Methodological Innovations in Polyketide Synthesis and their Application toward the Scalable Synthesis of Anti-Tumor Agent Spongistatin 1

Samuel Kaye Reznik

Submitted in partial fulfillment of the Requirement for the degree of Doctor of Philosophy in the Graduate School of Arts and Sciences

Columbia University

2012

Abstract

Methodological Innovations in Polyketide Synthesis and their Application toward the Scalable Synthesis of Anti-Tumor Agent Spongistatin 1

Samuel Kaye Reznik

This thesis describes the efforts of the Leighton laboratory to develop a scalable synthetic route to access anti-tumor agent spongistatin 1, or analogs thereof. In an effort to achieve this goal, several new chemical reaction platforms were established. Though these novel chemical transformations were developed specifically for use in the total synthesis of spongistatin 1, their potential application to general polyketide synthesis has been demonstrated. These methodological innovations have allowed our laboratory to take tremendous strides toward the longterm goal of helping to bring a potent chemotherapeutic agent to the global market.

Table of Contents

List of Schemes

List of Figures

List of Tables

Acknowledgements

As I approach the completion of my studies for the degree of Doctor of Philosophy in Organic Chemistry, numerous people come to mind whom I would like to acknowledge for the role they played in helping me arrive where I am today.

The true start to my career as a scientist began during my time at the Hopkins School in New Haven, CT. Under the guidance and encouragement of Dr. Sarah Leite, Dr. Albert Leger, Dr. Kellie Cox, Phillip Stewart and David McCord, I was imbued with a love of science that has served as a guiding light throughout my life.

My first opportunity to work in an academic research laboratory was afforded by Professor Alanna Schepartz at Yale University. I will be forever indebted to her for taking a chance on me as an undergraduate researcher despite my complete lack of laboratory experience. During my time in the Schepartz lab, my mentor, Dr. Olen Stephens, played a critical role in training me to think critically about scientific research. Over the past decade he has been a tremendous friend and has always been there to help me navigate life's many challenges.

From my time at the University of Pennsylvania, Professor Amos Smith played an incredibly influential role in my decision to pursue a Ph.D. in chemistry with a focus on organic synthesis. In one of life's small ironies, I was first exposed to the molecule spongistatin 1 in Professor Smith's second semester organic chemistry course. It was on the board the first day of class when he was describing the type of research his lab pursued. A few months later, Professor Smith gave me an opportunity to try my hand at polyketide synthesis myself. From that point until now, the focus of my professional career has been dedicated to becoming more adept at that art.

At Columbia University, I had the great fortune of joining the Leighton laboratory at a time when there were several incredible post-doctoral chemists who took a significant and sustained interest in my education and growth as a scientific researcher. Professor Uttam Tambar, Dr. Tyler Harrison and Dr. Jared Spletstoser were all tremendous mentors. In addition, I'd like to acknowledge Dr. Arash Soheili, in particular, as he spent a considerable portion of his final months in graduate school helping me get acclimated to work in the Leighton group and graduate school life in general.

In addition to meeting the colleagues above, I also had the distinct benefit of entering in the same graduate student class with Dr. Christopher Plummer. Though we were technically the same year, I always looked to Chris for advice both inside and outside of my fume hood. He has been a great friend over the years.

Within the Leighton group, I have had the pleasure of working directly with Professor Wesley Chalifoux, Dr. Ryan Shade, Linda Suen and Brian Marcus. All four of these Leighton group members helped me grow as a chemist, a mentor, a colleague and a friend, each in his or her own way.

Outside of the laboratory, I had the benefit of forming an incredible group of friends who have always been there to support me through the good times and bad. Dr. Daniel Wespe, Dr. Neal Miller, Dr. Christine Vanos Miller, Dr. Ferenc Kontes, Danielle Sedbrook, Trevor Sherwood and Kiel Beehler – thank you all.

I would also like to thank Daniel Chapman, who has been my roommate for the entirety of my graduate career. Chappy, thanks for always being so upbeat and cheerful; keep showing us all how to live the dream.

A special thank you must be paid to my Grandmother, Eleanore Reznik. Her never-ending supply of care packages sent to lab has kept me sustained through many long days and nights. I am so grateful to her for always thinking of and doing everything she can to support me.

On a similar note, I would like to thank my parents and sisters for their unending love and support. No matter how busy or stressed I have been over the years pursuing my Ph.D., they have always been there to lend an ear or a caring hand. I love you all very much and hope that I have made you proud.

And, of course, a heartfelt thank you must go to Danielle Bitterman. During a turbulent time in my life, Danielle helped me find my footing and inspired me to achieve as much as I could with the opportunities I had before me. I would not be where I am today if it weren't for her support, her encouragement, and the inspiring standard of excellence she adheres to every day.

Lastly, I would like to thank my advisor, Professor James Leighton. There were times during my Ph.D. where he may have been the only person who still believed I could succeed, even after I myself had lost hope. Thanks for giving me the chance to prove you right.

In Memory of Barry Reznik – A Beloved Chemist

Chapter 1:Toward a Scalable Synthesis of Spongistatin 1

1.1 Isolation and Bioactivity of Spongistatin 1

Polyketide natural products of the polypropionate/polyacetate type have attained a privileged position in the medicinal community, as they often possess important biological and therapeutic properties. In particular, spongistatin 1 (altohyrtin A) **1.1** has attracted a high level of interest from the medicinal community due to its extremely potent bioactivity as an antitumor agent (Figure 1.1).

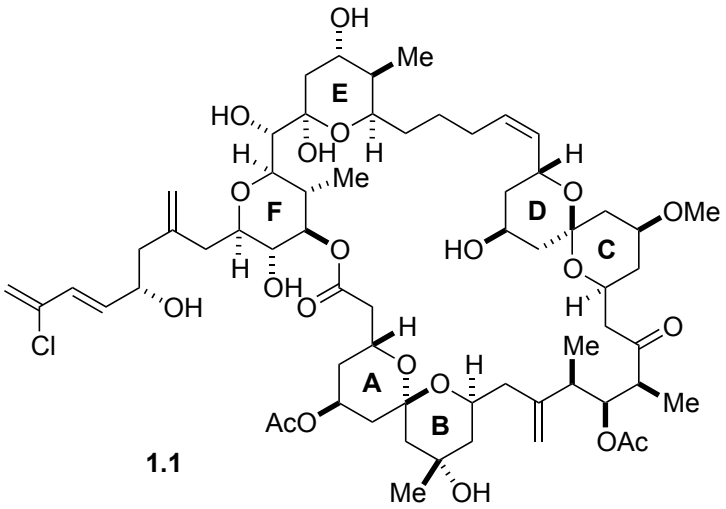

1.1

Figure 1.1: Spongistatin 1

First reported in 1993, spongistatin 1 was discovered independently and simultaneously by the Pettit,[1] Kitagawa/Kobayashi[2] and Fusetani[3] groups. This naturally occurring polyketide was harvested as part of a family of bioactive bis-spirocycle marine macrolides isolated from a variety of sea sponges found in the Indian Ocean as well as in the seas surrounding Japan. Spongistatin 1 itself was found to be quite scarce; degradation of nearly 400 kg of sponge produced only 14 mg of the natural product. Yet even with this small amount of isolated

material in hand, spongistatin 1's extraordinary bioactivity as an anti-mitotic, anti-tumor agent was quickly discovered. Spongistatin 1 was shown to have an average IC_{50} value of 0.12 nM against the NCI panel of 60 cancer cell lines, making it one of the most potent cancer cell growth inhibitory agents tested to date.[4] Furthermore, curative responses at extremely low doses of spongistatin 1 were also observed *in vivo* as part of later human melanoma and ovarian carcinoma xenograft studies.[5] Despite these promising preliminary biological results, however, the vanishingly small supply of the naturally product prevented comprehensive testing of spongistatin 1 as a potential chemotherapy agent.

1.2 Previous Syntheses of Spongistatin

Due to this confluence of scarcity and extraordinary potency, the spongistatin family has elicited an enormous amount of interest and effort from the synthetic chemistry community. While multiple research groups worldwide have completed numerous fragment syntheses, only seven research groups have been able to achieve complete total syntheses of spongistatin 1 and/or 2 to date. The work of Evans,[6] Kishi,[7] Smith,[8] Paterson,[9] Crimmins,[10] Heathcock[11] and Ley[12] represent a profound demonstration of synthetic creativity and resiliency in the face of an exceedingly daunting architectural task. Their syntheses of spongistatin necessitated the use of chemistry's most powerful tools for polyketide synthesis and provided a challenging proving ground for the development of important new methodologies employed by numerous chemists today.[13] In terms of increasing the medical community's supply of spongistatin 1, the Smith group notably succeeded in producing 1.0 g of spongistatin 1[8g] – an amount likely to be sufficient for all pre-clinical development trials – which has already produced some exciting *in vitro* and *in vivo* results, further elucidating the molecule's strong anticancer and low toxicity biological profile.[14]

1.3 The Goal of a More Scalable Synthesis and Overall Strategy

While the Smith group's preparation of 1.0 g of spongistatin 1 has already served as a boon toward firmly establishing its importance as a medicinal drug target, the prospect of turning spongistatin 1 into a viable chemotherapy agent remains a formidable challenge. The ultimate goal of making spongistatin 1, or an analog thereof, into a widely available antitumor agent still requires the development of a synthesis that can both facilitate the production of various analogs in addition to delivering the larger quantities necessary for clinical development. Especially in the context of new medical technologies that utilize a relatively small number of potent antitumor molecules as "warheads" attached to antibody-drug conjugates,[15] we believe that the development of a scalable, multi-gram synthesis of spongistain 1 would genuinely impact the scientific community's ability to develop a powerful and accessible chemotherapy agent.

To that end, we examined previous syntheses of spongistatin 1 and looked for opportunities to improve the overall efficiency and scalability of the total synthesis. The most efficient syntheses of spongistatin 1 to date divide the molecule into two separate syntheses of the ABCD and EF hemispheres, which are joined by a late-stage Wittig coupling followed by a macrolactonization sequence (Figure 1.2).[13] Seeing as the synthesis of these two hemispheres allows for a roughly convergent total synthesis, we opted to keep this late-stage hemisphere coupling strategy while looking to improve the overall efficiency of synthesizing the ABCD and EF hemisphere themselves.

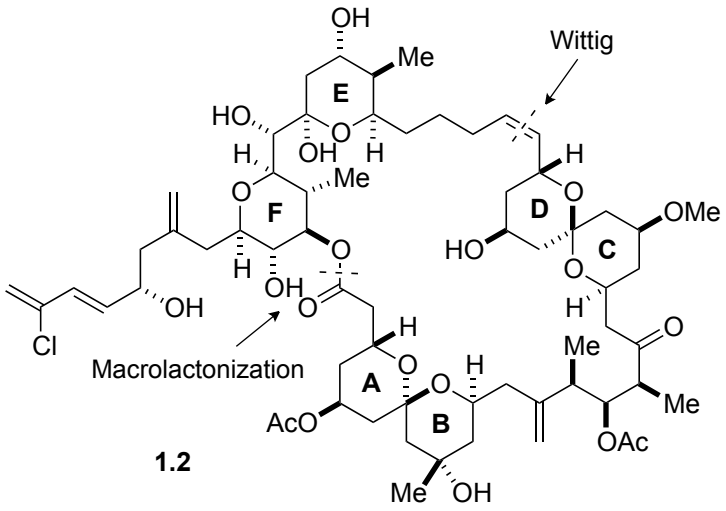

Figure 1.2: Established hemisphere coupling strategy

1.4 ABCD Hemisphere Retrosynthetic Analysis

Past efforts toward the synthesis of the ABCD hemisphere have frequently employed the Felkin-selective *anti*-aldol approach pioneered by the Evans group to join the AB and CD fragments.[6c] This original coupling strategy has continued to serve as a high-yielding fragment coupling reaction while also providing exquisite stereocontrol over the concomitantly formed C(15) and C(16) stereocenters (Scheme 1.1). Though this transformation could hardly be improved upon for use in small scale couplings, we felt that the multi-gram generation of the requisite complex fragment precursors, especially one as sensitive as the α-chiral-β,γ-unsaturated aldehyde **1.4**, would entail an unacceptable amount of risk for such precious, late-stage material. As such, we decided to explore an alternative approach to coupling the AB and CD spiroketals that, we hoped, would be more amenable to a large-scale synthesis.

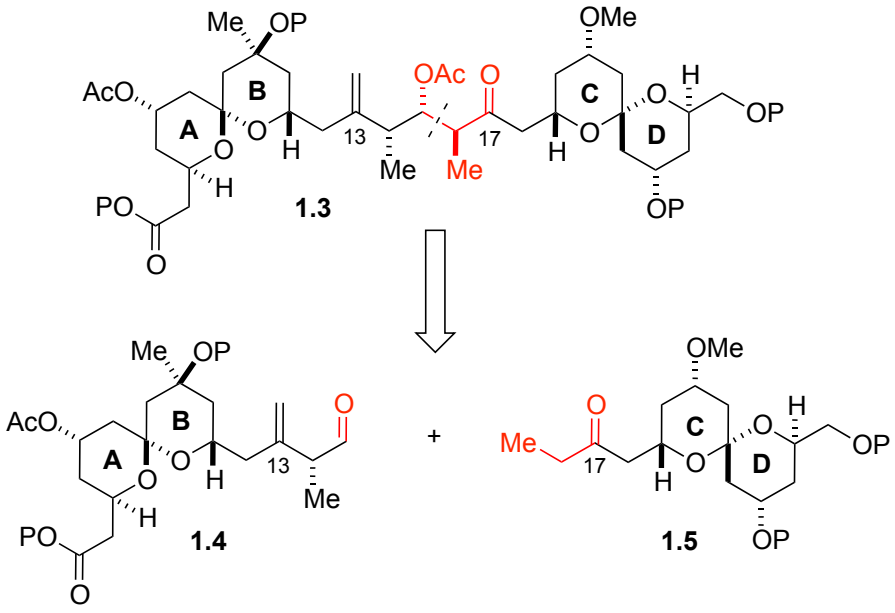

Scheme 1.1: The Evans aldol approach to the ABCD hemisphere

When considering an alternative fragment coupling approach to the ABCD hemisphere, we wanted to pursue a strategy that would allow for an efficient coupling of the AB and CD spiroketals while also requiring fewer total steps for generating the spiroketals themselves. With these goals in mind, the Leighton laboratory's previous work employing a tandem silylformylation / Tamao oxidation sequence to generate complex polyketide motifs began to serve as an inspirational cornerstone for our retrosynthetic strategy (Scheme 1.2).[16]

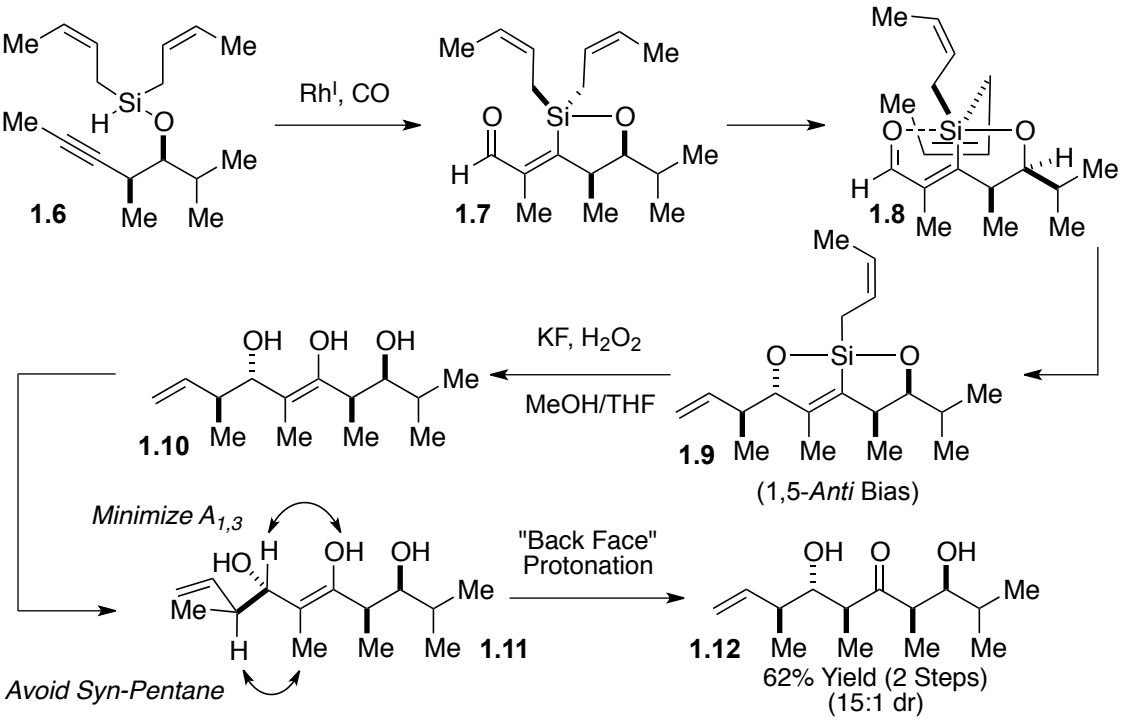

Scheme 1.2: Mechanism of tandem silylformylation / Tamao oxidation sequence

The tandem silylformylation / Tamao oxidation sequence depicted above not only provides access to complex polyketide stereochemical arrays such as **1.12** from simple homopropargylic silyl-ethers such as **1.6**, but does so in a high-yielding, scalable procedure only requiring purification at the end of the sequence. Since a reaction sequence with these characteristics was exactly the type of coupling strategy we wanted to employ in a multi-gram synthesis of spongistatin 1, we attempted to compare the product motif observed in substrate **1.12** to the pertinent region of the ABCD hemisphere **1.3** (Scheme 1.3). Satisfyingly, the highlighted C(13)-C(17) segment of the ABCD hemisphere mapped on quite closely to the product motif of our tandem sequence, indicating that the reaction platform could indeed serve as an effective method for installing the three requisite stereocenters as well as the desired olefin and ketone in the correct oxidation states.

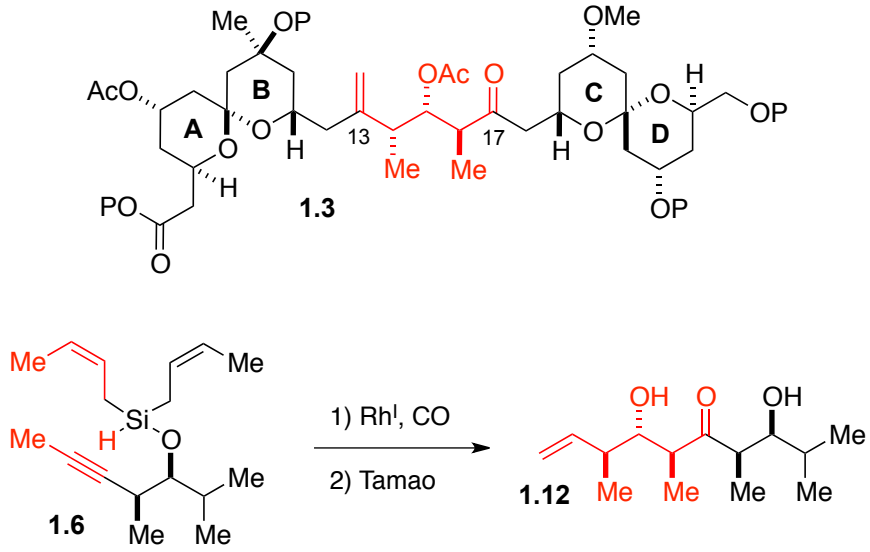

Scheme 1.3: Identification of ABCD fragment as tandem sequence substrate

Despite the already appealing prospect of employing our tandem silylformylation / Tamao oxidation methodology as a strategy to build the C(13)-C17) array from the CD spiroketal toward the AB spiroketal, we began to consider the notion that this methodology *might additionally be utilized as a fragment coupling procedure.* Though quite ambitious, this idea appeared to be a sound extension of the group's current reaction platform, since it simply necessitated that the AB spiroketal be tethered to the silicon as part of its "allyl" transfer moiety as shown in silyl-ether **1.13** (Scheme 1.4).

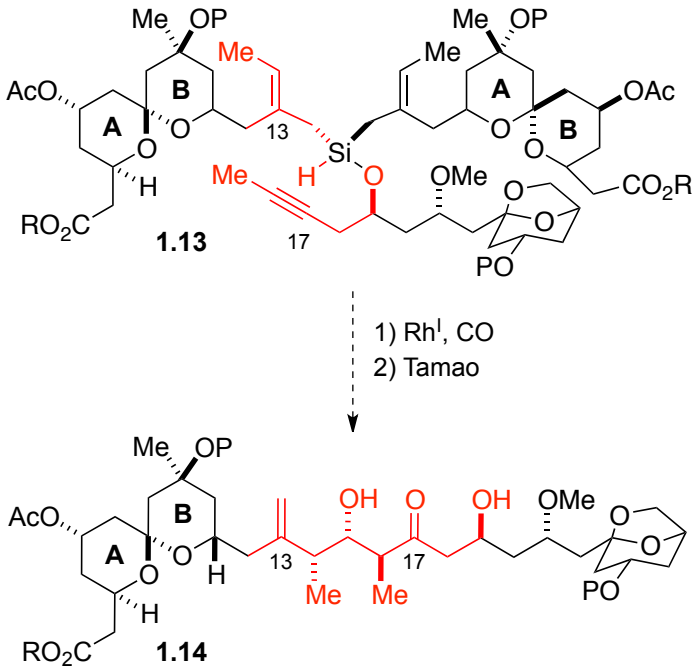

Scheme 1.4: Fragment coupling via tandem silylformylation/Tamao sequence

On closer examination of this potential coupling strategy, however, two main concerns came to light. The first being that the implementation of the tandem silylformylation / Tamao in its published form would require two equivalents of AB spiroketal – since only one undergoes the 1,5-*anti* allyl transfer (Scheme 1.2). The sacrifice of a full equivalent of the elaborated AB spiroketal would be unacceptable in a scalable total synthesis of spongistatin 1, so this aspect of the tandem sequence would need to be modified. The second concern centered on the fact that there was little precedence for making complex tiglic silanes (trans-crotyl silanes substituted at the 2 position), which is the required olefin geometry for obtaining the desired stereochemical triad seen in compound **1.14**.

With these concerns in mind, the initial goals of the synthesis of the ABCD hemisphere became clear. Before any major synthetic effort could be undertaken, new methodologies would have to be developed. These methods would need to allow for loading the AB spiroketal onto

silicon in a tiglic substitution pattern, in addition to selectively transferring a single equivalent of the AB spiroketal carried throughout the tandem sequence. Efforts toward these methodological goals will be described in the following chapter.

1.5 References and Notes

1. (a) Bai, R. L.; Cichacz, Z. A.; Herald, C. L.; Pettit, G. R.; Hamel, E., *Mol Pharmacol* **1993,** *44* (4), 757-766; (b) Pettit, G. R.; Cichacz, Z. A.; Gao, F.; Herald, C. L.; Boyd, M. R., *J. Chem. Soc. Chem. Comm.* **1993,** (14), 1166-1168; (c) Pettit, G. R.; Cichacz, Z. A.; Gao, F.; Herald, C. L.; Boyd, M. R.; Schmidt, J. M.; Hooper, J. N. A., *J. Org. Chem.* **1993,** *58* (6), 1302-1304; (d) Pettit, G. R., *Pure Appl Chem* **1994,** *66* (10-11), 2271-2281.

2. (a) Kobayashi, M.; Aoki, S.; Sakai, H.; Kawazoe, K.; Kihara, N.; Sasaki, T.; Kitagawa, I., *Tetrahedron. Lett.* **1993,** *34* (17), 2795-2798; (b) Kobayashi, M.; Aoki, S.; Sakai, H.; Kihara, N.; Sasaki, T.; Kitagawa, I., *Chem. Pharm. Bull.* **1993,** *41* (5), 989-991; (c) Kobayashi, M.; Aoki, S.; Kitagawa, I., *Tetrahedron. Lett.* **1994,** *35* (8), 1243-1246.

3. Fusetani, N.; Shimoda, K.; Matsunaga, S., *J. Am. Chem. Soc.* **1993,** *115* (10), 3977-3981.

4. Schyschka, L.; Rudy, A.; Jeremias, I.; Barth, N.; Pettit, G. R.; Vollmar, A. M., *Leukemia* **2008,** *22* (9), 1737-1745.

5. Pettit, R. K.; McAllister, S. C.; Pettit, G. R.; Herald, C. L.; Johnson, J. M.; Cichacz, Z. A., *Int J Antimicrob Ag* **1998,** *9* (3), 147-152.

6. (a) Evans, D. A.; Coleman, P. J.; Dias, L. C., *Angew. Chem. Int. Edit.* **1997,** *36* (24), 2738-2741; (b) Evans, D. A.; Trotter, B. W.; Cote, B.; Coleman, P. J., *Angew. Chem. Int. Edit.* **1997,** *36* (24), 2741-2744; (c) Evans, D. A.; Trotter, B. W.; Cote, B.; Coleman, P. J.; Dias, L. C.; Tyler, A. N., *Angew. Chem. Int. Edit.* **1997,** *36* (24), 2744-2747; (d) Evans, D. A.; Trotter, B. W.; Coleman, P. J.; Cote, B.; Dias, L. C.; Rajapakse, H. A.; Tyler, A. N., *Tetrahedron* **1999,** *55* (29), 8671-8726.

7. (a) Guo, J. S.; Duffy, K. J.; Stevens, K. L.; Dalko, P. I.; Roth, R. M.; Hayward, M. M.; Kishi, Y., *Angew. Chem. Int. Edit.* **1998,** *37* (1-2), 187-192; (b) Hayward, M. M.; Roth, R. M.; Duffy, K. J.; Dalko, P. I.; Stevens, K. L.; Guo, J. S.; Kishi, Y., *Angew. Chem. Int. Edit.* **1998,** *37* (1-2), 192-196.

8. (a) Smith, A. B.; Doughty, V. A.; Lin, Q. Y.; Zhuang, L. H.; McBriar, M. D.; Boldi, A. M.; Moser, W. H.; Murase, N.; Nakayama, K.; Sobukawa, M., *Angew. Chem. Int. Edit.* **2001,** *40* (1), 191-195; (b) Smith, A. B.; Lin, Q. Y.; Doughty, V. A.; Zhuang, L. H.; McBriar, M. D.; Kerns, J. K.; Brook, C. S.; Murase, N.; Nakayama, K., *Angew. Chem. Int. Edit.* **2001,** *40* (1), 196-199; (c) Smith, A. B.; Corbett, R. M.; Pettit, G. R.; Chapuis, J. C.; Schmidt, J. M.; Hamel,

E.; Jung, M. K., *Bioorg. Med. Chem. Lett.* **2002,** *12* (15), 2039-2042; (d) Smith, A. B.; Doughty, V. A.; Sfouggatakis, C.; Bennett, C. S.; Koyanagi, J.; Takeuchi, M., *Org. Lett.* **2002,** *4* (5), 783-786; (e) Smith, A. B.; Zhu, W. Y.; Shirakami, S.; Sfouggatakis, C.; Doughty, V. A.; Bennett, C. S.; Sakamoto, Y., *Org. Lett.* **2003,** *5* (5), 761-764; (f) Smith, A. B.; Sfouggatakis, C.; Gotchev, D. B.; Shirakami, S.; Bauer, D.; Zhu, W. Y.; Doughty, V. A., *Org. Lett.* **2004,** *6* (20), 3637-3640; (g) Smith, A. B.; Tomioka, T.; Risatti, C. A.; Sperry, J. B.; Sfouggatakis, C., *Org. Lett.* **2008,** *10* (19), 4359-4362; (h) Smith, A. B.; Doughty, V. A.; Sfouggatakis, C.; Bennett, C. S.; Koyanagi, J.; Takeuchi, M., *Org. Lett.* **2009,** *11* (3), 785-785; (i) Smith, A. B.; Lin, Q. Y.; Doughty, V. A.; Zhuang, L. H.; McBriar, M. D.; Kerns, J. K.; Boldi, A. M.; Murase, N.; Moser, W. H.; Brook, C. S.; Bennett, C. S.; Nakayama, K.; Sobukawa, M.; Trout, R. E. L., *Tetrahedron* **2009,** *65* (33), 6470-6488; (j) Smith, A. B.; Sfouggatakis, C.; Risatti, C. A.; Sperry, J. B.; Zhu, W. Y.; Doughty, V. A.; Tomioka, T.; Gotchev, D. B.; Bennett, C. S.; Sakamoto, S.; Atasoylu, O.; Shirakami, S.; Bauer, D.; Takeuchi, M.; Koyanagi, J.; Sakamoto, Y., *Tetrahedron* **2009,** *65* (33), 6489-6509.

9. (a) Paterson, I.; Chen, D. Y. K.; Coster, M. J.; Acena, J. L.; Bach, J.; Gibson, K. R.; Keown, L. E.; Oballa, R. M.; Trieselmann, T.; Wallace, D. J.; Hodgson, A. P.; Norcross, R. D., *Angew. Chem. Int. Edit.* **2001,** *40* (21), 4055-+; (b) Paterson, I.; Coster, M. J.; Chen, D. Y. K.; Acena, J. L.; Bach, J.; Keown, L. E.; Trieselmann, T., *Org. Biomol. Chem.* **2005,** *3* (13), 2420-2430; (c) Paterson, I.; Coster, M. J.; Chen, D. Y. K.; Gibson, K. R.; Wallace, D. J., *Org. Biomol. Chem.* **2005,** *3* (13), 2410-2419; (d) Paterson, I.; Coster, M. J.; Chen, D. Y. K.; Oballa, R. M.; Wallace, D. J.; Norcross, R. D., *Org. Biomol. Chem.* **2005,** *3* (13), 2399-2409.

10. Crimmins, M. T.; Katz, J. D.; Washburn, D. G.; Allwein, S. P.; McAtee, L. F., *J. Am. Chem. Soc.* **2002,** *124* (20), 5661-5663.

11. (a) Heathcock, C. H.; McLaughlin, M.; Medina, J.; Hubbs, J. L.; Wallace, G. A.; Scott, R.; Claffey, M. M.; Hayes, C. J.; Ott, G. R., *J. Am. Chem. Soc.* **2003,** *125* (42), 12844-12849; (b) Hubbs, J. L.; Heathcock, C. H., *J. Am. Chem. Soc.* **2003,** *125* (42), 12836-12843.

12. Ball, M.; Gaunt, M. J.; Hook, D. F.; Jessiman, A. S.; Kawahara, S.; Orsini, P.; Scolaro, A.; Talbot, A. C.; Tanner, H. R.; Yamanoi, S.; Ley, S. V., *Angew. Chem. Int. Edit.* **2005,** *44* (34), 5433-5438.

13. Paterson, I.; Yeung, K. S., *Chem Rev* **2005,** *105* (12), 4237-4313.

14. Xu, Q. L.; Huang, K. C.; Tendyke, K.; Marsh, J.; Liu, J. K.; Qiu, D. Y.; Littlefield, B. A.; Nomoto, K.; Atasoylu, O.; Risatti, C. A.; Sperry, J. B.; Smith, A. B., *Anticancer Res* **2011,** *31* (9), 2773-2779.

15. (a) Kovtun, Y. V.; Audette, C. A.; Ye, Y.; Xie, H.; Ruberti, M. F.; Phinney, S. J.; Leece, B. A.; Chittenden, T.; Blattler, W. A.; Goldmacher, V. S., *Cancer Res* **2006,** *66* (6), 3214-21; (b) Kovtun, Y. V.; Goldmacher, V. S., *Cancer letters* **2007,** *255* (2), 232-40; (c) Ducry, L.; Stump, B., *Bioconjugate chemistry* **2010,** *21* (1), 5-13.

16. Spletstoser, J. T.; Zacuto, M. J.; Leighton, J. L., *Org. Lett.* **2008,** *10* (24), 5593-5596.

Chapter 2: Methodology Work toward Intramolecular Fragment Coupling

2.1 Group Precedence for an Asymmetric Silane Alcoholysis

As described in the previous chapter, we believed we could achieve our goal of an efficient and scalable fragment coupling between the AB and CD spiroketals of spongistatin 1 through the use of the Leighton laboratory's tandem silylformylation / Tamao oxidation sequence.[1] However, to effectively employ this methodology, we would have to develop a way to load only a single equivalent of AB spiroketal onto silicon before the reaction sequence. Fortunately, our group had some useful precedent for accomplishing this task via an asymmetric silane alcoholysis (ASA) reaction.[2] In the ASA reaction platform, the silane in question contains a non-transferable *t*-butyl group in addition to the desired, transferable allyl subunit (Scheme 2.1). By establishing the silicon-oxygen bond diastereoselectively, the chirality at silicon serves to direct which face of the silylformylated substrate will be allylated during the tandem sequence.

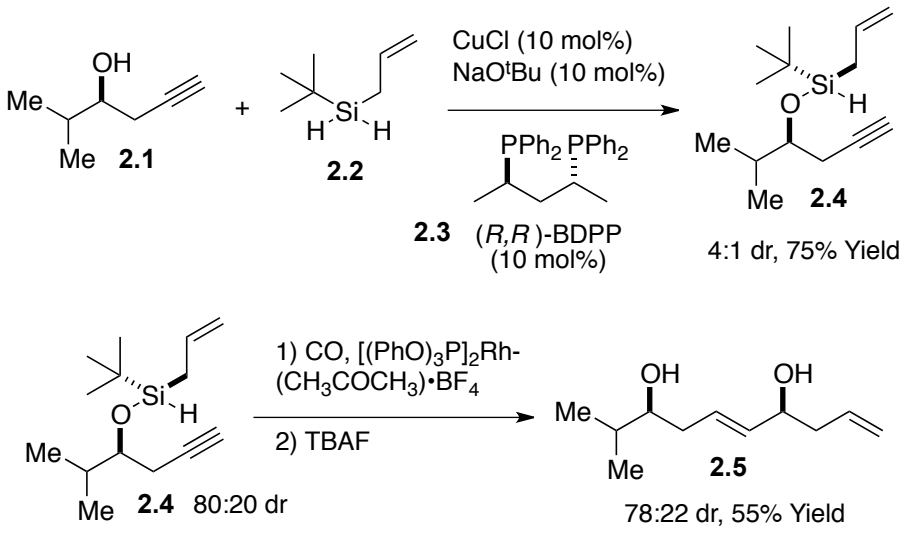

Scheme 2.1: Access to 1,5-*syn*-diols via asymmetric silane alcoholysis

Though it might seem that this precedent already allows for the use of a single "allyl" AB spiroketal unit on silicon in conjunction with the *t*-butyl moiety, the method falls short due to its resistance to the Tamao oxidation work-up required for our desired coupling procedure (Scheme 2.2).

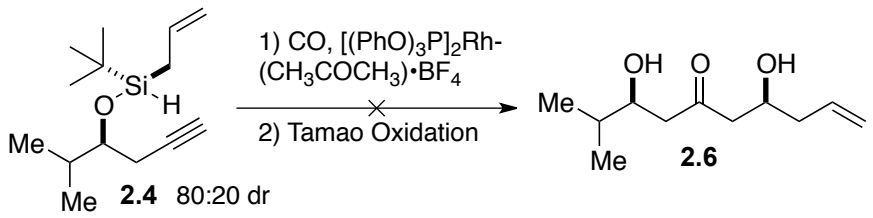

Scheme 2.2: *t*-Butyl subunit incompatibility with Tamao oxidation

As a result, the ASA reaction platform would have to be overhauled to find a suitable, non-transferable subunit that would allow for diastereoselective silicon-oxygen bond formation while still being amenable to a Tamao oxidation at the end of the silylformylation tandem reaction sequence (Scheme 2.3).

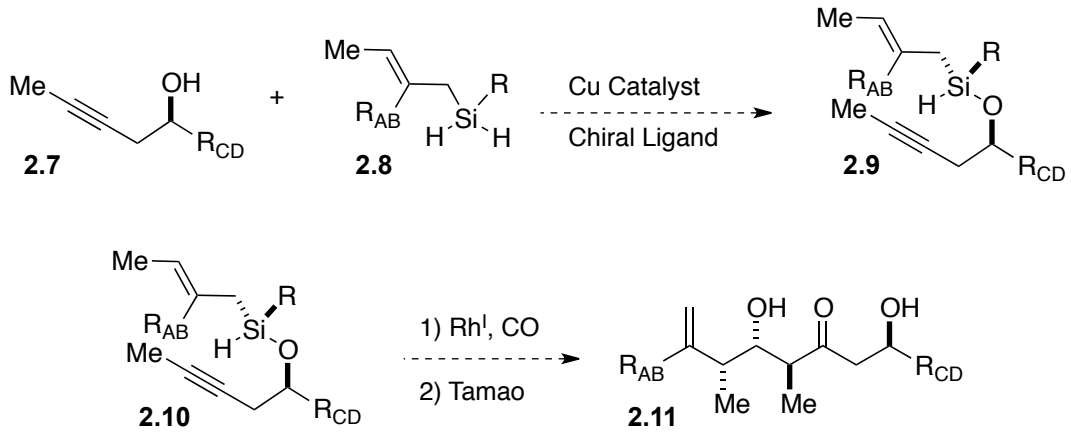

Scheme 2.3: Desired fragment coupling by ASA / silylformylation / Tamao sequence

2.2 Development of a Model ASA Reaction Assay and Initial Screening Results

When considering the optimization and extension of the Leighton laboratory's ASA reaction platform, it was important to think critically about the copper(I)-mediated reaction pathway and design a screening assay that would rapidly provide clear results. To that end, we examined the copper-mediated silane alcoholysis reaction mechanism as described by Oestreich and co-workers[3] and used it to develop a plausible catalytic sequence (Scheme 2.4).

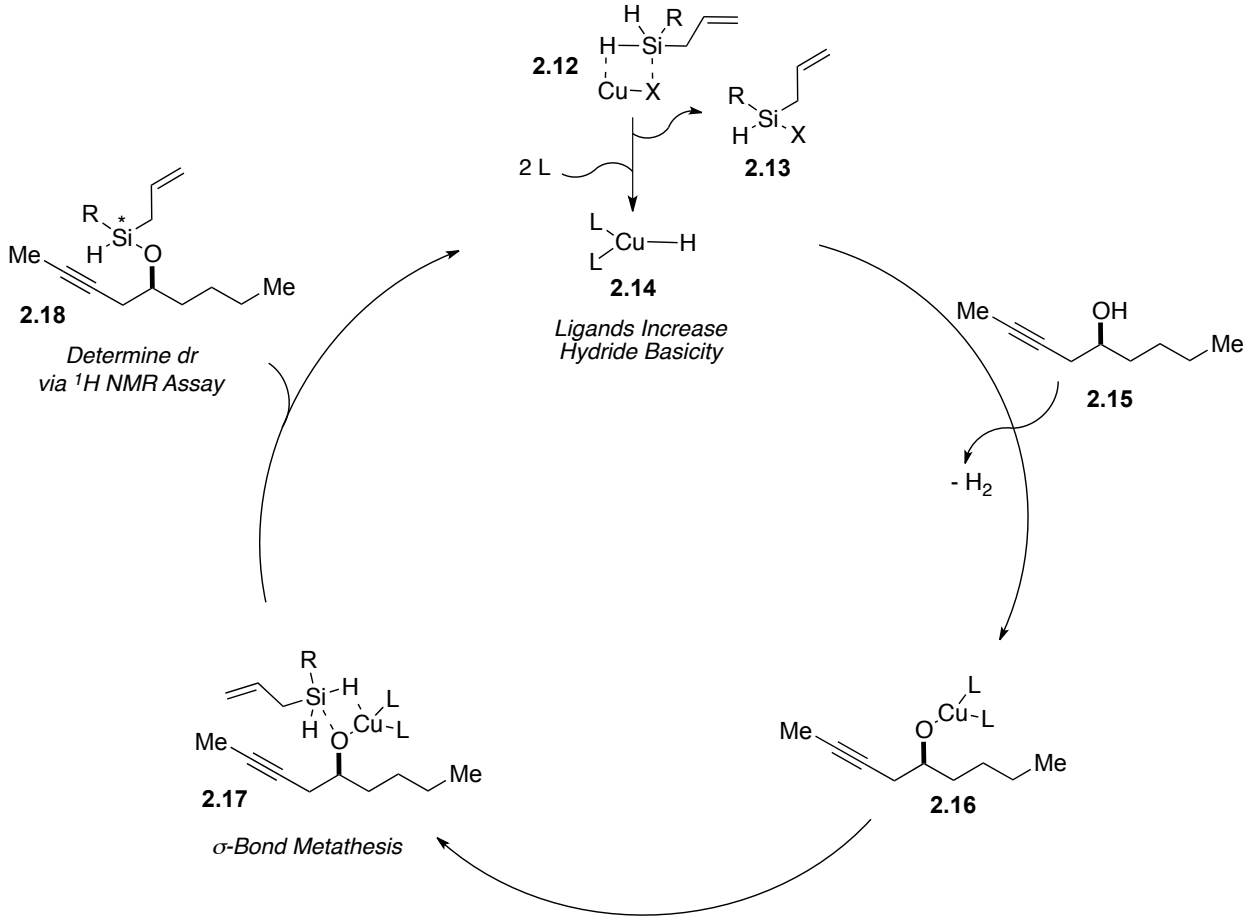

Scheme 2.4: Catalytic cycle for ASA model system

The proposed catalytic cycle depicted above helped us establish several variables that could be screened independently, such as the non-transferable group on silicon (R), the chiral ligand (L) and the source of copper (Cu-X).

To begin our investigation, we opted to use homopropargylic alcohol **2.15** (derived from the BF_3•OEt_2-mediated, propyne opening of enantioenriched epoxyhexane[4]) as a model for the CD spiroketal and a simple allyl subunit on silane **2.12** as a model for the AB spiroketal. We chose to explore aryl derivitives as our first group of R substituent since aryl-silicon bonds are known to be more amenable to Tamao oxidations than alkyl-silicon bonds.[5] To generate the desired aryl derivative silanes **2.12**, precursor aryl Grignards or aryl lithiates were reacted with allyltrichlorosilane and then reduced with excess LAH (Scheme 2.5).

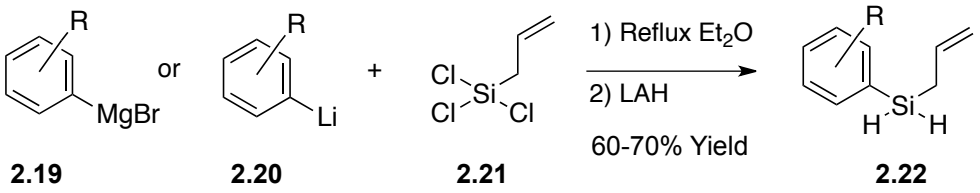

Scheme 2.5: Accessing aryl-allyl silanes

With the parent phenyl silane **2.23** in hand, a variety of chiral ligands and copper sources were screened. While none of these combinations served to provide any significant diastereoselectivity in setting the Si-O bond in silyl-ether **2.24**, the screen still provided useful information for determining the best copper(I) source and the optimal classes of phosphine ligands to pursue in further ASA studies (Scheme 2.6).

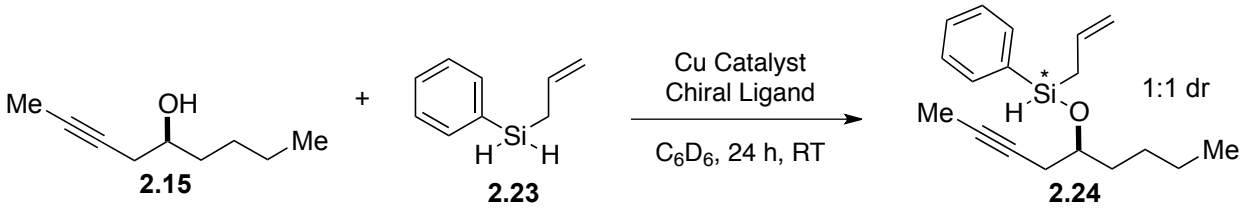

Scheme 2.6: Initial ASA screen with allylphenylsilane

It was determined from our initial screen that CuOAc was the best source of copper(I) for the ASA reaction as it smoothly generated copper hydride through its reaction with silane **2.23**

and released a relatively innocuous silyl-acetate **2.13** as its reaction byproduct. CuCl, CuBr and CuI were all found to have low reactivity in terms of generating the desired copper hydride for the catalytic cycle, while CuO^{t}Bu and CuOTf were found to be too reactive and led to a mixture of products.

As for the chiral phosphine ligands employed in the ASA reaction, two major trends became clear. While electron rich phosphines were required to increase the basicity of the copper hydride, and thus allow it to react with alcohol **2.15** in the first step of the catalytic cycle (Scheme 2.4), if the phosphines were too electron rich, overreaction of the copper hydride led to a mixture of products. A variety of phosphine classes and their relative reactivities in the ASA reaction are summarized below (Scheme 2.7, Scheme 2.8, Scheme 2.9, Scheme 2.10).

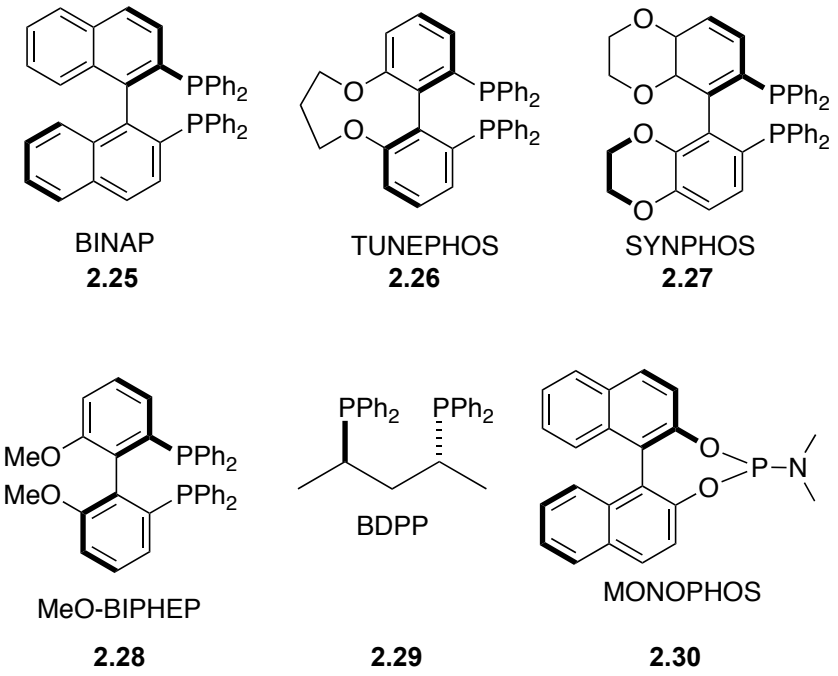

Scheme 2.7: Ligand classes that gave optimal copper-hydride reactivity in the ASA

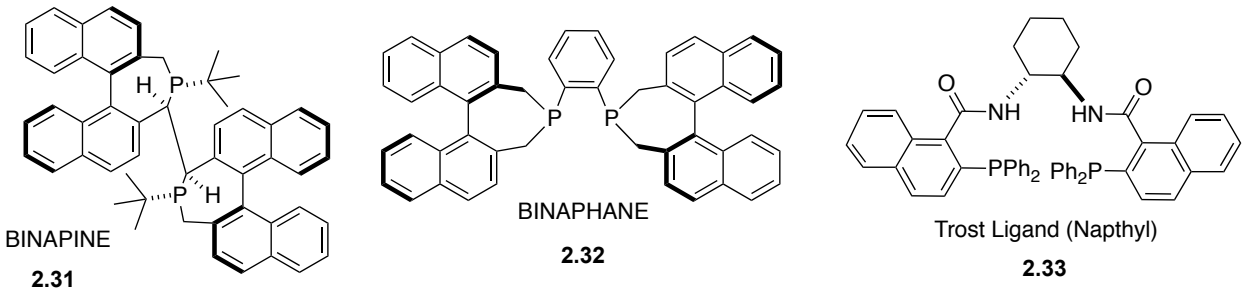

Scheme 2.8: Ligand classes that were too sterically hindered to promote the ASA

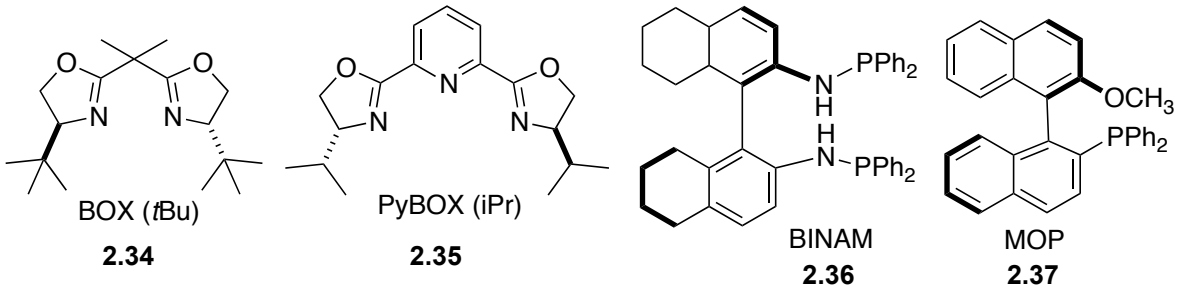

Scheme 2.9: Electron poor ligand classes that exhibited low reactivity in the ASA

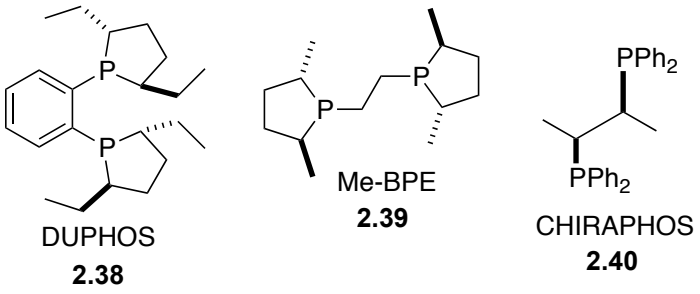

Scheme 2.10: Electron rich ligand classes that led to overreaction in the ASA

With a variety of ligands now known to effectively promote the desired silicon-oxygen bond formation (Scheme 2.7), we went on to explore the effect of modifying the aryl moiety on

silicon in an attempt to increase the reaction's diastereoselectivity in the silcon-oxygen bond forming step. Many aryl-allyl silanes were generated, all of which exhibited variable, albeit minimal, impacts on the diastereomeric ratio of products. The highest diastereoselectivities obtained for generating silyl-ethers **2.41** by utilizing silanes **2.22** in an ASA chiral ligand screen are indicated below (Scheme 2.11).

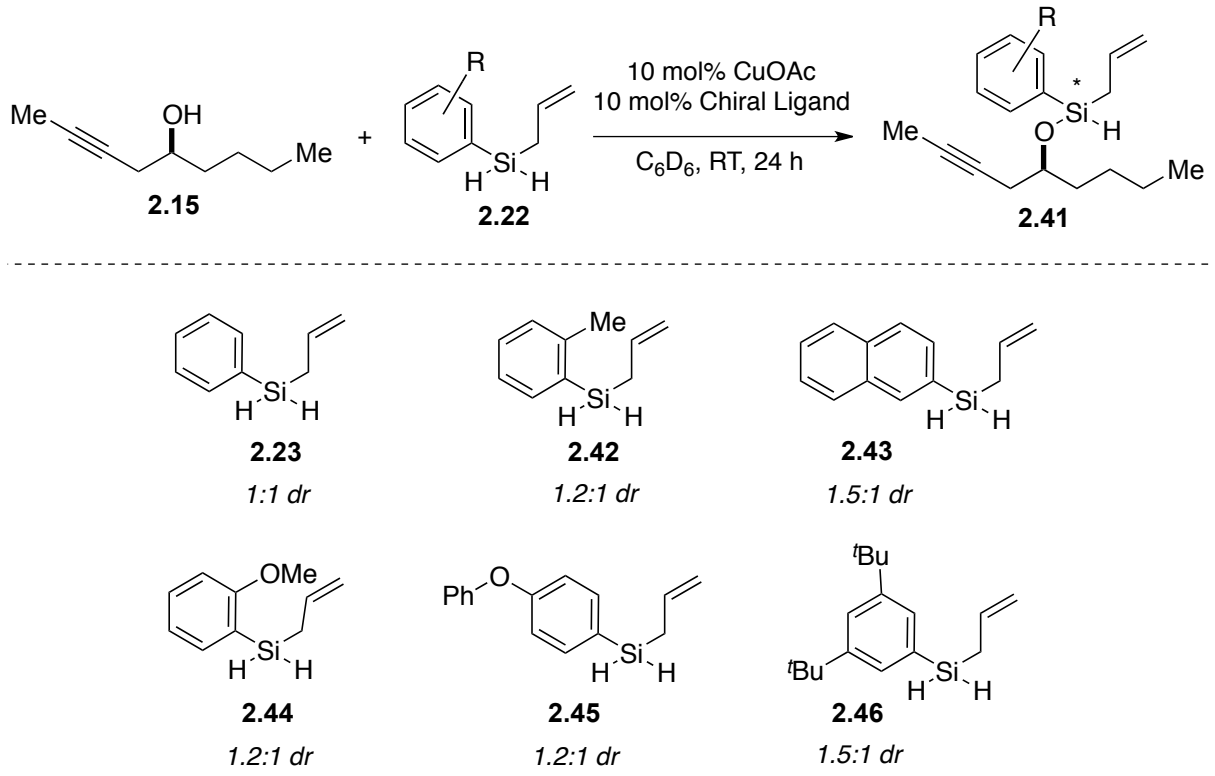

Scheme 2.11: Highest diastereoselectivities obtained using a variety of aryl silanes

Since the selectivities obtained using the aryl silanes shown above were not particularly promising, we sought to move the steric bulk of the aryl ring in **2.22** closer to the site at which the chiral silicon-oxygen bond was forming (Scheme 2.12). It was our hope that this modification would allow the aryl ring to better direct the chiral ligand on copper and thus increase the overall diastereoselectivity of the reaction.

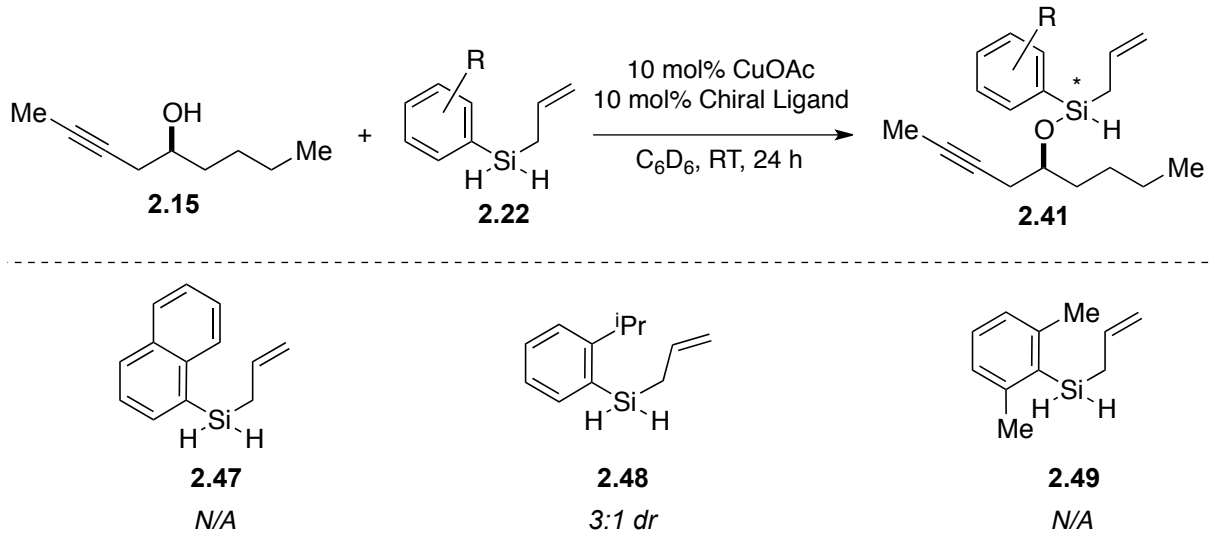

Scheme 2.12: Aryl-allyl silanes with steric bulk at the ortho position

While this modification did indeed serve to improve the diastereoselectivity of the ASA reaction to 3:1 dr when using isopropyl derived silane **2.48**, the increased steric bulk at the ortho position on the aryl ring was found to be incompatible with the requisite Tamao oxidation following the silylformylation tandem sequence. The performance of various silanes **2.22** in the tandem silylformylation / Tamao oxidation tandem sequence were evaluated by affecting a silane alcoholysis between the silane in question and achiral alcohol **2.50**. The resulting silyl ether **2.51** was then subjected to the tandem silylformylation / Tamao sequence (Scheme 2.13). If the silane was not compatible with the Tamao oxidation, its diastereoselectivity in the ASA reaction was not pursued (as with silanes **2.47** and **2.49** above).

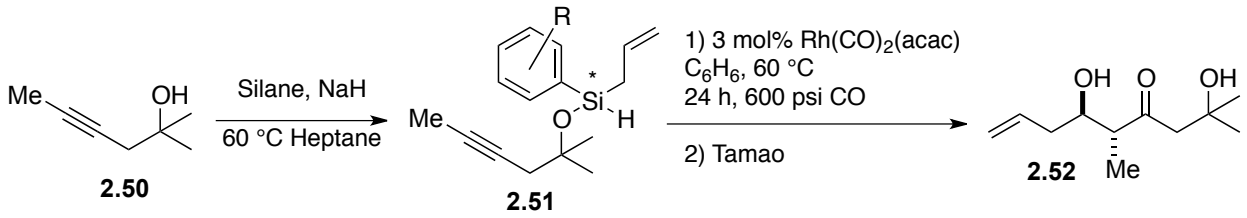

Scheme 2.13: Testing the compatibility of each silane with the Tamao oxidation

2.3 Exploring Alternative Silane Structural Motifs in the ASA Reaction

Following the lackluster screening results of the aryl derived, allylsilanes described in the previous section, we turned our attention to exploring alternative silane structural motifs in the ASA reaction. The first alternative we examined was a class of benzylic silane derivatives **2.53**. We hoped that by moving the steric bulk on silicon one carbon away that these derivatives might participate in distinct, diastereoselective interactions with the ASA chiral ligand while still remaining compatible with the Tamao oxidation required after the tandem sequence (Scheme 2.14).

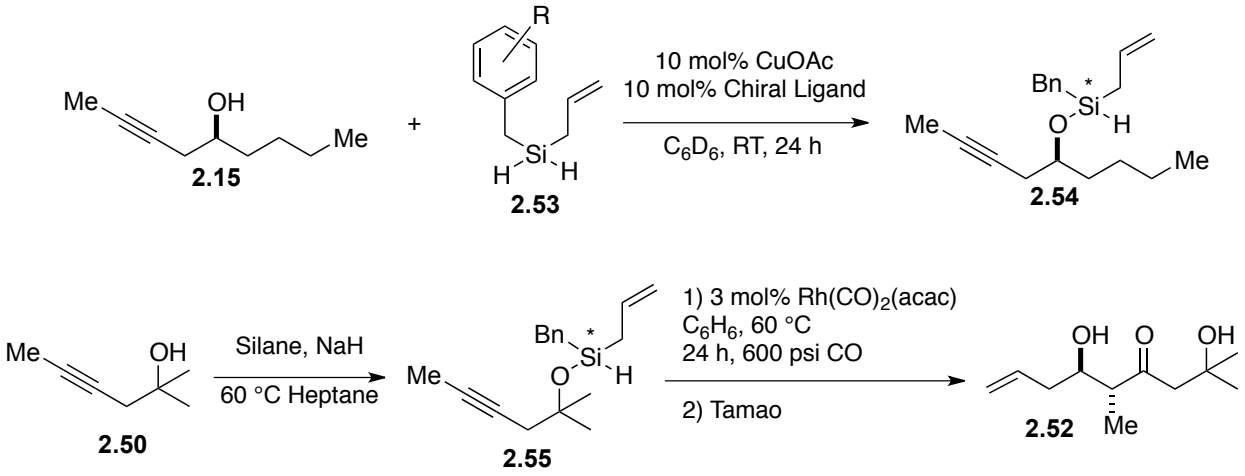

Scheme 2.14: Exploring benzylic silanes as an alternative structural motif

Because substituted benzyl Grignards and benzyl lithiates are often not commercially available, a method for generating silanes of type **2.53** had to be identified. As first demonstrated by Benkeser, the combination of trichlorosilane **2.56** and trialkylamines such as **2.57** generates a reactive source of anionic trichlorosilicon **2.58** which can then act as a nucleophile in S_N2, S_N2' or 1,2-carbonyl additions.[6] This methodology was used to generate a

variety of substituted benzylic silanes **2.53** from their precursor benzyl chlorides **2.60** as shown below (Scheme 2.15).

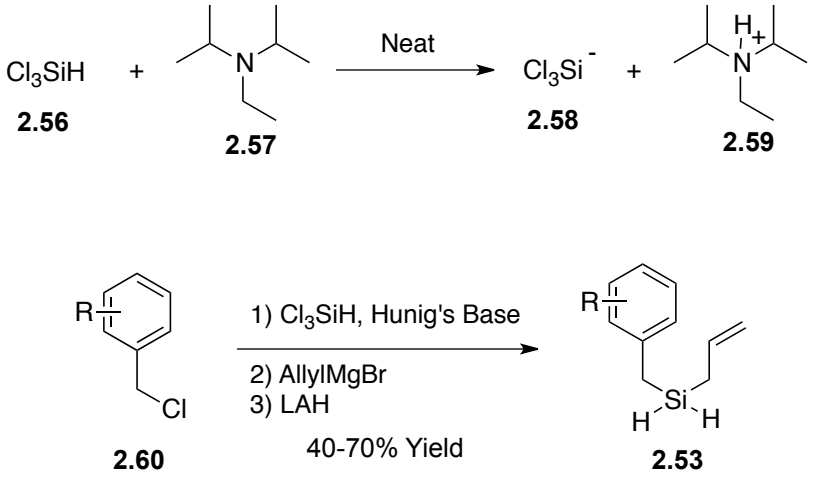

Scheme 2.15: Accessing benzyl-allyl silanes

As with the substituted aryl silanes **2.22** (Scheme 2.11), the benzylic silanes **2.53** were subjected to a battery of ASA reactions (Scheme 2.14) utilizing several classes of chiral ligands (Scheme 2.7). The best diastereomeric ratios obtained with each silane are depicted below (Scheme 2.16).

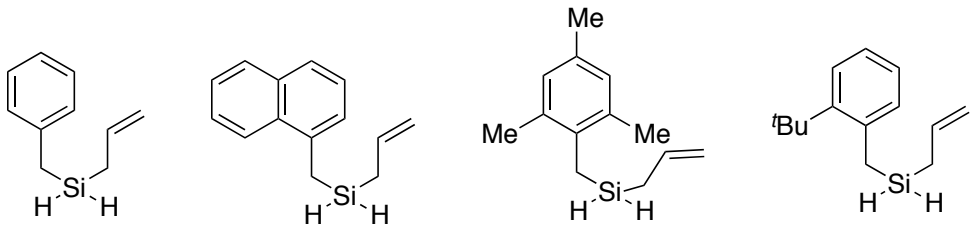

1:1 dr **2.61**

1.3:1 dr **2.62**

1.5:1 dr **2.63**

1.5:1 dr **2.64**

Scheme 2.16: Highest diastereoselectivities obtained using a variety of benzylic silanes

Though more highly substituted benzylic silanes, such as 2,6-di-*t*-butyl benzyl silane, could perhaps have been synthesized and examined in the ASA reaction, the disappointing results seen with the more readily accessible substrates depicted above led us to abandon benzylic silanes **2.53** as a potential ASA structural motif.

Inspired by related work by Benkeser,[6b] we next turned our attention to benzhydryl silane **2.67** as a potential parent compound for a new ASA structural motif that would still be amenable to Tamao oxidation. Unfortunately, the synthesis of benzhydryl silane **2.67** was low yielding from known trichlorosilane **2.66**[6b] (Scheme 2.17).

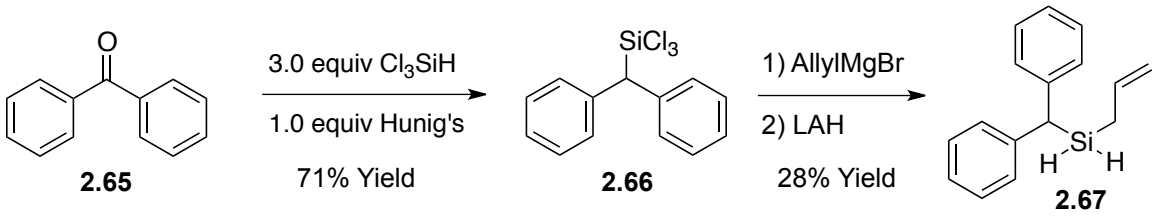

Scheme 2.17: Accessing benzhydryl silane

Nonetheless, with some pure material in hand, we attempted to examine the effectiveness of silane **2.67** in the ASA reaction. Surprisingly, we found that as the reaction progressed, diphenylmethane **2.69** was steadily cleaved from both silanes **2.67** and **2.68** (Scheme 2.18).

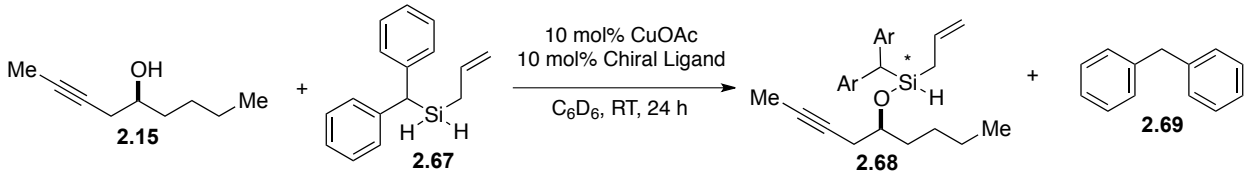

Scheme 2.18: Exploring benzhydryl silane as an alternative ASA structural motif

This result seemingly indicated that the doubly-benzylic, stabilized anion of diphenylmethane becomes a viable leaving group in the presence of nucleophilic copper-hydride. This theory

would also explain the low yield of the allyl Grignard addition / LAH reduction of compound **2.66**. Attempts to synthesize electron rich derivatives of benzhydryl silane **2.67**, in the hope that they would be less susceptible to the benzhydryl cleavage pathway, were unsuccessful.

Undaunted by these repeated failures to find a structural class of silanes that would deliver high diastereoselectivities in the ASA reaction while still being amenable to Tamao oxidation following the tandem silylformylation sequence, we thought that the utilization of a chiral, α-substituted, benzylic silane **2.70** might allow us to achieve our methodological goals (Scheme 2.19).

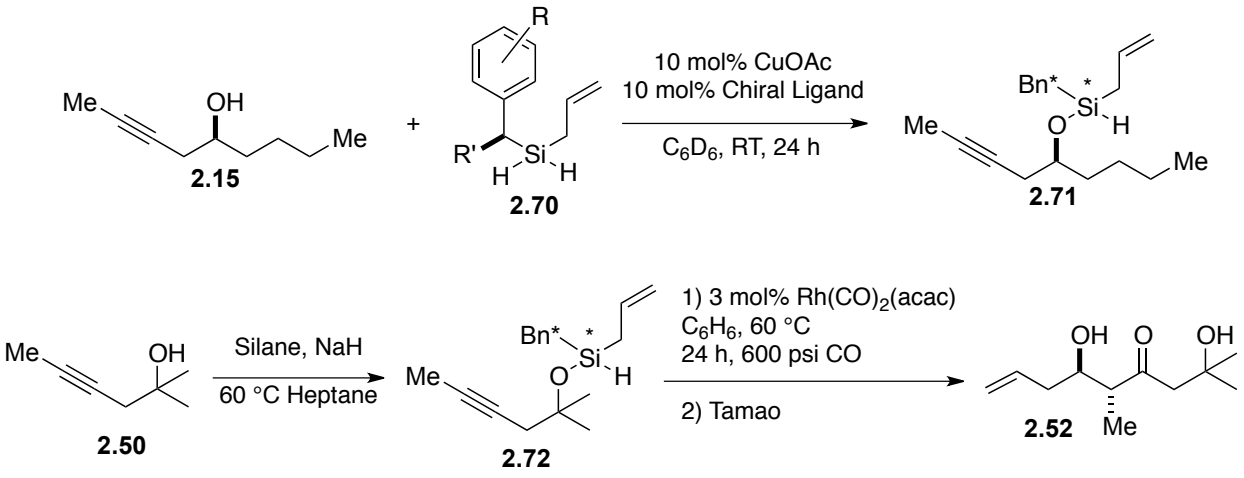

Scheme 2.19: Exploring chiral benzylic silanes as an alternative structural motif

While adding an extra layer of chiral induction to the ASA reaction platform might be seen as undesirable from an academic standpoint, given the practical ease by which the chiral, benzylic trichlorosilanes **2.74** could be accessed from their commercially available styrene precursors **2.73** (Scheme 2.20),[7] we felt it was quite appropriate to explore this structural motif. These sentiments were even more pronounced given our proposed use of the ASA reaction in the

context of a fragment coupling sequence, where the value of the late-stage coupling components would far outweigh that of a chiral silane.

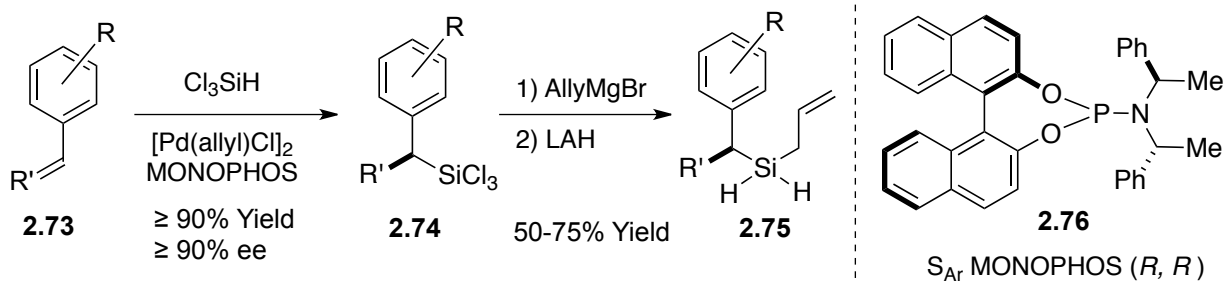

Scheme 2.20: Accessing chiral benzylic-allyl silanes

Employing the reaction sequence shown above, a family of chiral, benzylic-allyl silanes **2.75** were prepared for screening in the ASA reaction with a variety of chiral ligands (Scheme 2.21). (Note: ee's of all chiral, benzylic silanes were determined via Tamao oxidation to the benzylic alcohol followed by Mosher's ester analysis).[8] To our delight, we obtained our first significant increase in the diastereoselectivity of the ASA reaction, observing a diasetereoselectivity of 3.9:1, when chiral, benzylic silane **2.79** was utilized in conjunction with the chrial ligand (*S*)-Tol-BINAP to generate silyl-ether **2.71** (Scheme 2.19).

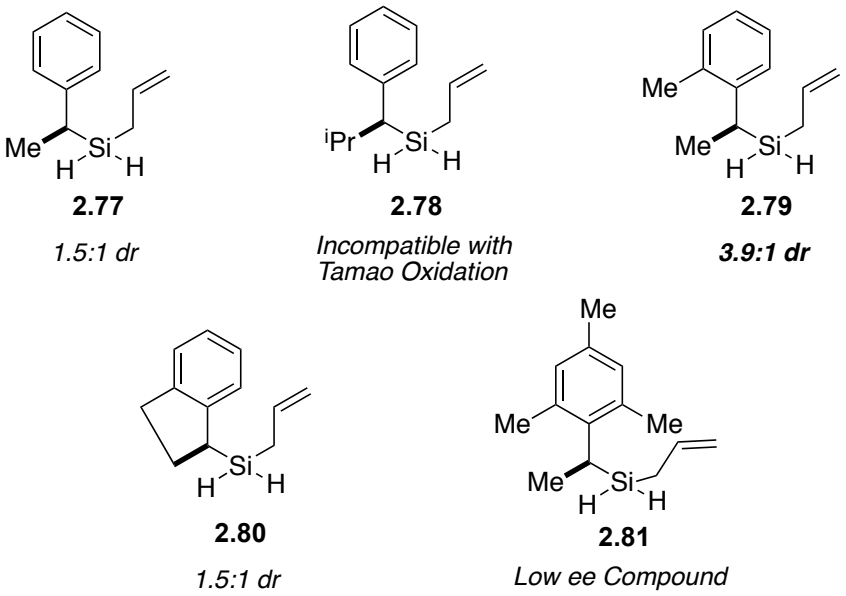

Scheme 2.21: Highest diastereoselectivities obtained using chiral, benzylic silanes

Attempts to modify the ortho-methyl, α-methyl substitution pattern on chiral, benzylic silane **2.79** in the hopes of further improving the silane's performance in the ASA and tandem sequence were met with some difficulty. As shown above, an attempt to utilize the α-isopropyl substituted chiral, benzylic silane **2.78** proved to be too hindered to undergo our requisite Tamao oxidation. Further efforts to tether the α-methyl substituent to the ortho-methyl substituent through use of indene-derived silane **2.80** only served to decrease the substrate's diastereoselectivity in the ASA reaction. Since free rotation seemed critical for high diastereoselectivity, we next attempted to bulk up the chiral, benzylic silane by using a mesityl-type substitution on the aryl ring. Unfortunately, the 2,6-methyl-substitution on the precursor styrene ring proved incompatible with the enantioselective hydosilylation reaction,[7a] generating silane **2.81** in an unacceptable 30% ee.

These difficulties not withstanding, we felt that silane **2.79** generated enough diastereoselectivity to allow for a more in-depth analysis of the ASA reaction manifold.

Considering there were now three stereocenters participating in the ASA reaction (specifically, the alcohol stereocenter, the benzylic silane stereocenter and the chiral ligand on copper), we felt it would be instructive to analyze the relative strength of the chiral matching components by running a series of experiments summarized in Table 2.1. As can be seen in the data table below, the strongest matching effect was observed between the (*S*)-BINAP ligand **(*S*)-2.87** and the (*S*)-chiral, benzylic silane **(*S*)-2.79** (entries 1 and 3 vs. entries 2 and 4). The chirality of the alcohol substrate **2.15**, in contrast, exhibited a much weaker match/mismatch effect on the diastereoselectivity (entries 1 and 2 versus entries 3 and 4). These results were reassuring in the sense that for the real fragment coupling of spongistatin 1 the chirality of the CD spiroketal alcohol **2.7** would be set, while the enantiomer of silane **2.75** and the chiral ligand on copper could be independently matched to give the desired stereochemical product.

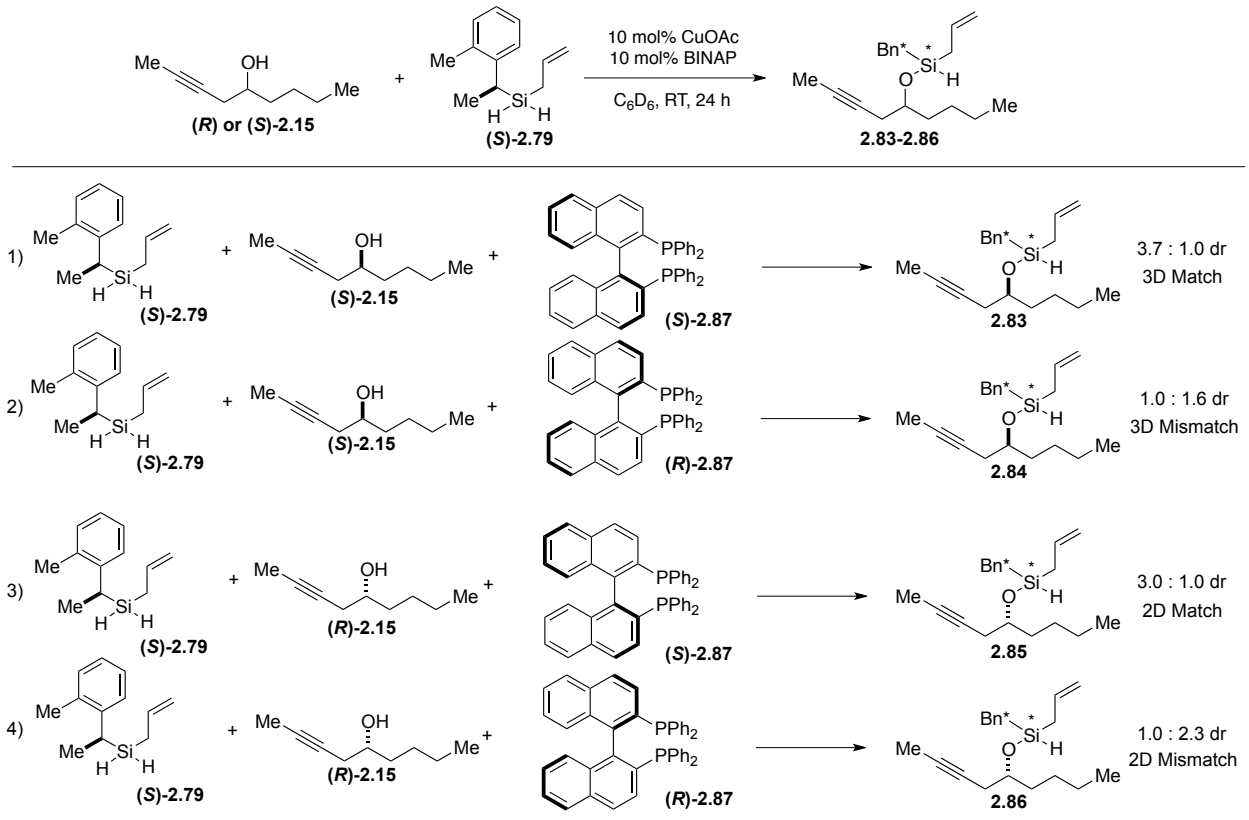

Table 2.1: Match / Mismatch analysis for ASA reaction with three chiral centers

With these exciting ASA diastereoselectivity results for chiral, benzylic, allylsilane **2.79** in hand, we next turned our attention toward the synthesis of tiglic silanes. The tiglic silane motif more accurately represents the AB spiroketal coupling fragment **2.8**, and we were hopeful that the increase in differentiated steric bulk on silicon would lead to even greater diastereoselectivities in the ASA reaction.

2.4 Development of a Robust *Anti*-1,4-Hydrosilylation Reaction

Though the 1,4-hydrosilylation of dienes is well precedented,[9] the most effective strategies employ late transition metal catalyst (such as palladium) and proceed via a *syn*-1,4-hydrosilylation mechanism to give Z-allylsilane products.[10] To our knowledge, only one example of a method for *anti*-1,4-hydrosilylation has been reported.[11] This method, pioneered by the Le Gendre group, utilizes a titanium catalyst to affect the unusual regio- and diastereoselectivity seen in the reaction (Scheme 2.22).

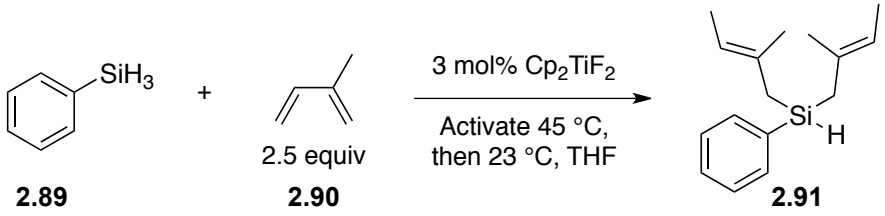

Scheme 2.22: *Anti*-1,4-bis-hydrosilylation reported by the Le Gendre group

The bis-hydrosilylation shown above allows for the use of Cp_2TiF_2 as an inexpensive, bench stable pre-catalyst, which, upon heating in the presence of phenylsilane **2.89**, converts to the active titanium hydride species **2.92** required for the catalytic cycle proposed by the Le Gendre group (Scheme 2.23).

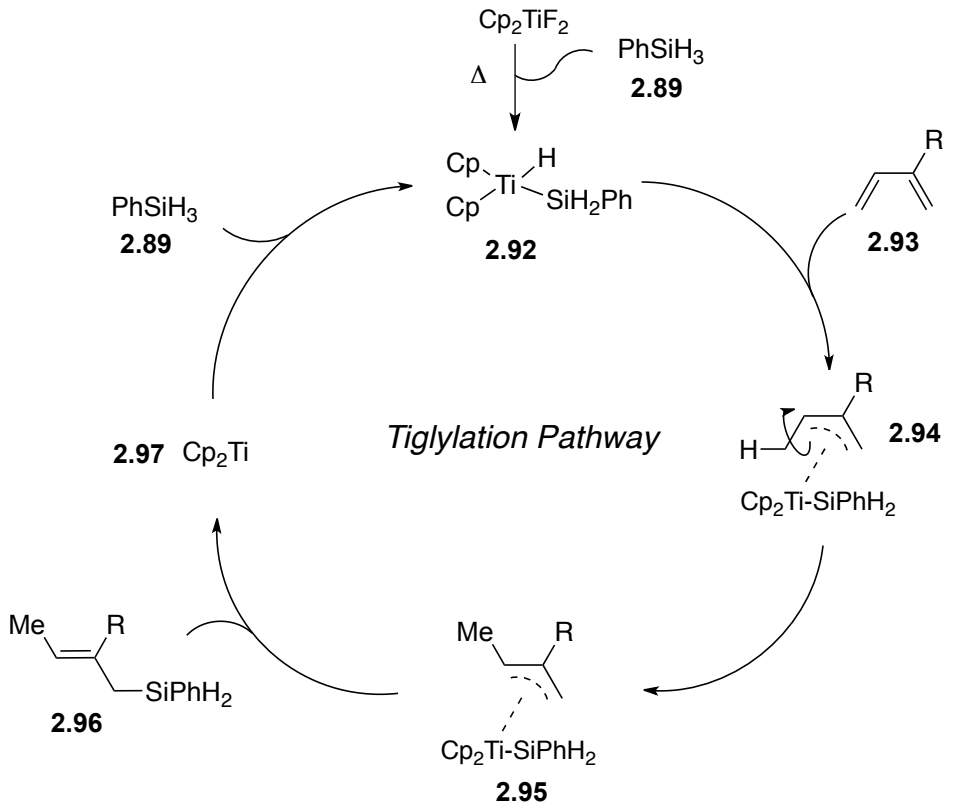

Scheme 2.23: Postulated tiglylation catalytic cycle (Le Gendre)

[Note: the σ-bond rotation of intermediate **2.94** has been added for mechanistic clarity].

While this *anti*-1,4-hydrosilylation reaction looked promising for generating tiglic silanes of type **2.8**, the reaction described by Le Gendre begins to follow an unproductive pathway when only one equivalent of diene **2.93** is used (Scheme 2.24).

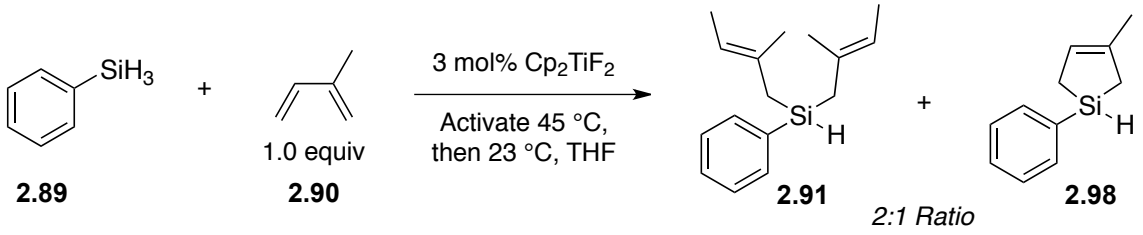

Scheme 2.24: Mixture of products observed while attempting mono-tiglylation

This undesired dehydrogenative, double silylation mechanism was further explored by the Le Gendre group, and their postulated mechanism for the dehydrogenative pathway is shown below (Scheme 2.25).

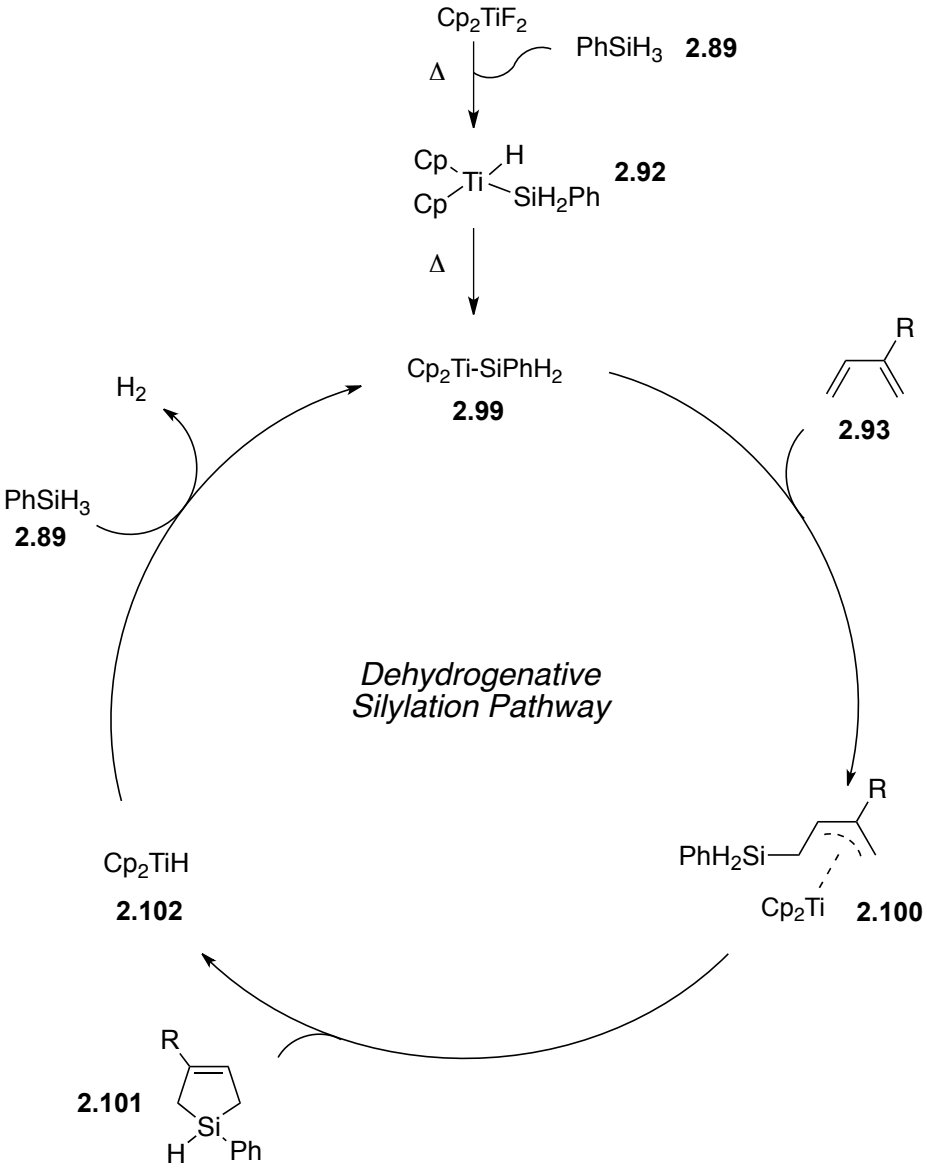

Scheme 2.25: Postulated dehydrogenative silylation catalytic cycle (Le Gendre)

As depicted at the start of the catalytic cycle, the Le Gendre group proposed that continued heating of tiglylation catalyst **2.92** converts it to titanium species **2.99,** presumably by reaction of two equivalents of titanium catalyst **2.92** to release H_2 and binuclear titanium(III) silyl complex $[Cp_2Ti(SiH_2Ph)]_2$ as a secondary pre-catalyst.[12] This new titanium(III) species then undergoes a series of σ-bond metatheses to catalyze the dehydrogenative double silylation reaction that generates silacycle **2.101**. This mechanism was further supported by the Le Gendre group's demonstration that extended heating of Cp_2TiF_2 in THF followed by the later addition of isoprene **2.90** at room temperature led to exclusive silacycle **2.98** formation. In contrast, the large excess of isoprene **2.90** used in Scheme 2.22 likely prevented the conversion of tiglylation catalyst **2.92** to dehydrogenative catalyst **2.99** through a concentration-dependent competitive inhibition of the catalytic breakdown pathway by the diene substrate.

While the dehydrogenative double silylation pathway (Scheme 2.25) is certainly fascinating, if we were to effectively employ the titanium mediated tiglylation reaction (Scheme 2.23) to generate our AB spiroketal fragment coupling partner **2.8**, a method for exclusively accessing the *anti*-1,4-hydrosilylation pathway in the presence of ca. 1.0 equivalent of the precious AB-silane precursor would need to be devised. Fortunately, the Le Gendre group did indicate one successful example of affecting mono-tiglylation (Scheme 2.26).

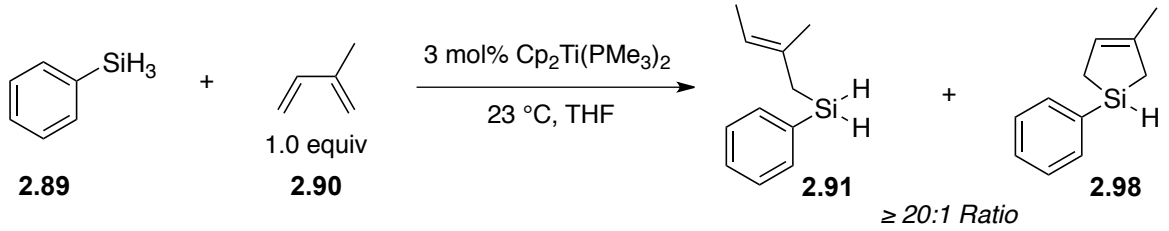

Scheme 2.26: Use of a titanium(II) catalyst to directly affect mono-tiglylation

By using a pre-made titanium(II) catalyst ($Cp_2Ti(PMe_3)_2$) to initiate the desired titanium(II)-titanium(IV) tiglylation cycle at room temperature, the undesired generation of a titanium(III) catalytic species at higher temperatures is completely obviated. Thus, using $Cp_2Ti(PMe_3)_2$ as the reaction catalyst, the *anti*-1,4-hydrosilylation chemistry was successfully extended to the mono-tiglylation of benzylic silanes in the Leighton laboratory.

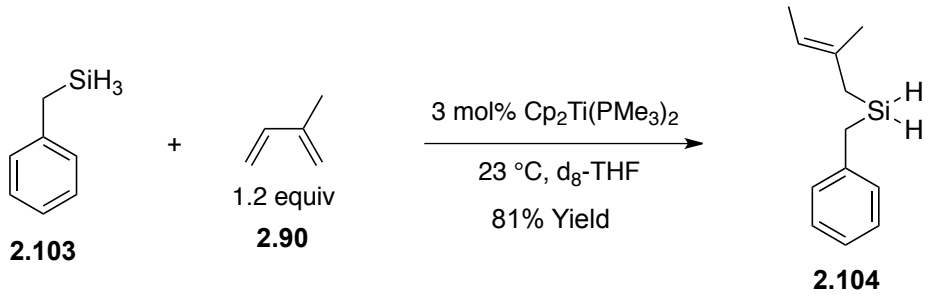

Scheme 2.27: Successful mono-tiglylation of benzylsilane with $Cp_2Ti(PMe_3)_2$

While the extension of this mono-tiglylation reaction to benzylsilane **2.103** gave us hope that the titanium-mediated *anti*-1,4-hydrosilylation could be compatible with the chiral, benzylic silanes necessary for high diastereoselectivities in the ASA reaction (Chapter 2, Section 3), we found the required $Cp_2Ti(PMe_3)_2$ catalyst to be quite unstable and difficult to rely on for reproducible results. Considering our ultimate goal was to use this methodology in the context of a multi-gram fragment coupling between two late-stage intermediates, the need to find a robust method for carrying out this transformation was of the utmost importance. As such, we decided to revisit the use of stable catalyst precursor Cp_2TiF_2 to hopefully affect the mono-tiglylation of benzylic silane **2.103** without forming any undesirable and inseparable silacyle side-product **2.105** (Scheme 2.28).

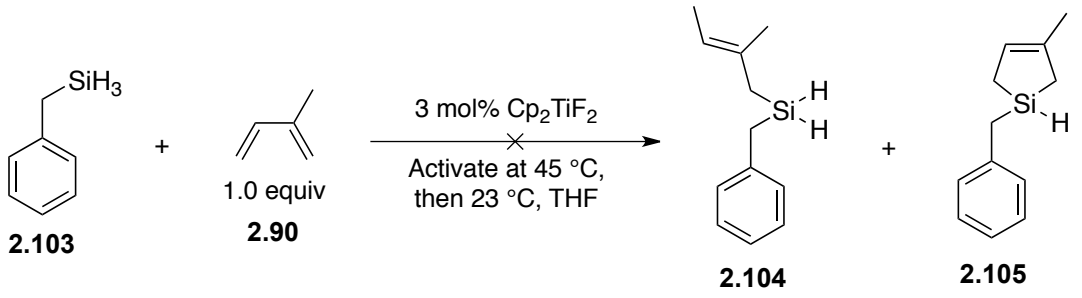

Scheme 2.28: Attempt to mono-tiglylate benzylsilane with Cp_2TiF_2 precatalyst in THF

To our surprise, all attempts to activate Cp_2TiF_2 for the tiglylation of benzylsilane **2.103** in dry THF were unsuccessful. After some screening, it was found that 1,4-dioxane was better suited for promoting the activation of the titanium pre-catalyst. While it was not completely clear why switching to this more Lewis-basic solvent was necessary to successfully alter the reaction substrate from phenylsilane **2.89** to benzylsilane **2.103**, we have tentatively attributed it to a subtle augmentation of the electron density on Cp_2TiF_2 that allows it to undergo initial activation with the presumably less reactive benzylsilane. Unfortunately, even after discovering the efficacy of 1,4-dioxane in promoting the catalyst activation, we still found the ratio of desired mono-tiglylated product **2.104** to undesired silacycle product **2.105** to be 2:1 (Scheme 2.29).

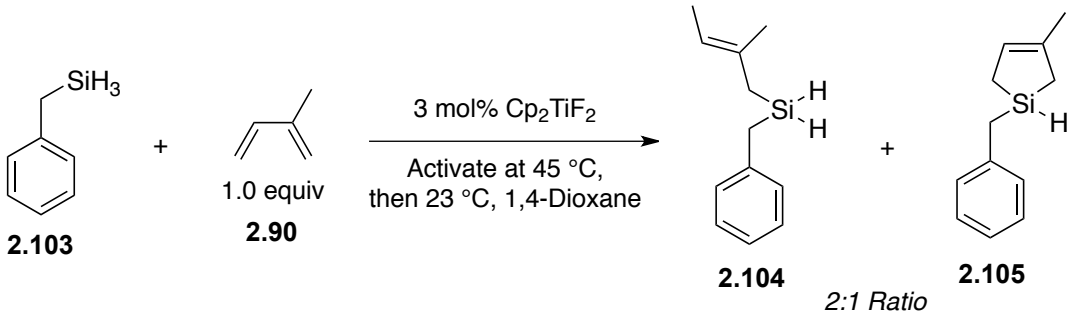

Scheme 2.29: Mono-tiglylation of benzylsilane using Cp_2TiF_2 in 1,4-dioxane

Following this disappointing result, we became increasingly concerned that we would be unable to find a robust reaction platform to efficiently generate tiglic silane **2.8**. In a final attempt to modify the reaction conditions in order to promote the exclusive formation of tiglic silane **2.104** by minimizing the production of silacycle **2.105**, we reanalyzed the pathway in which the undesired dehydrogenative catalyst forms.

As previously discussed, the desired titanium(IV) catalytic species **2.92** converts to the undesired titanium(III) species **2.99** when heated (Scheme 2.25). The degree to which this catalyst breakdown is observed is heavily dependent on the concentration of the substrate diene **2.93**, presumably because it takes two free titanium(IV) species **2.92** reacting with one another to degrade to the unwanted titanium(III) species **2.99** (*vide supra*). We took this to mean that when the titanium(IV) species **2.92** engages diene **2.93** it becomes unavailable for participation in the catalytic breakdown pathway with other titanium(IV) molecules **2.92**. Given our belief that this was the case, we thought that we could perhaps disrupt the catalyst breakdown pathway by adding a Lewis-basic phosphine to the reaction mixture in order to stabilize the free titanium(IV) species **2.92** as it forms under the Cp_2TiF_2 activation conditions.

Given the ability of $Cp_2Ti(PMe_3)_2$ to promote the desired mono-tiglylation, we first thought to use PMe_3 as a source of stabilizing phosphine. However, due to the pyrophoricity of PMe_3, we opted to screen more stable phosphine additives instead. The results of this screen are summarized in Table 2.1.

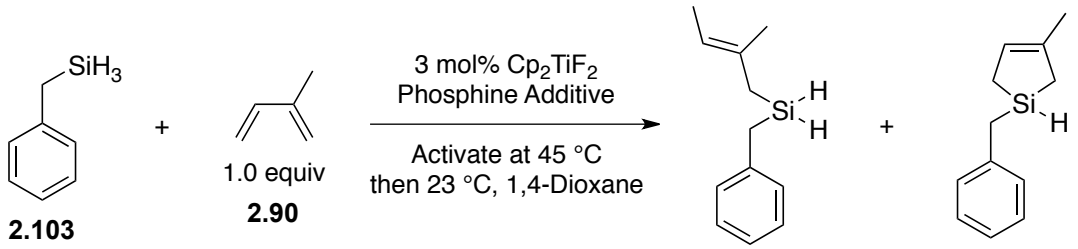

	Phosphine Additive	*Phosphine : Titanium*	*Product : Silacycle*
1)	PEt_3	4 equiv	2:1
2)	PBu_3	4 equiv	3:1
3)	**PCy_3**	**4 equiv**	**20:1 (88% Isolated Yield)**
4)	PCy_3	2 equiv	2:1
5)	PCy_3	10 equiv	9:1

Table 2.2: Phosphine additive screen in 1,4-*anti*-hyrosilylation reaction

To our delight, the addition of certain phosphine ligands had a dramatic impact on the degree to which the undesired dehydrogenative silylation pathway was observed. As seen in Table 2.2, there was a direct relationship between the phosphine cone-angle and stabilization of the desired titanium(IV) species at the start of the catalytic cycle. The addition of PEt_3, which has a small cone angle, did not improve the product to silacycle ratio beyond what was initially observed when the reaction was run in the absence of phosphine (Scheme 2.29). On the other hand, the use of PCy_3, which has a large cone angle, prevented the breakdown of the titanium(IV) species almost entirely, giving a 20:1 ratio of product to silacycle. It was found that utilization of 4 equivalents of phosphine relative to titanium (12 mol%) was the optimal amount needed to promote the desired tiglylation pathway (Entry 3), as the beneficial effect disappeared

when only 2 equivalents were used (Entry 4) and diminished when 10 equivalents were used (Entry 5).

Having optimized the reaction conditions for the mono-tiglylation of benzylsilane **2.103**, we eagerly synthesized chiral, benzylic silane **2.108** (Scheme 2.30), so that we could attempt the *anti*-1,4-hydrosilylation on this key substrate.

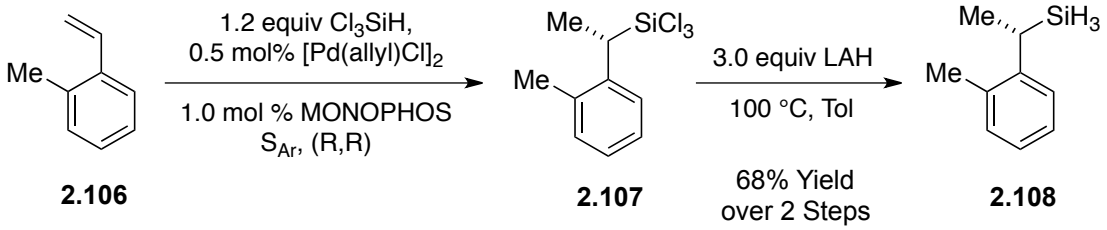

Scheme 2.30: Generation of chiral, benzylic silane 2.108

To further define the dependence of monotiglylation on the phosphine ligand for silane **2.108**, several more phosphine additives were screened, with the results summarized in Table 2.3 below. Somewhat surprisingly, no reaction was observed when the mono-tiglylation was attempted in the absence of a phosphine additive (Entry 1). Though this was an unexpected result, it was plausibly consistent with our previous observation that the titanium pre-catalyst required a more Lewis-basic solvent (*i.e.* 1,4-dioxane) in order to react with deactivated benzylsilane substrates (Scheme 2.29). Given the deactivation of our more hindered α-substituted, benzylic silane **2.108**, it now seemed that an even greater amount of Lewis-base activation was required for the Cp_2TiF_2 pre-catalyst to initiate the tiglylation process. Fortunately, our phosphine additives readily imparted this increased Lewis-base activation, as a variety of electron-rich phosphines with large cone-angles were found to effectively promote the mono-tiglylation reaction (Entries 2-4). After comparing several phosphine additives, PCy_3 remained the optimal ligand, providing the desired product in 78% isolated yield (Entry 3).

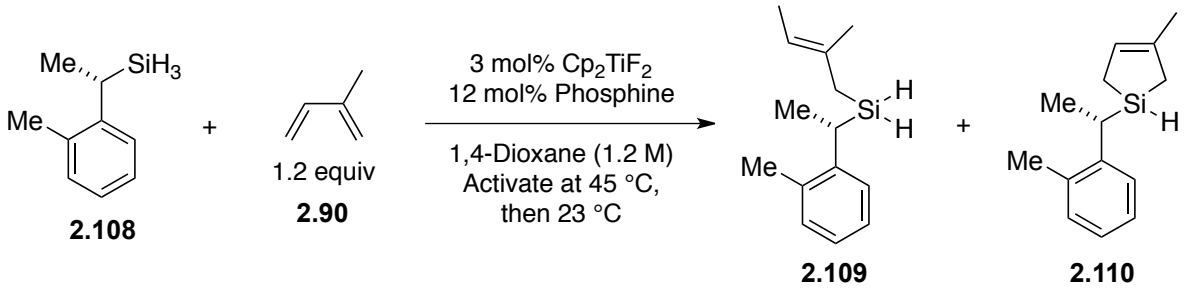

	Phosphine Additive	*Product : Silacycle*
1)	None	S.M.
2)	PPh_3	11:1
3)	**PCy_3**	**20:1 (78% Isolated Yield)**
4)	$P(o\text{-}Tol)_3$	14:1

Table 2.3: Phosphine screen for mono-tiglylation of chiral, benzylic silane 2.108

2.5 Synergistic Effects of Chiral, Benzylic, Tiglyl-Silanes in the ASA Reaction

With the synthesis of chiral, benzylic, tiglyl-silane **2.109** fully optimized, it was time to examine its performance in the ASA reaction. As stated previously, the tiglic silane motif more accurately represents the AB spiroketal coupling fragment **2.8** depicted in Scheme 2.3, and we were hopeful that the increased differentiation in the steric bulk on silicon would lead to even greater diastereoselectivities in the ASA reaction.

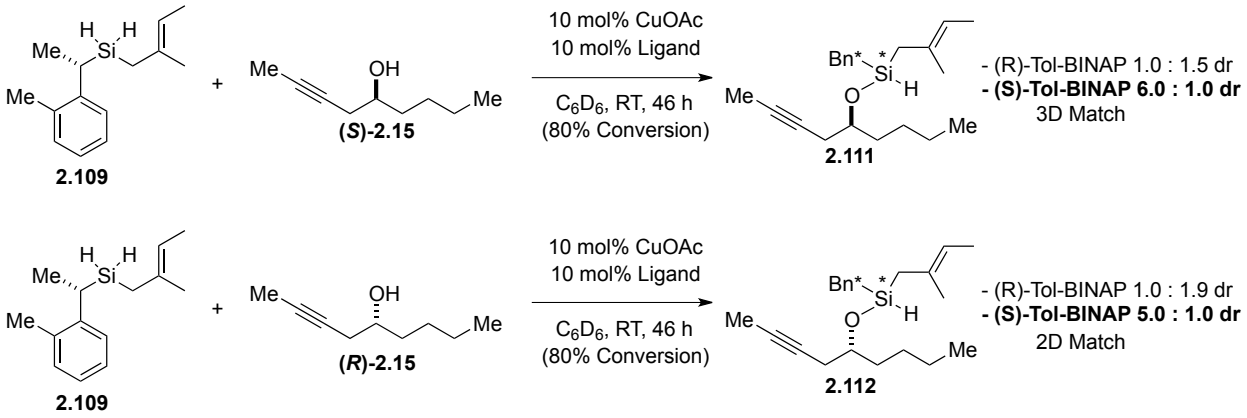

Scheme 2.31: Synergistic match case of chiral, benzylic, tiglyl-silane in ASA

Gratifyingly, tiglic silane **2.109** indeed showed a strong synergistic effect with the chiral phosphine ligand employed in the ASA (Scheme 2.31). Though the reaction was a bit slower (80% conversion after two days at RT), the triply differentiated and doubly differentiated matched cases now gave selectivities as high as 6:1 and 5:1 dr respectively – a substantial improvement over the chiral, benzylic, allyl-silane **2.79** examined in Table 2.1. In the cases where the chiral phosphine and chiral silane were mismatched, selectivities less than 1:2 were observed, with chiral induction of the phosphine ligand found to be slightly dominant over the chiral induction from the silane.

With good diastereoselectivities finally being observed in the ASA reaction, we were emboldened to attempt the synthesis of an even more sterically congested chiral, benzylic silane in the hopes of achieving excellent diastereoselectivity in the ASA. While we had already determined that increasing the steric bulk at the α-position on the chiral, benzylic silanes was incompatible with the Tamao oxidation following the tandem silylformylation sequence (silane **2.78** in Scheme 2.21), we thought there might still be an opportunity to expand the steric bulk at the ortho position on the aryl ring. More specifically, we hoped that by changing the substituent

at the ortho position in silane **2.109** from methyl to isopropyl, we might be able to increase the benzylic silane's interaction with the chiral ligand used in the ASA while minimally disrupting the steric environment at silicon during the Tamao oxidation.

After some experimentation, it was found that the synthesis of the precursor ortho-isopropyl styrene **2.114** could either be achieved through a one-step Stille coupling procedure[13] or a more economical, two-step Suzuki-Molander coupling procedure[14] (Scheme 2.32).

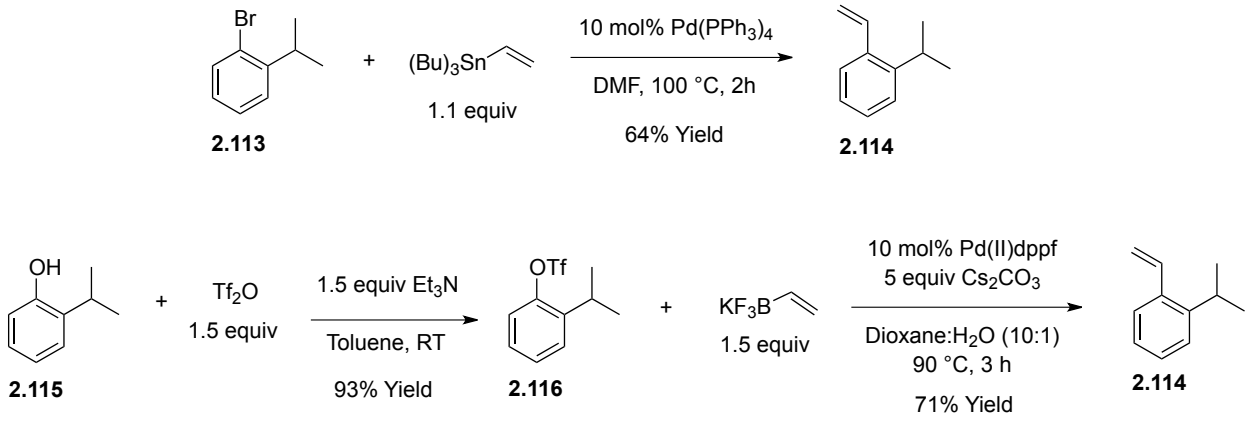

Scheme 2.32: Syntheses of ortho-isopropyl styrene precursor 2.114

With ortho-isopropyl styrene **2.114** in hand, a gram-scale enantioselective hydrosilylation / reduction procedure was performed to give chiral, benzylic silane **2.118** in good yield with minimal catalyst loading (Scheme 2.33).

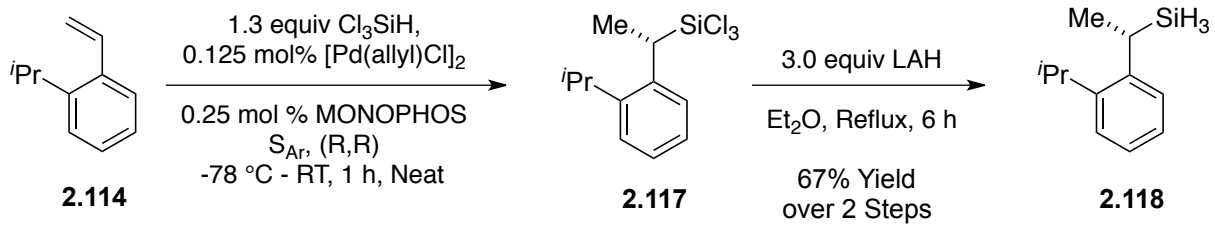

Scheme 2.33: Optimized, gram-scale synthesis of ortho-isopropyl silane 2.118

With significant quantities of ortho-isopropyl, chiral, benzylic silane **2.118** at our disposal, we next carried out our first gram-scale *anti*-1,4-hydrosilylation, which proceeded quite smoothly to generate chiral, benzylic tiglylsilane **2.119** in good yield (Scheme 2.34).

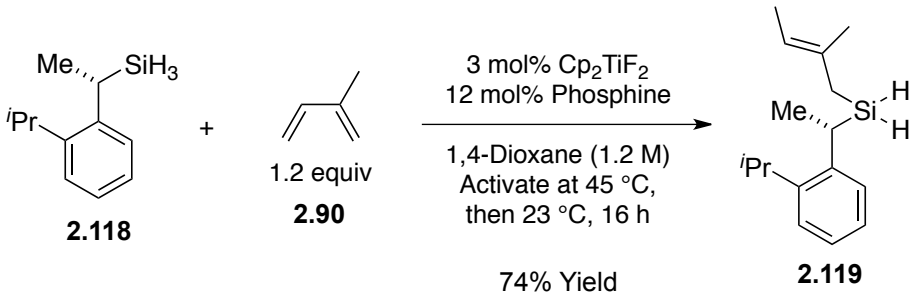

Scheme 2.34: Gram-scale synthesis of ortho-isopropyl tiglylsilane 2.119

Our newly accessed ortho-isopropyl tiglylsilane was next screened with a wide variety of chiral ligands in the ASA reaction, a small sampling is represented in Table 2.4. As was the case for ortho-methyl tiglylsilane **2.109** (Scheme 2.31) the (*S*)-Tol-BINAP triply differentiated matched case proved to be the most diastereoselective chiral ligand in the ASA reaction (Entry 1). Although switching from ortho-methyl tiglylsilane **2.109** to ortho-isopropyl tiglylsilane **2.119** only resulted in a modest boost in diastereoselectivity (6:1 to 7:1), a substantial effect on the overall ASA reaction rate was observed across a variety of ligands. For example, using the ortho-isopropyl tiglylsilane **2.119** and the matched (*S*)-Tol-BINAP ligand, full conversion was reached for the ASA in 24 h (Entry 1), a marked improvement over the 80% conversion reached in 48 h using the ortho-methyl tiglylsilane **2.109** (Scheme 2.31). Even the mismatched (*R*)-Tol-BINAP was found to go to complete conversion after two days (Entry 2). Notably, both the achiral PCy_3 and (*S*)-Xylyl-MeO-BIPHEP ligands rapidly proceeded to full conversion in only 6 h (Entries 4-5), with the (*S*)-Xylyl-MeO-BIPHEP giving a matched diastereoselectivity of nearly 5.7 : 1.0.

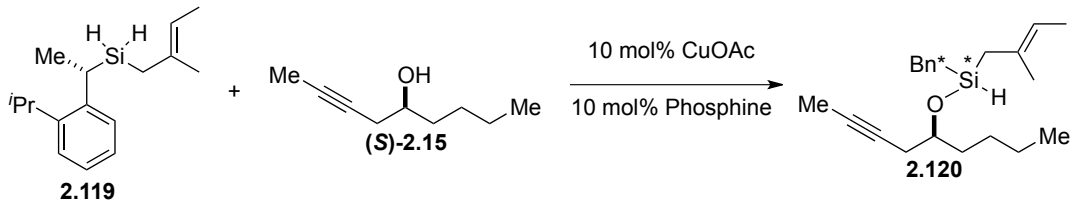

	Solvent	*Temp*	*Time*	*Phosphine*	*dr*
1)	C_6D_6	RT	24 h	(S)-Tol-BINAP	7.0 : 1.0
2)	C_6D_6	RT	48 h	(R)-Tol-BINAP	1.0 :1.3
3)	C_6D_6	RT	24 h	(S)-Tol-MeO-BIPHEP	6.4 : 1.0
4)	C_6D_6	RT	6 h	(S)-Xyl-MeO-BIPHEP	5.7 : 1.0
5)	C_6D_6	RT	6 h	PCy_3	1.0 : 1.4

Table 2.4: ASA Ligand screen with ortho-isopropyl, chiral, benzylic tiglylsilane

Given that (*S*)-Xylyl-MeO-BIPHEP exhibited good diastereoselectivity at a relatively fast rate, we though we might be able to increase the ASA diastereomeric ratio by cooling this reaction down. To our immense satisfaction, we found that this ASA reaction could successfully be run at 0 °C for 24 h in deuterated toluene to give the desired product in 10.7 : 1.0 dr (Scheme 2.35).

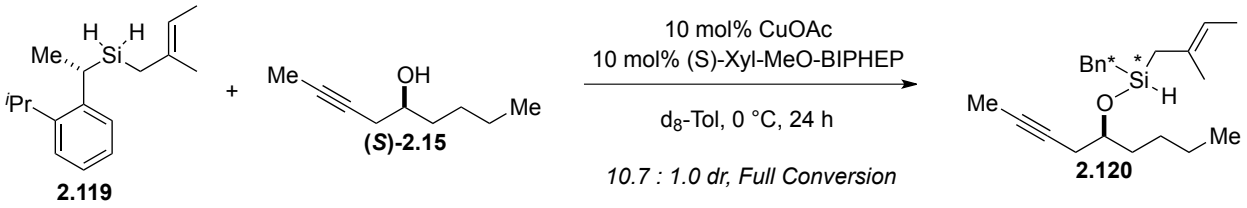

Scheme 2.35: Optimized ASA substrate and conditions resulting in >10:1 dr

This groundbreaking result marked the end of our search for new ASA substrate and ligand combinations as we felt the information obtained from this model study could be readily applied to the real coupling system (Scheme 2.3). The last methodological hurdle that remained was the confirmation that the ortho-isopropyl, chiral, benzylic, tiglic silyl-ether **2.120** was still a competent substrate for our tandem silylformylation / Tamao oxidation protocol.

Up until this point, the absolute stereochemical configuration of the ASA reaction product had yet to be assigned. Though one might imagine a series of derivitizations that would allow us to either grow a crystal or run an extensive array of nOe experiments to assign the silicon stereocenter, we felt that a simpler, indirect method would suffice for the time being. As demonstrated in our group's recent publication,[1] the tandem silylformylation / Tamao oxidation sequence is most diastereoselective when the 1,5-*anti* diol can simultaneously direct protonation of the transient enol species to give a 1,2-*anti* relationship between the adjacent methyl and alcohol stereocenters (Chapter 1, Section 1, Scheme 1.2). Given our newfound ability to direct the tiglic transfer fragment to either alcohol face via the ASA reaction platform, we could potentially generate a 1,5-*syn* diol tandem silylformylation product that would be expected to give lower diastereoselectivity in the Tamao oxidation as the 1,5-*syn* alcohols each direct the proton to opposite faces of the intermediate enol. Thus, if these two tandem silylformylation / Tamao oxidation reactions were set up side-by-side, the reaction that proceeds more smoothly and with higher overall diastereoselectivity could be tentatively assigned as the one generating the desired 1,5-*anti* diol product.

Following this line of reasoning, a series of reactions were carried out to generate the pertinent silyl-ether starting materials (Scheme 2.36). Achiral alcohol **2.50** was first converted to a 1:1 mixture of silyl-ether **2.121** to be used as a control in the tandem silylformylation / Tamao

oxidation sequence. Next, silyl-ethers **2.122** and **2.123** were formed using opposite enantiomers of alcohol **2.15** with unknown, albeit identical, stereochemistry at silicon derived from the ASA matched case reaction utilizing tiglic silane **(*S*)-2.119** and (S)-Tol-BINAP.

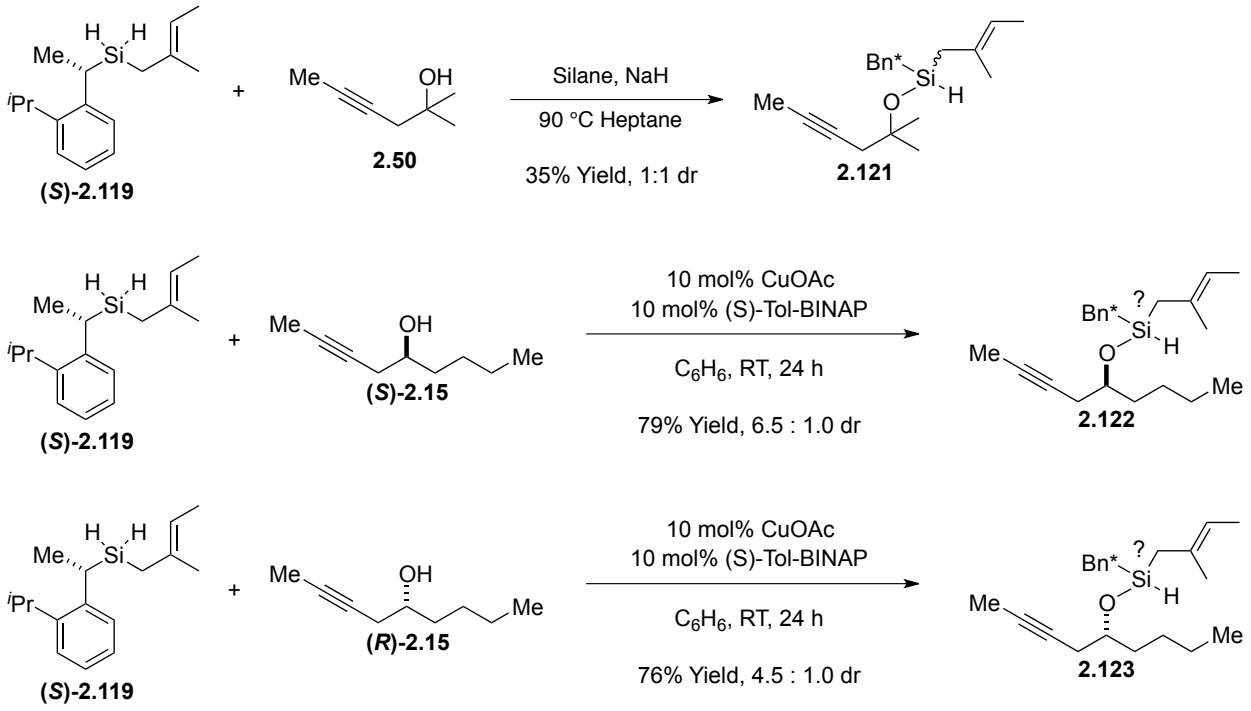

Scheme 2.36: Generation of key silyl-ethers for tandem silylformylation / Tamao

With silyl-ethers **2.121, 2.122** and **2.123** successfully synthesized, the tandem silylformylation / Tamao oxidation sequence was carried out for each substrate. As summarized in Scheme 2.37, the results of these experiments were clear. First and foremost, the viability of the tandem fragment coupling sequence as envisioned in Scheme 2.3 was established as silyl-ether **2.121** cleanly afforded complex polyketide fragment **2.126** in approximately 75% yield and in 6:1 overall dr. Furthermore, the stereochemistry of silyl-ethers **2.122** and **2.123** at silicon was also established as shown in silyl-ethers **2.124** and **2.125** since only silyl-ether **2.125** went on to

give complex polyketide fragment **2.128** in good yield and good overall diastereoselectiviy – thus indicating the formation of the desired, 1,5-*anti* diol product.

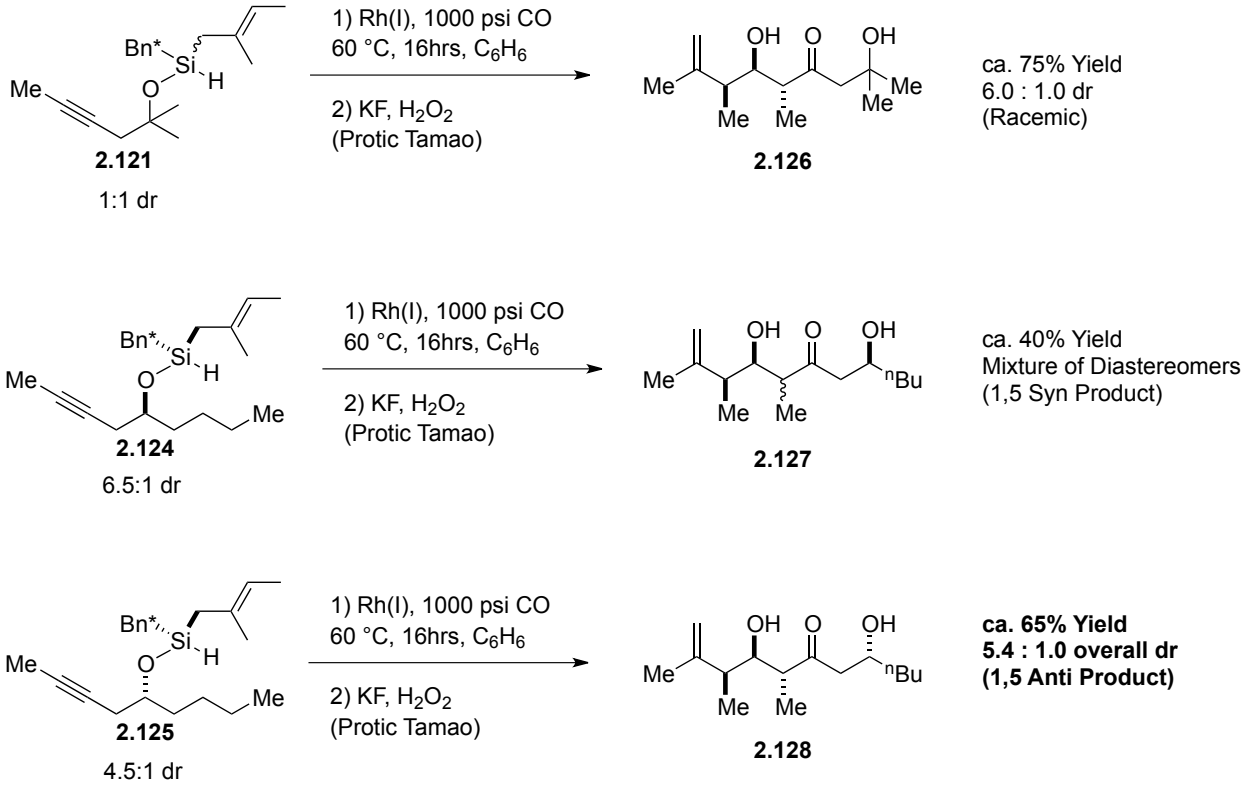

Scheme 2.37: Tandem silylformylation / Tamao sequence establishing chirality at Si

The exciting results depicted in Scheme 2.37 served as a strong proof-of-concept for our overarching goal of efficiently coupling the AB and CD spiroketals of spongistatin 1 via an intramolecular, tandem silylformylation / Tamao oxidation sequence to generate the complex polyketide motif observed in compound **2.128**. With both the ASA reaction and the tandem silylformylation / Tamao oxidation sequence successfully demonstrated on model system **2.125**, it was time to devote our attention to the total synthesis of the AB and CD fragments of spongistatin 1, in order to attempt our fragment coupling strategy on the real system.

2.6 References and Notes

1. Spletstoser, J. T.; Zacuto, M. J.; Leighton, J. L., *Org. Lett.* **2008,** *10* (24), 5593-5596.

2. Schmidt, D. R.; O'Malley, S. J.; Leighton, J. L., *J. Am. Chem. Soc.* **2003,** *125* (5), 1190-1191.

3. Weickgenannt, A.; Mewald, M.; Muesmann, T. W. T.; Oestreich, M., *Angew. Chem. Int. Edit.* **2010,** *49* (12), 2223-2226.

4. Schaus, S. E.; Brandes, B. D.; Larrow, J. F.; Tokunaga, M.; Hansen, K. B.; Gould, A. E.; Furrow, M. E.; Jacobsen, E. N., *J. Am. Chem. Soc.* **2002,** *124* (7), 1307-1315.

5. Jones, G. R.; Landais, Y., *Tetrahedron* **1996,** *52* (22), 7599-7662.

6. (a) Benkeser, R. A.; Gaul, J. M.; Smith, W. E., *J. Am. Chem. Soc.* **1969,** *91* (13), 3666; (b) Benkeser, R. A., *Accounts Chem Res* **1971,** *4* (3), 94.

7. (a) Jensen, J. F.; Svendsen, B. Y.; la Cour, T. V.; Pedersen, H. L.; Johannsen, M., *J. Am. Chem. Soc.* **2002,** *124* (17), 4558-4559; (b) Feringa, B. L.; Pineschi, M.; Arnold, L. A.; Imbos, R.; de Vries, A. H. M., *Angew. Chem. Int. Edit.* **1997,** *36* (23), 2620-2623.

8. (a) Dale, J. A.; Dull, D. L.; Mosher, H. S., *J. Org. Chem.* **1969,** *34* (9), 2543; (b) Dale, J. A.; Mosher, H. S., *J. Am. Chem. Soc.* **1973,** *95* (2), 512-519; (c) Ward, D. E.; Rhee, C. K., *Tetrahedron. Lett.* **1991,** *32* (49), 7165-7166.

9. Sarkar, T. K., *Synthesis-Stuttgart* **1990,** (11), 969-983.

10. (a) Hara, M.; Ohno, K.; Tsuji, J., *J Chem Soc Chem Comm* **1971,** (6), 247; (b) Tsuji, J.; Hara, M.; Ohno, K., *Tetrahedron* **1974,** *30* (14), 2143-2146.

11. Bareille, L.; Becht, S.; Cui, J. L.; Le Gendre, P.; Moise, C., *Organometallics* **2005,** *24* (24), 5802-5806.

12. Aitken, C. T.; Harrod, J. F.; Samuel, E., *J. Am. Chem. Soc.* **1986,** *108* (14), 4059-4066.

13. Stille, J. K., *Angew Chem Int Edit* **1986,** *25* (6), 508-523.

14. Molander, G. A.; Ito, T., *Org. Lett.* **2001,** *3* (3), 393-396.

Chapter 3: Syntheses of AB and CD Fragments and Attempted Coupling

3.1 Synthesis of the CD Fragment and Preliminary ASA Results

As described in Chapter 1 and more specifically depicted in Chapter 2, Scheme 2.3, our main goal in the scalable synthesis of the ABCD hemisphere of spongistatin 1 was to affect the large-scale coupling of the AB and CD spiroketal from simplified coupling partners **3.2** and **3.3** while simultaneously establishing the complex C(13)-C(17) polyketide stereochemical array highlighted in compound **3.1** (Scheme 3.1).

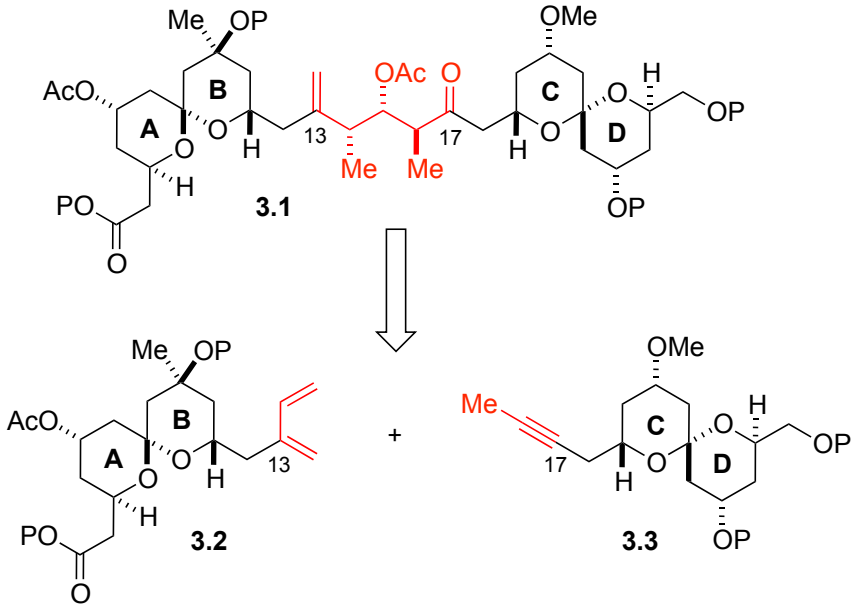

Scheme 3.1: Retrosynthetic analysis for AB and CD spiroketal fragment coupling

In order to utilize the asymmetric silane alcoholysis (ASA) reaction platform developed in Chapter 2, however, the CD fragment would have to be coupled pre-spiroketalization in order to access the requisite alcohol moiety at C(19). Thus, we designed an acyclic CD spiroketal equivalent **3.5** that could be readily transketalized to the desired CD spiroketal following the key ASA / tandem silylformylation / Tamao oxidation coupling sequence (Scheme 3.2).

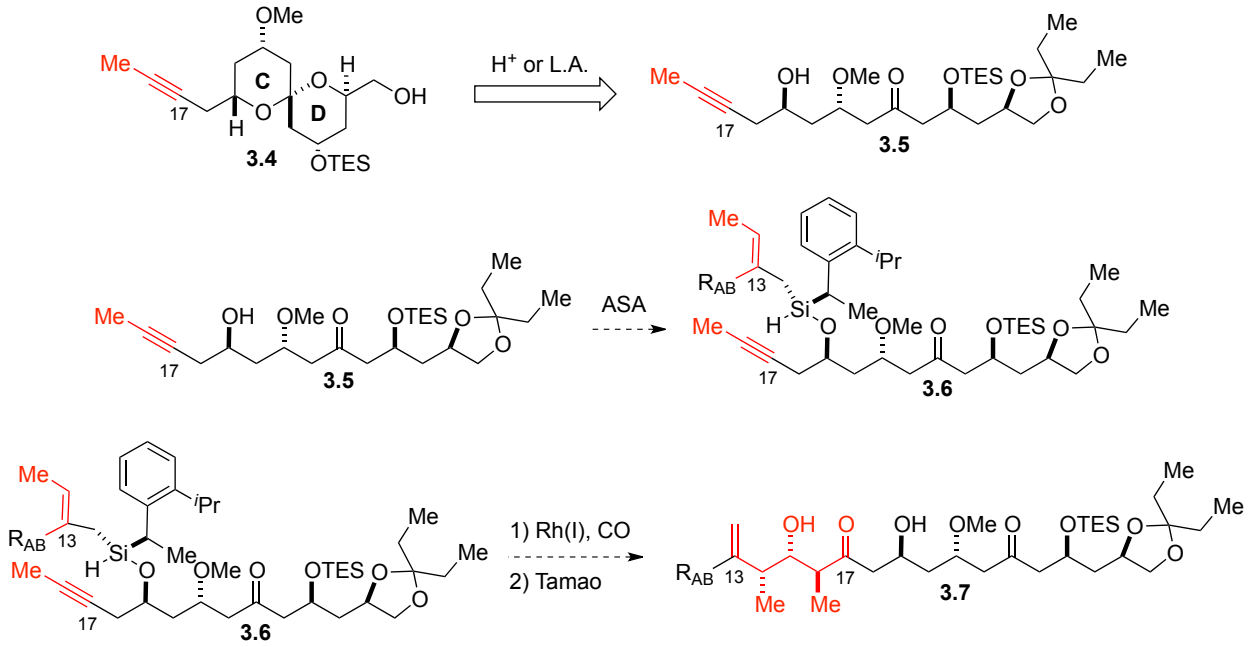

Scheme 3.2: Acyclic CD spiroketal equivalent 3.5 for use in fragment coupling

Since our main goal was to quickly discern whether or not acyclic CD fragment **3.5** could be a competent coupling partner in the ASA / tandem sequence depicted above, our first generation retrosynthesis was fairly straightforward, utilizing aldol technology to bring several subunits together while simultaneously setting multiple fragment stereocenters (Scheme 3.3).

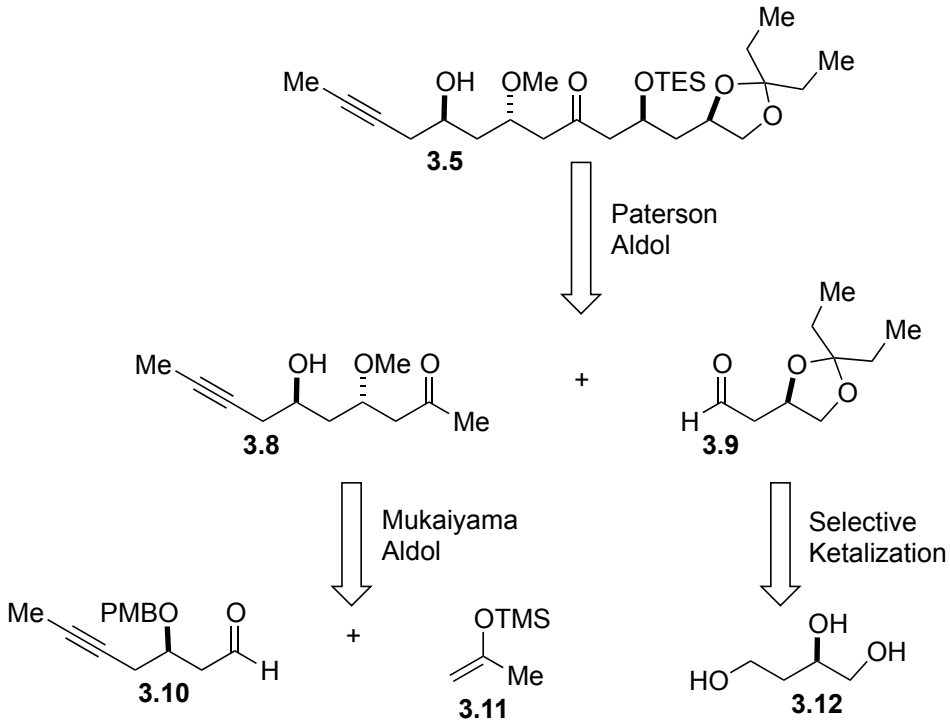

Scheme 3.3: Retrosynthetic strategy for generating acyclic CD fragment 3.5

Though the synthesis of aldehyde **3.9** was already known,[1] we modified the route to improve its operational ease and scalability (Scheme 3.4). The stereocenter present in target aldehyde **3.9** comes from the chiral pool, as this subunit synthesis begins with the reduction of (D)-malic acid **3.13**. Though previous syntheses called for a tedious chromatographic purification of the extremely polar triol **3.12**, we found this to be unnecessary, as protection of the crude material provided ketal **3.15** in good yield over the two-step sequence. It is worth noting that the diethyl-ketal thermodynamically prefers to form the desired 5-membered ring in compound **3.15** as opposed to the alternative 6-membered ring.[2] The requisite 3,3-dimethoxypentane **3.14** for this protection was prepared by pre-ketalization of 3-pentanone in good yield and high purity. Previous syntheses utilized PCC to oxidize alcohol **3.15** to aldehyde

3.9, but we found the Swern oxidation procedure to be equally effective and easier to run on a multi-gram scale.

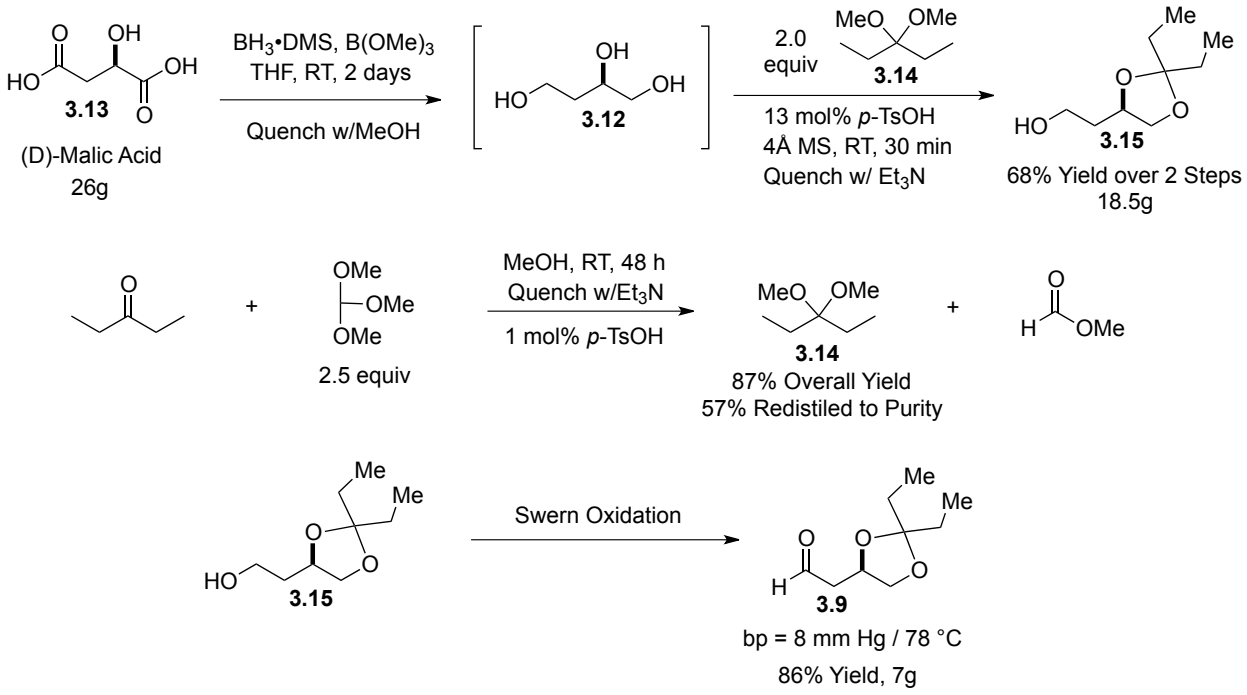

Scheme 3.4: Approach to CD subunit aldehyde 3.9

With ready access to aldehyde **3.9**, we next turned our attention to the synthesis of aldehyde **3.10** and silyl-enol ether **3.11** (Scheme 3.3). Silyl-enol ether **3.11** is commercially available, but could also be prepared in low to moderate yields via an Organic Syntheses prep.[3] The synthesis of aldehyde **3.10** commenced with the hydrolytic kinetic resolution of epichlorohydrin to give (***R*)-3.16** in high ee (Scheme 3.5).[4] The enantioenriched epichlorohydrin was next regioselectively opened with propyne in moderate yield to provide alkynol **3.17** on large scale. The primary chloride on **3.17** was then displaced with NaCN to generate nitrile **3.18** in good yield (Caution: it was critical to avoid an aqueous workup of this reaction to prevent the release of cyanide gas from any unreacted NaCN). After some experimentation, muti-gram access to compound **3.20** was achieved in good yield using an acid-mediated PMB-

trichloroacetimidate **3.19** protection. Though usable, this procedure was not ideal, as it required the tedious removal of the resulting trichloroacetamide reaction byproduct (alternative base-mediated protection conditions using PMB-Cl were found to be ineffective).

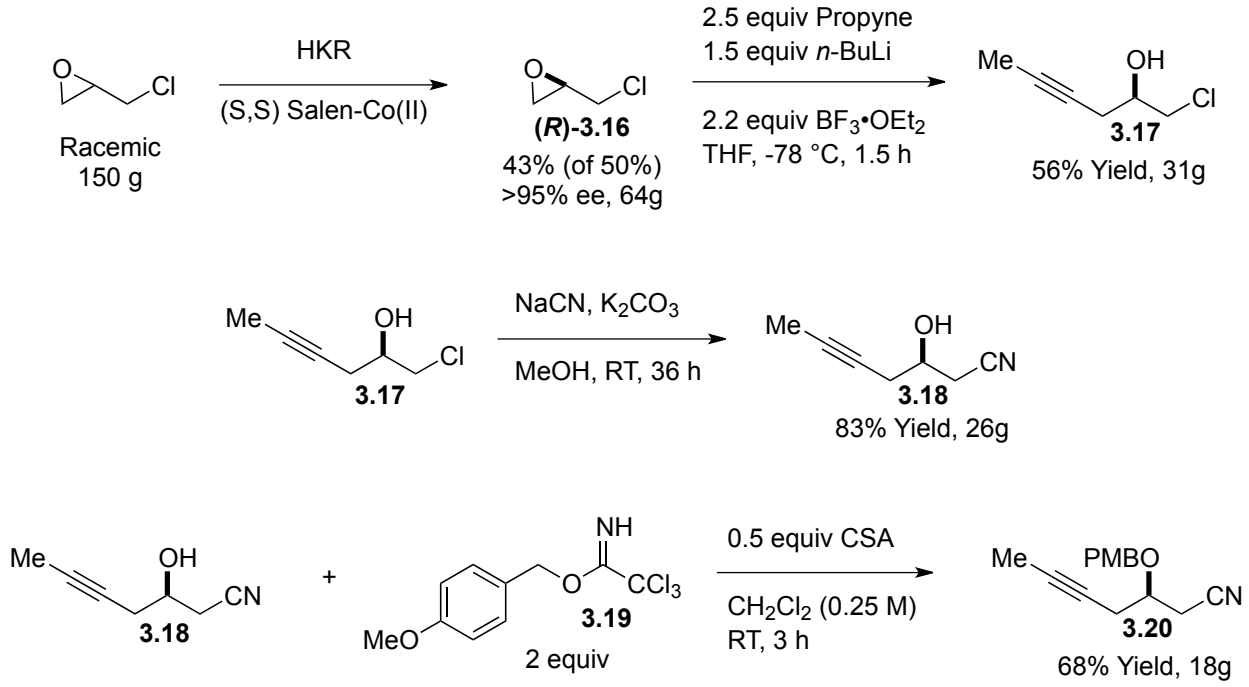

Scheme 3.5: Multi-gram synthesis of nitrile 3.20 in route to aldehyde 3.10

With large amounts of nitrile **3.20** in hand, we attempted to convert it to desired aldehyde **3.10** using a variety of DIBAl-H reduction conditions (Table 3.1). Though this reaction was occasionally successful, we found it to be unacceptably inconsistent in terms of yield, reproducibility and purity of the isolated product. Despite several weeks of attempted optimization we had no choice but to abandon this route to aldehyde **3.10** (and our stockpile of nitrile **3.20**) in search of a more effective strategy.

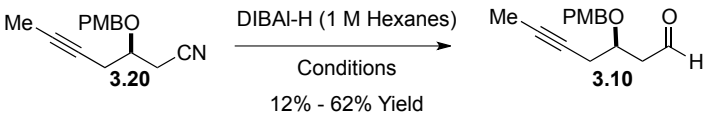

Entry	*Solvent*	*Temp*	*DIBAl-H*	*Time*	*Quench*	Results
1	Et_2O	-78 °C	5.0 eq	1 hr	10% Tartaric Acid	3 Rxn Spots, 20% Yield
2	Hexanes	-78 °C	5.0 eq	1 hr	EtOAc / H_2O	No Rxn (Insoluble S.M.)
3	CH_2Cl_2	-78 °C	5.0 eq	1 hr	0.5 M HCl	Trace Pdt
4	CH_2Cl_2	-78 °C	5.0 eq	1 hr	10% Tartaric Acid	12% Pdt
5	THF	0 °C	2.5 --> 5.0 eq	2 hr	Saturated Tartaric Acid	Clean Rxn, Trace Pdt post work-up
6	THF	0 °C	2.5 --> 5.0 eq	2.5 hr	10 % Tartaric Acid	35% Pdt (Brown Crud...)
7	THF	0 °C	2.5 --> 5.0 eq	5 hr	10 % Tartaric Acid	25% Pdt (Brown Crud) + PMB-OH!
8	THF	0 °C	2.5 --> 5.0 eq	2.5 hr	10% Tartaric Acid Wash w/$NaHCO_3$	45% Pdt (Brown Crud...)
9	**THF**	**0 °C**	**2.5 --> 5.0 eq**	**4 hr**	**10% Tartaric Acid 3x Wash w/$NaHCO_3$**	**62% Pdt but still brown!**

Table 3.1: DIBAl-H reduction conditions

In an effort to design a more robust synthesis of CD subunit **3.10**, we hoped to use an ozonolysis reaction to generate the desired aldehyde from terminal alkene **3.24** (Scheme 3.6). Our new synthesis began again with the hydrolytic kinetic resolution of epichlorohydrin, this time with the opposite catalyst enantiomer, to generate large quantities of compound **(*S*)-3.16**. This epoxide was opened with vinyl Grignard and the resulting crude hydroxyalkene was distilled from KOH to give allyl epoxide **3.22**. Epoxide **3.22** was then opened with propyne to give alkynol **3.23** in good yield. This alcohol was far more amenable to PMB protection as standard NaH/PMB-Br conditions provided multi-gram quantitates of desired alkene **3.24** in excellent yield.

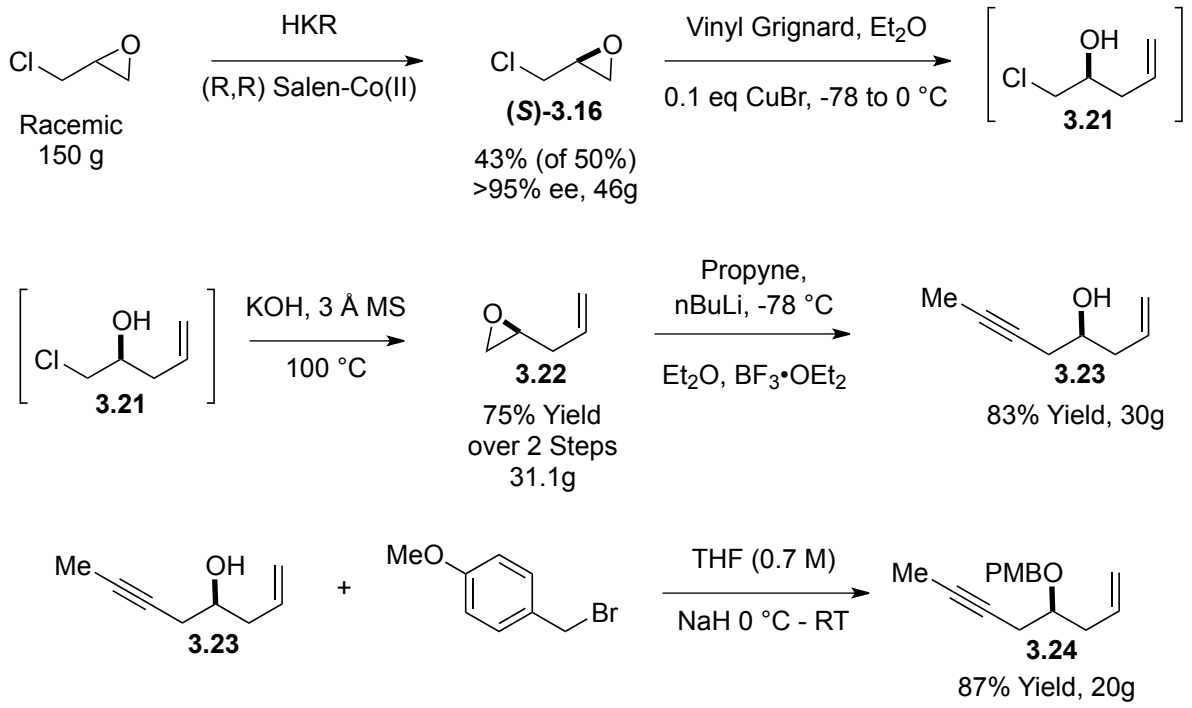

Scheme 3.6: Multi-gram synthesis of alkene 3.24 in route to aldehyde 3.10

Gratifyingly, alkene **3.24** was readily converted to aldehyde **3.10** via ozonolysis using trace sudan(III) dye to carefully monitor consumption of the alkene,[5] since overreaction led to some degradation of the alkyne. With clean aldehyde **3.10** finally in hand, we were able to probe its selectivity in the BF_3•OEt_2 mediated Mukaiyama aldol reaction with silyl-enol ether **3.11**. As predicted by Evans,[6] the β-OPMB substituted aldehyde effectively controlled the open transition-state addition of the silyl-enol ether to give the 1,3-*anti* addition product **3.25** in 5:1 dr. Next, alcohol **3.25** was methylated using Meerwein salt (Me_3OBF_4) and Proton Sponge to circumvent the standard NaH/MeI conditions, which caused alcohol **3.25** to eliminate to its corresponding enone. Though a large excess of methylating reagent was required for full conversion (ca. 5 equiv), CD fragment subunit **3.8** could be obtained in good yield following a critical 1.0 M acetic acid extraction to remove the excess Proton Sponge (Scheme 3.7).

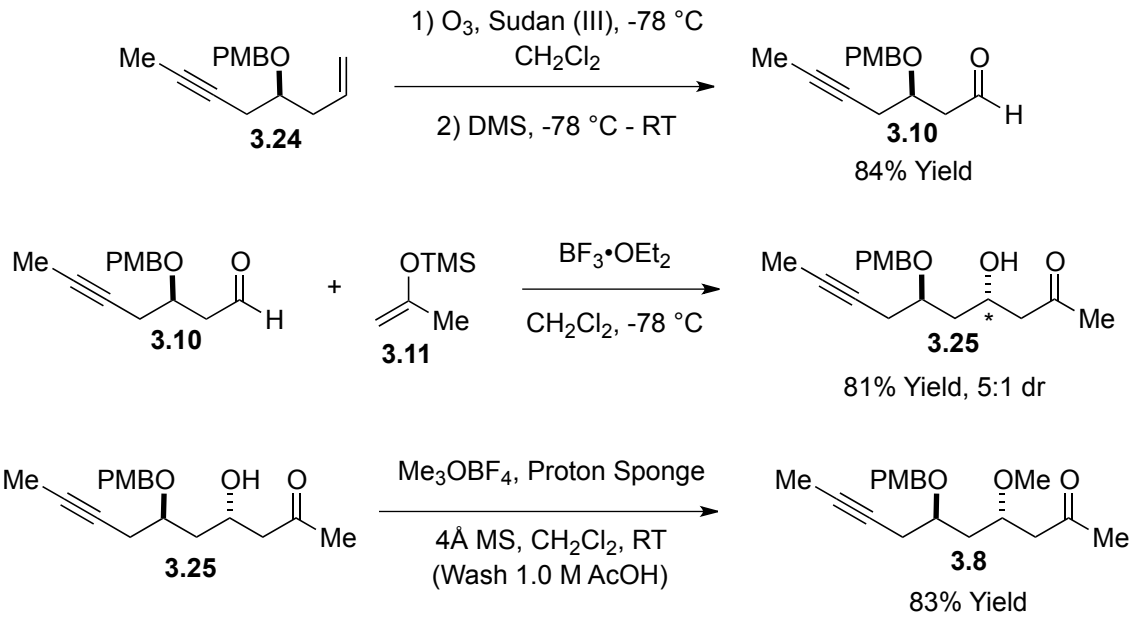

Scheme 3.7: Generation of CD fragment subunit 3.8 via Mukaiyma aldol

Given that the methylation step to generate compound **3.8** was less than ideal, requiring a large excess of reagents, we paused to consider an alternative strategy for generating methyl-ether **3.8** (Scheme 3.8). By simply modifying the ozonolysis conditions used to react alkene **3.24**, we were able to generate dimethyl acetal **3.26** in good yield. With this acetal in hand, we attempted to generate methyl-oxocarbenium species **3.27** in situ and directly add silyl-enol ether **3.11** to this reactive species in an effort to selectively generate compound **3.8** in one step. Unfortunately, all attempts toward this goal were met with little success. Despite screening a variety of Lewis acids (BF_3, TMSOTf, TiCl, $Ti(O^iPr)_4$) the reaction yield was quite low and showed little diastereoselectivity, with a slight preference for the undersired methyl-ether diastereomer. In light of these disappointing results, we returned to the reasonably effective strategy depicted in Scheme 3.7 and continued onward with the CD fragment synthesis.

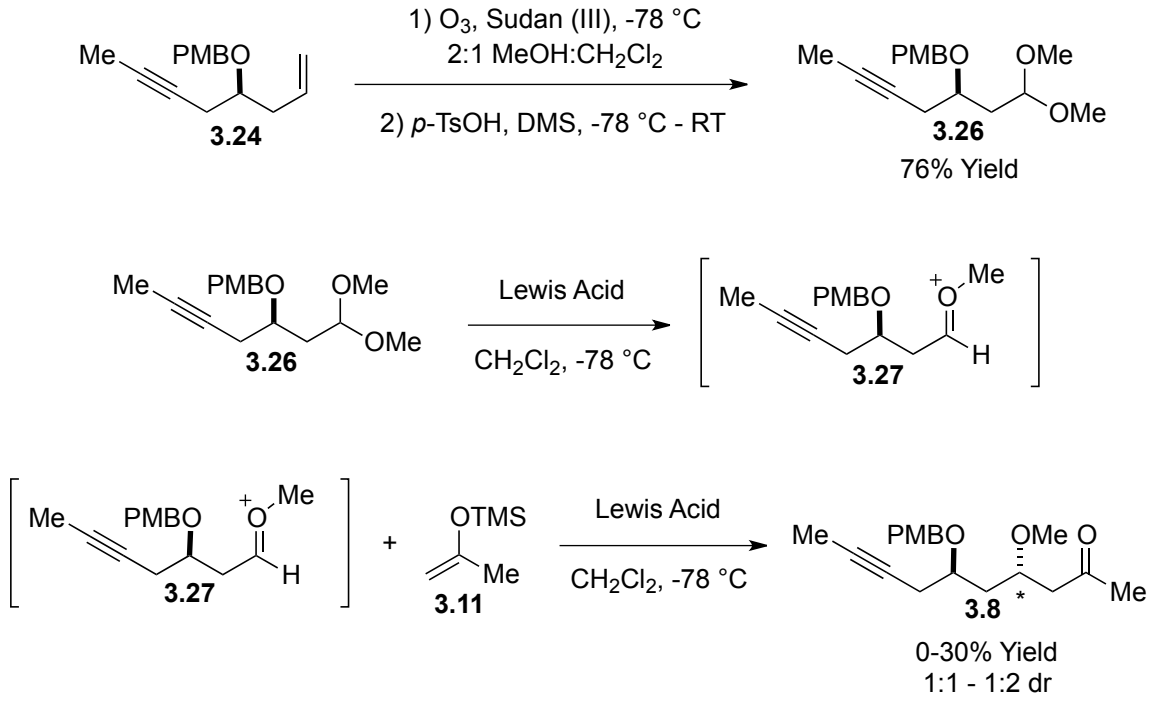

Scheme 3.8: Attempt to generate methyl-ether 3.8 from oxocarbenium 3.27

With both ketone **3.8** and aldehyde **3.9** in hand, we set out to join them stereoselectively through a Paterson aldol reaction. To our great satisfaction, this reaction not only proved to be highly efficient in terms of yield, but also provided the desired alcohol **3.28** in 10:1 dr – an impressive display of chiral reagent control using (-)-DIP-Chloride. Furthermore, the minor diastereomer at the methyl-ether center, resulting from the earlier Mukaiyama aldol reaction, could be chromatographically separated from the desired product at this point. Alcohol **2.28** was readily TES protected to give compound **2.29**, but the final reaction required to generate ASA precursor alcohol **3.5** failed, as PMB deprotection only afforded undesired lactol **3.30** upon purification (Scheme 3.9).

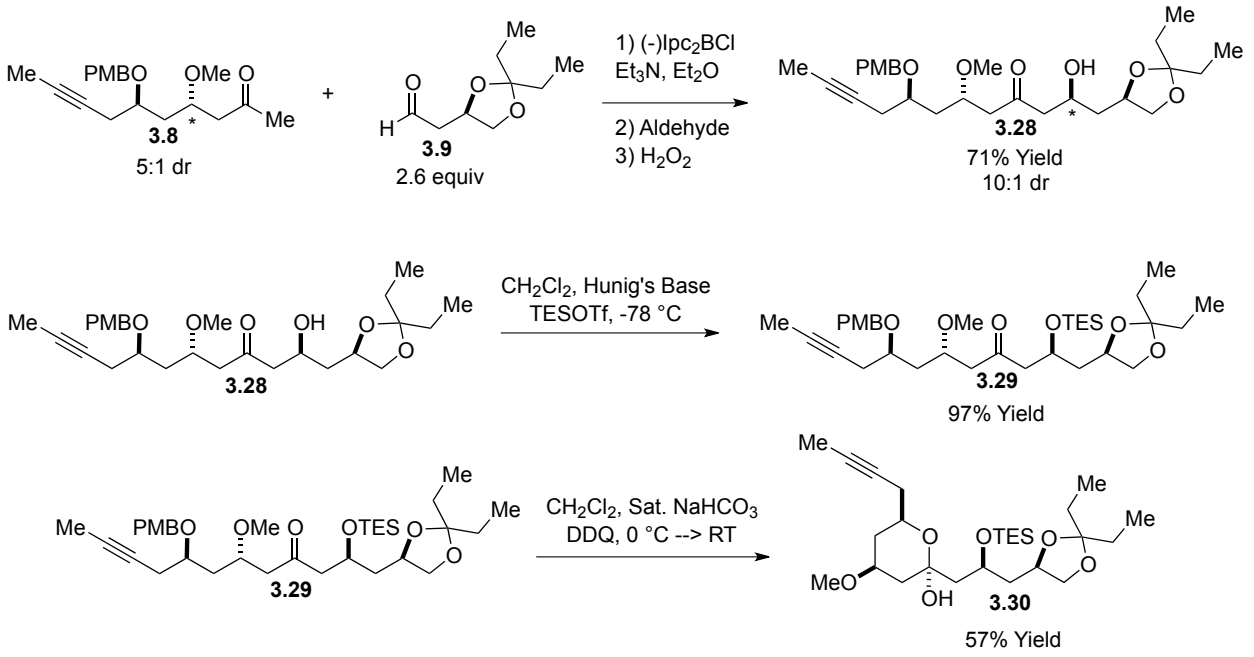

Scheme 3.9: Paterson aldol and attempted completion of acyclic CD fragment

Considering the propensity of δ-substituted keto-alcohols to cyclize to their corresponding lactols, we sought an alternative approach to reveal the requisite alcohol for the ASA reaction while masking the ketone in another form. The strategy we hoped to employ involved packaging the ketone as bicyclic-ketal **3.31**, which we were able to successfully generate through a modified $In(OTf)_3$ catalyzed transketalization procedure.[7] The resulting bicyclic alcohol **3.31** was readily protected with TBSOTf, incidentally providing a solid, crystalline intermediate (not shown), and the requisite free-alcohol **3.32** was revealed through a DDQ-mediated PMB deprotection (Scheme 3.10). (Note: It is critical to use free alcohol **3.32** shortly after its synthesis, as it slowly spiroketalizes over time).

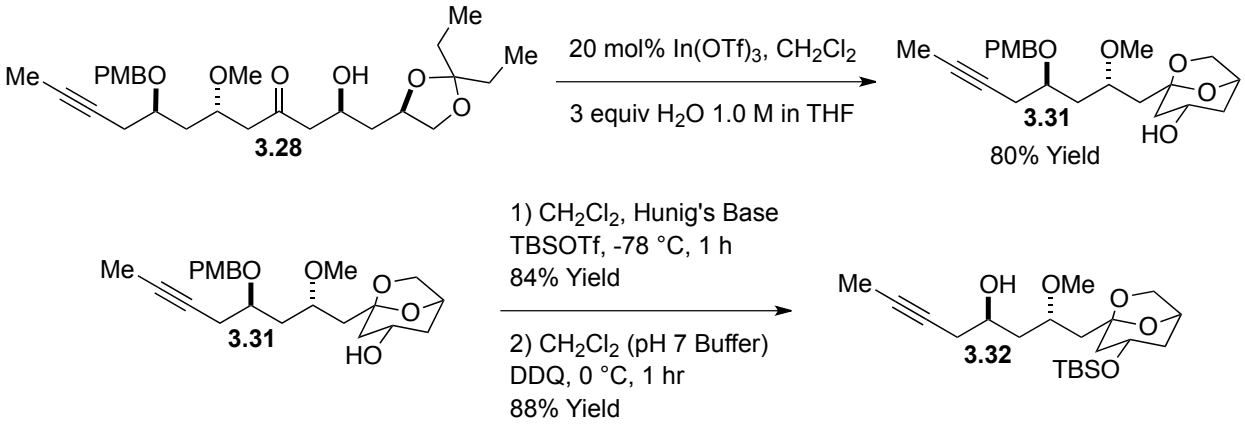

Scheme 3.10: Synthesis of revised CD fragment - bicyclic alcohol 3.32

With our route to the revised CD fragment **3.32** complete, we eagerly tested this functionalized, homopropargylic alcohol in preliminary ASA reactions (Chapter 2, Section 5) with ortho-isopropyl, chiral, benzylic tigylsilane **(R)-3.33** (Scheme 3.11).

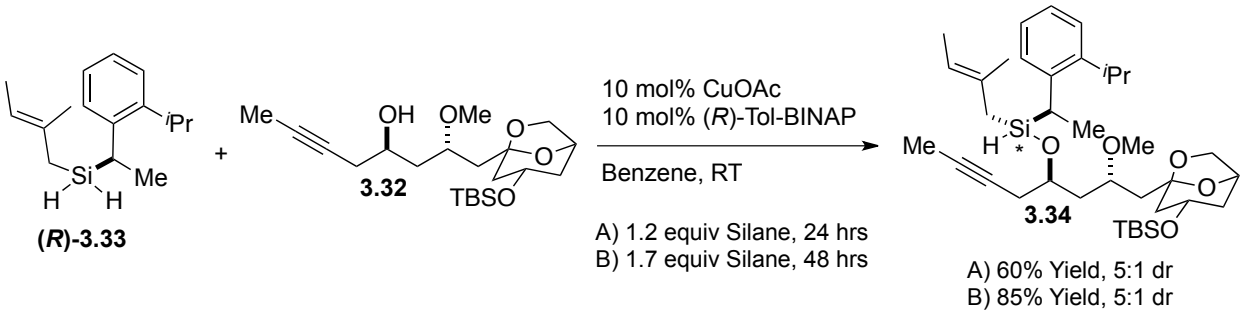

Scheme 3.11: Preliminary ASA reactions with CD fragment bicyclic alcohol 3.32

Though far from optimized, the preliminary results above served as a clear proof-of-concept that the ASA reaction conditions were indeed compatible with our revised CD fragment **3.32**. Upon isolation of silyl-ether **3.34**, the ASA adduct was immediately subjected to our standard silylformylation / Tamao oxidation conditions (Scheme 3.12).

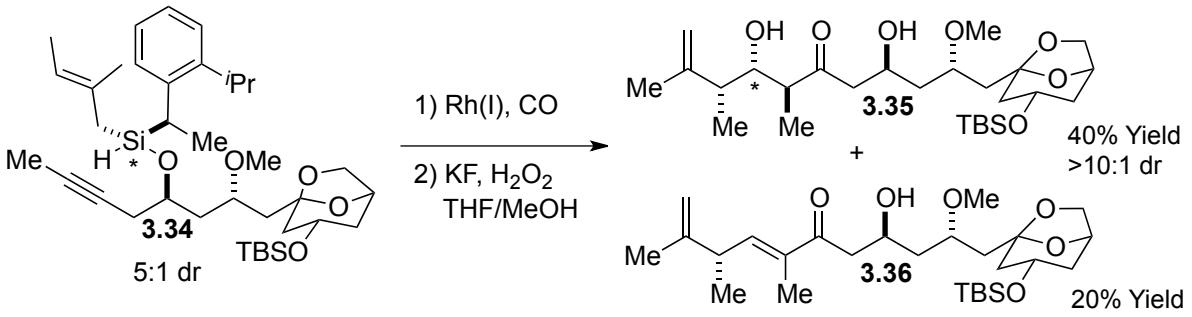

Scheme 3.12: Preliminary tandem silylformylation / Tamao oxidation sequence

Following isolation of the major reaction products, we were delighted to find that the tandem silylformylation / Tamao oxidation sequence worked reasonably well, providing tandem sequence products **3.35** and **3.36** in about 60% combined yield. Complex polyketide fragment **3.35** was our desired tandem sequence product, so we were quite pleased to isolate it in 40% yield and >10:1 dr. It was at first puzzling that compound **3.35** could be isolated in such high diastereopurity given that the starting material silyl-ether **3.34** was only a 5:1 dr mixture. However, considering the bias of the tandem silylformylation sequence to provide 1,5-*anti* diol products[8] in addition to the increased steric bulk provided by the substituted bicyclic ketal in silyl-ether **3.34**, one might assume that the minor diastereomer was unable to undergo the tiglylation event following silylformylation; thus, allowing for its ready removal from the desired reaction products during purification. Generation of complex polyketide enone **3.36** could only have resulted from elimination of the desired keto-diol **3.35** (presumably during the Tamao oxidation), so its isolation still served to demonstrate that the majority of silyl-ether **3.34** diastereomer successfully underwent the tandem silylformylation sequence.

The exciting results depicted in Scheme 3.11 and Scheme 3.12 firmly convinced us that the ASA / tandem silylformylation / Tamao oxidation sequence could indeed serve as the key fragment coupling strategy we first envisioned in Chapter 1. Though the yields and selectivities

of the preliminary key reactions shown above were only moderate, we felt that a full optimization of all the reaction conditions would best be reserved for the "real" coupling between the fully elaborated AB spiroketal and CD fragment. As such, we next shifted our focus to the synthesis of the AB spiroketal for participation in our complete fragment coupling procedure.

3.2 Synthesis of the AB Fragment and Attempted *Anti*-1,4-Hydrosilylation

When considering the synthesis of the AB fragment of spongistatin 1, we attempted to design a convergent synthesis that would allow for rapid access to desired diene **3.37**. Our first generation retrosynthesis is shown below (Scheme 3.13). This initial retrosynthetic strategy also relies on an aldol coupling for joining key subunits **3.39** and **3.40** and employs an enyne methathesis to generate diene **3.40** from alkyne **3.41**. The tertiary carbinol in subunit **3.41** would hopefully be set utilizing a novel, silane-mediated methallylation reaction that will be described in detail below.

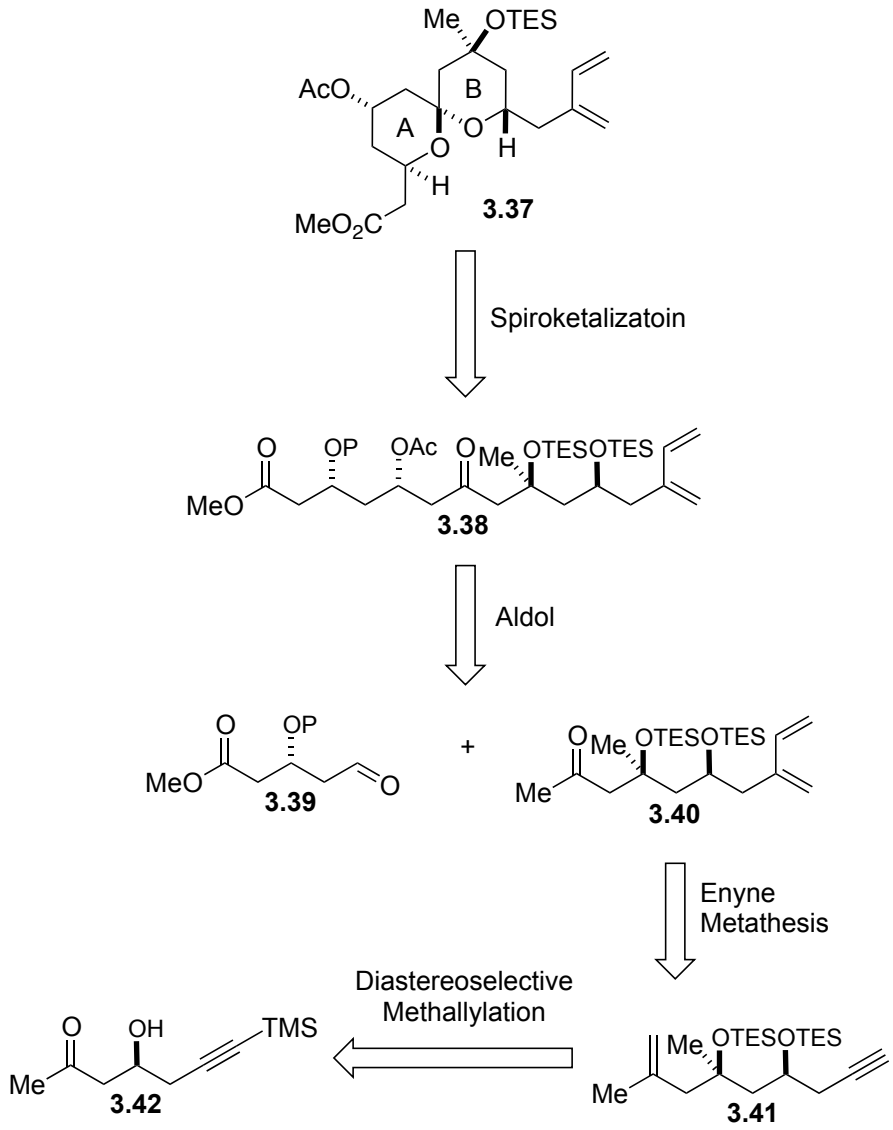

Scheme 3.13: First generation retrosynthesis of AB spiroketal diene 3.37

Our initial efforts directed toward the synthesis of subunit **3.42** attempted to parlay the scalable chemistry demonstrated in the beginning of Scheme 3.6 to our new synthetic target (Scheme 3.14). Thus, we attempt to convert allyl epoxide **(*S*)-3.22** to desired subunit **3.42** via a BF_3•OEt_2 mediated TMS-acetylene opening followed by a Wacker oxidation. Though the epoxide opening provided alkynol **3.43** in high yields, all attempts to affect a Wacker oxidation

on this substrate afforded none of the desired product, seemingly due to functional group incompatibility with the electron-rich, internal alkyne.

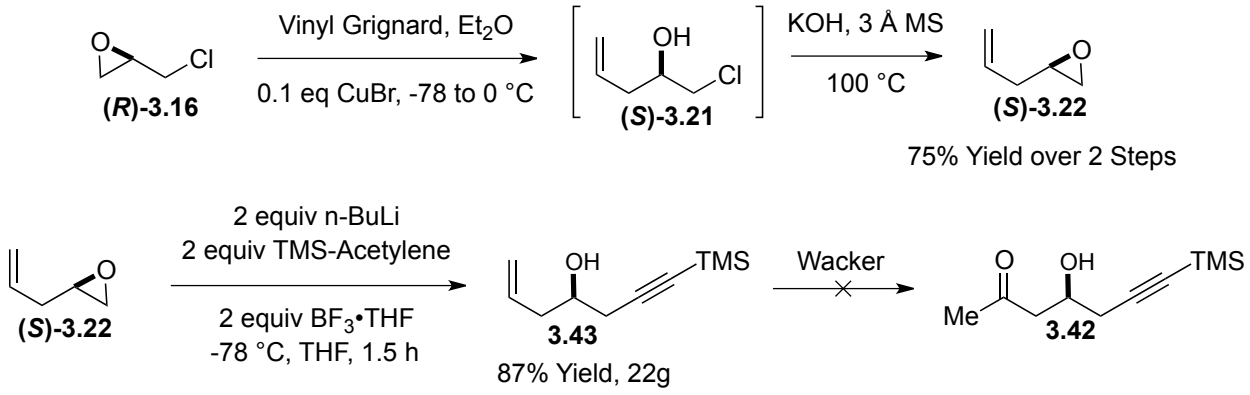

Scheme 3.14: First efforts toward the synthesis of AB fragment subunit 3.42

In light of the failed Wacker oxidation shown in Scheme 3.14, we devised an alternative approach to AB fragment subunit **3.42** (Scheme 3.15). In this new strategy, we again employed the epoxide opening/closing/opening sequence successfully utilized above, only this time adding an isopropenyl group to epichlorohydrin **(*R*)-3.16**, instead of an allyl group, to provide alkynol **3.46** in large quantities. 1,1-disubstituted alkene **3.46** was then subjected to several ozonolysis conditions, but side-reactions with the electron rich TMS-alkyne again prevented the isolation of desired product **3.42**. Despite this setback, we eventually found compound **3.46** to be amenable to the operationally simple, one-pot oxidative cleavage conditions reported by Nicolaou,[9] providing desired AB fragment subunit **3.42** in excellent yields.

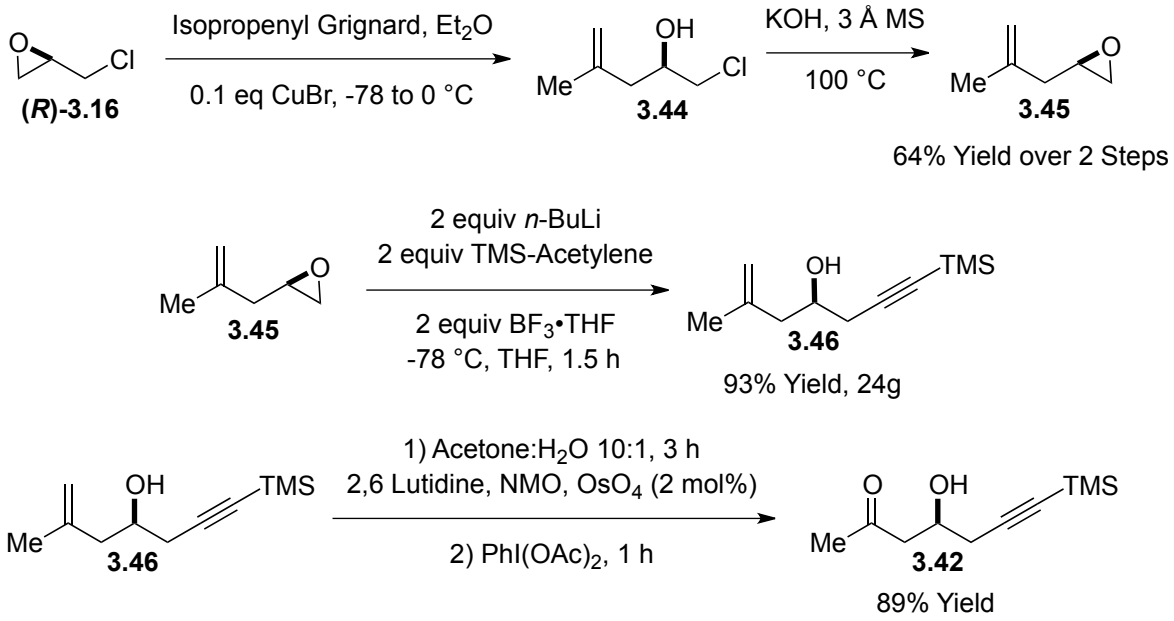

Scheme 3.15: Successful synthesis of AB fragment subunit 3.42 via oxidative cleavage

With a route to AB fragment subunit **3.42** firmly established, we next turned our attention to the proposed diasteresoselective methallylation of this β-hydroxy ketone. Based on literature precedent from our research group, it was known that strained silanes could affect a tandem aldol-allylation sequence on aldehydes to produce tertiary carbinols (Scheme 3.16).[10]

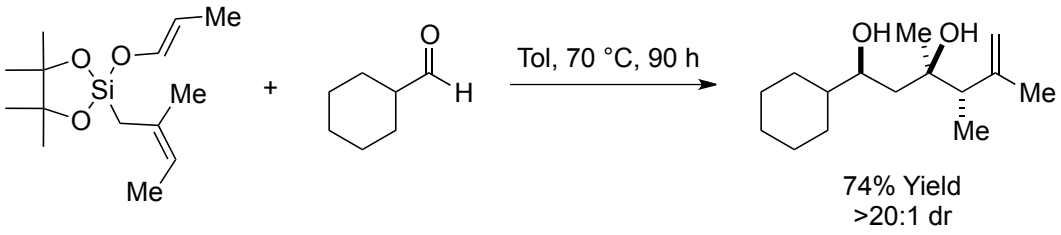

Scheme 3.16: Group precedence for tandem aldol-allyation chemistry

It was our hope that a modification of this procedure could be applied to the synthesis of the AB spiroketal to potentially generate either intermediate **3.53** or intermediate **3.55** (Scheme 3.17).

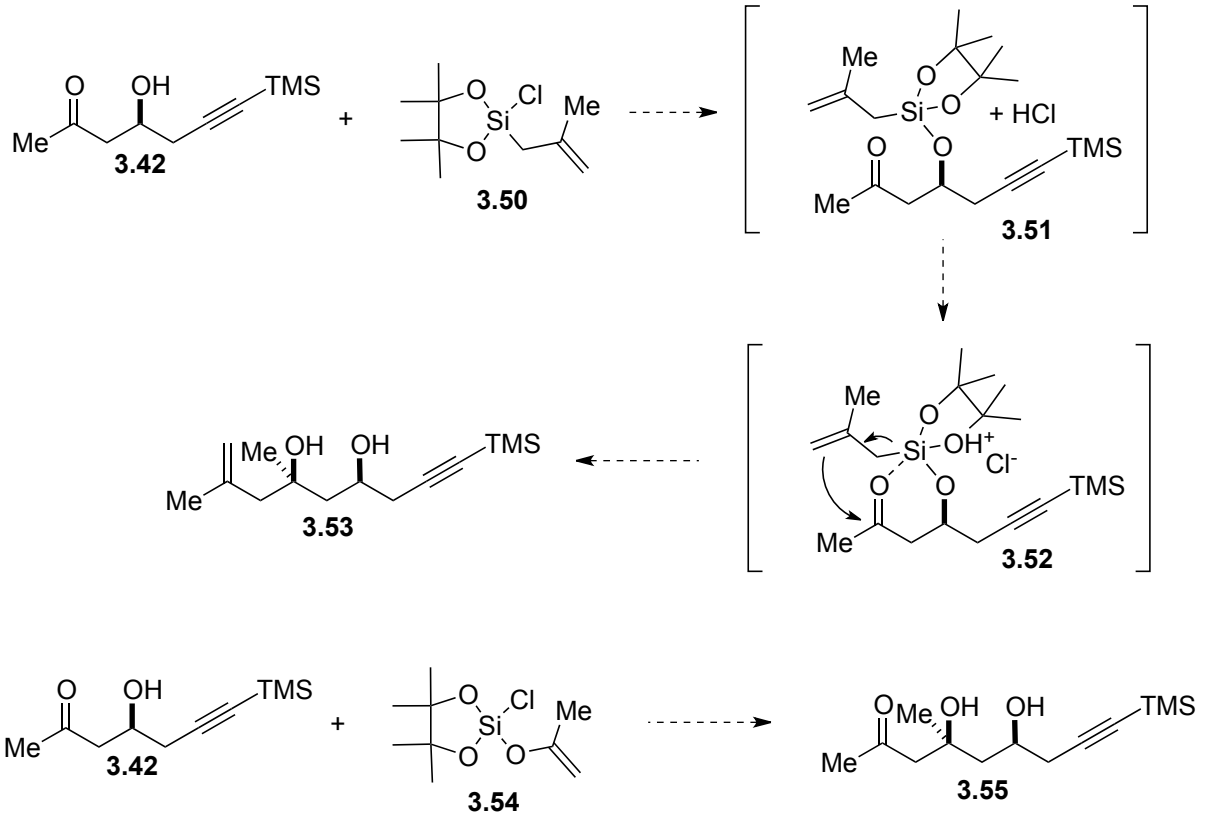

Scheme 3.17: *Syn* selective generation of 1,3- tertiary carbinol using a pinacol-silane

To probe the strategy laid out above, we first sought to synthesize methallyl-trichlorosilane **3.56** and use it to generate pinacol-silane **3.50** (Scheme 3.18).

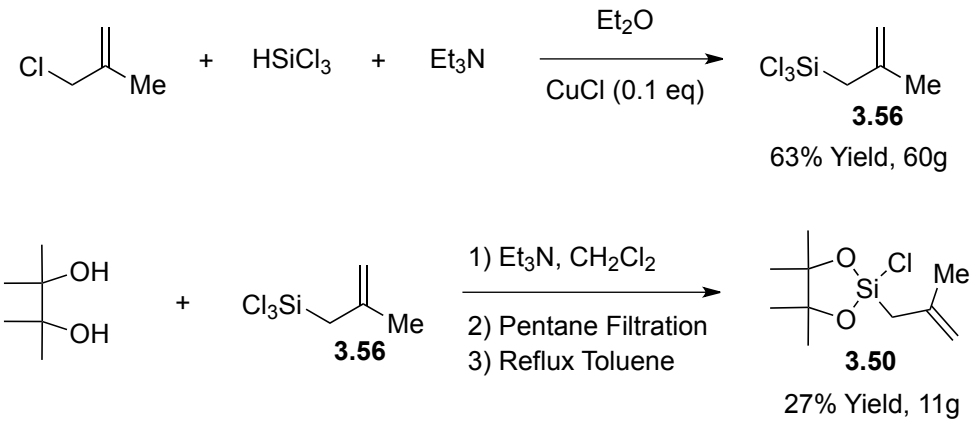

Scheme 3.18: Synthesis of methallyl, pinacol-silane 3.50

Though the synthesis of pinacol-silane **3.50** depicted above was low yielding, it did serve to provide the desired reagent in multi-gram quantities. Thus, using pinacol-silane **3.50** we screened several reaction temperatures in benzene to see if we could affect the desired diastereoselective, methallylation of β-hydroxy ketone **3.42**. To our great satisfaction, this reaction platform, which was originally only applicable to aldehydes,[10] worked quite nicely on our β-hydroxy ketone substrate **3.42**, presumably through the activation pathway depicted in Scheme 3.17. As seen below, the best diastereoselectivities were obtained when the reaction was allowed to proceed slowly over 4 days at 40 °C (Scheme 3.19).

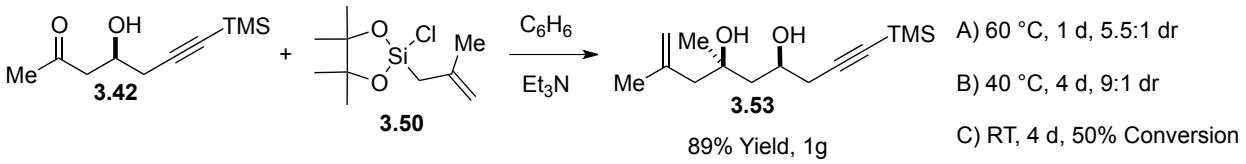

Scheme 3.19: Temperature screen for methallylation of β-keto alcohol 3.42

Given our success with reagent **3.50** we opted to continue with our synthesis of the AB spiroketal fragment instead of pursuing the slightly more step-economical reaction with silane **3.54** to directly generate ketone **3.55** (Scheme 3.17). To access ketone **3.55**, we subjected alkene **3.53** to the oxidative cleavage conditions describe above (Scheme 3.15).[9] Unfortunately, as observed in the case of δ-substituted hydroxy ketone **3.29** cyclizing to form lactol **3.30** (Scheme 3.9), the desired δ-substituted hydroxy ketone could only be isolated as lactol **3.57** in moderate yields following the oxidation. Incidentally, this result implies that the use of silane **3.54** to directly generate ketone **3.55** from alcohol **3.42** would likely have been unsuccessful. To obviate this lactolization problem, we first bis-protected diol **3.53** with TESOTf and then proceeded with the oxidative cleavage of alkene **3.58**. This new protocol proceeded smoothly, providing ketone **3.59** in good yield (Scheme 3.20).

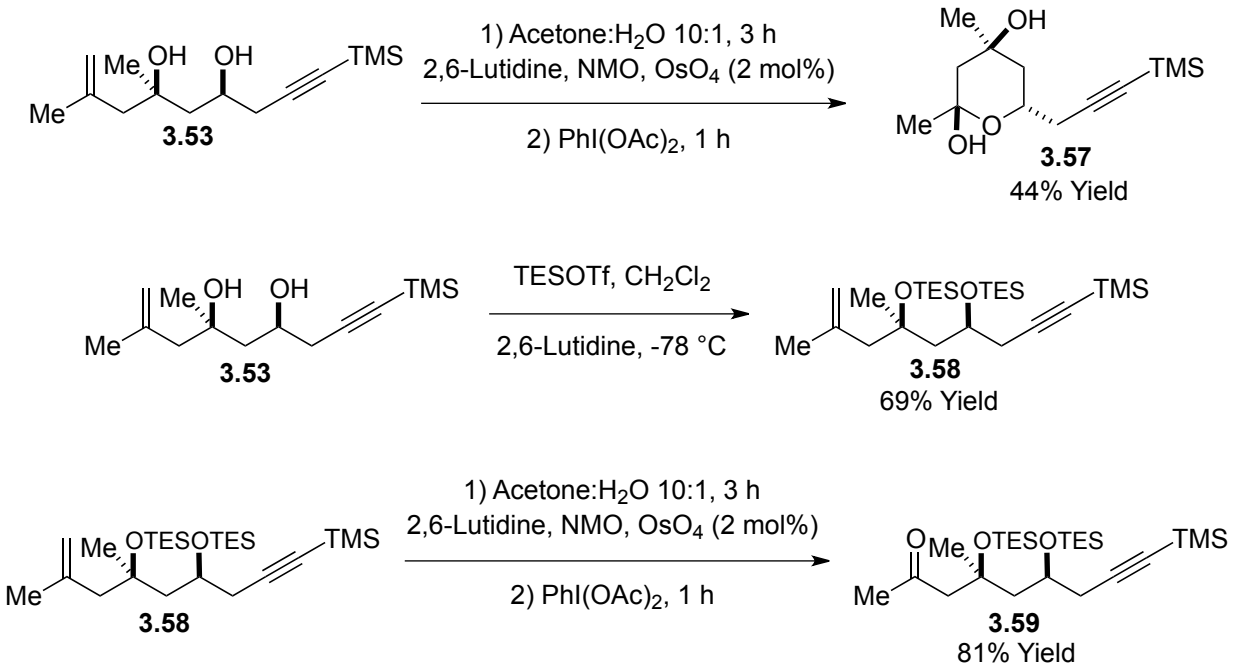

Scheme 3.20: Accessing aldol coupling partner, keto-alkyne 3.59

With potential aldol coupling partner **3.59** in hand, we shifted our efforts toward the generation of aldehyde **3.64** (Scheme 3.21). As seen below, the synthesis once again began with the vinyl Grignard opening of enantioenriched epichlorohydrin **(R)-3.16** to give allyl-alcohol **(*S*)-3.21**. This primary chloride was displaced with NaCN to give nitrile **3.60** in good yield (Caution: it was critical to avoid an aqueous workup of this reaction to prevent the release of cyanide gas from any unreacted NaCN). Nitrile **3.60** was then converted to methyl ester **3.62** through a base mediated hydrolysis followed by methylation of the intermediate free acid **3.61**. Alkene **3.63** was successfully obtained using an acid-mediated PMB protection using PMB-trichloroacetimidate **3.19**. Finally, the desired aldehyde **3.64** was accessed in moderate yield via ozonolysis.

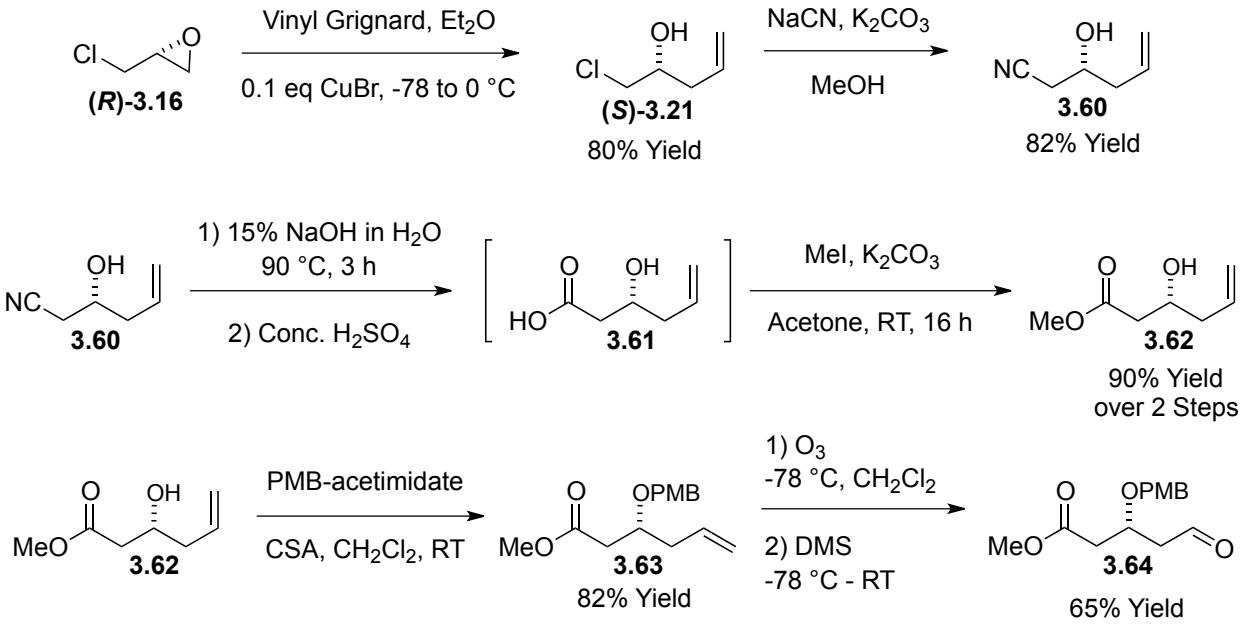

Scheme 3.21: Accessing aldol coupling partner, aldehyde 3.64

Our first attempt to couple ketone **3.59** and aldehyde **3.64** using a Mukaiyama aldol reaction was only met with moderate success (Scheme 3.22). Complex polyketide fragment **3.66** was obtained in 60% yield and 4:1 dr as the β-OPMB substituted aldehyde **3.64** controlled the approach of silyl-enol ether **3.65** to give the expected 1,3-*anti* addition product **3.66** as the major diastereomer.[6] Since the 1,3-*syn* stereochemical relationship shown in compound **3.67** was desired, we hoped to simultaneously install the requisite acetate functionality as well as invert the carbinol stereocenter by using a Mitsunobu reaction procedure.[11] Unfortunately, all efforts to employ the Mitusnobu reaction only resulted in elimination to the undesired enone **3.68**, forcing us to reexamine our aldol coupling strategy.

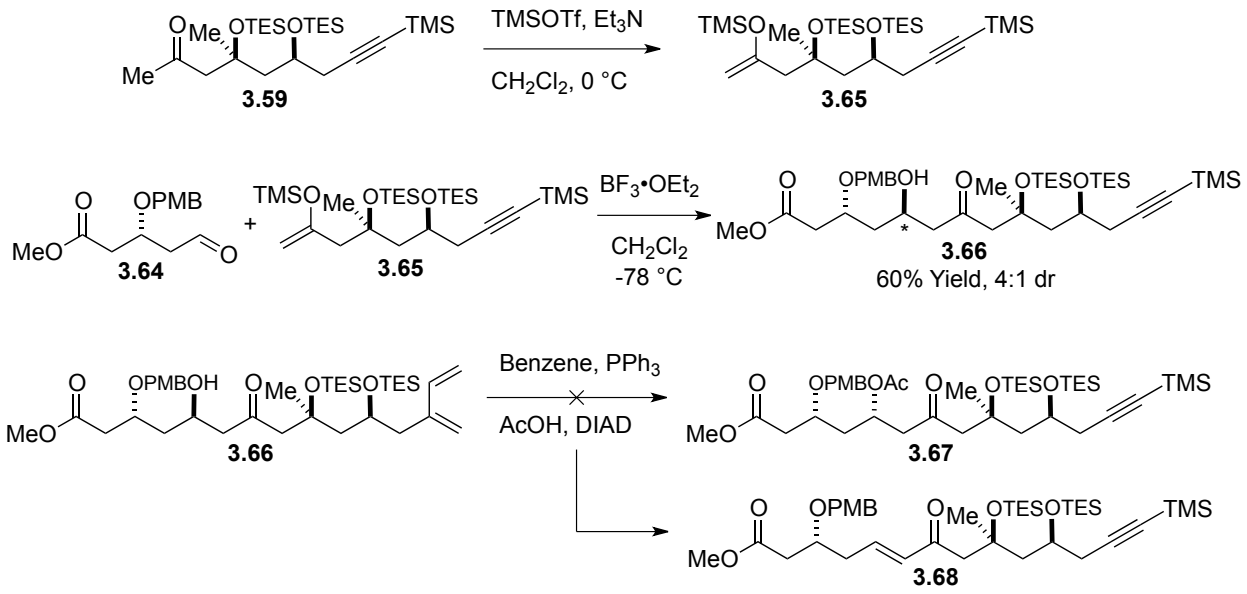

Scheme 3.22: Mukaiyama aldol followed by attempted Mitsunobu reaction

Given that Mukaiyama aldol conditions gave the undesired stereochemical outcome at the newly formed carbinol center, we sought to explore closed transition-state, boron-enolate aldol chemistry in the hopes of directly obtaining the desired stereocenter shown in compound **3.70** (Scheme 3.23).

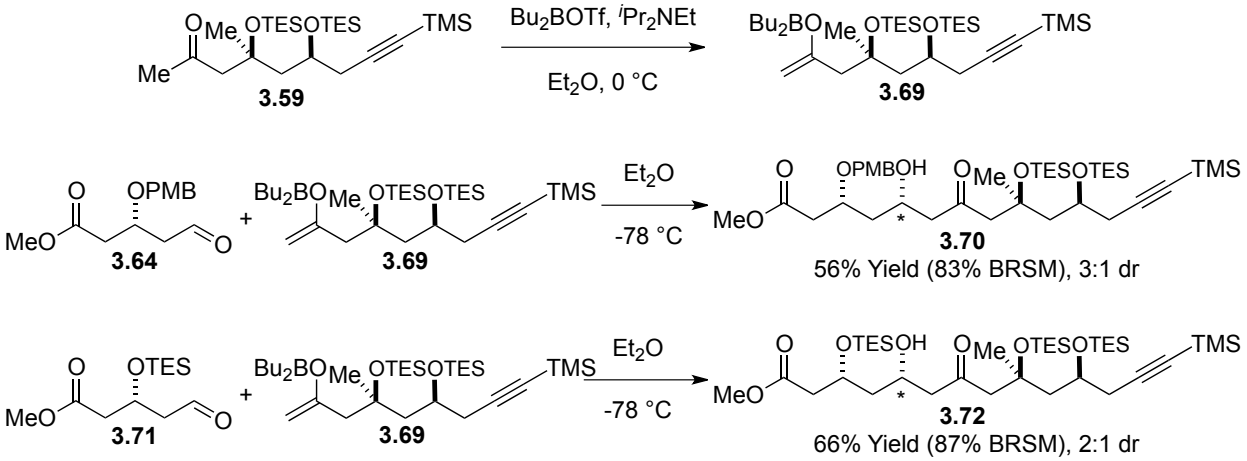

Scheme 3.23: Attempted boron mediated aldol coupling

Though we did succeed in overturning the stereochemical outcome of the aldol coupling, as the results in Scheme 3.23 show, we only did so in moderate diastereoselectivity even when the β-OPMB substituted aldehyde **3.64** was replaced with a β-OTES substituted aldehyde **3.71**.

In light of these unsatisfactory results, we next attempted to employ a Paterson aldol protocol in the hopes that the chiral boron reagent would override any substrate preference in directing the stereochemical outcome of the coupling (Scheme 3.24). Fortunately, this reaction did serve to provide compound **3.72** in 13:1 dr, though only in moderate yield following its acetylation and complete purification as compound **3.73**.

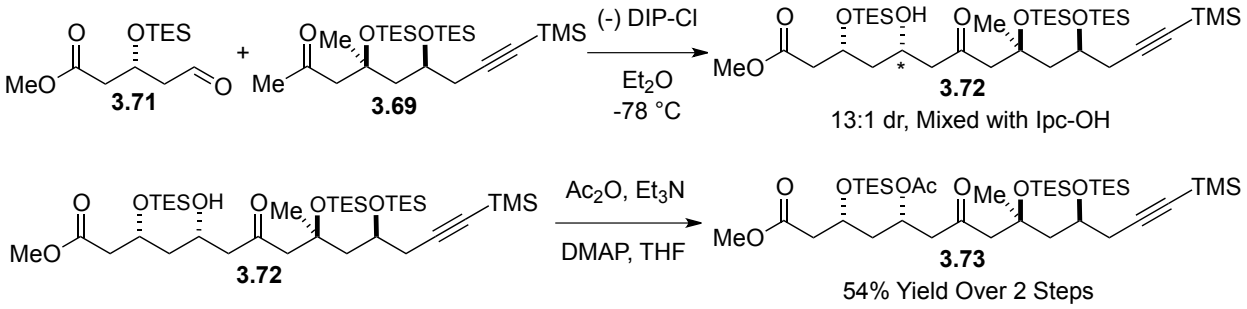

Scheme 3.24: Paterson aldol coupling to form acyclic AB fragment alkyne 3.73

With reliable methods established to set all of the stereocenters in the AB fragment, we next worked to install the critical diene moiety necessary for the ultimate fragment coupling between the AB and CD spiroketals (Scheme 3.25). Going back to TMS-alkyne **3.69**, we screened several conditions to remove the TMS group and provide free alkyne **3.74**. Standard K_2CO_3/MeOH and TBAF/AcOH conditions were both found to be indiscriminant, causing unwanted deprotection of the TES ethers during the reaction. A more exotic method utilizing $AgNO_3$ in a mixture of protic solvents, however, proved to be quite effective, so long as a solution of sat. NH_4Cl was added at the end of the reaction to precipitate out AgCl and protonate the free alkyne. Consistent with results disclosed by Driver, the enyne metathesis of compound

3.74 proceeded in high yields due to the ruthenium catalyst's ability to coordinate the homopropargylic heteroatom.[12] Small amounts of dimerized diene products were observed (ca. 5%) in addition to desired diene **3.75**, but these could be effectively separated from the product through careful chromatographic purification.

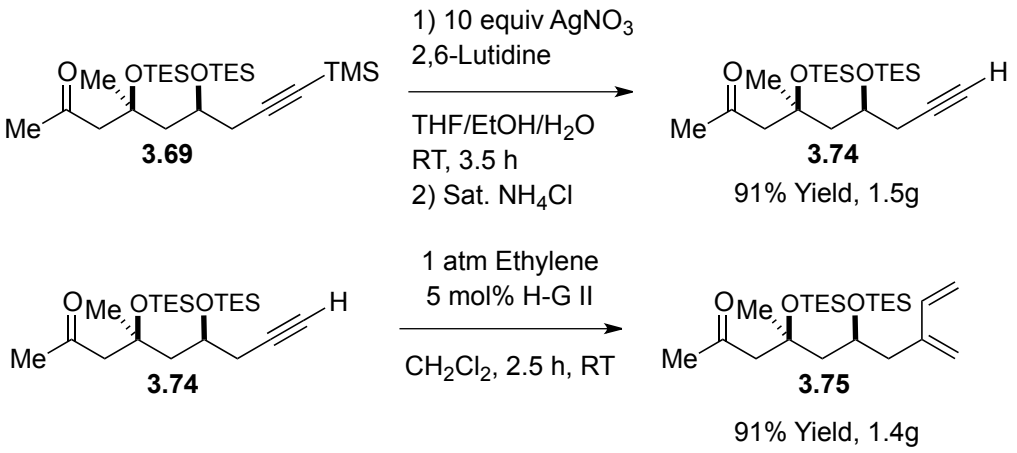

Scheme 3.25: Conversion of alkyne 3.69 to diene 3.75 via enyne metathesis

With gram-quantities of keto-diene **3.75** in hand, we returned to our Paterson aldol subunit coupling reaction and were pleased to obtain similar results to those reported in Scheme 3.24 (Scheme 3.26).

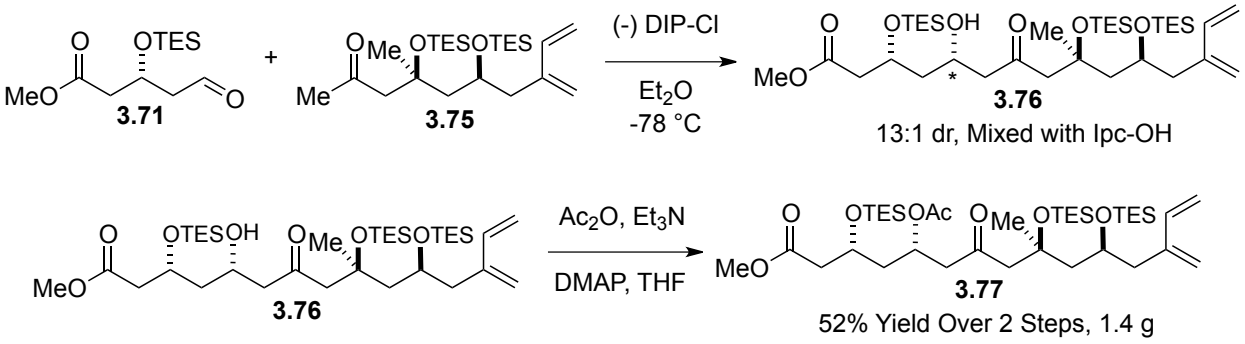

Scheme 3.26: Paterson aldol coupling to form acyclic AB fragment diene 3.77

Our next objective was to affect the spiroketalization of acyclic precursor **3.77**. To that end, subjection of compound **3.77** to CSA/MeOH conditions, served to cleave all of the molecule's silyl-ether bonds and effectively promoted spiroketalization to provide the thermodynamically preferred, doubly-anomeric spiroketal **3.78** in excellent yield (Scheme 3.27). The axial, tertiary alcohol of **3.78** was then reprotected using an excess of TESOTf to give key AB fragment intermediate **3.37** in good yield. It should be noted that while this reaction was somewhat sluggish, attempts to subject alcohol **3.78** to more forcing protection conditions led to unwanted silylation of the acetate α to its carbonyl. Several mild spiroketalization conditions were also screened in an attempt to spiroketalize acyclic compound **3.78** without removing the desired tertiary TES group. Unfortunately, the best of these conditions (PPTS/EtOH, RT, 1 h) only provided spiroketal **3.79** in 66% yield and as a 1:3 mixture of diastereomers, with the undesired, non-anomeric spiroketal predominating as the preferentially formed kinetic product.

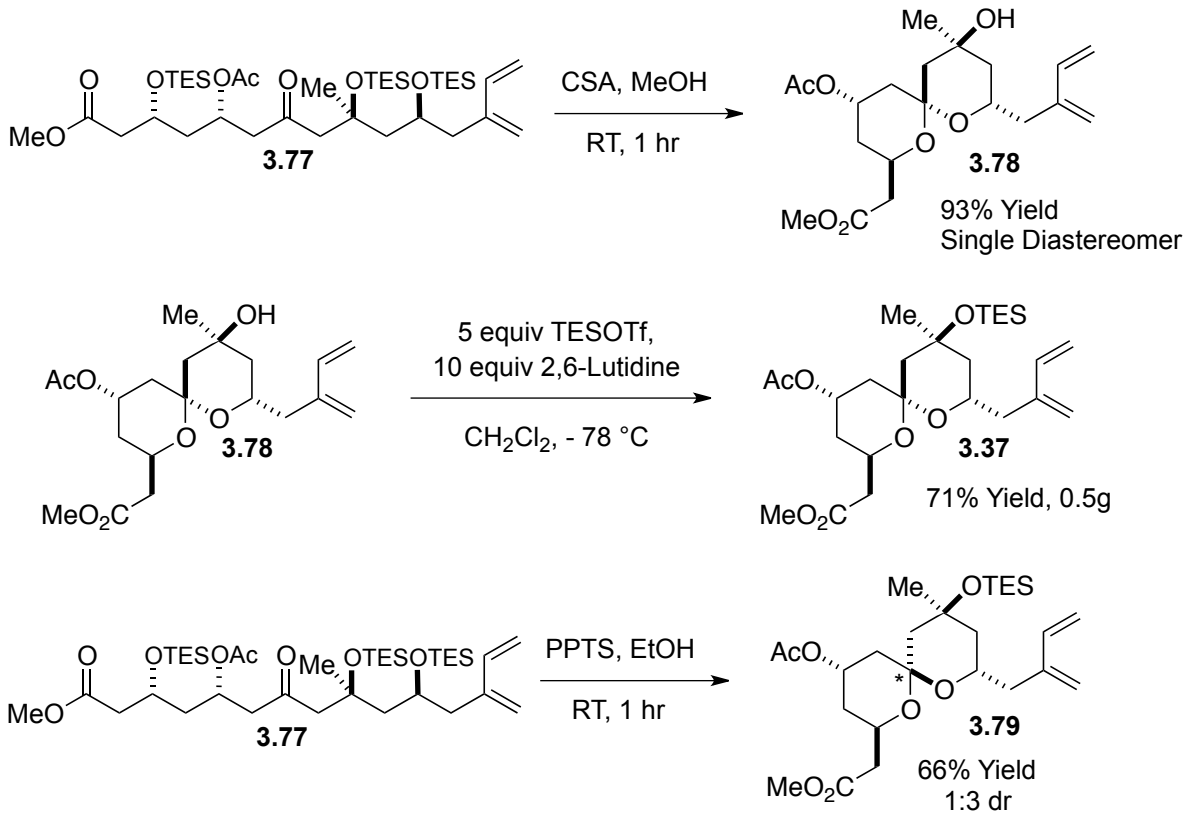

Scheme 3.27: Spiroketalization to generate key AB fragment 3.37

With AB spiroketal fragment **3.37** finally in hand, we eagerly subjected it to our optimized *anti*-1,4-hydrosilylation conditions (Chapter 2, Scheme 2.34) to begin the key ABCD fragment coupling procedure envisioned in Scheme 3.2. To our deep dismay, none of the desired tiglic silane **3.81** could be isolated, despite numerous attempts to execute the hydrosilylation (Scheme 3.28). After running a battery of control experiments, it was eventually determined that the titanium mediated *anti*-1,4-hydrosilylation chemistry was incompatible with several Lewis-basic functional groups. In particular, model esters such as **3.82** prevented the reaction entirely, returning only unreacted starting material.

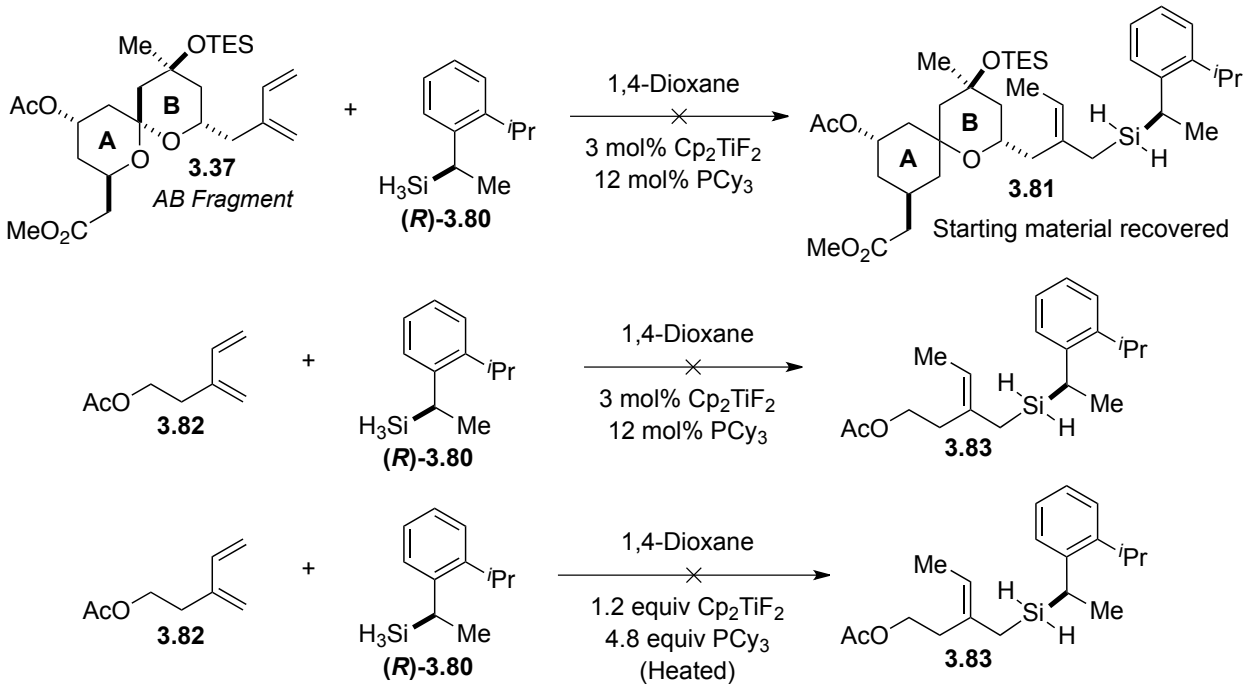

Scheme 3.28: Failed *anti*-1,4-hydrosilylation of AB fragment 3.37

The distressing results shown above stuck a major blow to our hopes of attaining a high-yielding and scalable fragment coupling sequence as first described in Chapter 1. Though one might envision a synthetic strategy that allows for the masking of the offending ester functionalities in AB fragment **3.37**, in order to allow for the use of the methodology developed in Chapter 2, we felt this would add an unacceptable level of inefficiency to what we hoped would ultimately be one of several streamlined fragment syntheses ultimately brought together to generate multi-gram quantities of spongistatin 1.

Yet while the application of our proposed ASA / tandem silylformylation / Tamao oxidation fragment coupling strategy was fading into improbability, a potential solution to our fragment coupling conundrum was manifesting itself in the work of a Leighton group post-doc named Dr. Hyunwoo Kim. This alternative approach will be described in the following chapter.

3.3 References and Notes

1. Smith, A. B.; Chen, S. S. Y.; Nelson, F. C.; Reichert, J. M.; Salvatore, B. A., *J. Am. Chem. Soc.* **1997,** *119* (45), 10935-10946.
2. (a) Huggins, M. J.; Kubler, D. G., *J. Org. Chem.* **1975,** *40* (19), 2813-2815; (b) Masamune, S.; Ma, P.; Okumoto, H.; Ellingboe, J. W.; Ito, Y., *J. Org. Chem.* **1984,** *49* (15), 2834-2837.
3. Walshe, N. A., Goodwin, T. B., Smith, G. C., Woodward, F. E., *Org Synth* **1987,** *65*, 1.
4. Furrow, M. E.; Schaus, S. E.; Jacobsen, E. N., *J. Org. Chem.* **1998,** *63* (20), 6776-6777.
5. Veysoglu, T.; Mitscher, L. A.; Swayze, J. K., *Synthesis-Stuttgart* **1980,** (10), 807-810.
6. Evans, D. A.; Duffy, J. L.; Dart, M. J., *Tetrahedron. Lett.* **1994,** *35* (46), 8537-8540.
7. Gregg, B. T.; Golden, K. C.; Quinn, J. F., *J. Org. Chem.* **2007,** *72* (15), 5890-5893.
8. Spletstoser, J. T.; Zacuto, M. J.; Leighton, J. L., *Org. Lett.* **2008,** *10* (24), 5593-5596.
9. Nicolaou, K. C.; Adsool, V. A.; Hale, C. R. H., *Org. Lett.* **2010,** *12* (7), 1552-1555.
10. (a) Wang, X. L.; Meng, Q. L.; Nation, A. J.; Leighton, J. L., *J. Am. Chem. Soc.* **2002,** *124* (36), 10672-10673; (b) Wang, X. L.; Meng, Q. L.; Perl, N. R.; Xu, Y.; Leighton, J. L., *J. Am. Chem. Soc.* **2005,** *127* (37), 12806-12807.
11. Swamy, K. C. K.; Kumar, N. N. B.; Balaraman, E.; Kumar, K. V. P. P., *Chem Rev* **2009,** *109* (6), 2551-2651.
12. Smulik, J. A.; Diver, S. T., *Org. Lett.* **2000,** *2* (15), 2271-2274.

Chapter 4: Methodology Work toward Intermolecular Fragment Coupling

4.1 Developing a Fragment Coupling Procedure by Intermolecular Crotylation

As described at the conclusion of Chapter 3, our intramolecular fragment coupling strategy for joining the AB and CD spiroketals of spongistatin 1 was facing some potentially irreconcilable difficulties. Fortunately, the contemporary work of Dr. Hyunwoo Kim would prove to be the inspiration for a revised fragment coupling strategy (Scheme 4.1).[1]

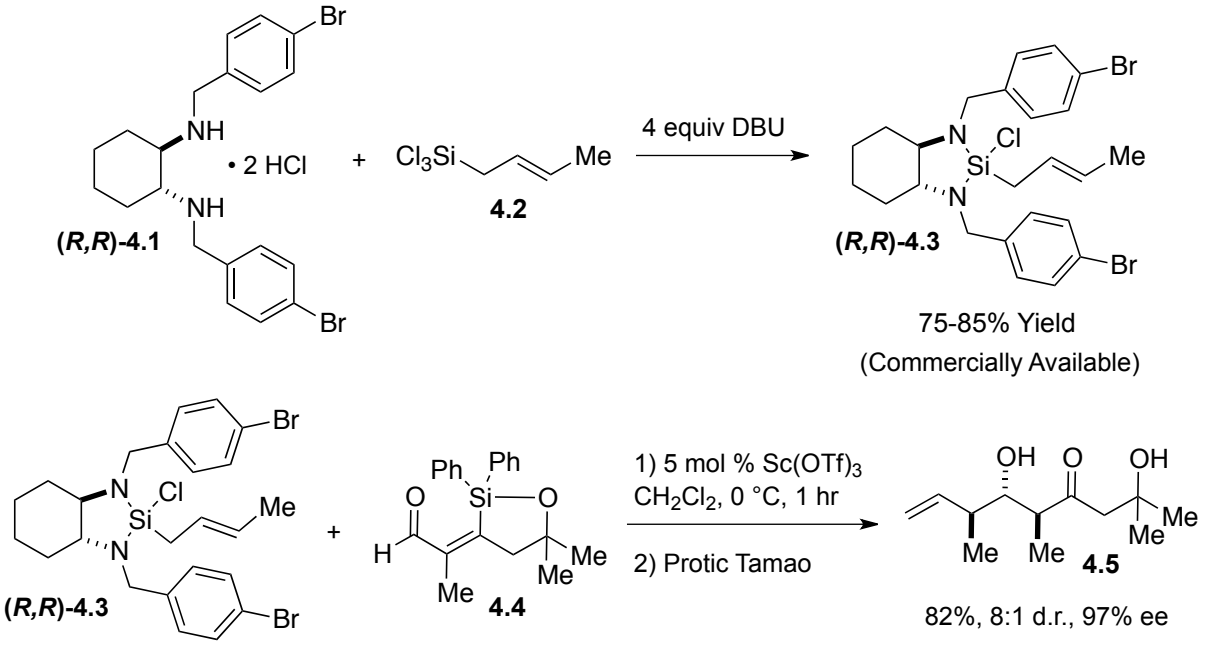

Scheme 4.1: $Sc(OTf)_3$ mediated crotylation of hindered aldehydes

As depicted above, Dr. Kim's key insight was that the Leighton laboratory's known allylation and crotylation reagents derived from diamine **4.1**[2] could be activated with catalytic quantities of $Sc(OTf)_3$, imbuing them with the reactivity required to selectively crotylate even the most sterically hindered and electronically deactivated classes of aldehydes. Most notably, aldehyde **4.4** was shown to undergo crotylation followed by immediate Tamao oxidation to

provide complex polyketide fragment **4.5** in excellent yield, diastereoselectivity and enantioselectivity.

Given the exciting results depicted in Scheme 4.1, we began to consider the possibility of attaining our scalable and efficient coupling of the AB and CD fragments of spongistatin 1 through a similar $Sc(OTf)_3$ catalyzed intermolecular crotylation / Tamao oxidation sequence depicted below (Scheme 4.2).

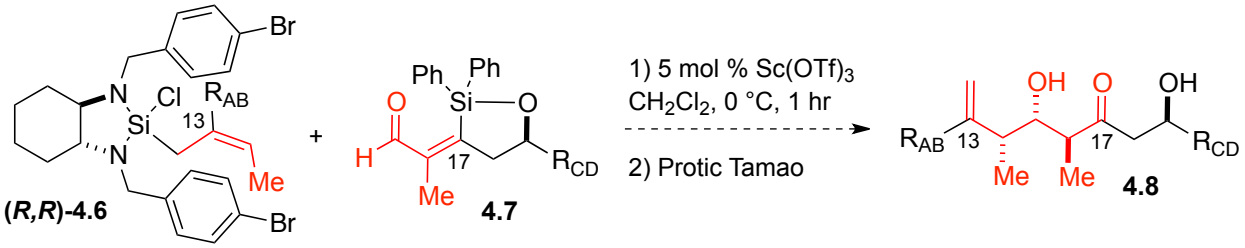

Scheme 4.2: Proposed intermolecular crotylation / Tamao oxidation coupling

In order to utilize this revised coupling strategy, however, a method for generating the angelic silane motif shown in compound **(*R*,*R*)-4.6** would have to be identified. The stereochemical rationale for the use of an angelic silane coupling partner in the intermolecular approach as opposed to the tiglic silane coupling partner formerly required in the intramolecular approach is shown below (Scheme 4.3).

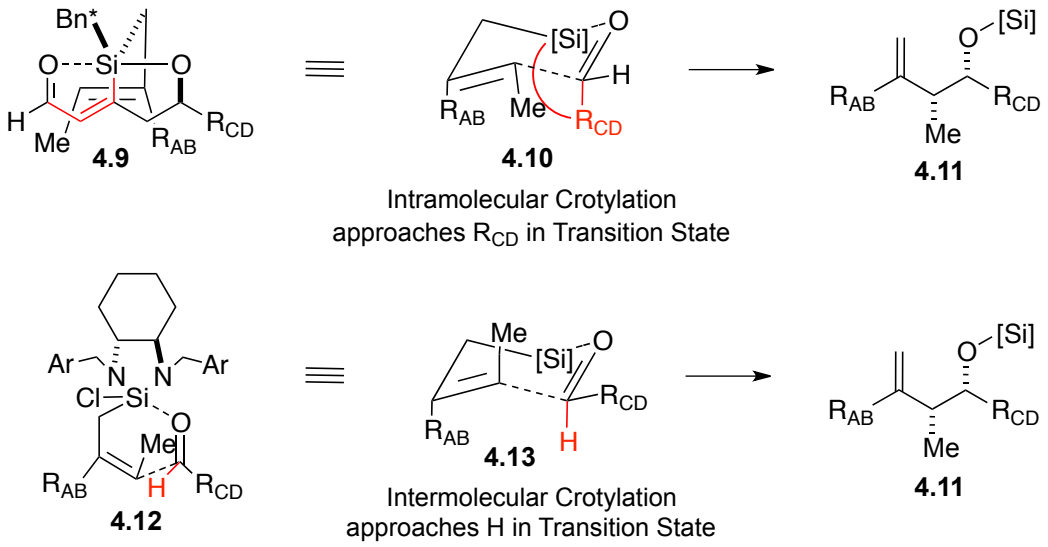

Scheme 4.3: Stereochemical consequences of silane olefin geometry

As can be seen in Scheme 4.3, generation of the desired 1,2-*syn* stereochemical outcome in compound **4.11** requires opposite olefin geometries in the "allyl" moiety depending on whether the transfer from silicon occurs intermolecularly or intramolecularly. In the intramolecular case, the *trans* olefin geometry is required to deliver the 1,2-*syn* methyl relationship, since the allylation necessarily approaches the tethered R_{CD} portion of the aldehyde (transition state **4.10**). For the intermolecular case, the *cis* olefin geometry is required to deliver the 1,2-*syn* methyl relationship, since the R_{CD} portion of the aldehyde can achieve the equatorial orientation shown in transition state **4.13**.

Fortunately, unlike the synthesis of tiglic silanes (Chapter 2, Section 4), the synthesis of angelic silanes is well precedented, with several 1,4-hydrosilyaltion reactions known to give the desired product motif.[3] Selecting Tsuji's *syn*-1,4-hydrosilylation of dienes with trichlorosilane[3b] as our desired reaction platform, we first sought to determine this transformation's functional group compatibility, since this was the ultimate undoing of the *anti*-1,4-hydrosilylation

chemistry previously described (Chapter 2, Section 4 and the conclusion of Chapter 3). To that end, we ran several control experiments shown below (Scheme 4.4).

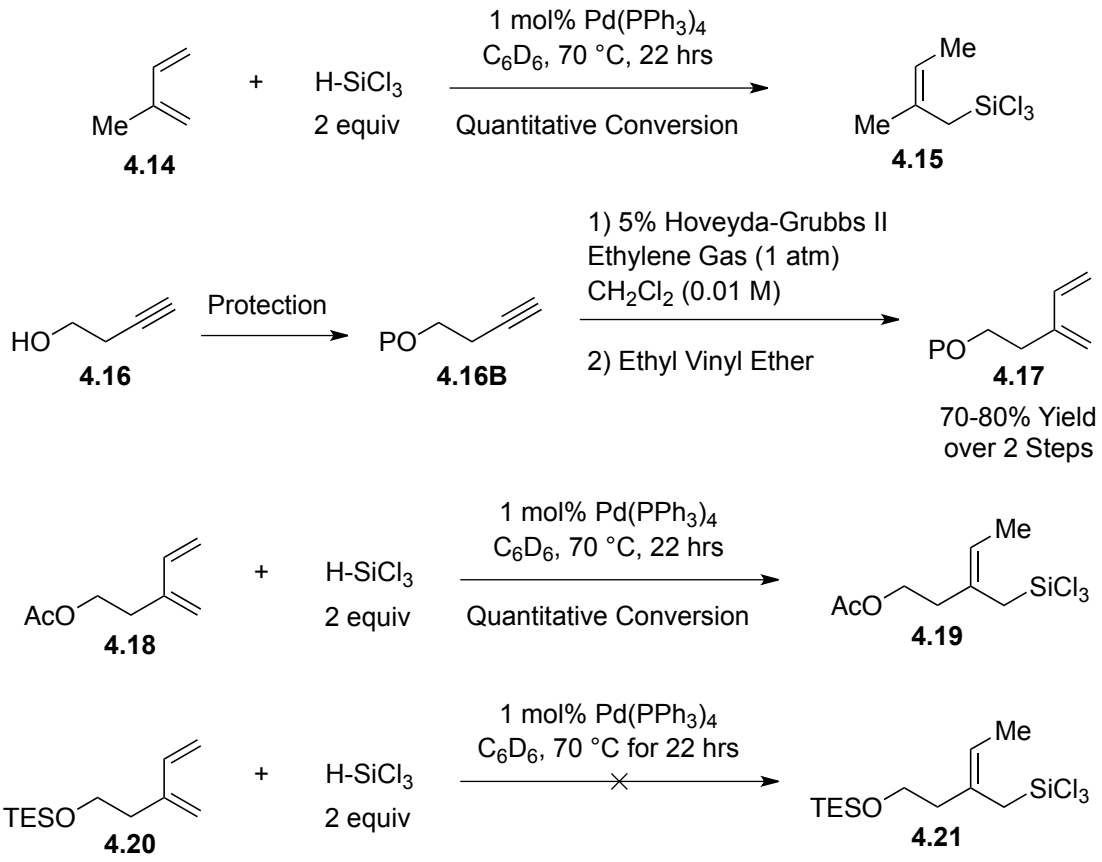

Scheme 4.4: Functional group compatibility with *syn*-1,4-hydrosilylation reaction

The conversion of isoprene **4.14** to trichlorosilane **4.15** was simply a reproduction of Tsuji's extraordinarily efficient and selective hydrosilylation chemistry.[3b] Following that first control experiment, several dienes of type **4.17** were synthesized to probe the functional group compatibility of the *syn*-1,4-hydrosilylation. After some experimentation, it was found that this reaction manifold was completely compatible with esters and carbonates to provide products such as **4.19**. These results gave us hope that the *syn*-1,4-hydrosilylation protocol could be effectively applied to our fully elaborated AB fragment spiroketal, which contains two ester

moieties. However, the *syn*-1,4-hydrosilylation functional group was found to be wholly incompatible with silyl ethers, as subjection of diene **4.20** led to deprotection and subsequent decomposition of the resulting alcohol. Though not ideal, this silyl-ether incompatibility was an inconvenience we felt we could design our AB fragment synthesis around. Thus, with the functional group compatibility of this *syn*-1,4-hydrosilylation procedure established, we continued our exploration of the proposed intermolecular coupling reaction in a simple model system.

Our first task in designing a model system for the intramolecular fragment coupling of the AB and CD fragments of spongistatin 1 was to generate an appropriate surrogate for CD silacycle-aldehyde **4.7** (Scheme 4.2). This proved to be reasonably straightforward (Scheme 4.5), as we once again employed Jacobsen's HKR to generate enantioenriched 1,2-epoxyhexane **(*S*)-4.22**[4] and used a BF_3•THF-mediated propyne opening reaction to generate homopropargylic alcohol **4.23** in excellent yield. This alcohol **4.23** was then protected with chlorodiphenylsilane and immediately subjected to silylformylation conditions that successfully provided model silacycle-aldehyde **4.25** in excellent yield.

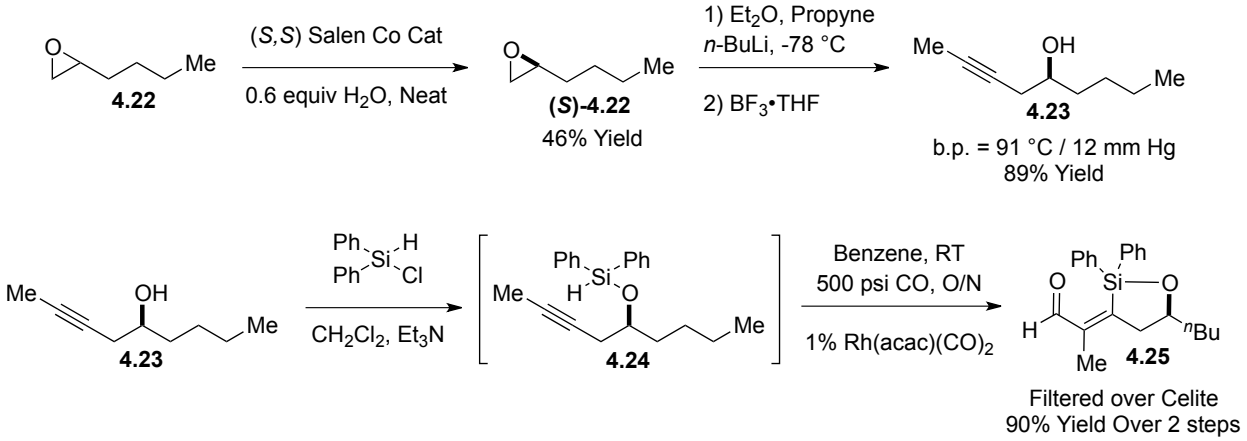

Scheme 4.5: Synthesis of model silacycle-aldehyde 4.25

With model aldehyde **4.25** in hand, we next set up the intermolecular fragment coupling procedure using angelic-trichlorosilane **4.19** complexed with diamine **(*R,R*)-4.1** to form **(*R,R*)-4.26** (Scheme 4.6) as a surrogate for AB coupling partner **(*R,R*)-4.6** (Scheme 4.2).

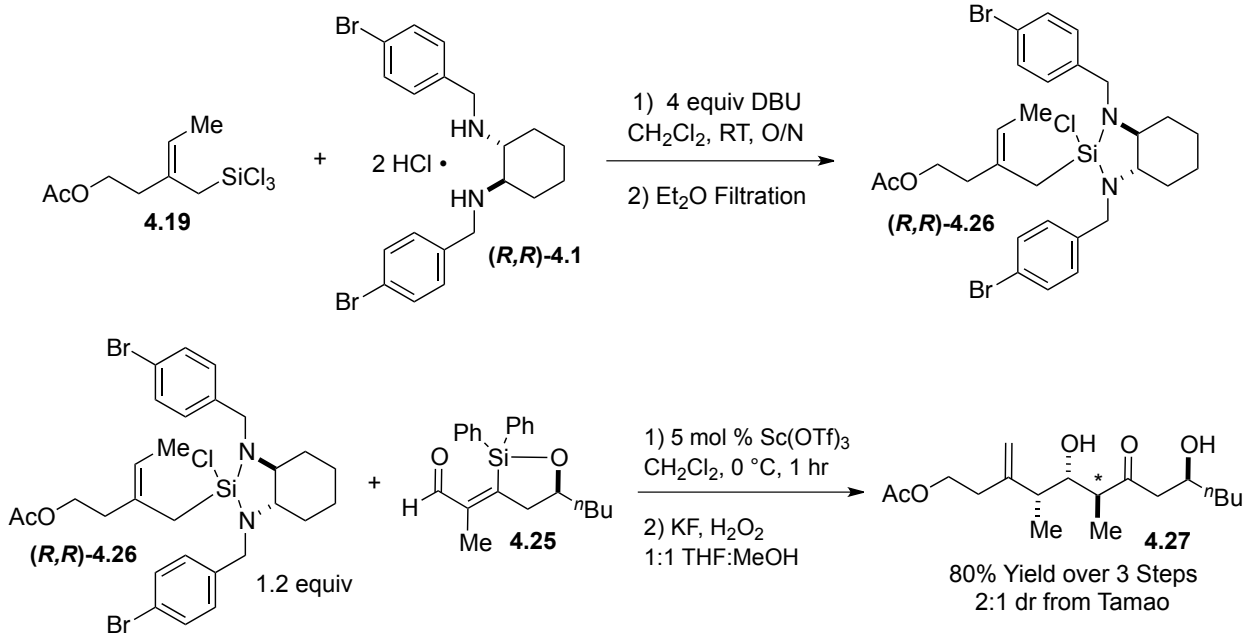

Scheme 4.6: Fragment coupling by crotylation / Tamao oxidation – Model System

The results depicted above were very exciting in the sense that coupled complex polyketide fragment **4.27** was successfully isolated in excellent yield over the 2 step sequence. This constituted the first example of fragment coupling by crotylation mediated by the Leighton group's chiral diamine ligand **4.1** in conjunction with catalytic quantities of $Sc(OTf)_3$. Yet much to our surprise, though compound **4.27** was obtained in high yield, it was only isolated as a 2:1 mixture of diastereomers under our standard Tamao oxidation conditions.[5] Because our standard protic Tamao conditions provided high diastereoselectivity in both our tandem silylformylation / Tamao oxidation sequences as well as in the *trans*-crotylation of silacycle-aldehyde **4.4** (Scheme

4.1), we felt that its unexpected failure in this intermolecular fragment coupling sequence merited an in-depth analysis.

It seemed that the main difference between the highly selective crotylation / Tamao oxidation sequence shown in Scheme 4.1 and the failure to achieve high diastereoselectivity in the intermolecular fragment coupling sequence shown in Scheme 4.6 was the substitution at the 2 position of the allyl transfer moiety (*i.e.* the angelic position). As such, we sought to generate a sample set of complexed silanes with varying substitution patterns at the 2 position in order to determine their impact on the Tamao oxidation selectivity. The results of these experiments are summarized below (Scheme 4.7).

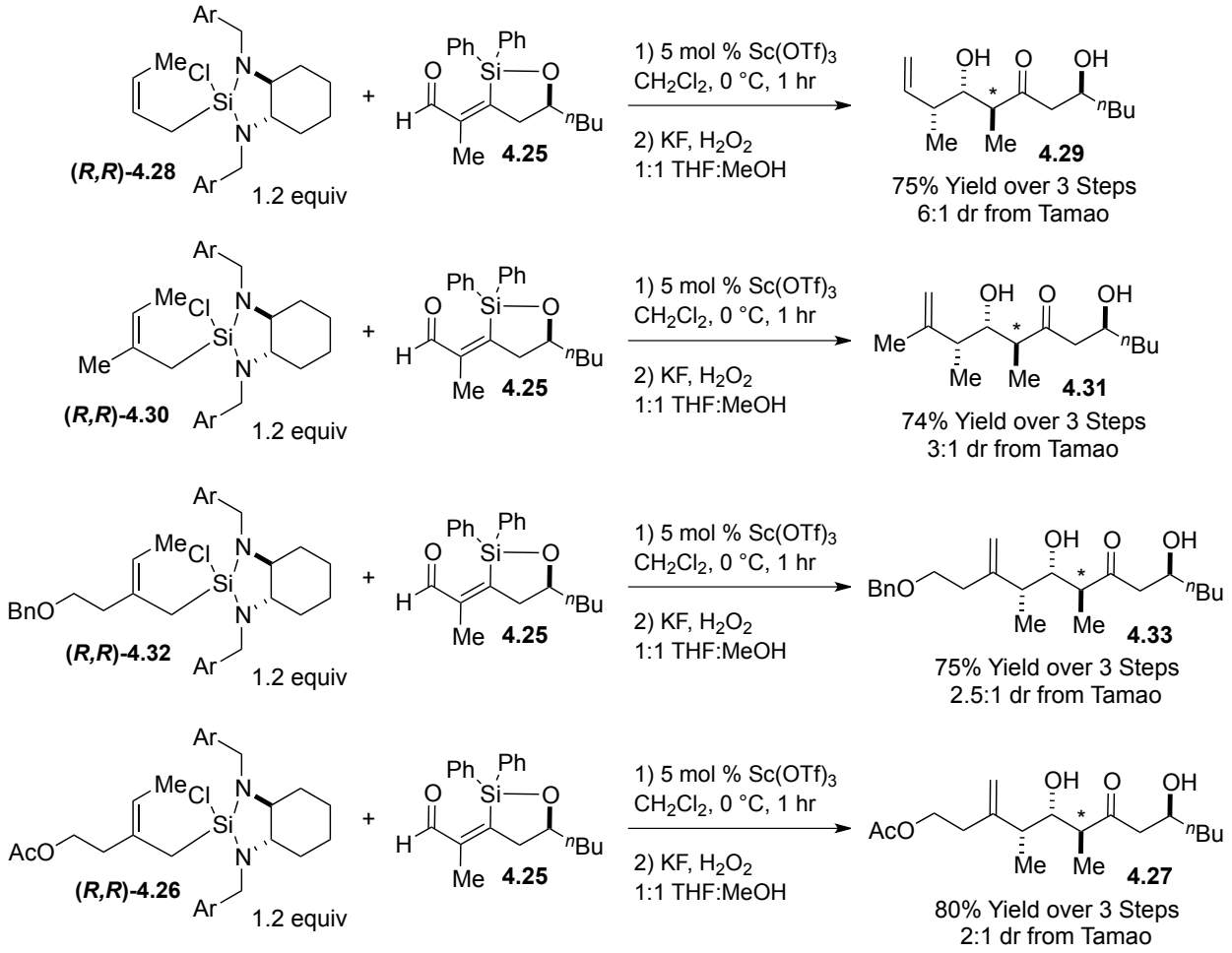

Scheme 4.7: Remote steric effect on Tamao oxidation diastereoselectivity

As can be seen in the scheme above, the larger the substituent at the 2 position, the worse the Tamao oxidation selectivity became. This remote steric effect was very disheartening as the envisioned angelication coupling partner **(*R,R*)-4.6** would necessarily be substituted with the entire AB spiroketal at the 2 position. Given this requirement, it became critical for us to identify alternative Tamao oxidation conditions that would restore the reaction's diastereoselectivity if we were to succeed in utilizing our revised fragment coupling strategy to synthesize the ABCD hemisphere of spongistatin 1.

Fortunately, the Tamao oxidation is an extremely well investigated transformation, and there were a myriad of conditions to be examined.[6] A summary of our extensive exploration is represented in Table 4.1 below.

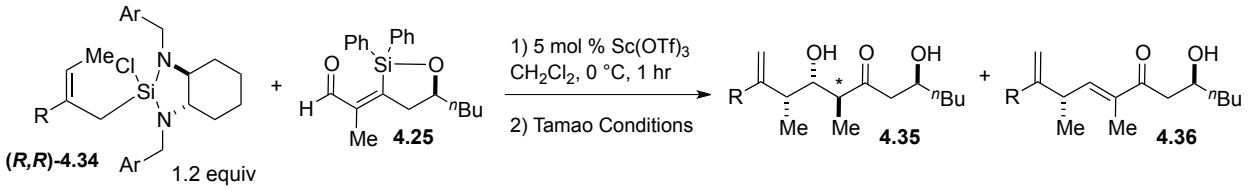

	R	Solvent	Peroxide	Additive	Time (Temp)	dr / Elim.
1)	-OAc	THF/MeOH	13x H_2O_2	4x KF	1 h (RT)	2:1 / >6:1
2)	**H**	**THF/MeOH**	**13x H_2O_2**	**4x KF**	**1 h (RT)**	**6:1 / >6:1**
3)	-OBn	THF/MeOH	13x H_2O_2	4x KF	1 h (RT)	2.5:1 / 5:1
4)	-OBn	THF/MeOH	13x H_2O_2	4x TBAF	3 h (RT)	1:1/None
5)	-OBn	DMF	*m*-CPBA	4x KF	20 h (RT)	Mess
6)	-OBn	DMF	13x H_2O_2	4x KHF_2	20 h (RT)	1.3:1 / 2:1
7)	-OBn	DMF	13x H_2O_2	Ac_2O/KHF_2	20 h (RT)	Mess
8)	**-OBn**	**THF/MeOH**	**13x H_2O_2**	**13x $KHCO_3$**	**<20 h (RT)**	**5:1 / 2:1**
9)	Me	THF/MeOH	13x H_2O_2	13x $NaHCO_3$	4 h (RT)	10:1 / 2:1
10)	Me	THF / pH 7	13x H_2O_2	13x $KHCO_3$	24 h (RT)	Little Pdt
11)	Me	THF/MeOH	13x H_2O_2	1x $NaHCO_3$	4 h (RT)	8:1 / 2.3:1

12)	**Me**	**THF/MeOH**	**13x H_2O_2**	**1x $KHCO_3$**	**4 h (RT)**	**10:1 / 2:1**
13)	Me	THF/MeOH	13x H_2O_2	0.2x $KHCO_3$	8 hr (RT)	8:1 / 2.4:1
14)	Me	THF/MeOH	13x H_2O_2	0.2x$NaHCO_3$	8 h (RT)	8:1 / 2.3:1
15)	Me	THF/MeOH	13x H_2O_2	1x KH_2PO_4	2 days (RT)	6:1 / 2.8:1
16)	Me	THF/MeOH	13x H_2O_2	1x K_2HPO_4	8 h (RT)	8:1 / 2.3:1
17)	Me	THF/MeOH	13x H_2O_2	1 x K_3PO_4	30 min (RT)	6:1 / 2.3:1
18)	Me	MeOH	13x H_2O_2	1x K_2HPO_4	1.5 h (RT)	5:1 / 1.3:1
19)	Me	THF/MeOH	13x H_2O_2	1x Hunig's	8 h (RT)	8:1 / 2.3:1
20)	Me	THF/MeOH	13x H_2O_2	13x KOH	10 min (RT)	All Elim
21)	Me	THF/MeOH	13x H_2O_2	AcOH/TBAF	24 h (RT)	1.5:1/None
22)	Me	THF/MeOH	13x H_2O_2	4x HF•Pyr	24 h (RT)	Minimal Rxn
23)	Me	THF/MeOH	13x H_2O_2	4x KF	1.5 h (RT)	3:1 / 3:1
24)	Me	THF/MeOH	13x H_2O_2	4x KHF_2	24 h (RT)	Minimal Rxn
25)	Me	THF/MeOH	13x H_2O_2	4x CsF	10 min (RT)	4:1 / 4:1
26)	**Me**	**THF/MeOH**	**13x H_2O_2**	**4x CsF**	**1.5 h (0°C)**	**4:1 / 6:1**
27)	Me	THF/^{i}PrOH	13x H_2O_2	CsF	24 h (RT)	5:1 / 20:1
28)	**Me**	**^{i}PrOH**	**13x H_2O_2**	**CsF**	**1.5 h (RT)**	**5:1 / 20:1**
29)	Me	^{i}PrOH	13x H_2O_2	KF	<10 h (RT)	5:1 / 7:1
30)	Me	^{i}PrOH	13x H_2O_2	1x $KHCO_3$	<10 h (RT)	10:1 / 8:1
31)	**Me**	**^{i}PrOH**	**13x H_2O_2**	**1x $KHCO_3$**	**5 h (RT)**	**10:1 / 8:1**
32)	**-OBn**	**^{i}PrOH**	**13x H_2O_2**	**1x $KHCO_3$**	**24 h (RT)**	**8:1 / 8:1**

Table 4.1: Optimization of Tamao oxidation reaction conditions

Table Notes: -OAc and -OBn indicate CH_2CH_2OAc and CH_2CH_2OBn, respectively. "Elim." refers to the product distribution ratio of **4.35** to **4.36**.

As can be seen in the above table, utilization of mild base mediated Tamao conditions, instead of fluoride, as well as switching to isopropanol as a solvent system led to improved diastereoselectivities of coupled product **4.35** while minimizing unwanted elimination to side-product **4.36**. The best results (Entries 31 and 32) are shown below with their isolated yields (Scheme 4.8).

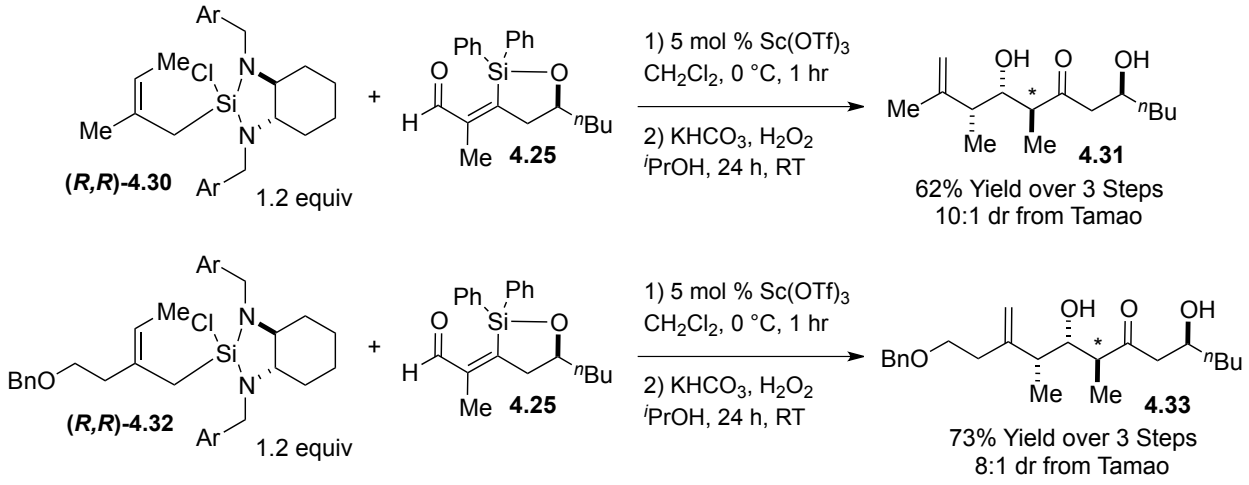

Scheme 4.8: Optimized Tamao oxidation following fragment coupling by crotylation

With the diastereoselectivity of the Tamao oxidation restored, our model system results gave us confidence that our revised, intermolecular fragment coupling strategy could indeed be employed to bring the fully elaborated AB and CD spiroketals together while simultaneously installing the full stereochemical array depicted in compound **4.8** (Scheme 4.2).

4.2 Fragment Coupling by Crotylation - Staged by Asymmetric Isoprenylation

Given the exciting results achieved in our fragment coupling model systems (Scheme 4.8), we felt it was important to divert some attention away from the total synthesis of spongistatin 1 in an effort to make this procedure more generally applicable to a variety of polyketide targets.

Since not all alkyne substrates are amenable to enyne metathesis, we sought to develop a more general method for installing the diene functionality required for our fragment coupling by crotylation procedure.

When considering various strategies for installing a diene moiety in the context of polyketide total synthesis, we thought that the asymmetric isoprenylation of aldehydes would be a useful approach, as it would additionally serve to set a carbinol stereocenter. Though two distinct methods for the enantioselective isoprenylation of aldehydes are known,[7] neither of them posses the scope, practicality and scalability we hoped to achieve in a general fragment coupling method. This being the case, we sought to extend our robust, strained silane reaction platform[1] to this new synthetic application. In practice, it seemed that if we could generate strained silane reagent **4.37** from isoprenyl-trichlorosilane **4.38** we would be well on our way toward achieving our goal (Scheme 4.9). All efforts to synthesize reagent precursor **4.38** by directly metallating isoprene **4.39**[8] and reacting it with tetrachlorosilane were met with significant purification difficulties. After some experimentation, however, a scalable, two-step approach was developed to provide clean isoprenyl-trichlorosilane **4.38** in reasonable yield.[9]

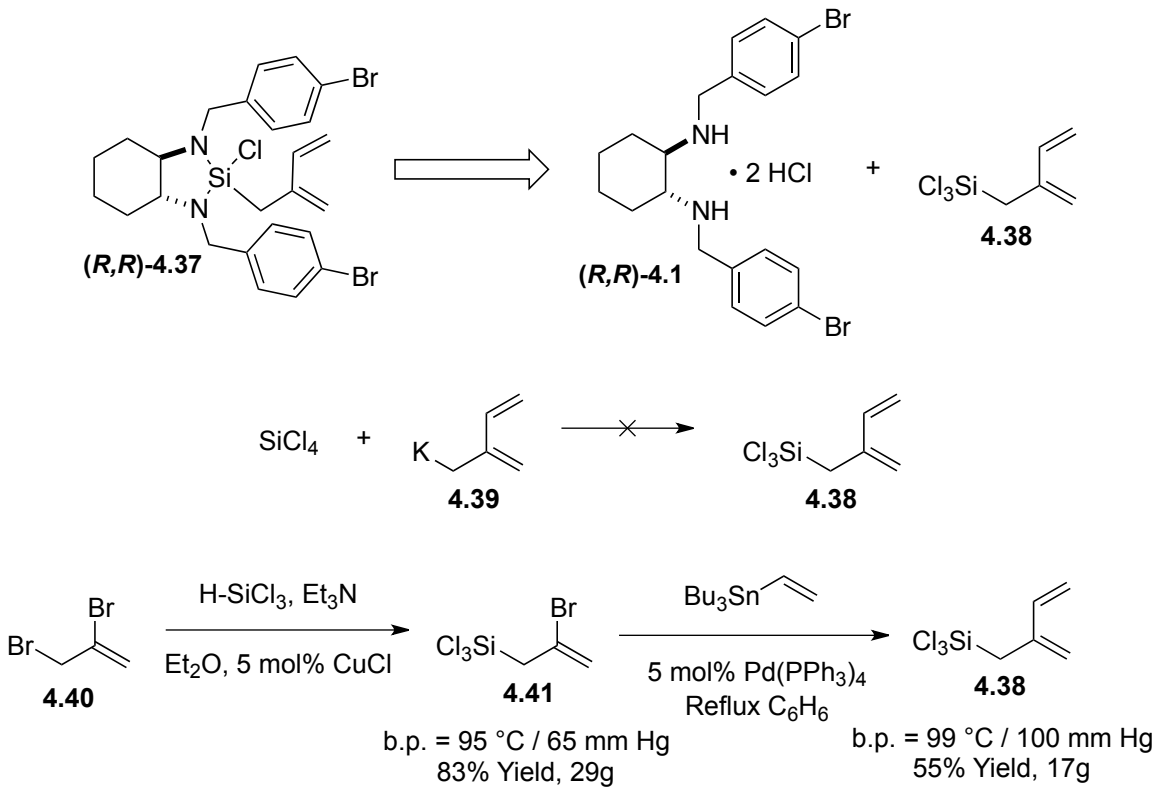

Scheme 4.9: Synthesis of isopenyl-trichlorosilane 4.38

With multi-gram quantities of trichlorosilane **4.38** in hand, we next performed a large scale complexation reaction with diamine **(*R,R*)-4.1** to generate desired reagent **(*R,R*)-4.37** (~80% yield, 80g). This reagent was stored as a stock solution in CH_2Cl_2 for use in a variety of isoprenylation reactions (Scheme 4.10). To our great satisfaction, our new stained silane isoprenylation reagent **(*R,R*)-4.37** provided the desired diene products in high yield and high enantioselectivity for a variety of aldehyde substrates, including the strongly deactivated α-methylcinnamaldehyde **4.48**.

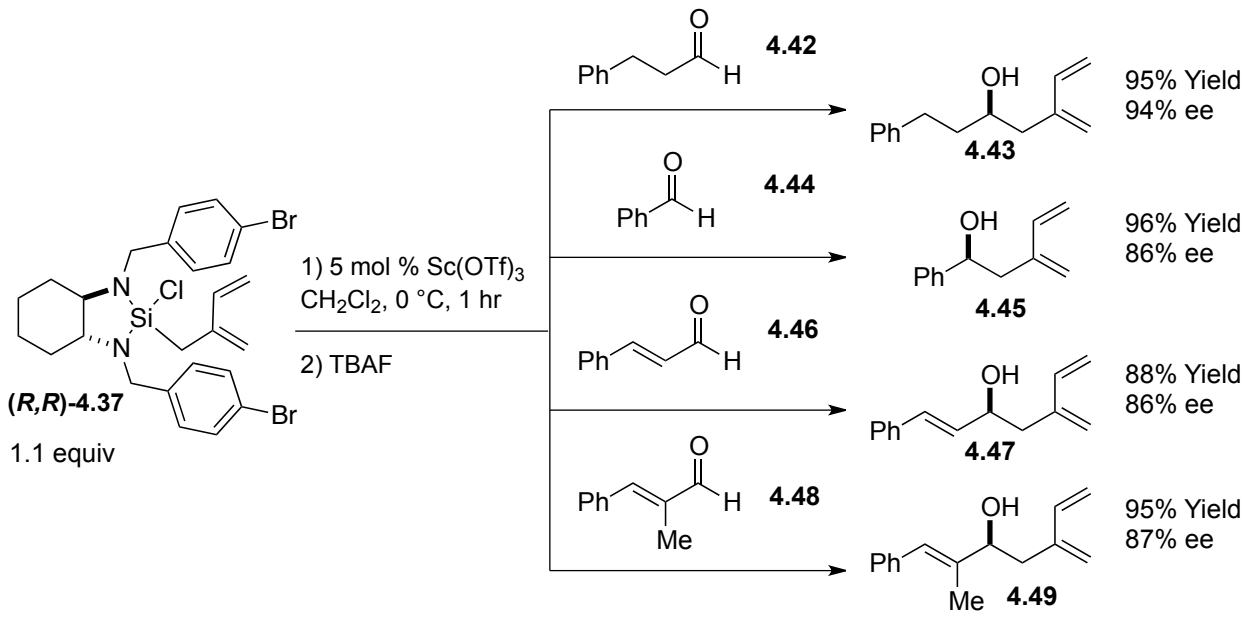

Scheme 4.10: Enantioselective isoprenylation of aldehydes with strained silane 4.37

Given the successful application of our new reagent **(*R,R*)-4.37** on a variety of simple aldehydes, we sought to test its efficacy on a more complex, chiral aldehyde of the type likely to be encountered in polyketide synthesis. Thus, we embarked on the synthesis of chiral aldehyde **4.53** beginning with an enantioselective *syn*-crotylation of hydrocinnamaldehyde **4.42** using our known silane reagent **(*R,R*)-4.50**. The product of this reaction, alcohol **4.51**, was subsequently TES protected and ozonized to give desired chiral aldehyde **4.53** in excellent overall yield (Scheme 4.11).

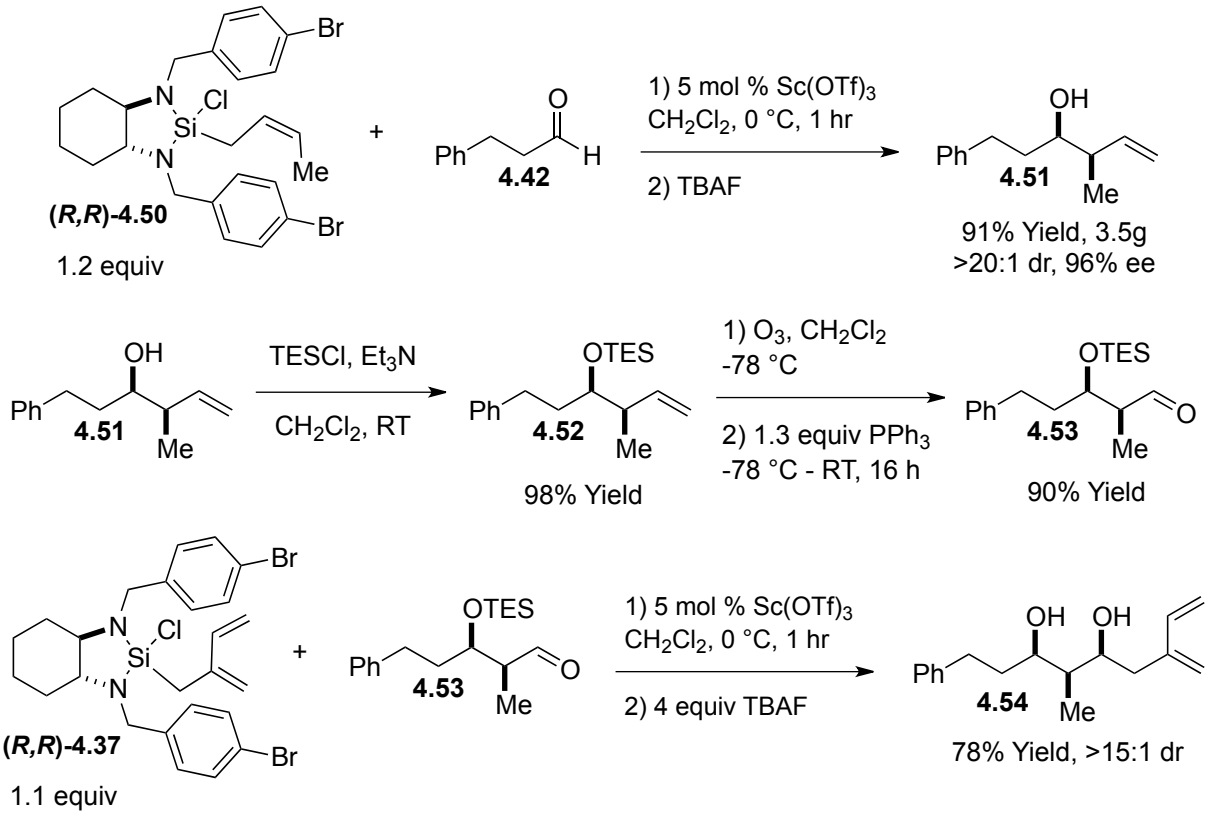

Scheme 4.11: Synthesis and successful isoprenylation of chiral aldehyde 4.53

Following the subjection of chiral aldehyde **4.53** to our new isoprenylation reagent **(*R,R*)-4.37**, we were pleased to isolate diol **4.54**, following an exhaustive TBAF work-up, in good yield and excellent diastereoselectivity as shown above.

With ready access to a variety of relevant diene-polyketide fragments now possible, our next goal was to demonstrate their viability in our intermolecular fragment coupling by crotylation method. Acetylation of dienes **4.43** and **4.54** provided fragment coupling precursors **4.55** and **4.58**. These dienes were subjected to the *syn*-1,4-hydrosilylation and diamine complexation conditions described in Scheme 4.4 and Scheme 4.6 to give angelic silane coupling partners **(*R,R*)-4.57** and **(*R,R*)-4.60** (Scheme 4.12).

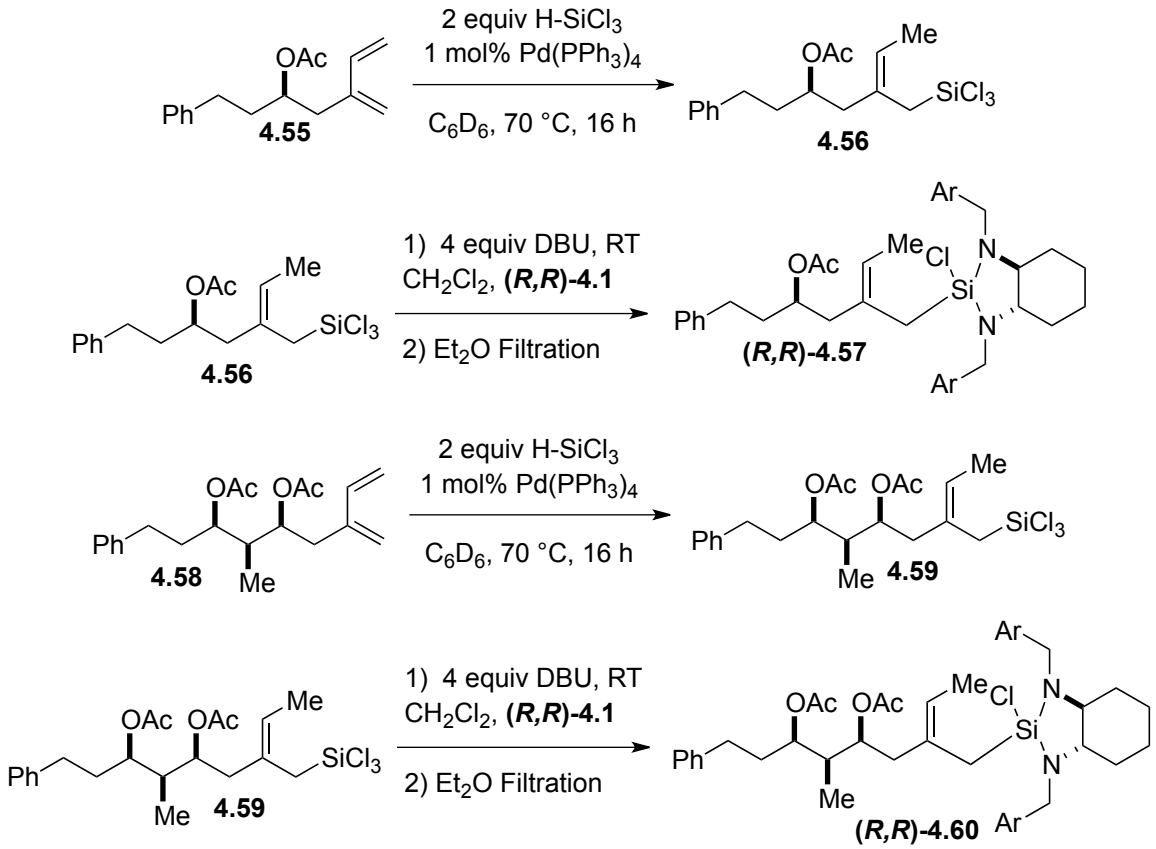

Scheme 4.12: Generation of angelic silane fragment coupling partners

The angelic silanes generated in Scheme 4.12 were immediately reacted with aldehyde coupling partners **4.42** and **4.53** to complete the fragment coupling procedure (Scheme 4.13). The products of these reactions were worked up with excess TBAF to provide the corresponding complex polyketide fragment products. To our delight, this general procedure worked quite well, providing complex polyketide fragments in 73-79% overall yield (3 step yield from starting dienes **4.55** and **4.58**). Also, the procedure was amenable to using the isoprenylation reagent's opposite enantiomer **(*S*,*S*)-4.57** to provide complex polyketide fragment **4.63** in excellent overall yield and comparable selectivities.

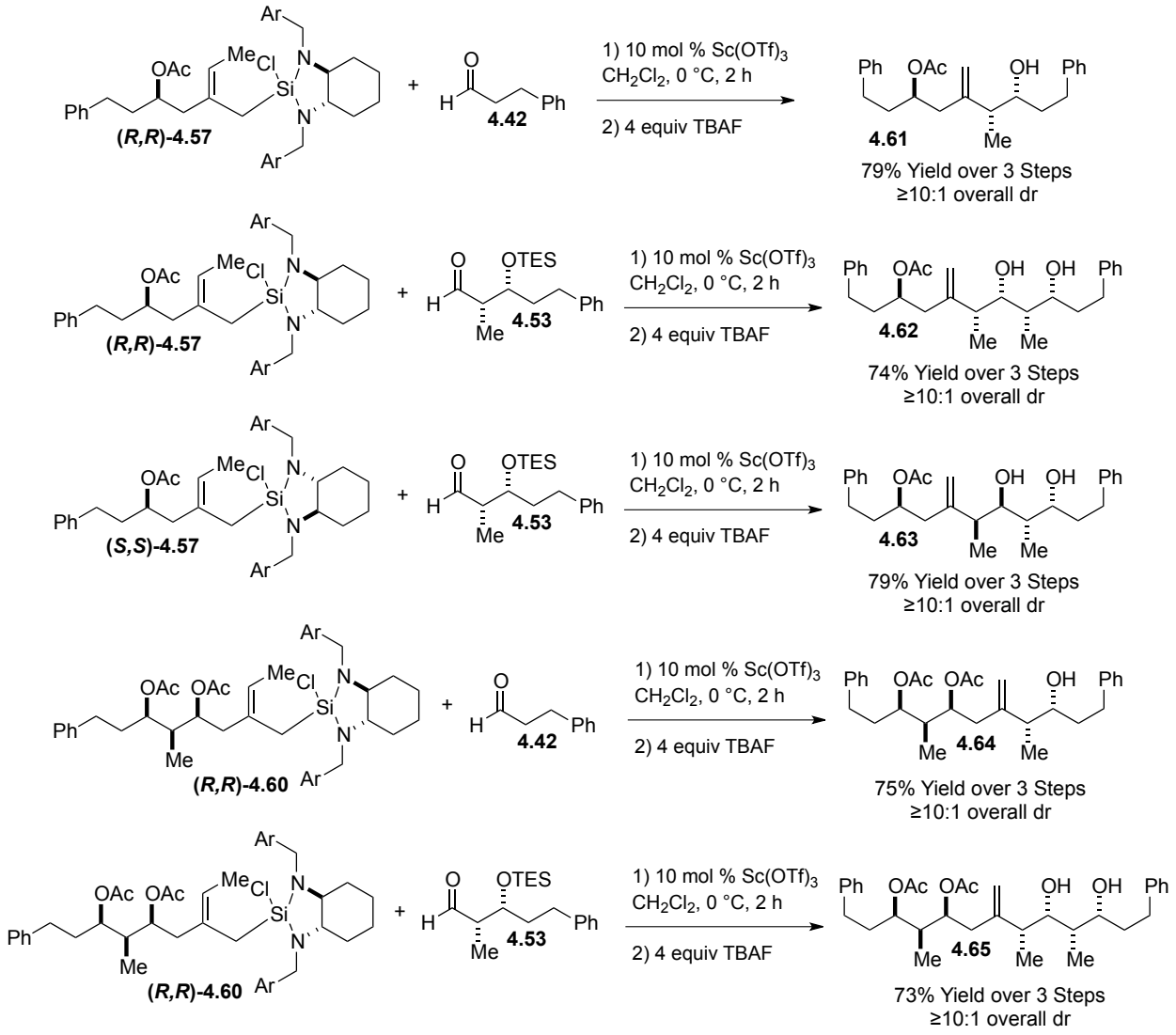

Scheme 4.13: Fragment coupling by crotylation as a general method

The final application of our newly established fragment coupling by crotylation procedure was to use it to crotylate a silacycle aldehyde of type **4.7** followed by our optimized Tamao oxidation to provide the polyketide array highlighted in structure **4.8** (Scheme 4.2). Thus, acetate **4.58** was converted to angelic silane **(*R*,*R*)-4.60** (Scheme 4.12) and reacted with silacycle-aldehyde **4.25** (Scheme 4.14). Pleasingly, we were able to isolate silacycle product **4.66** in excellent overall yield and diastereoselectivity following a mild TBAF•3H_2O work-up.

This silacycle **4.66** was then subjected to our optimized Tamao oxidation conditions (Scheme 4.8) to gratifyingly provide complex polyketide fragment **4.67** in 73% yield and 5:1 overall dr. (Note: Sterochemical proofs verifying the newly formed stereocenters are included in the experimtental section for Chapter 4).

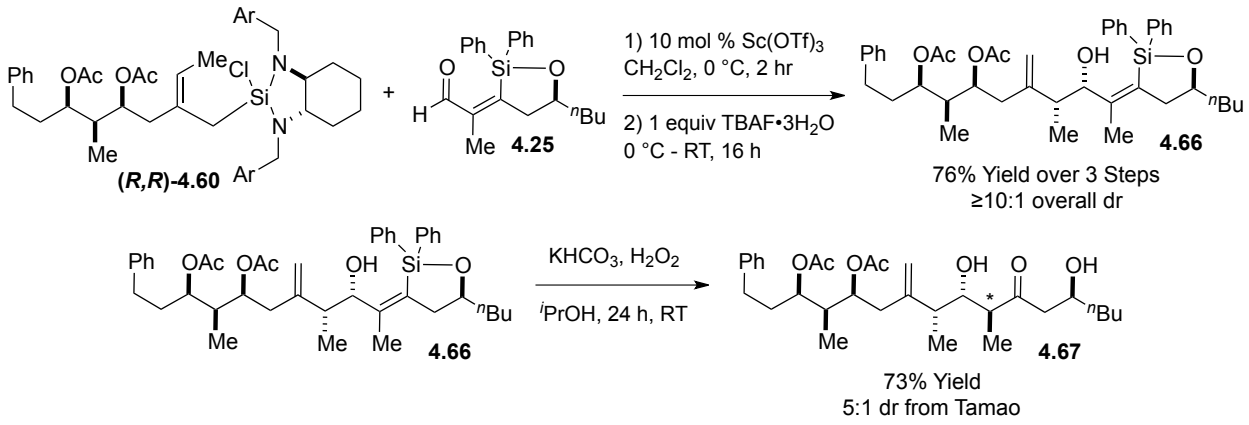

Scheme 4.14: Fragment coupling by crotylation / Tamao oxidation sequence

With our intermolecular fragment coupling by crotylation / Tamao oxidation strategy successfully showcased on the model substrates shown above, we eagerly looked forward to applying this method to the fully elaborated AB and CD fragments of spongistatin 1. Work toward attempting this exciting reaction sequence will be discussed in the following chapter.

4.3 References and Notes

1. Leighton, J. L.; Kim, H.; Ho, S., *J. Am. Chem. Soc.* **2011,** *133* (17), 6517-6520.

2. (a) Kubota, K.; Leighton, J. L., *Angew. Chem. Int. Edit.* **2003,** *42* (8), 946-948; (b) Hackman, B. M.; Lombardi, P. J.; Leighton, J. L., *Org. Lett.* **2004,** *6* (23), 4375-4377.

3. (a) Hara, M.; Ohno, K.; Tsuji, J., *J Chem Soc Chem Comm* **1971,** (6), 247-&; (b) Tsuji, J.; Hara, M.; Ohno, K., *Tetrahedron* **1974,** *30* (14), 2143-2146; (c) Sarkar, T. K., *Synthesis-Stuttgart* **1990,** (11), 969-983.

4. Tokunaga, M.; Larrow, J. F.; Kakiuchi, F.; Jacobsen, E. N., *Science* **1997,** *277* (5328), 936-938.

5. Spletstoser, J. T.; Zacuto, M. J.; Leighton, J. L., *Org. Lett.* **2008,** *10* (24), 5593-5596.

6. Jones, G. R.; Landais, Y., *Tetrahedron* **1996,** *52* (22), 7599-7662.

7. (a) Yu, C. M.; Jeon, M.; Lee, J. Y.; Jeon, J., *Eur. J. Org. Chem.* **2001,** (6), 1143-1148; (b) Brown, H. C.; Randad, R. S., *Tetrahedron* **1990,** *46* (13-14), 4463-4472.

8. Klusener, P. A. A.; Tip, L.; Brandsma, L., *Tetrahedron* **1991,** *47* (10-11), 2041-2064.

9. (a) Furuya, N.; Sukawa, T., *J Organomet Chem* **1975,** *96* (1), C1-C3; (b) Stille, J. K.; Groh, B. L., *J. Am. Chem. Soc.* **1987,** *109* (3), 813-817.

Chapter 5: Large Scale Synthesis of AB Fragment and ABCD Coupling

5.1 The Scalable Synthesis of AB Fragment Spiroketal-Diene

Confident that our intermolecular fragment coupling by crotylation / Tamao oxidation sequence described in Chapter 4 could be employed to join the AB and CD fragments of spongistatin 1, we next embarked on the development of a truly scalable synthesis of the AB fragment of spongistatin 1. Though a first generation synthesis of the AB fragment had already been established (Chapter 3, Section 2), the advent of our enantioselective isoprenylation methodology (Chapter 4, Section 2) inspired the more concise retrosynthesis of the AB spiroketal-diene **5.1** shown below (Scheme 5.1).

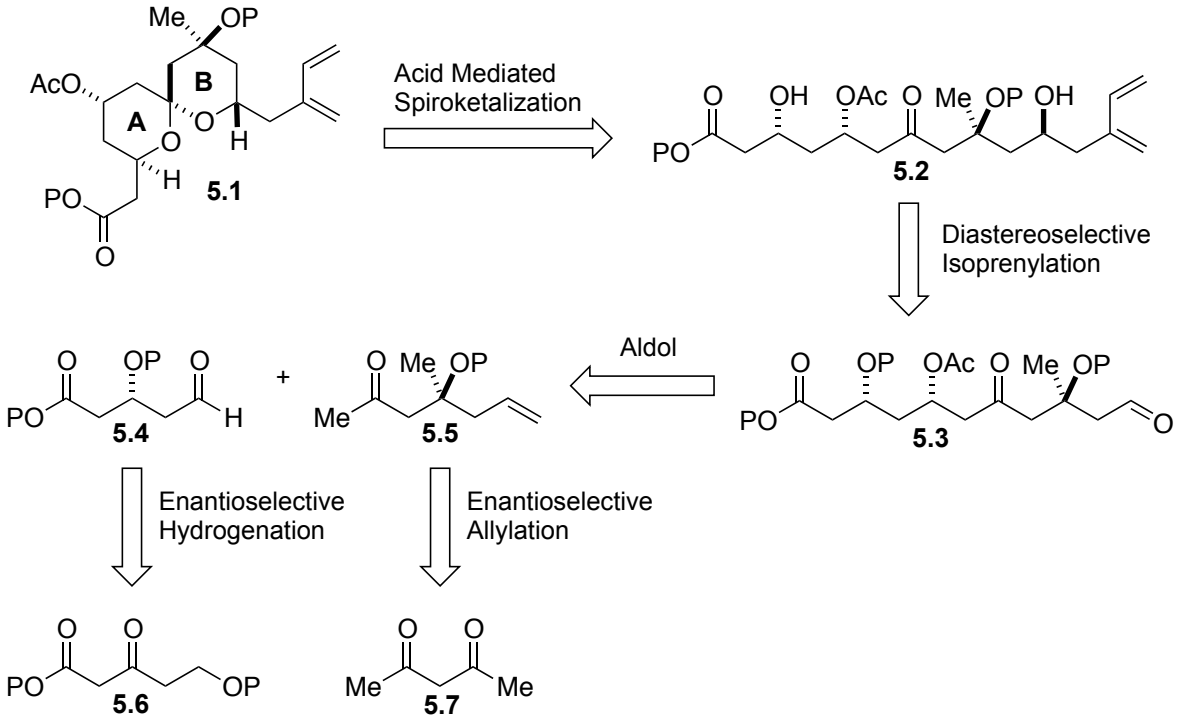

Scheme 5.1: Revised retrosynthetic analysis for AB fragment spiroketal-diene 5.1

As depicted above, our retrosynthesis takes advantage of the doubly-anomeric nature of the AB spiroketal **5.1** by concluding with an acid-mediated, thermodynamically controlled spiroketalization of acyclic diene **5.2**. We proposed that diene **5.2** would arise from the implementation of our asymmetric isoprenylation reaction on an aldehyde **5.3** and that aldehyde **5.3** would be formed through a convergent aldol coupling of aldehyde subunit **5.4** and densely functionalized ketone **5.5**. The chirality of these key subunits could potentially be set through the use of an enantioselective hydrogenation and an enantioselective allylation procedure, which will be described below.

When considering the synthesis of tertiary alcohol **5.5**, it came to our attention that there were no direct methods to obtain it through the enantioselective allylation of acetylacetone **5.7**, as proposed in Scheme 5.1. This seemed to be a consequence of the fact that the vast majority of known enantioselective ketone allylation strategies are only effective on aryl ketone substrates.[1] Furthermore, even if the most promising of these allylation strategies[1f] were found to be amenable to our particular substrate, in order to obtain the desired product in high-yield, one of the ketone moieties in acetylacetone **5.5** would have to be selectively protected and then revealed following the allylation procedure.

Given our unwavering commitment to the development of an expedient and scalable synthesis to access large quantities of the AB spiroketal **5.1**, this multi-step work-around for the enantioselective allylation of acetylacetone was deemed unacceptable. As such, we considered a novel application of our strained silane reagents[2] in the context of β-diketone allylation. Though our strained silane reagents were known to be wholly incapable of allylating ketones, even in the presence of $Sc(OTf)_3$, we thought that the latent nature of β-diketones to exist as their enol tautomers could perhaps allow for a uniquely effective mode of reactivity (Scheme 5.2).

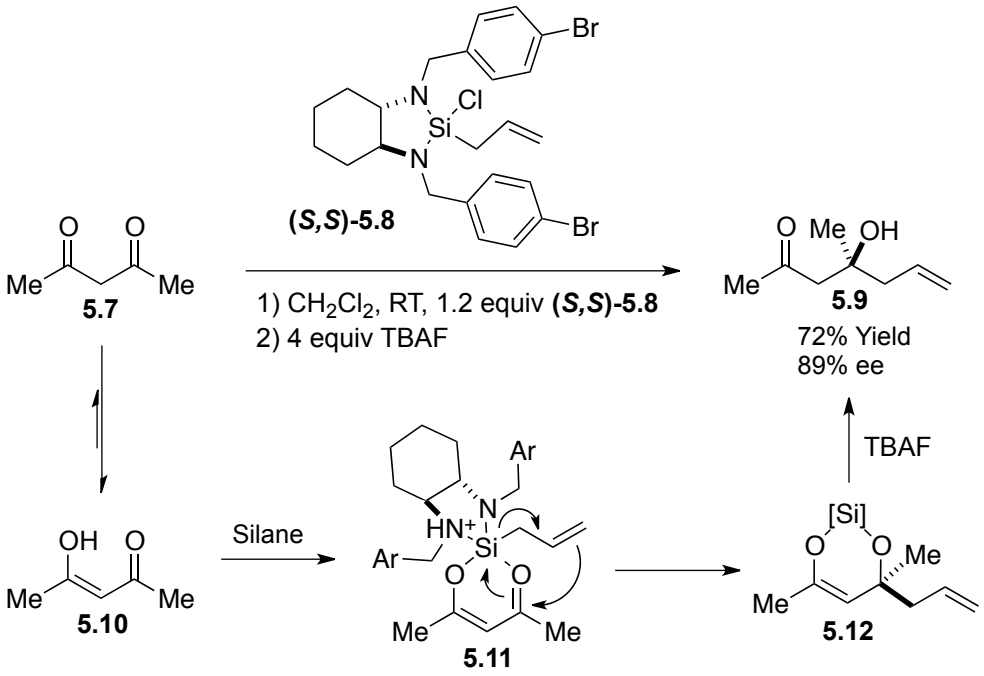

Scheme 5.2: Seminal enantioselective allylation of β-diketones

To our delight, our proposed application of strained silane **(*S,S*)-5.8** to the enantioselective allylation of acetylacetone **5.7** worked exceedingly well. As depicted in our mechanistic scheme above, we believe that the enol form of acetylacetone **5.10** initially reacts with chlorosilane **(*S,S*)-5.8** to generate a local equivalent of HCl. As seen in other applications of the Leighton laboratory's silane reagents,[3] protonation by Brønsted acid strongly augments the electrophilicity of the strained silanes. Given that silane **(*S,S*)-5.8** was tethered to acetylacetone **5.10** in the form of a vinylogous silyl-ester **5.11**, the intramolecular proximity of the otherwise unreactive carbonyl allows for the enantioselective allylation event to occur. In-depth mechanistic elucidation, expansion of the substrate scope to unsymmetrical β-diketones, and extension of this reaction platform to enantioselective crotylations have been dutifully and beautifully achieved through the tireless work of Dr. Wesley Chalifoux. The culmination of these studies has resulted in an unprecedented, general strategy for the enantioselecive allylation of β-diketones.[4]

For the purposes of our scalable synthesis of the AB fragment of spongistatin 1, we felt it was important to develop conditions under which chiral diamine **(*S,S*)-5.13** could be recovered following the enantioselective allylation of acetylacetone **5.7** (Scheme 5.3). To this end, we developed a sequential TBAF/HCl work-up that allowed for the isolation of alcohol **5.9** in good yield and facilitated excellent recovery of the chiral diamine **(*S,S*)-5.13**. Tertiary alcohol **5.9** was then TES protected to afford ketone **5.14** in excellent yield.

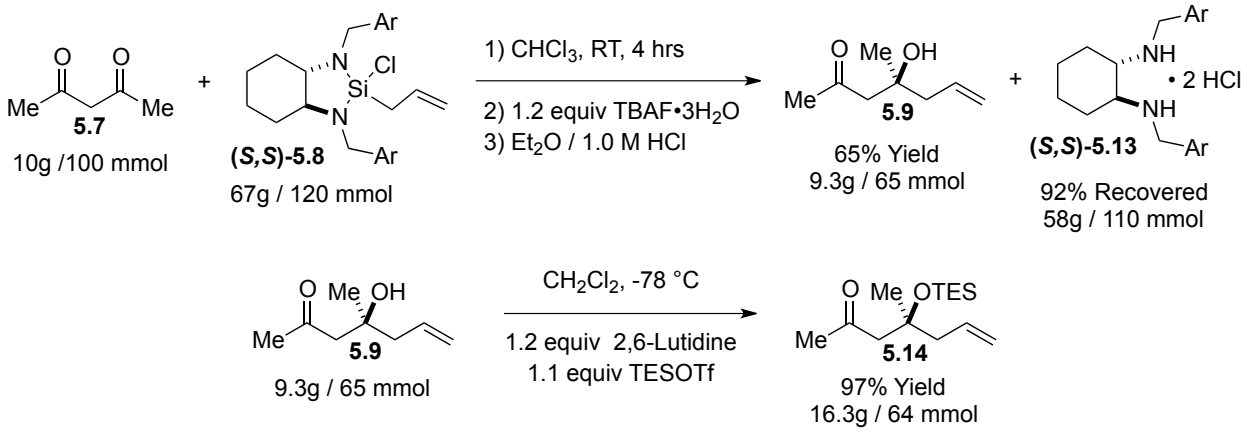

Scheme 5.3: Large-scale access to ketone subunit 5.14

With large quantities of ketone **5.14** in hand, we turned our attention to the scalable synthesis of subunit **5.6** (Scheme 5.1). Before beginning this task, we first had to select an appropriate protecting group for the ester functionality that could be carried through the ABCD fragment coupling sequence. A survey of the spongistatin literature[5] indicated that the alloc group would be most amenable to late-stage deprotection,[6] but considering that our key fragment coupling by crotylation procedure required a palladium(0) mediated 1,4-hydroslilylation (Chapter 4, Section 1), we worried that this protecting group would not survive. This fear was confirmed in model study experiments, which led us to ultimately select the TMSE protecting group instead (Scheme 5.4).

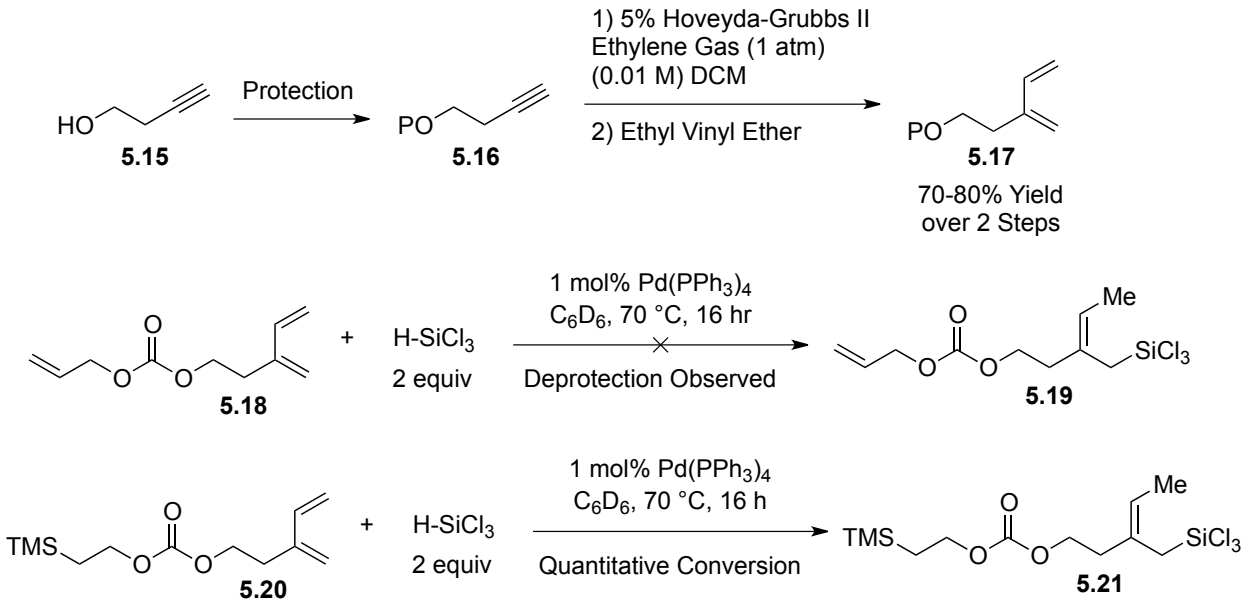

Scheme 5.4: Protecting group screen under 1,4-hydrosilylation conditions

Once we had selected an appropriate ester protecting group, we sought to synthesize β-keto ester **5.24** (Scheme 5.5). Our first efforts toward this synthetic goal centered on using a Claisen-type reaction between chloroformate **5.22** and ketone **5.23** to access the desired β-keto ester **5.24**. This proved to be unsuccessful under a variety of conditions. We also attempted to augment the overall functional group reactivity in the Claisen-type reaction by replacing substrates **5.22** and **5.23** with ester **5.25** and acyl chloride **5.26**, respectively. This method did provide some of the desired product, albeit in unacceptably low yields. Next, we attempted to access β-keto ester **5.24** through a successive aldol coupling between ketone **5.25** and aldehyde **5.27** followed by oxidation. Though this method worked to some degree, the results of these experiments were both low yielding and irreproducible. Finally, we attempted a bis-acetylation of TMS-ethanol followed by a dianionic BOM-Cl alkylation[7] of the resulting β-keto ester **5.29** to obtain desired product **5.24**. This two-step sequence worked in good yield and was quite amenable to large-

scale production as shown below (Note: the 1 M HCl work-up of compound **5.29** was critical to preventing its rearrangement to an unknown side-product).

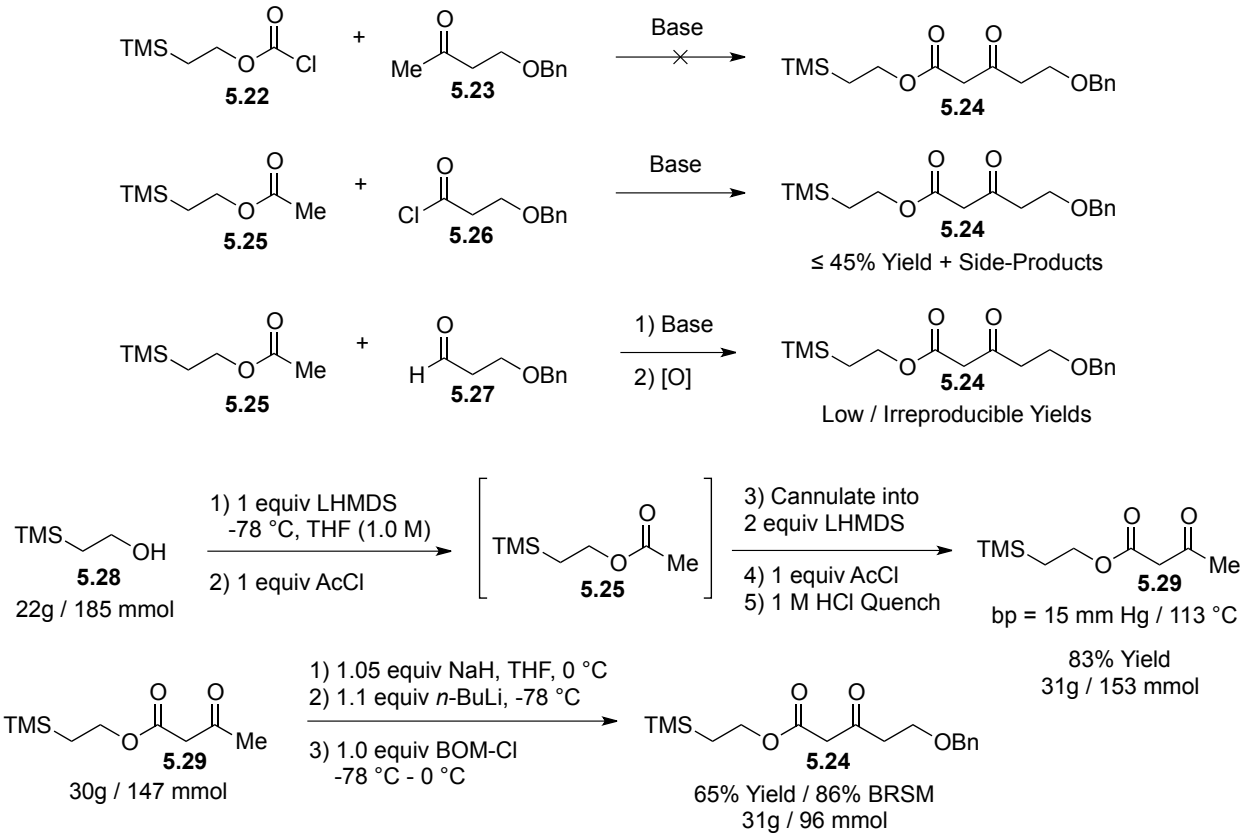

Scheme 5.5: Large-scale bis-acetylation and alkylation to give β-keto ester 5.24

The conversion of β-keto ester **5.24** to alcohol subunit **5.32** proceeded smoothly over a three-step operation, only requiring chromatography at the conclusion of the sequence (Scheme 5.6). β-keto ester **5.24** successfully underwent Noyori hydrogenation to establish the alcohol stereocenter in 96% ee.[8] Though this reaction was performed under typical hydrogenation conditions, it was found that the use of 1:1 THF:MeOH mixed solvent system was critical for clean conversion to product. Alcohol **5.30** was readily TES protected to give compound **5.31**, which was subsequently subjected to debenzylation conditions that provided alcohol **5.32** in

excellent overall yield. It is worth noting, however, that the rate of debenzylation was greatly dependent on the quality of the $Pd(OH)_2$ employed, requiring anywhere from 1.5-6 h. The reaction progress was carefully monitored and stopped before significant hydrogenative cleavage of the TES-ether could occur.[9] (Note: Due to these inconsistent reaction times, a continued search for a reliable combination of reaction solvent and palladium source is recommended).

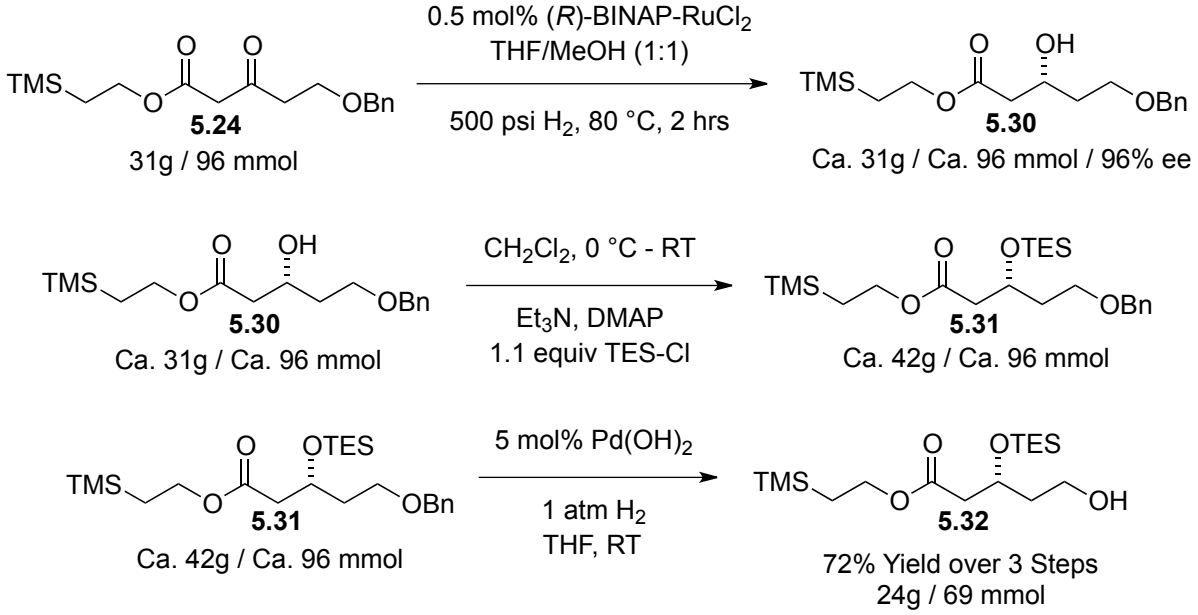

Scheme 5.6: Large-scale hydrogenations used to access alcohol 5.32

With ketone subunit **5.14** and alcohol subunit **5.32** in hand, we sought to bring these compounds together through a Paterson aldol reaction (Scheme 5.7). First, alcohol **5.32** was oxidized to aldehyde **5.33** using Swern oxidation conditions. The crude aldehyde **5.33** was filtered over a pad of pH 7 buffered SiO_2 gel and taken on to the Paterson aldol reaction without further purification. The Paterson aldol proceeded smoothly to provide desired coupled fragment **5.34** in high overall diastereoselectivity. Though this product was difficult to separate from the isopinocamphenol reaction byproduct, exhaustive acetylation of the semi-crude mixture allowed

for the straightforward purification of acetate **5.35** by column chromatography. The entire three-step sequence was highly efficient, providing acetate **5.35** in 72% overall yield on large-scale.

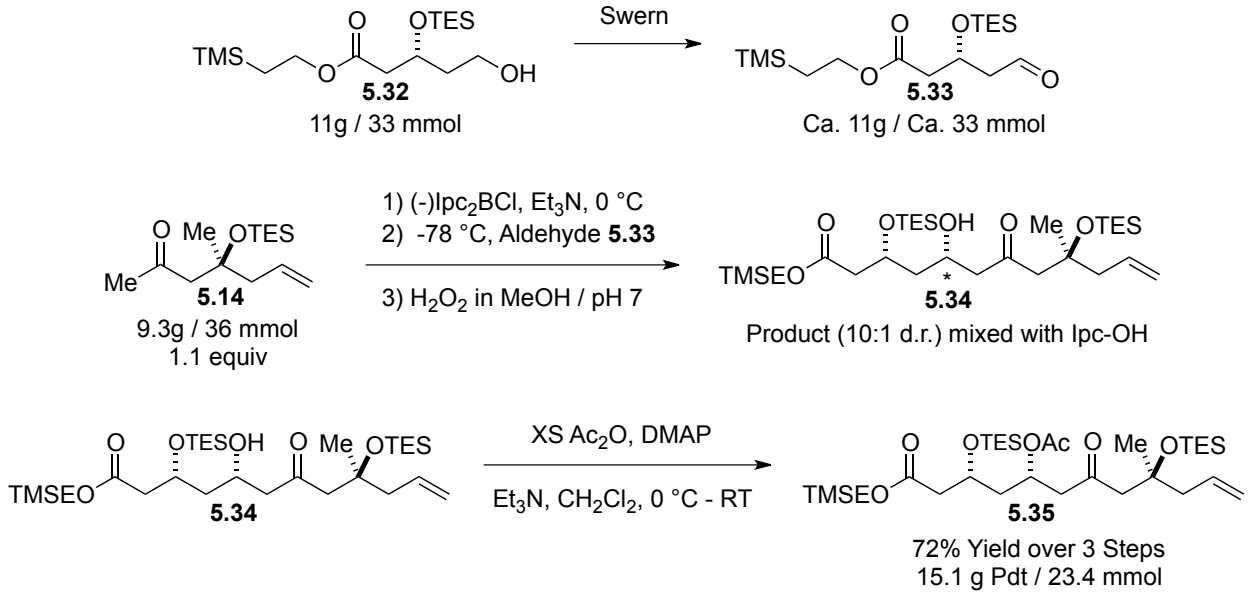

Scheme 5.7: Large-scale Paterson aldol providing access to alkene 5.35

After producing large quantities of alkene **5.35** we next converted it to desired aldehyde **5.36** through the use of an ozonolysis procedure followed by a PPh_3-mediated reduction of the resulting ozonide. Though we found aldehyde **5.36** to be sensitive to purification by SiO_2 gel chromatography, we were able to isolate the desired compound in acceptable purity by triturating out the unwanted phosphines from a solution of hexanes. (Note: Small amounts of leftover phosphines exhibited no deleterious effects on the subsequent chemistry). With aldehyde **5.36** finally in hand, we subjected it to the asymmetric isoprenylation reagent **(*R,R*)-5.37** developed in Chapter 4, Section 2 (Scheme 4.10). Gratifyingly, the isoprenylation procedure worked quite well on this highly functionalized polyketide fragment, providing lactol **5.38** following a mild TBAF•$3H_2O$ work up and filtration over a plug of SiO_2 gel to remove the chiral diamine (Scheme 5.8). This lactol **5.38** was taken on without further purification to the acid-mediated

spiroketalization, which pleasingly cleaved both of the silyl-ethers in the molecule and provided the doubly-anomeric AB-spiroketal **5.39** as a single isolable diastereomer in 66% yield over the three-step sequence.

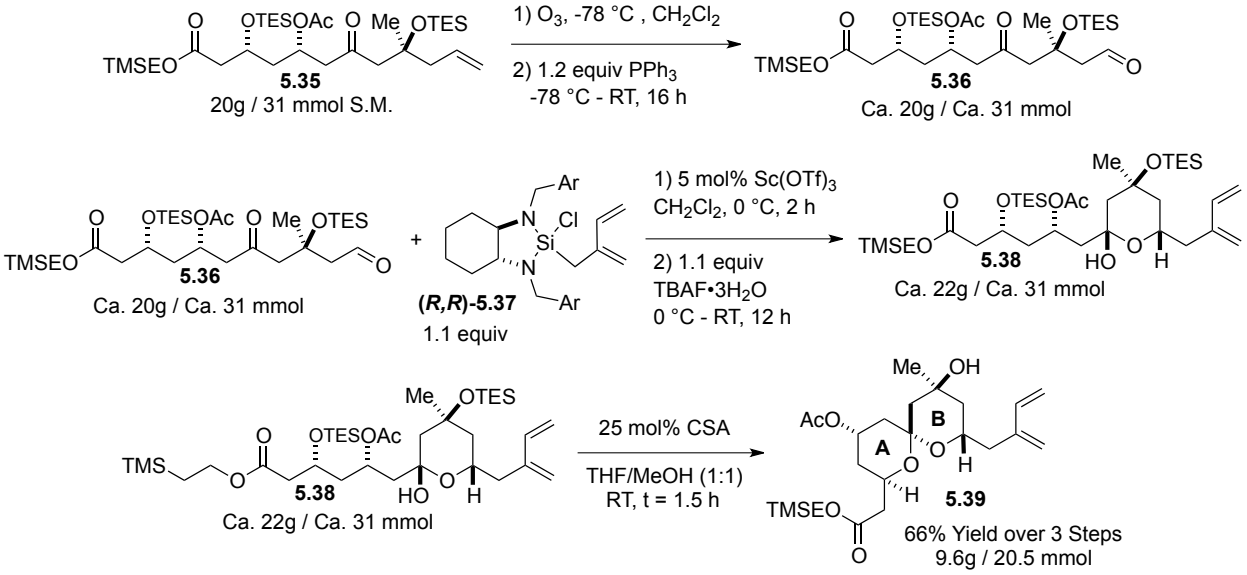

Scheme 5.8: Large-scale diastereoselective isoprenylation and spiroketalization

Since none of the intermediates on our route were crystalline solids that could be readily submitted for X-ray analysis, we paused at this point to run a battery of COSY and nOe experiments on AB-spiroketal **5.39** in order to confirm the molecule's relative stereochemical configuration. To our satisfaction, all of the pertinent nOe relationships were observed (Scheme 5.9). Furthermore, if we are to assume that the absolute stereochemical induction of the well precedented Noyori hydrogenation[8] held true for the generation of alcohol **5.30**, then this nOe analysis served to confirm the correct absolute stereochemical configuration of AB-spiroketal **5.39** as well.

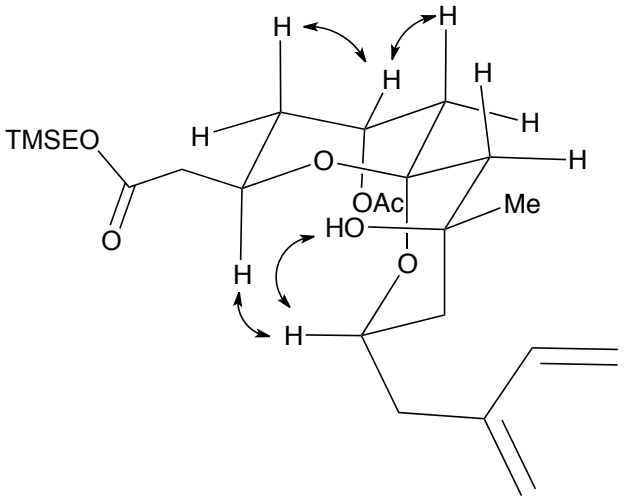

Scheme 5.9: nOe correlations assigning all stereocenters in AB spiroketal 5.39

With the relative stereochemistry of AB-spiroketal diene **5.39** fully established, it was nearly time to test the AB fragment in the key intermolecular fragment coupling sequence. All that remained was the protection of the free, tertiary alcohol in compound **5.39**. Though we had previously been able to TES protect this position with TESOTf (Chapter 3, Section 2, Scheme 3.27) we also knew from control studies performed in Chapter 4, Section 1 (Scheme 4.4) that silyl-ethers were not compatible with the upcoming *syn*-1,4-hydrosilylation procedure. Thus, we embarked on a lengthy search for a suitable protecting group that would satisfy all our synthetic needs (Table 5.1).

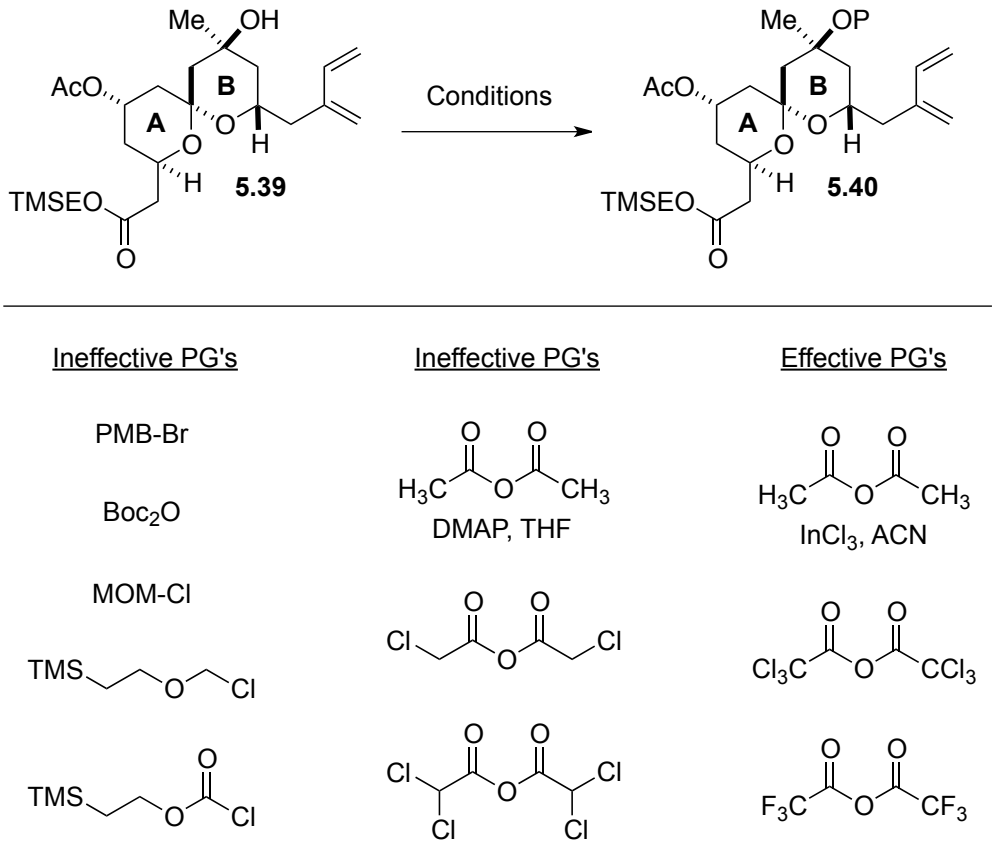

Table 5.1: Protecting group screen for hindered, axial 3° alcohol 5.39

As seen in the table above, due to the extraordinarily hindered stereochemical environment surrounding the axial, tertiary alcohol position of spiroketal **3.59**, very few functional groups were amenable to its protection. Though we were able to affect its protection using acetetic anhydride in conjunction with a somewhat exotic $InCl_3$ catalyzed procedure,[10] it was not clear how we would selectively deprotect this group in the presence of spongistatin 1's secondary acetate on the A ring. Trichloroacetic anhydride turned out to provide reasonable protection of alcohol **3.59** (ca. 75% yield), but it was later found to be incompatible with the 1,4-hydrosilylation procedure. Somewhat surprisingly, trifluoracetic anhydride (TFAA) was discovered to be an extremely effective protecting group, serving to provide protected tertiary

trifluoroacetate **5.41** in nearly quantitative yields (Scheme 5.10). The TFA ester was remarkably stable on our molecule, including its ability to survive the 1,4-hydrosilylation reaction, presumably as a consequence of its extremely congested steric environment and short bond-lengths. Furthermore, it was found after some experimentation that the TFA ester could be mildly and selectively cleaved by stirring compound **5.41** in a concentrated solution of NH_3 in ethanol.

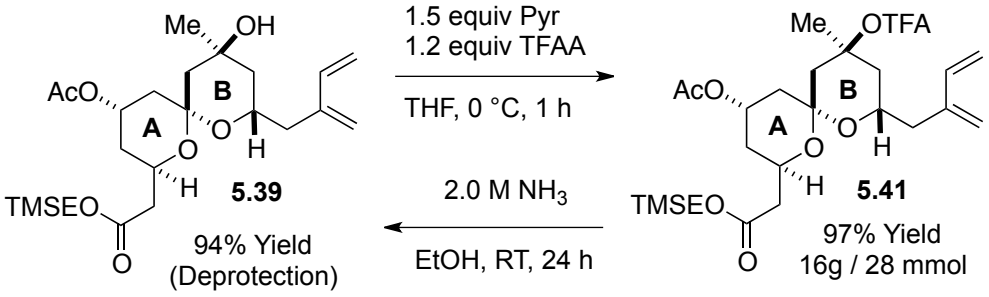

Scheme 5.10: Trifluoroacetate as a suitable protecting group for 3° alcohol 3.59

With the full elaboration of the AB fragment spiroketal-diene **5.41** complete, it is worth taking a moment to comment on the remarkable scalability of the synthetic route described in this section. As has been noted throughout the schemes, every reaction in this sequence has been performed on greater than a 10g scale (and often greater than a 20g scale) while still giving high yields of product. The longest linear sequence for the entire AB fragment is 12 steps with only 14 total steps required for the entire sequence. The overall yield of the elaborated AB fragment synthesis is 17.9% (23.7% BRSM). Furthermore, the number of chromatographies in the sequence has been minimized to just 5 full chromatographic purifications. This last accomplishment has greatly facilitated the large-scale execution of the route, resulting in the ability for a single chemist to readily synthesize over 34.5g of the complete AB fragment **5.41** in merely 3 months time, and for less than $10,000 of chemical reagents and supplies. To date, the

synthetic efforts of this author have resulted in the generation of 43.5g of the AB fragment, a picture of which is included below (Figure 5.1).

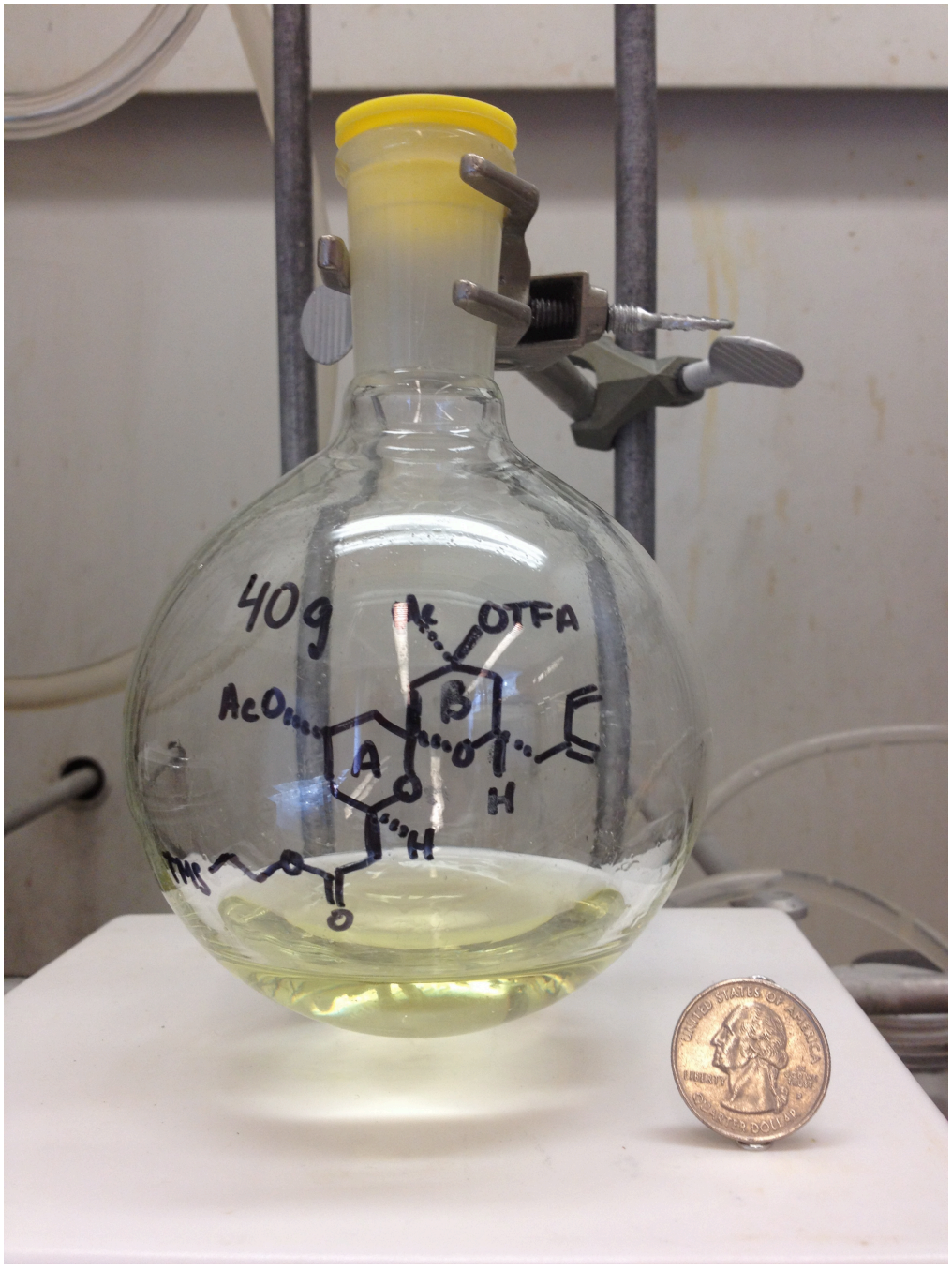

Figure 5.1: Over 40g of the fully elaborated AB fragment of spongistatin 1

5.2 Key Coupling Reaction and Final Elaboration of the ABCD Hemisphere

Given the unexpected failure of our previous intramolecular coupling strategy at the end of Chapter 3, we approached the intermolecular coupling of the fully elaborated AB and CD fragments with some trepidation. Thanks to the diligent work of Dr. Ryan Shade, several grams of the PMB protected CD fragment bicycle **5.42** (Chapter 3, Section 1) were available for immediate use with the large stockpile of AB fragment diene **5.41** generated above.

The first task required for the intermolecular coupling sequence was the conversion of PMB protected CD fragment bicycle **5.42** to silacycle-aldehyde **5.44** (Scheme 5.11). This sequence proceeded smoothly, efficiently providing compound **5.44**. Due to the sensitivity of the silacycle-aldehyde moiety to purification by SiO_2 gel chromatography, compound **5.44** was taken on to the key coupling reaction without purification.

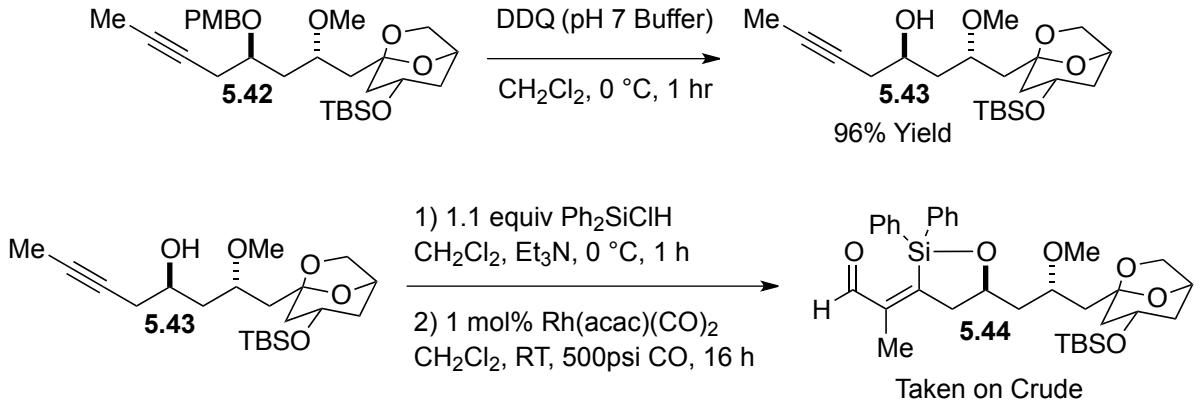

Scheme 5.11: Preparation of CD silacycle-aldehyde fragment coupling partner 5.44

At this point, AB spiroketal diene **5.41** was converted to angelic silane **(*R,R*)-5.46** according to the method developed in Chapter 4, Section 1 (Scheme 5.12). Pleasingly, this operation proceeded smoothly on the fully functionalized AB spiroketal, efficiently providing silane **(*R,R*)-5.46**, which was also taken on to the key coupling without purification.

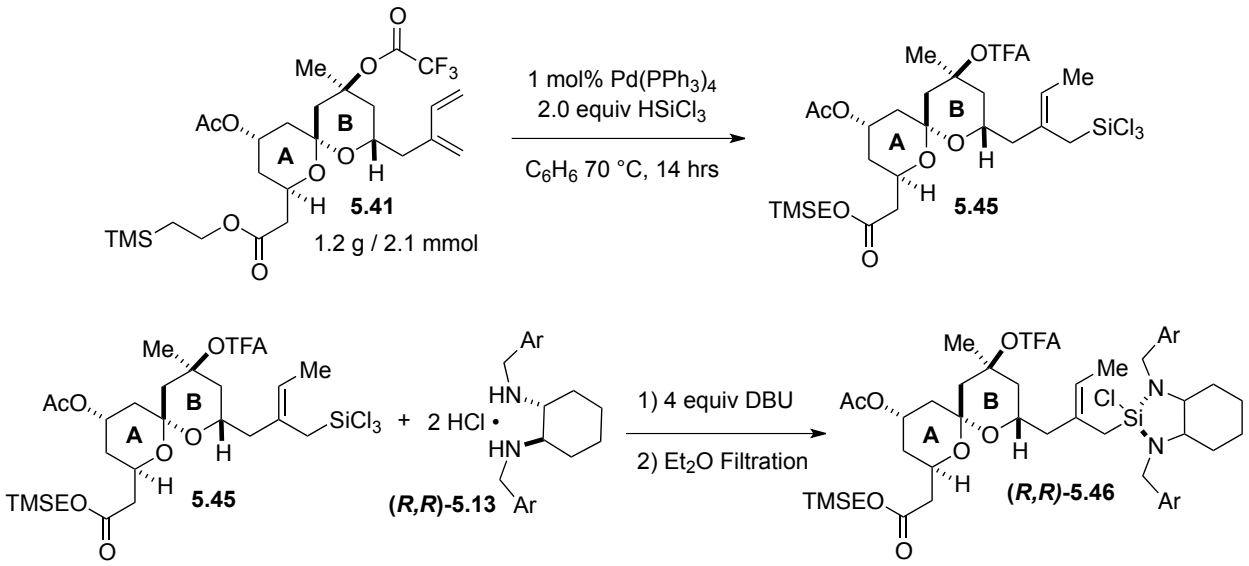

Scheme 5.12: Preparation of angelic-silane coupling partner (*R,R*)-5.46

Now that coupling partners **5.44** and **(*R,R*)-5.46** had been fully prepared, the stage was set to attempt our key intermolecular fragment coupling by crotylation / Tamao oxidation sequence with the aim of uniting the ABCD hemisphere of spongistatin 1. Thus, we reacted angelic-silane **(*R,R*)-5.46** with silacycle-aldehyde **5.44** in the presence of catalytic $Sc(OTf)_3$ and utilized our mild TBAF•$3H_2O$ conditions to work up the reaction (Scheme 5.13). To our unparalleled delight, the key fragment coupling worked as envisioned, providing the coupled ABCD hemisphere silacycle **5.47** in 55% yield over the three-step sequence from diene **5.41**. The efficiency of this fragment coupling averages to over 80% yield per step, a remarkable achievement considering the complexity of the fragment coupling substrates involved and the number of chemical manipulations successfully achieved. It is worth noting that a significant amount of unreacted silacycle-aldehyde **5.44** was recovered during the reaction purification (ca. 30%), indicating that the conversion of diene **5.41** to angelic-silane **(*R,R*)-5.46** was the limiting factor in the sequence and perhaps merited further optimization. Finally, it should also be noted

that this reaction was performed on the gram-scale (1.3g / 1.1 mmol of coupled ABCD fragment was isolated), effectively demonstrating the transformation's general robustness and potential for use in a muli-gram synthesis of spongistatin 1.

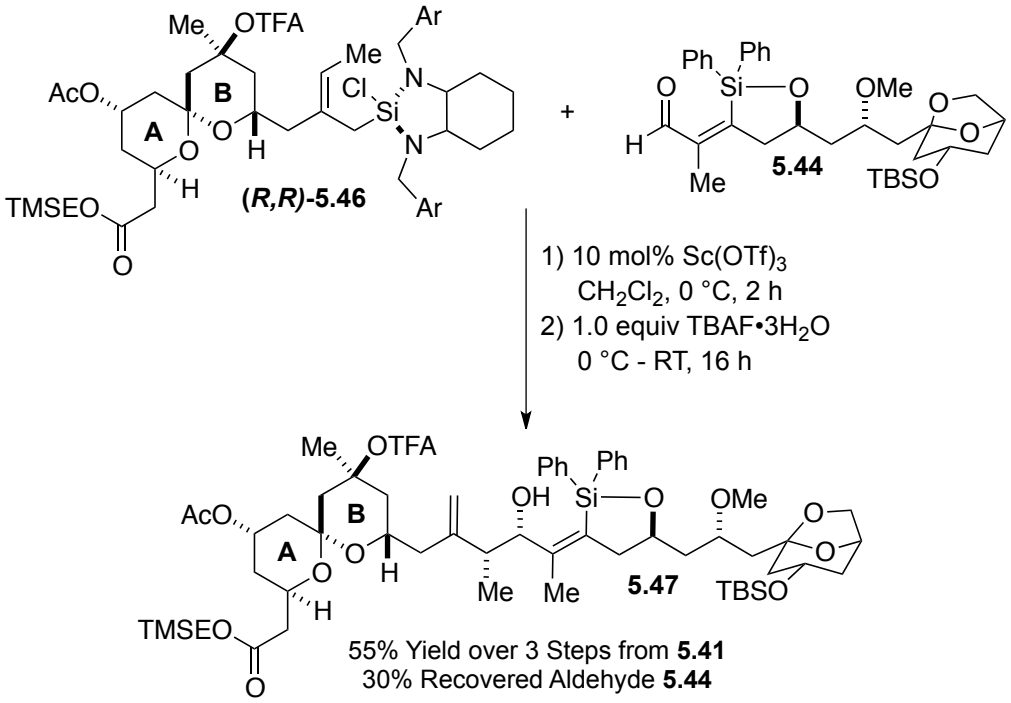

Scheme 5.13: Intermolecular ABCD fragment coupling by crotylation

With successfully coupled ABCD silacycle **5.47** in hand, we next subjected it to our optimized Tamao oxidation conditions described in Chapter 4, Section 1 and shown in Scheme 5.14 below. As was expected, the large steric bulk of the AB spiroketal had a detrimental effect on the diastereoselectivity of our protic Tamao oxidation (4:1 dr). Despite this result, we were still able to generate compound **5.48** in good overall yield, fully establishing the highly functionalized polyketide array that bridges the AB and CD spiroketals of spongistatin 1. Though the diastereoselectivity of the Tamao oxidation was only moderate, it was possible to

cleanly isolate the desired diastereomer of compound **5.48** through careful chromatographic purification.

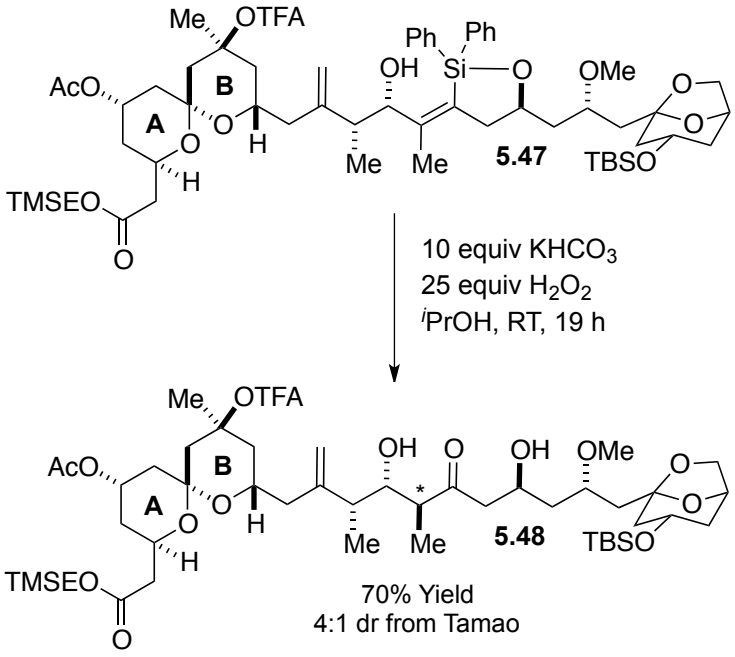

Scheme 5.14: Tamao oxidation to establish complex ABCD polyketide array

Having successfully employed our fragment coupling by crotylation / Tamao oxidation sequence to join the AB and CD fragments of spongistatin 1, all that remained in our synthesis was the formation of the CD spiroketal and final elaboration of the ABCD fragment. Unfortunately, a cursory screen of potential Lewis and Brønsted acids gave us little hope of kinetically setting the desired "non-anomeric" CD spiroketal;[11] the doubly-anomeric CD spiroketal was consistently isolated in a ratio ranging from 3:1 dr using HF•H_2O to 8:1 dr using CSA. However, since the Smith group had already demonstrated the ability to reequilibrate the C(23) center of spongistatin 1 to the desired anomer using $HClO_4/Ca(ClO_4)_2$ once the entire macrolide was assembled,[12] we chose to simply carry the undesired, but readily prepared, doubly-anomeric CD spiroketal through the remainder of our synthesis (Scheme 5.15).

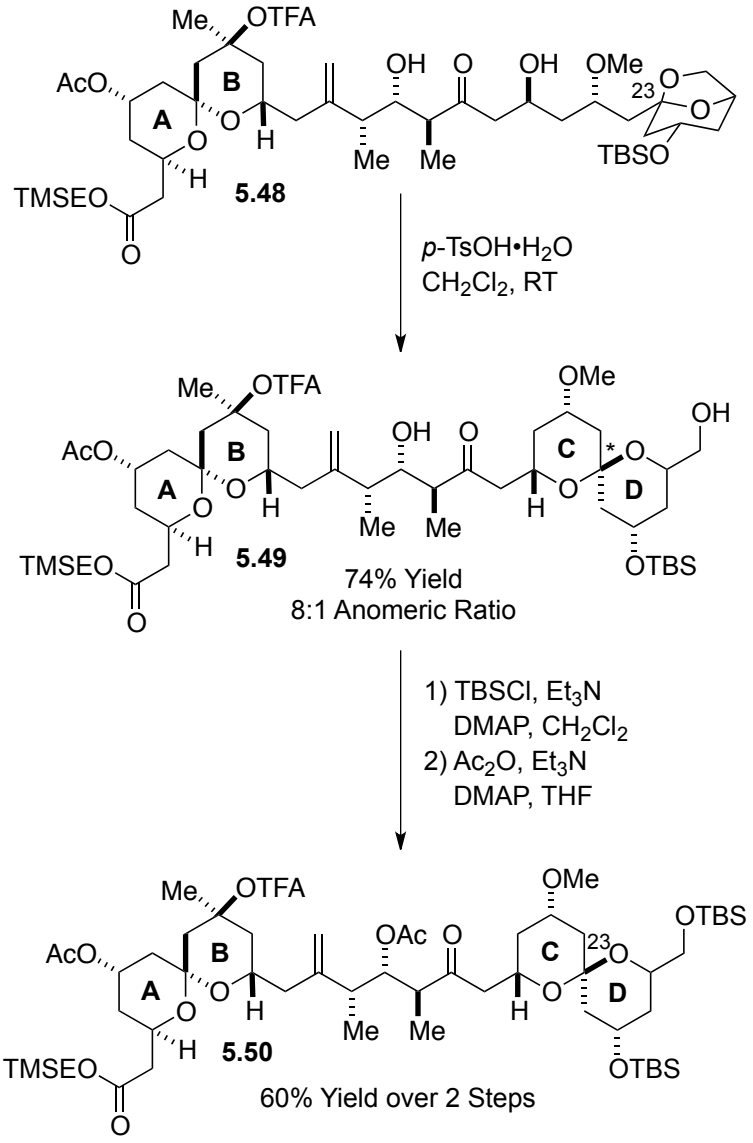

Scheme 5.15: Final elaboration of the protected C(23)-*epi*-ABCD hemisphere 5.50

As shown above, the final elaboration of the C(23)-epimer of ABCD hemisphere **5.50**, was achieved in good yield over a three-step sequence. This marked the completion of our ABCD fragment synthesis. Though not technically a formal synthesis of spongistatin 1 due to modifications in the protecting group strategy, we have preliminary evidence indicating that

compound **5.50** could be converted to known intermediates from previous total syntheses of spongistatin 1.[5]

5.3 Long-Term Goals of the Leighton Group's Spongistatin Research Program

Though the completed synthesis of the ABCD fragment of spongistatin 1 was an exciting achievement, the overarching goal of the Leighton laboratory always centered on the desire to develop a synthetic strategy that would allow spongistatin 1, or an analog thereof, to reach the global market as a potent chemotherapy agent. In light of the recent discovery by the Smith group, that a diminutive, ABEF congener of spongistatin 1 **5.51** retains a significant amount of anti-tumor bioactivity relative to the natural product **5.52** (Scheme 5.16),[13] we began to consider a plausible strategy for the rapid the synthesis of a variety of bioactive analogs of spongistatin 1.

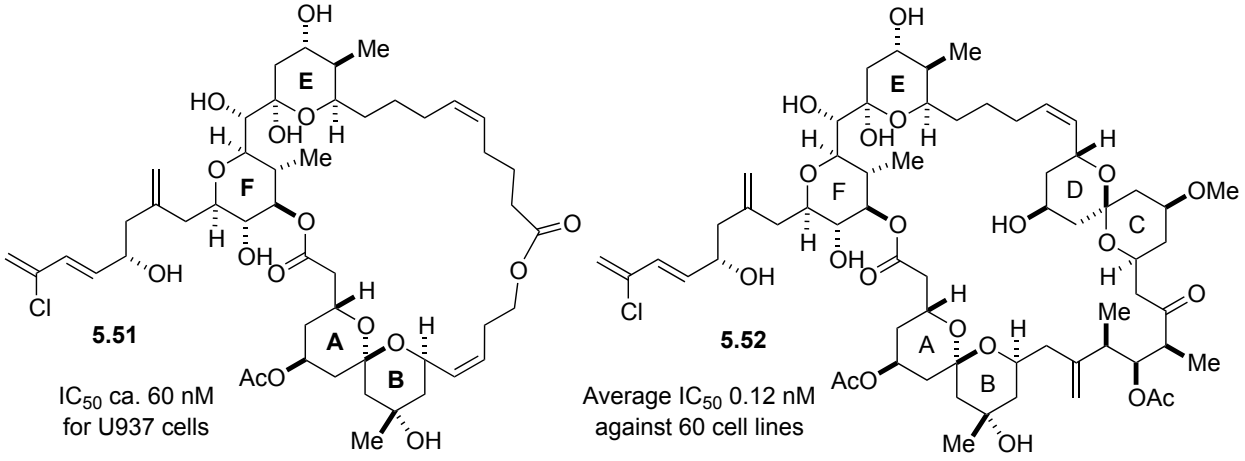

Scheme 5.16: Relative bioactivity of a diminutive ABEF congener of spongistatin 1

The findings above imply that the CD spiroketal is the least critical structural motif contributing to spongistatin's breathtaking biological potency. Though Smith's diminutive form **5.51** no longer possessed the type of potency that would make it a likely drug target, we felt that

a slightly more elaborate, yet still simplified, version of the CD fragment could potentially restore the level of bioactivity that captured the interest of the medicinal chemistry community. This modification could serve to drastically decrease the overall effort required to synthesize the entire molecule, bringing the spongistatin class of anti-tumor molecules a significant step closer to implementation as a chemotherapy agent.

For the biological screening of these spongistatin CD-analogs to be realized, however, we would need to have ready access to large quantities of both the AB and EF fragments of spongistatin 1 in order to couple them with a variety of CD fragment variants. As described in Chapter 5, Section 1, a substantial supply of the AB fragment of spongistatin 1 has been supplied through the work of this author. Using the intermolecular fragment coupling by crotylation chemistry, developed in Chapter 4, Section 1 and successfully implemented in Chapter 5, Section 2, we believe we have a powerful reaction platform in place to join the AB fragment to a variety of CD analogs, so long as they possess pendant aldehyde functionality. To this end, we thought it prudent to work on further optimizing our fragment coupling conditions with the fully elaborated AB-spiroketal **5.41** by testing it on two model aldehydes representing potential CD analogs (Scheme 5.17, Scheme 5.18).

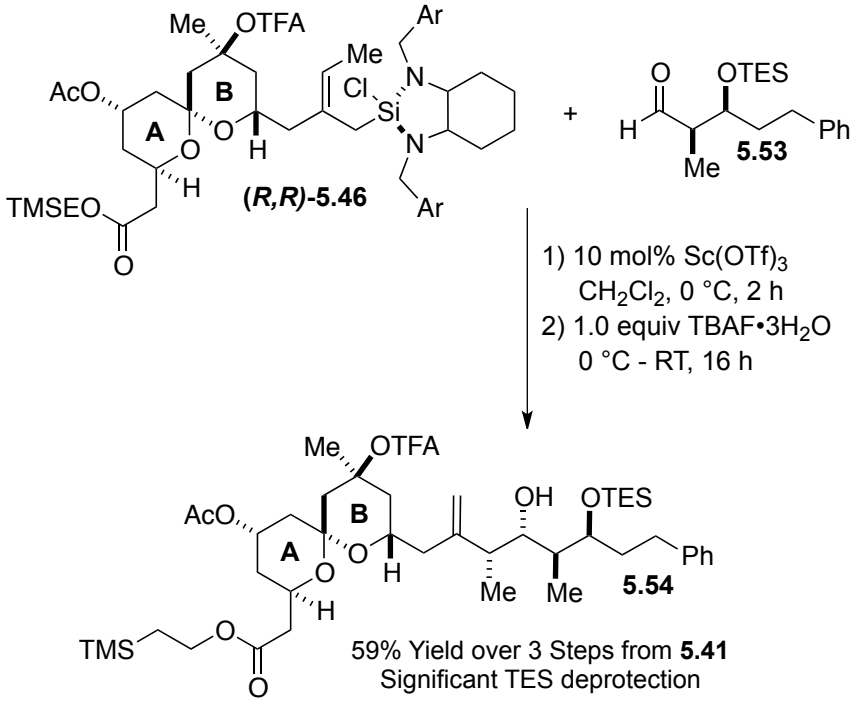

Scheme 5.17: AB spiroketal fragment coupling with a model TES-aldehyde

As depicted above, use of the fragment coupling procedure with simple aldehyde **5.53** afforded a modest improvement in yield over our initial coupling of the AB and CD fragments of spongistatin 1 (Scheme 5.13). Though we had expected this reaction to be high yielding, a significant loss in yield was attributed to the deprotection of the TES ether seen in compound **5.54** during the TBAF work-up – a presumably fixable problem. Much greater improvement in yield was observed when our optimized coupling conditions were applied to the union of the AB spiroketal to silacycle-aldehyde **5.55**, providing coupled silacycle product **5.56** in an excellent 74% yield over the three step sequence (Scheme 5.18). This silacycle was further converted to complex polyketide **5.57** in good yield and selectivity following our optimized Tamao oxidation conditions.

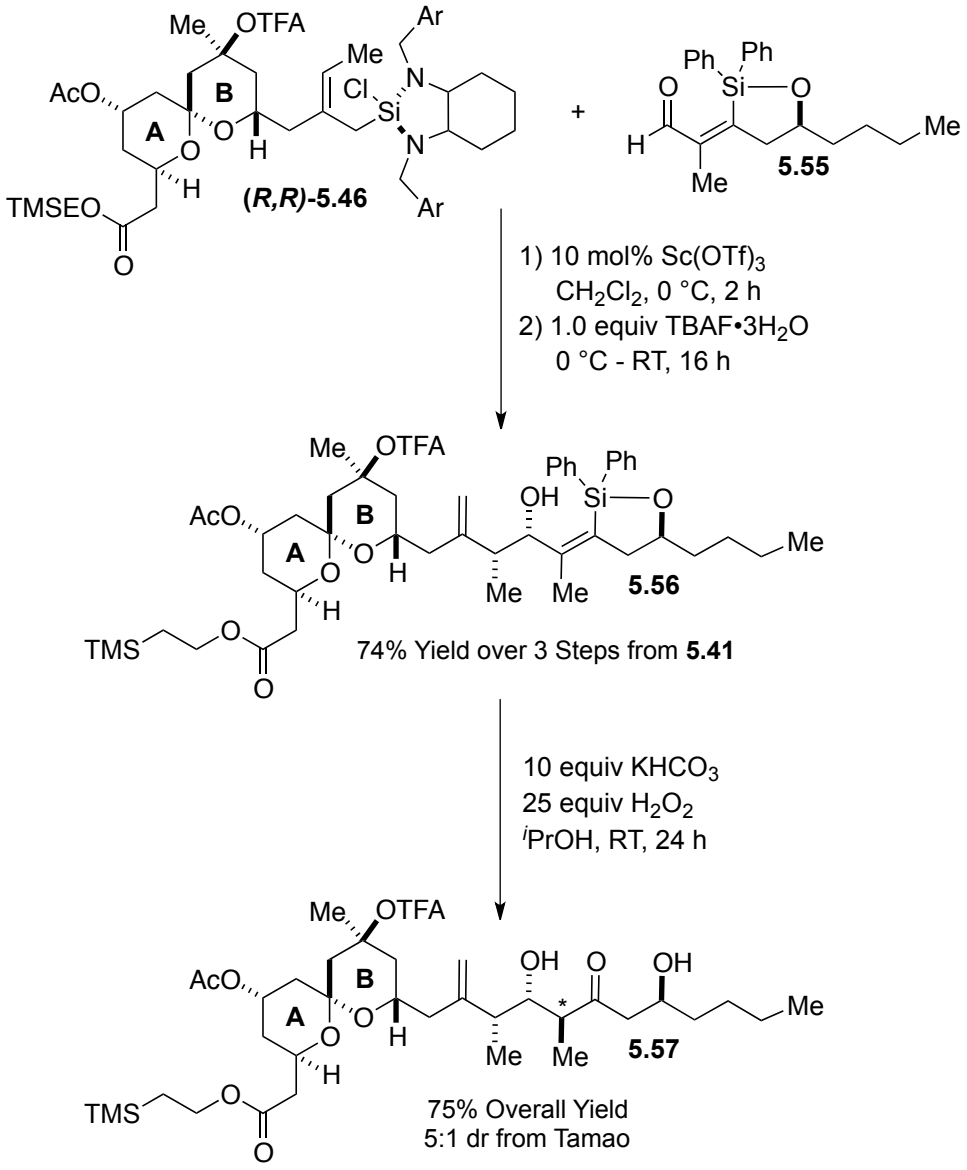

Scheme 5.18: AB spiroketal fragment coupling with a model silacycle-aldehyde

With these exciting results firmly demonstrating the viability of appending our large stockpile of AB spiroketal to a variety of CD fragment analogs, we believe that the Leighton group's spongistatin research program has taken tremendous strides toward achieving our ultimate goal of developing a synthetic strategy that would allow spongistatin 1, or an analog thereof, to be employed as an effective chemotherapy agent. Impressive work toward the multi-

gram synthesis of the EF fragment of spongistatin 1 is currently being pursued by Dr. Paul Tanis, while the very capable Linda Suen concurrently explores the development of CD fragment analogs rationally designed to accommodate potential antibody-drug conjugation.[14] Though this author's direct contribution to the Leighton laboratory's spongistatin research program has come to a conclusion, he eagerly awaits the continued success of his mentor and colleagues that is soon to come.

5.4 References and Notes

1. (a) Nakamura, M.; Hirai, A.; Sogi, M.; Nakamura, E., *J. Am. Chem. Soc.* **1998,** *120* (23), 5846-5847; (b) Waltz, K. M.; Gavenonis, J.; Walsh, P. J., *Angew. Chem. Int. Edit.* **2002,** *41* (19), 3697-3699; (c) Wadamoto, M.; Yamamoto, H., *J. Am. Chem. Soc.* **2005,** *127* (42), 14556-14557; (d) Miller, J. J.; Sigman, M. S., *J. Am. Chem. Soc.* **2007,** *129* (10), 2752-2753; (e) Barnett, D. S.; Moquist, P. N.; Schaus, S. E., *Angew. Chem. Int. Edit.* **2009,** *48* (46), 8679-8682; (f) Shi, S. L.; Xu, L. W.; Oisaki, K.; Kanai, M.; Shibasaki, M., *J. Am. Chem. Soc.* **2010,** *132* (19), 6638-6639.

2. (a) Kubota, K.; Leighton, J. L., *Angew. Chem. Int. Edit.* **2003,** *42* (8), 946-948; (b) Hackman, B. M.; Lombardi, P. J.; Leighton, J. L., *Org. Lett.* **2004,** *6* (23), 4375-4377; (c) Kim, H.; Ho, S.; Leighton, J. L., *J. Am. Chem. Soc.* **2011,** *133* (17), 6517-6520.

3. (a) Berger, R.; Duff, K.; Leighton, J. L., *J. Am. Chem. Soc.* **2004,** *126* (18), 5686-5687; (b) Bou-Hamdan, F. R.; Leighton, J. L., *Angew. Chem. Int. Edit.* **2009,** *48* (13), 2403-2406; (c) Valdez, S. C.; Leighton, J. L., *J. Am. Chem. Soc.* **2009,** *131* (41), 14638-14369.

4. Chalifoux, W. A.; Reznik, S. K.; Leighton, J. L., *Nature* **2012,** *487* (7405), 86-89.

5. Paterson, I.; Yeung, K. S., *Chem Rev* **2005,** *105* (12), 4237-4313.

6. Crimmins, M. T.; Katz, J. D.; Washburn, D. G.; Allwein, S. P.; McAtee, L. F., *J. Am. Chem. Soc.* **2002,** *124* (20), 5661-5663.

7. Brooks, D. W.; Kellogg, R. P.; Cooper, C. S., *J. Org. Chem.* **1987,** *52* (2), 192-196.

8. Kitamura, M.; Ohkuma, T.; Inoue, S.; Sayo, N.; Kumobayashi, H.; Akutagawa, S.; Ohta, T.; Takaya, H.; Noyori, R., *J. Am. Chem. Soc.* **1988,** *110* (2), 629-631.

9. Ikawa, T.; Hattori, K.; Sajiki, H.; Hirota, K., *Tetrahedron* **2004,** *60* (32), 6901-6911.

10. Chakraborti, A. K.; Gulhane, R., *Tetrahedron. Lett.* **2003,** *44* (35), 6749-6753.

11. Favre, S.; Vogel, P.; Gerber-Lemaire, S., *Molecules* **2008,** *13* (10), 2570-2600.

12. Smith, A. B.; Lin, Q.; Doughty, V. A.; Zhuang, L.; McBriar, M. D.; Kerns, J. K.; Boldi, A. M.; Murase, N.; Moser, W. H.; Brook, C. S.; Bennett, C. S.; Nakayama, K.; Sobukawa, M.; Lee Trout, R. E., *Tetrahedron* **2009,** *65* (33), 6470-6488.

13. Smith, A. B.; Risatti, C. A.; Atasoylu, O.; Bennett, C. S.; Liu, J. K.; Cheng, H. S.; TenDyke, K.; Xu, Q. L., *J. Am. Chem. Soc.* **2011,** *133* (35), 14042-14053.

14. (a) Kovtun, Y. V.; Audette, C. A.; Ye, Y.; Xie, H.; Ruberti, M. F.; Phinney, S. J.; Leece, B. A.; Chittenden, T.; Blattler, W. A.; Goldmacher, V. S., *Cancer Res* **2006,** *66* (6), 3214-21; (b)

Kovtun, Y. V.; Goldmacher, V. S., *Cancer letters* **2007,** *255* (2), 232-40; (c) Ducry, L.; Stump, B., *Bioconjugate chemistry* **2010,** *21* (1), 5-13.

Chapter 6:Experimental Information for Chapter 4

General Information. Unless otherwise stated, all chemical compounds were purchased from common commercial sources. All reactions were carried out under an atmosphere of nitrogen in flame or oven-dried glassware with magnetic stirring unless otherwise indicated. Degassed solvents were purified by passage through an activated alumina column. Thin-layer chromatography (TLC) was carried out on glass backed silica gel TLC plates (250 μm) from Silicycle; visualization by UV light, phosphomolybdic acid (PMA), *p*-Anisaldehyde (*p*-Anis) or potassium permanganate ($KMnO_4$) stain. Gas chromatographic analyses were performed on a Hewlett-Packard 6890 Series Gas Chromatograph equipped with a capillary split-splitless inlet and flame ionization detector with electronic pneumatics control using either a Supelco β-Dex 120 (30 m x 0.25 mm) or Supelco β-Dex 325 (30 m x 0.25 mm) capillary GLC column. HPLC analysis was carried out on an Agilent 1200 Series using either a Chiralpak AD-H (250 × 4.5 mm ID) column or Chiralcel OD (250 × 4.5 mm ID) column. ^1H NMR spectra were recorded on a Bruker DPX-300 (300 MHz), Bruker DRX-300 (300 MHz), Bruker AVIII nano bay-400 (400 MHz), Bruker AVIII single bay-400 (400 MHz), Avance III 500 (500 mHz) or a Avance III 500 Ascend magnet (500 MHz) spectrometer and are reported in ppm from $CDCl_3$ internal standard (7.26 ppm). Data are reported as follows: (bs= broad singlet, s = singlet, d = doublet, t = triplet, q = quartet, p = quintet, h = hextet, sep = septet, m = multiplet, dd = doublet of doublets, ddd = doublet of doublet of doublets, dddd = doublet of doublet of doublet of doublets; coupling constant(s) in Hz; integration). Proton decoupled ^{13}C NMR spectra were recorded on a Bruker DRX-300

(300 MHz), Bruker AVIII single bay-400 (400 MHz), Bruker AVIII nano bay-400 (400 MHz), Avance III 500 (500 mHz) or a Avance III 500 Ascend magnet (500 MHz) spectrometer and are reported in ppm from $CDCl_3$ internal standard (77.0 ppm). Infrared spectra were recorded on a Nicolet Avatar 370DTGS FT-IR. Optical rotations were recorded on a Jasco DIP-1000 digital polarimeter. (APCI)-MS was conducted on a JMS-LCmate LCMS (JEOL).

General Procedure 1: Isoprenylation of Aldehydes

A solution of aldehyde (1.0 equiv) in anhydrous CH_2Cl_2 (0.1 M) was cooled to 0 °C and isoprenylation reagent **(*R,R*)-4.37** (1.1 equiv a from a 0.6 M stock solution in CH_2Cl_2) was added followed by $Sc(OTf)_3$ (0.05 equiv). The resulting mixture was stirred vigorously at 0 °C until complete consumption of aldehyde was observed by reaction aliquot ^1H NMR analysis (typically 1-2 h). The reaction was quenched at 0 °C with a 1 M solution of TBAF in THF (3.0 equiv) and then allowed to warm to room temperature. (Note: For concomitant TES removal during work-up, 4.0 equiv of TBAF was used). The resulting mixture was concentrated to an amber oil, and the crude product was purified by silica gel chromatography to afford the desired diene.

General Procedure 2: Fragment Coupling by Crotylation

A flame-dried sealed tube was charged with $Pd(PPh_3)_4$ (0.01 equiv), evacuated and back-filled with N_2. The starting material diene (1.0 equiv) was transferred to the sealed tube in a solution of anhydrous C_6H_6 (0.1 M) under an atmosphere of N_2. Trichlorolsilane (2.0 equiv) was added to the solution and the sealed tube was screwed closed. The reaction vessel was placed in a 70 °C bath and the light yellow solution was stirred for 12-16 h. The resulting amber solution was allowed to cool to room temperature before being cannulated into a flame-dried, 2-neck roundbottom flask. The sealed tube was rinsed with anhydrous C_6H_6 (2 x 0.4 M), and the wash solution was cannulated into the 2-neck roundbottom flask. The reaction mixture was concentrated down to a crude amber oil using air-free technique. (Note: air-free technique involved placing the roundbottom flask in a 40 °C water bath, connecting it to an adjacent -78 °C cold-finger and carefully reducing the pressure with a manometer partitioned through the pump manifold. Upon complete removal of solvent, the entire system was back-filled with N_2).

The resulting hydrosilylated product was retaken in anhydrous CH_2Cl_2 (0.1 M) and diamine•2HCl salt **(*R,R*)-4.1** or **(*S,S*)-4.1** (1.0 equiv) was added at room temperature. The resulting white slurry was cooled to 0 °C and distilled DBU (4.0 equiv) was added to the reaction mixture over 10 min. As DBU was added, the white salts solvated upon deprotonation and the solution took on an amber hue. After an additional 5 min of stirring, the solution was thawed to room temperature. After 2 h, the solvent was removed using air-free technique until the resulting yellow oil became opaque and foamy. (Note: air-free technique involved placing the roundbottom flask in a room

temperature water bath, connecting it to an adjacent -78 °C cold-finger and carefully reducing the pressure with a manometer partitioned through the pump manifold. Upon complete removal of solvent, the entire system was back-filled with N_2). The resulting oil was retaken in anhydrous Et_2O (0.1 M) and shaken vigorously for 5-15 min until the DBU•HCl salts precipitated out as a white solid. This heterogeneous solution was stirred vigorously for an additional 3-5 h to until the DBU•HCl salts became a very fine white precipitate. The tinted yellow supernatant was filter-cannulated using Teflon tubing into a flame-dried, 2-neck roundbottom flask. Et_2O (0.2 M) was added to rinse the leftover DBU•HCl salts and the flask was shaken vigorously. The supernatant was again filter-cannulated into the new 2-neck roundbottom flask. This process was repeated a second time with a final Et_2O wash (0.4 M). The solvent was again removed using air-free technique (room temperature bath) until the resulting yellow oil became opaque and foamy.

The resulting crotyl-silane was retaken in anhydrous CH_2Cl_2 (0.1 M) and cooled to 0 °C. The aldehyde coupling partner (1.0 equiv) was added to the cooled mixture followed by $Sc(OTf)_3$ (0.10 equiv). The reaction mixture was stirred vigorously at 0 °C for 2 h before being quenched with TBAF. (Note: For concomitant TES removal during work-up, 4.0 equiv of TBAF in a 1 M solution of THF was used, and the solution was subsequently allowed to warm to room temperature. For more mild removal of the diamine-silane, the reaction was quenched with 1.0 equiv of solid TBAF•$3H_2O$ and the surrounding 0 °C bath was allowed to slowly expire over 12-16 h). The quenched reaction mixture was concentrated down to a thick oil, and this crude material was

purified by silica gel chromatography to afford the desired fragment coupled product as well as any unreacted starting material aldehyde.

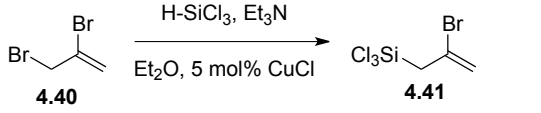

b.p. = 95 °C / 65 mm Hg
83% Yield, 29g

A flame-dried, 2-neck, 500 mL roundbottom flask was charged with CuCl (684 mg, 6.91 mmol, 0.05 equiv) and equipped with a flame-dried reflux condenser (Note: a 24/40 glass adapter joint was attached to the top of the condenser to allow for adequate reaction ventilation and N_2 flow). Et_2O (280 mL, 0.5 M) was added to the flask, and the mixture was stirred to create a green slurry. Et_3N (23.1 mL, 166 mmol, 1.2 equiv) was added and the mixture took on a green/brown color. The flask was cooled to 0 °C and 2,3-dibromopropene **4.40** (13.5 mL, 138 mmol, 1.0 equiv) was added. Trichlorosilane (16.7 mL, 166 mmol, 1.2 equiv) was slowly added to the solution at 0 °C in 4 mL portions every 10 min (Caution: HCl salts immediately formed upon each trichlorosilane addition and a strong exotherm occurred! The reaction solvent occasionally refluxed in the condenser, but was effectively contained). 10 min after the final trichlorosilane addition, the reaction mixture was allowed to thaw to room temperature. After 2.5 h of stirring, full conversion to product was confirmed by ^1H reaction aliquot NMR analysis. The thick reaction mixture was filter-cannulated into a flame-dried, 2-neck, 1-L roundbottom flask. The remaining HCl salts were washed with additional Et_2O (2 x 100 mL) which were also filter-cannulated into the new 1-L flask. The majority of the solvent was removed using air-free technique until the crude reaction product was highly

concentrated in Et_2O. (Note: air-free technique involved placing the roundbottom flask in a room temperature water bath, connecting it to an adjacent -78 °C cold-finger and carefully reducing the pressure to 100 mm Hg with a manometer partitioned through the pump manifold. Upon adequate concentration of solvent, the entire system was back-filled with N_2). This salty, concentrated oil was transferred to a flame-dried distillation apparatus via syringe (Note: lots of smoke fumed off the salty, brown/yellow reaction crude during this purification process). Distillation (b.p. 95 °C at 65 mm Hg) afforded allyl-trichlorosilane **4.41** (29.2g, 115 mmol, 83% yield) as a smoky, colorless oil (Note: the product is moisture sensitive and fumes if exposed to air). ^{1}H NMR (500 MHz, $CDCl_3$) δ 5.74 (dt, *J* = 2.3, 1.1 Hz, 1H), 5.63 (d, *J* = 2.2 Hz, 1H), 2.92 (d, *J* = 1.2 Hz, 2H); ^{13}C NMR (125 MHz, $CDCl_3$) δ 121.7, 120.6, 38.8.

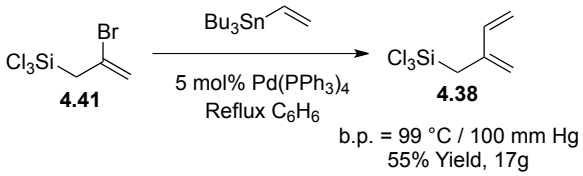

A flame-dried 500 mL roundbottom flask was charged with $Pd(PPh_3)_4$ (9.02g, 7.8 mmol, 0.05 equiv).[1] The flask was evacuated and back-filled with N_2 before being charged with benzene (165 mL, 1.0 M) to create a yellow solution. Allyl-trichlorosilane **4.41** (39.7g, 156 mmol, 1.0 equiv) was added to the solution followed by tributyl(vinyl)tin (50.3 mL, 172 mmol, 1.1 equiv). The roundbottom flask was equipped with a flame-dried reflux condenser, and the resulting mixture was heated to reflux. The refluxing solution turned dark red over time. After refluxing for 2 h, nearly full

[1] $Pd(PPh)_3$ was supplied by Acros

conversion to the desired product was observed by reaction aliquot ^{1}H NMR analysis. The reflux condenser was replaced with a flame-dried, 8 in. vigreux column and distillation head. The majority of the reaction solvent was boiled off over 1 hour (120 °C oil bath). The resulting concentrated reaction crude was carefully transferred to a flame-dried distillation apparatus via syringe. Distillation (b.p. 99 °C at 100 mm Hg) afforded isoprenyl-trichlorosilane **4.38** (17.3g, 86 mmol, 55% yield) as a smoky colorless oil (Note: the product is moisture sensitive and fumes if exposed to air). ^{1}H NMR (400 MHz, $CDCl_3$) δ 6.46 (ddd, J = 17.6, 10.8, 0.8 Hz, 1H), 5.34-5.17 (m, 4H), 2.60 (d, J = 1.1 Hz, 2H); ^{13}C NMR (100 MHz, $CDCl_3$) δ 138.0, 137.2, 119.5, 115.3, 28.0.

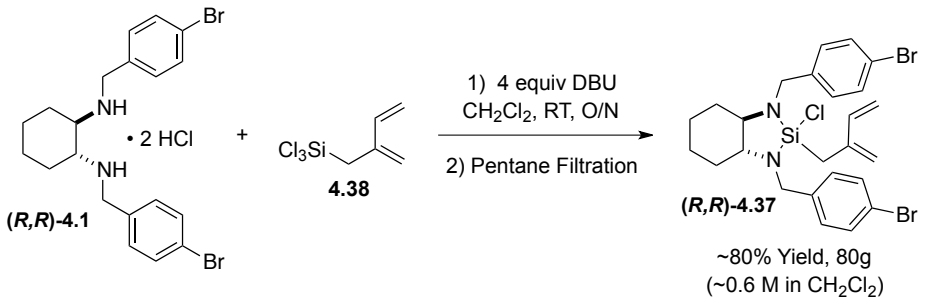

A flame-dried 3-L, 2-neck roundbottom flask was charged with diamine•2HCl salt **(*R,R*)-4.1** (96.6g, 184 mmol, 1.0 equiv) and CH_2Cl_2 (615 mL, 0.3 M). The slurry was cooled to 0 °C and isoprenyl-trichlorosilane **4.38** (37g, 184 mmol, 1.0 equiv) was added. Distilled DBU (110 mL, 736 mmol, 4.0 equiv) was added to the mixture at 0 °C over 10 min. As DBU was added, the white salts solvated upon deprotonation and the solution took on an amber hue. After an additional 5 min of stirring, the solution was thawed to room temperature. After 1 h, reaction aliquot NMR analysis showed full conversion to the desired product. The solvent was removed using air-free technique until the resulting oil became opaque and foamy. (Note: air-free technique involved

placing the roundbottom flask in a room temperature water bath, setting up an adjacent -78 °C cold-finger and carefully reducing the pressure with a manometer partitioned through the pump manifold. Upon complete removal of solvent, the entire system was back-filled with N_2). Pentane (600 mL) was then added to the oil at room temperature, and the solution was shaken vigorously for 5-15 min until the DBU•HCl salts precipitated out into a fine white solid. This heterogeneous mixture was stirred vigorously for an additional 1 h. The tinted yellow supernatant was filter-cannulated using Teflon tubing into a dry 1-L, 2-neck roundbottom flask. Pentane (300 mL) was added to the leftover DBU•HCl salts and the flask was shaken vigorously. The supernatant was again filter-cannulated into the new 1L, 2-neck roundbottom flask. This process was repeated a second time with a final pentane wash (150 mL). The solvent was again removed using air-free technique until the resulting oil became opaque and foamy. The product oil was transferred to a flame-dried 500 mL roundbottom flask to provide isoprenylation reagent **(*R*,*R*)-4.37** (ca. 85g, 147 mmol, 80% Yield) as a stock solution in CH_2Cl_2 (~0.6 M). A small aliquot of this stock solution was concentrated for characterization. ^{1}H NMR (500 MHz, $CDCl_3$) δ 7.43 (dd, *J* = 8.4, 2.5 Hz, 4H), 7.30 (t, *J* = 8.8 Hz, 4H), 6.38 (dd, *J* = 17.4, 10.4 Hz, 1H), 5.17 (d, *J* = 17.4 Hz, 1H), 5.08 (d, *J* = 12.0 Hz, 3H), 4.16 (d, *J* = 16.3 Hz, 1H), 4.03 (d, *J* = 15.2 Hz, 1H), 3.89 (d, *J* = 15.2 Hz, 1H), 3.80 (d, *J* = 16.3 Hz, 1H), 2.81 (ddd, *J* = 11.9, 9.2, 2.9 Hz, 1H), 2.73 (ddd, *J* = 11.9, 9.3, 3.0 Hz, 1H), 1.97 (d, *J* = 15.4 Hz, 1H), 1.88 (d, *J* = 15.5 Hz, 1H), 1.84-1.54 (m, 4H), 1.13 (tt, *J* = 12.7, 10.2 Hz, 2H), 1.01 (qd, *J* = 13.6, 12.7, 4.1 Hz, 1H), 0.91 (tt, *J* = 12.0, 6.4 Hz, 1H); ^{13}C NMR (125 MHz, $CDCl_3$) δ 141.5, 140.3, 139.9, 139.5, 131.2, 129.9, 129.0, 120.5, 120.2, 117.3, 114.3, 66.5, 65.3, 48.2, 47.5, 31.0, 30.4, 24.7, 21.3.

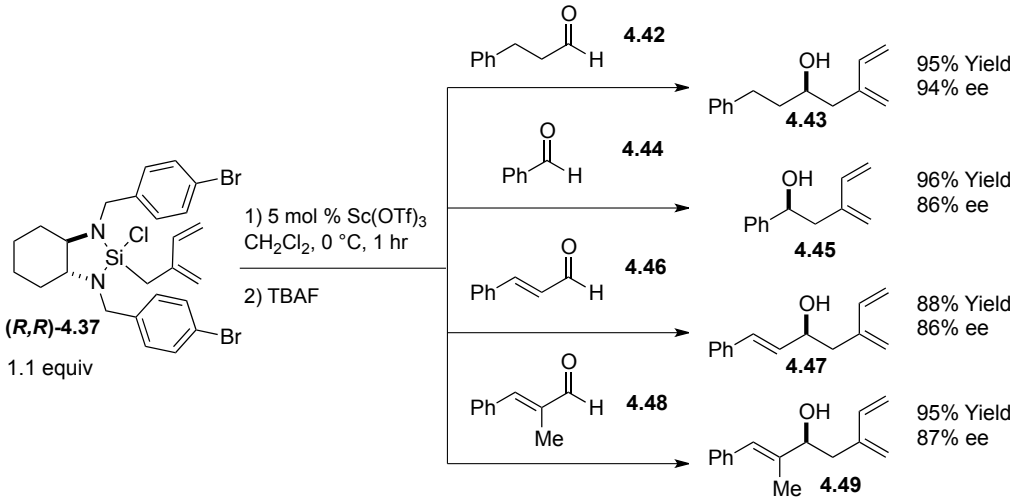

Hydrocinnamaldehyde **4.42** (3.8 mL, 28.8 mmol, 1.0 equiv) was reacted with **(*R,R*)-4.37** (1.1 equiv) according to general procedure 1. Purification by silica gel chromatography (gradient 10%, 25% EtOAc/Hexanes) afforded **4.43** (5.56g, 27.5 mmol, 95% Yield) as a pale yellow oil. The isolated diene was either used immediately or frozen in a solution of benzene for long-term storage. The enantiomeric excess of **4.43** was determined to be 94% ee by chiral HPLC analysis (see HPLC chromatogram below). $[\alpha]_D$ = +21° (c 2.0, CH_2Cl_2); R_f = 0.3 (15% EtOAc/Hexanes, PMA); ^{1}H NMR (500 MHz, $CDCl_3$) δ 7.37-7.28 (m, 2H), 7.28-7.18 (m, 3H), 6.42 (dd, *J* = 17.6, 11.0 Hz, 1H), 5.25 (d, *J* = 17.6 Hz, 1H), 5.22-5.09 (m, 3H), 3.82 (dq, *J* = 8.9, 4.7 Hz, 1H), 2.88 (dt, *J* = 13.9, 8.3 Hz, 1H), 2.79-2.70 (m, 1H), 2.56 (dd, *J* = 13.9, 3.7 Hz, 1H), 2.32 (dd, *J* = 13.9, 9.0 Hz, 1H), 1.94-1.80 (m, 2H), 1.72 (bs, 1H); ^{13}C NMR (125 MHz, $CDCl_3$) δ 143.0, 142.1, 138.4, 128.4, 128.4, 125.8, 118.5, 114.3, 69.1, 40.1, 38.8, 32.2; IR (cast film) 3382, 3027, 2931, 1594, 1496, 1454, 1392, 1083, 993, 900 cm^{-1}; LRMS (FAB+) calc'd for $C_{14}H_{18}O$ $[M]^+$ 202.29, found 202.28.

Benzaldehyde **4.44** (51 μL, 0.5 mmol, 1.0 equiv) was reacted with **(*R,R*)-4.37** (1.1 equiv) according to general procedure 1. Purification by silica gel chromatography (10% EtOAc/Hexanes) afforded **4.45** (84 mg, 0.48 mmol, 96% Yield) as a pale yellow oil. The enantiomeric excess of **4.45** was determined to be 86% ee by chiral HPLC analysis (see HPLC chromatogram below). $[\alpha]_D$ = -41° (c 1.8, CH_2Cl_2); R_f = 0.3 (10% EtOAc/Hexanes, PMA); ^{1}H NMR (400 MHz, $CDCl_3$) δ 7.35-7.17 (m, 5H), 6.33 (dd, *J* = 17.6, 10.8 Hz, 1H), 5.24 (d, *J* = 17.6 Hz, 1H), 5.11-4.98 (m, 3H), 4.75 (ddd, *J* = 9.3, 4.0, 2.0 Hz, 1H), 2.62 (ddd, *J* = 14.1, 4.0, 1.1 Hz, 1H), 2.47 (ddd, *J* = 14.2, 9.2, 0.8 Hz, 1H), 1.94 (d, *J* = 2.4 Hz, 1H); ^{13}C NMR (125 MHz, $CDCl_3$) δ 144.1, 142.7, 138.3, 128.4, 127.6, 125.8, 118.9, 114.3, 72.2, 42.2; IR (cast film) 3382, 3086, 3032, 2930, 1594, 1454, 1393, 1137, 1083, 1054, 993, 901cm^{-1}; LRMS (FAB+) calc'd for $C_{12}H_{14}O$ $[M]^+$ 174.24, found 174.22.

Cinnamaldehyde **4.46** (63 μL, 0.5 mmol, 1.0 equiv) was reacted with **(*R,R*)-4.37** (1.1 equiv) according to general procedure 1. Purification by silica gel chromatography (15% EtOAc/Hexanes) afforded **4.47** (88 mg, 0.44 mmol, 88% Yield) as a pale yellow oil. The enantiomeric excess of **4.47** was determined to be 86% ee by chiral HPLC analysis (see HPLC chromatogram below). $[\alpha]_D$ = +7° (c 0.6, CH_2Cl_2); R_f = 0.3 (15% EtOAc/Hexanes, PMA); ^{1}H NMR (400 MHz, $CDCl_3$) δ 7.46-7.38 (m, 2H), 7.38-7.31 (m, 2H), 7.31-7.23 (m, 1H), 6.65 (dd, *J* = 15.9, 1.1 Hz, 1H), 6.45 (dd, *J* = 17.6, 11.0 Hz, 1H), 6.28 (dd, *J* = 15.9, 6.4 Hz, 1H), 5.35 (d, *J* = 17.6 Hz, 1H), 5.26-5.14 (m, 3H), 4.50 (ddddd, *J* = 7.9, 6.1, 4.5, 3.1, 1.2 Hz, 1H), 2.65 (ddd, *J* = 14.0, 4.8, 1.0 Hz, 1H), 2.52 (ddd, *J* = 14.0, 8.4, 0.8 Hz, 1H), 1.92 (d, *J* = 3.2 Hz, 1H); ^{13}C NMR (125 MHz, $CDCl_3$) δ

142.4, 138.5, 136.8, 131.7, 130.2, 128.6, 127.7, 126.5, 119.0, 114.4, 70.8, 40.1; IR (cast film) 3369, 3027, 2929, 1595, 1494, 1449, 1392, 1099, 1026, 992, 966, 902 cm^{-1}; LRMS (FAB+) calc'd for $C_{14}H_{16}O$ $[M]^+$ 200.28, found 200.08.

α-Methyl-*trans*-cinnamaldehyde **4.48** (70 μL, 0.5 mmol, 1.0 equiv) was reacted with **(*R*,*R*)-4.37** (1.1 equiv) according to general procedure 1. Purification by silica gel chromatography (10% EtOAc/Hexanes) afforded **4.49** (102 mg, 0.475 mmol, 95% Yield) as a pale yellow oil. The enantiomeric excess of **4.49** was determined to be 87% ee by chiral HPLC analysis (see HPLC chromatogram below). $[\alpha]_D$ = +18° (c 2.4, CH_2Cl_2); R_f = 0.3 (10% EtOAc/Hexanes, PMA); ^{1}H NMR (400 MHz, $CDCl_3$) δ 7.42-7.19 (m, 5H), 6.58 (s, 1H), 6.46 (dd, *J* = 17.6, 11.0 Hz, 1H), 5.37 (d, *J* = 17.7 Hz, 1H), 5.26-5.16 (m, 3H), 4.38 (ddd, *J* = 8.9, 4.3, 1.9 Hz, 1H), 2.70 (ddd, *J* = 14.0, 4.2, 1.1 Hz, 1H), 2.49 (dd, *J* = 14.0, 8.9 Hz, 1H), 1.96 (d, *J* = 1.4 Hz, 2H), 1.88 (d, *J* = 6.0 Hz, 1H); ^{13}C NMR (125 MHz, $CDCl_3$) δ 142.9, 139.6, 138.4, 137.6, 129.0, 128.1, 126.5, 125.8, 118.6, 114.3, 75.5, 38.6, 13.6; IR (cast film) 3384, 3086, 2952, 1595, 1492, 1444, 1390, 1335, 1154, 1074, 1010, 994, 900 cm^{-1}; LRMS (FAB+) calc'd for $C_{15}H_{18}O$ $[M]^+$ 214.30, found 214.03.

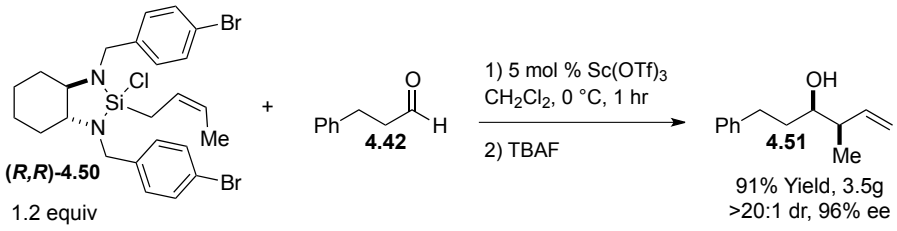

To a solution of **4.42** hydrocinnamaldehyde (2.63 mL, 20.0 mmol, 1.0 equiv) solvated in anhydrous CH_2Cl_2 (200 mL, 0.1 M) was added (*R*,*R*)-*cis* EZ-CrotylMix™

(*R,R*)-4.50 (14.1g, 24.0 mmol, 1.2 equiv) at 0 °C.[2] The reaction mixture was stirred for 1 h at 0 °C before being quenched with a 1 M solution of TBAF in THF (60 mL, 60 mmol, 3.0 equiv). The resulting mixture was allowed to warm to room temperature and was then concentrated down to a thick oil. This crude residue was purified by silica gel chromatography (gradient 5%, 15% EtOAc/Hexanes) to afford alkene **4.51** (3.47g, 18.24 mmol, 91% Yield) as a colorless oil. The diastereoselectivity of the reaction was determined to be >20:1 by ^{1}H NMR analysis. The enantiomeric excess of **4.51** was determined to be 96% ee by chiral HPLC analysis (see HPLC chromatogram below). $[\alpha]_D$ = +30° (c 5.0, CH_2Cl_2); R_f = 0.6 (25% EtOAc/Hexanes, PMA); ^{1}H NMR (400 MHz, $CDCl_3$) δ 7.42-7.30 (m, 2H), 7.30-7.20 (m, 3H), 5.93-5.73 (m, 1H), 5.21-5.08 (m, 2H), 3.58 (ddd, *J* = 8.9, 5.2, 3.2 Hz, 1H), 2.93 (ddd, *J* = 13.7, 10.1, 5.3 Hz, 1H), 2.71 (ddd, *J* = 13.7, 9.8, 6.7 Hz, 1H), 2.44-2.29 (m, 1H), 1.89 (dddd, *J* = 13.5, 10.0, 6.7, 3.2 Hz, 1H), 1.82-1.63 (m, 2H), 1.10 (d, *J* = 6.9 Hz, 3H); ^{13}C NMR (100 MHz, $CDCl_3$) δ 142.3, 140.9, 128.5, 128.4, 125.8, 115.5, 74.1, 43.8, 35.9, 32.5, 14.4; IR (cast film) 3384, 2936, 2866, 1496, 1454, 1417, 1373, 1037, 997, 914 cm^{-1}; LRMS (FAB+) calc'd for $C_{13}H_{18}O$ $[M]^+$ 190.28, found 190.11.

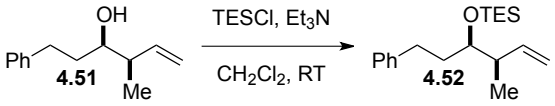

98% Yield

To a solution of alcohol **4.51** (1.90g, 10.0 mmol, 1.0 equiv) in anhydrous CH_2Cl_2 (100 mL, 0.1 M) was added Et_3N (2.1 mL, 15.0 mmol, 1.5 equiv) followed by TES-Cl

[2] Commercially available asymmetric crotylation and allylation reagents such as EZ-CrotylMix and can be purchased from Sigma-Aldrich.

(2.0 mL, 12.0 mmol, 1.2 equiv) and DMAP (367mg, 0.3 mmol, 0.3 equiv). The mixture was stirred at room temperature, and the reaction progress was monitored by TLC analysis. At 1.5 h, the reaction was quenched with MeOH (0.6 mL, 15.0 mmol, 1.5 equiv) and concentrated down to a salty oil. This oil was retaken in hexanes and filtered. The resulting solution was concentrated and purified by silica gel chromatography (gradient 0%, 3% EtOAc/Hexanes) to afford silyl-ether **4.52** (2.98g, 9.78 mmol, 98% Yield) as a colorless oil. $[\alpha]_D$ = +14° (c 4.0, CH_2Cl_2); R_f = 0.8 (5% EtOAc/Hexanes, PMA); ^{1}H NMR (400 MHz, $CDCl_3$) δ 7.35 (t, *J* = 7.5 Hz, 2H), 7.25 (d, *J* = 7.4 Hz, 3H), 5.94 (ddd, *J* = 17.5, 10.5, 7.3 Hz, 1H), 5.22-5.02 (m, 2H), 3.71 (q, *J* = 5.5 Hz, 1H), 2.93-2.74 (m, 1H), 2.65 (ddd, *J* = 13.5, 9.8, 6.7 Hz, 1H), 2.45 (h, *J* = 6.8 Hz, 1H), 1.81 (dtd, *J* = 9.8, 6.2, 3.5 Hz, 2H), 1.22-0.97 (m, 12H), 0.72 (q, *J* = 7.9 Hz, 6H); ^{13}C NMR (100 MHz, $CDCl_3$) δ 142.8, 141.1, 128.4, 125.7, 114.2, 75.9, 43.3, 36.2, 31.8, 15.5, 7.1, 5.3; IR (cast film) 2955, 2912, 2877, 1456, 1415, 1239, 1074, 1006, 912 cm^{-1}; LRMS (FAB+) calc'd for $C_{19}H_{31}OSi$ $[M-H]^+$ 303.53, found 303.31.

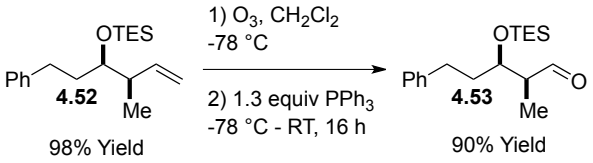

Oxygen gas was bubbled through a solution of alkene **4.52** (1.0g, 3.28 mmol, 1.0 equiv) solvated in CH_2Cl_2 (33 mL, 0.1 M). The solution was cooled to -78 °C while still being sparged with oxygen. O_3 was bubbled through the solution at -78 °C until the solution took on a dark blue color (15 min). The solution was then purged with oxygen until the blue color fully dissipated (10 min). PPh_3 (1.12g, 4.36 mmol, 1.3 equiv) was

added to the cold solution, which was then removed from the cold bath and allowed to thaw to room temperature under an atmosphere of N_2. After 15 h, the reaction was concentrated down to a yellow oil caked with solids. This oil was retaken in hexanes (33 mL, 0.1 M) and stirred vigorously for 10 min to triturate out most of the phosphines. The white slurry was filtered and concentrated to an oil with intermittent solids. The trituration process was repeated a second time to provide a pale yellow oil with minimal solids. The crude material was purified by silica gel chromatography (gradient 1%, 3% EtOAc/Hexanes, pH 7 buffered SiO_2 gel[3]) to afford aldehyde **4.53** (904 mg, 2.95 mmol, 90% Yield) as a pale yellow oil. $[\alpha]_D$ = +39° (c 1.5, CH_2Cl_2); R_f = 0.4 (5% EtOAc/Hexanes, PMA); ^{1}H NMR (500 MHz, $CDCl_3$) δ 9.82 (d, *J* = 1.1 Hz, 1H), 7.37-7.26 (m, 2H), 7.26-7.16 (m, 3H), 4.20 (td, *J* = 6.3, 3.8 Hz, 1H), 2.73 (ddd, *J* = 13.7, 10.7, 6.0 Hz, 1H), 2.66-2.58 (m, 1H), 2.58-2.50 (m, 1H), 1.86 (dddd, *J* = 26.1, 13.8, 11.0, 6.4 Hz, 2H), 1.13 (d, *J* = 7.0 Hz, 3H), 0.99 (t, *J* = 7.9 Hz, 9H), 0.63 (q, *J* = 8.2 Hz, 6H); ^{13}C NMR (125 MHz, $CDCl_3$) δ 205.0, 141.6, 128.5, 128.2, 126.0, 71.9, 51.4, 36.5, 32.2, 8.0, 6.9, 5.2; IR (cast film) 2954, 2913, 2878, 1707, 1645, 1457, 1238, 1103, 1009 cm^{-1}; LRMS (FAB+) calc'd for $C_{18}H_{30}O_2Si$ $[M]^+$ 306.52, found 306.29.

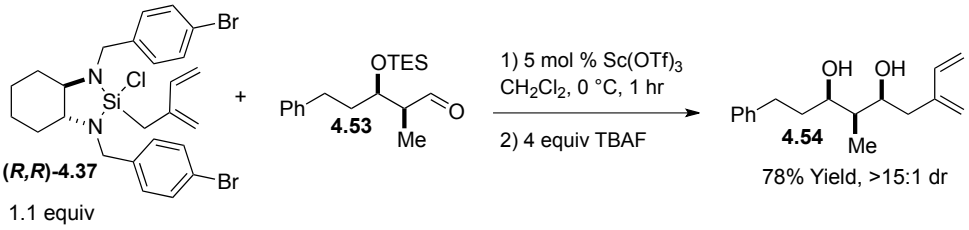

[3] pH 7 buffered SiO_2 gel was prepared my adding 10% pH 7 buffer (by mass) to a roundbotttom flask half filled with SiO_2 gel. The resulting mixture was rotated on a rotary evaporated for >12 h (at atmospheric pressure) and then stored for future use.

Aldehyde **4.53** (904 mg, 2.95 mmol, 1.0 equiv) was reacted with **(*R,R*)-4.37** (1.1 equiv) according to general procedure 1. Purification by silica gel chromatography (25% EtOAc/Hexanes) afforded diol **4.54** (599 mg, 2.30 mmol, 78% Yield) as a pale yellow oil. The isolated diene was either used immediately or frozen in a solution of benzene for long-term storage. The diastereoselectivity of the reaction was determined to be >15:1 by ^{1}H NMR analysis. $[\alpha]_D$ = +18° (c 3.5, CH_2Cl_2); R_f = 0.3 (25% EtOAc/Hexanes, PMA); ^{1}H NMR (400 MHz, $CDCl_3$) δ 7.37-7.28 (m, 2H), 7.28-7.16 (m, 3H), 6.42 (dd, *J* = 17.6, 10.8 Hz, 1H), 5.29 (d, *J* = 17.6 Hz, 1H), 5.22-5.08 (m, 3H), 4.03 (td, *J* = 6.7, 6.1, 1.9 Hz, 1H), 3.91 (ddd, *J* = 8.7, 4.4, 1.8 Hz, 1H), 2.98 (bs, 1H), 2.82 (ddd, *J* = 13.8, 10.0, 5.7 Hz, 1H), 2.68 (ddd, *J* = 13.8, 9.6, 6.4 Hz, 1H), 2.50-2.36 (m, 3H), 2.03-1.83 (m, 1H), 1.81-1.67 (m, 1H), 1.62 (qt, *J* = 6.9, 2.0 Hz, 1H), 1.02 (d, *J* = 7.0 Hz, 3H); ^{13}C NMR (100 MHz, $CDCl_3$) δ 142.9, 142.1, 138.3, 128.5, 128.4, 125.8, 118.4, 114.4, 76.1, 74.6, 40.8, 37.7, 37.0, 32.5, 4.7; IR (cast film) 3357, 2943, 1594, 1496, 1454, 1389, 1094, 1030, 973, 901 cm^{-1} ; LRMS (FAB+) calc'd for $C_{17}H_{25}O_2$ $[M+H]^+$ 261.38, found 261.25.

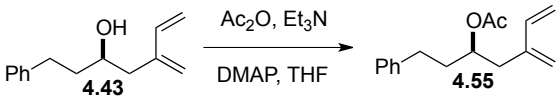

To a solution of alcohol **4.43** (5.56g, 27.5 mmol, 1.0 equiv) solvated in anhydrous THF (275 mL, 0.1 M) was added Et_3N (5.8 mL, 41.3 mmol, 1.5 equiv) followed by Ac_2O (3.1 mL, 33.0 mmol, 1.2 equiv) and DMAP (1.0g, 8.25 mmol, 0.3 equiv). The mixture was stirred at room temperature and the reaction progress was monitored by TLC analysis. At 1.5 h, the reaction was concentrated down to a white, salty oil. This crude residue was purified by silica gel chromatography (gradient 3%, 5% EtOAc/Hexanes) to

afford acetate **4.55** (6.50g, 26.6 mmol, 97% Yield) as a pale yellow oil. The isolated diene was either used immediately or frozen in a solution of benzene for long-term storage. $[\alpha]_D$ = -5° (c 2.0, CH_2Cl_2); R_f = 0.8 (10% EtOAc/Hexanes, PMA); ^{1}H NMR (500 MHz, $CDCl_3$) δ 7.35-7.27 (m, 2H), 7.24-7.16 (m, 3H), 6.38 (dd, *J* = 17.6, 10.7 Hz, 1H), 5.38 (d, *J* = 17.7 Hz, 1H), 5.18-5.09 (m, 3H), 5.05 (t, *J* = 1.5 Hz, 1H), 2.73 (ddd, *J* = 13.9, 10.1, 6.0 Hz, 1H), 2.68-2.56 (m, 2H), 2.44 (ddd, *J* = 13.9, 6.6, 1.0 Hz, 1H), 2.05 (s, 3H), 1.99-1.84 (m, 2H); ^{13}C NMR (125 MHz, $CDCl_3$) δ 170.7, 142.3, 141.6, 138.3, 128.4, 128.3, 125.9, 118.5, 114.2, 72.4, 36.7, 35.6, 31.9, 21.2; IR (cast film) 3028, 2932, 1736, 1596, 1454, 1373, 1239, 1029, 994, 902 cm^{-1} ; LRMS (FAB+) calc'd for $C_{16}H_{21}O_2$ $[M+H]^+$ 245.34, found 245.23.

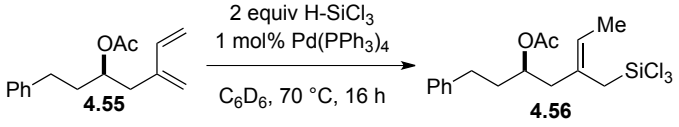

Diene **4.55** (17 mg, 0.07 mmol, 1.0 equiv) was reacted according to the first section of general procedure 2 in a sealed NMR tube. This small scale reaction was performed in C_6D_6 so that the intermediate, hydrosilylated compound **4.56** could be observed and confirmed by ^{1}H and ^{13}C NMR. ^{1}H NMR (400 MHz, C_6D_6) δ 7.20-7.11 (m, 2H), 7.06 (td, *J* = 6.7, 1.7 Hz, 3H), 5.23 (qt, *J* = 6.7, 1.0 Hz, 1H), 5.08 (tdd, *J* = 8.0, 5.3, 4.4 Hz, 1H), 2.66-2.41 (m, 2H), 2.36-2.15 (m, 4H), 1.86-1.59 (m, 2H), 1.68 (s, 3H), 1.36 (d, *J* = 6.6 Hz, 3H); ^{13}C NMR (100 MHz, C_6D_6) δ 169.3, 141.3, 128.4, 128.3, 127.9, 127.7, 127.4, 126.9, 126.0, 125.4, 71.1, 43.5, 35.7, 31.9, 27.4, 20.3, 14.0. Some excess trichlorosilane was also observed by ^{1}H NMR (400 MHz, C_6D_6) δ 5.40 (s).

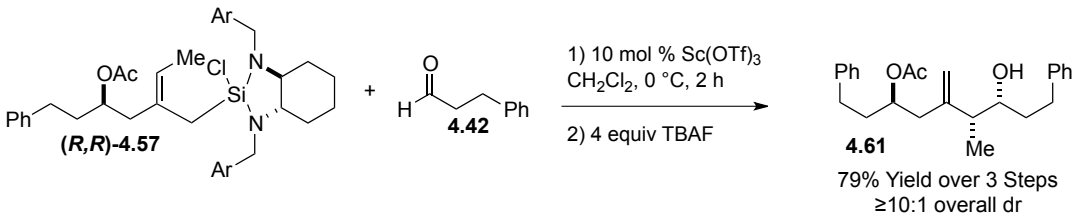

Diene **4.55** (452 mg, 1.85 mmol, 1.0 equiv) was coupled with hydrocinnamaldehyde (244 μL, 1.85 mmol, 1.0 equiv) according to general procedure 2 using diamine **(*R,R*)-4.1**. The crude material was purified by silica gel chromatography (20% EtOAc/Hexanes) to afford compound **4.61** (556 mg, 1.46 mmol, 79% Yield over 3 steps) as a colorless oil. The diastereoselectivity of the reaction was determined to be >10:1 by ^{1}H NMR analysis. $[\alpha]_D$ = +46° (c 1.9, CH_2Cl_2); R_f = 0.3 (15% EtOAc/Hexanes, PMA); ^{1}H NMR (400 MHz, $CDCl_3$) δ 7.37-7.27 (m, 4H), 7.27-7.15 (m, 6H), 5.12 (tt, *J* = 8.5, 4.6 Hz, 1H), 4.98 (d, *J* = 1.3 Hz, 1H), 4.92 (s, 1H), 3.58 (dt, *J* = 8.1, 3.9 Hz, 1H), 2.86 (ddd, *J* = 13.7, 9.7, 5.8 Hz, 1H), 2.77-2.56 (m, 3H), 2.37-2.17 (m, 3H), 2.03 (s, 3H), 1.99-1.70 (m, 4H), 1.58 (bs, 1H), 1.05 (d, *J* = 6.9 Hz, 3H); ^{13}C NMR (100 MHz, $CDCl_3$) δ 170.6, 148.2, 142.1, 141.4, 128.4, 128.4, 128.3, 126.0, 125.8, 113.4, 71.6, 71.1, 43.8, 41.1, 36.1, 32.8, 31.9, 21.1, 12.4; IR (cast film) 3460, 3027, 2930, 1735, 1496, 1454, 1373, 1242, 1030, 901 cm^{-1} ; LRMS (FAB+) calc'd for $C_{25}H_{33}O_3$ $[M+H]^+$ 381.53, found 381.15.

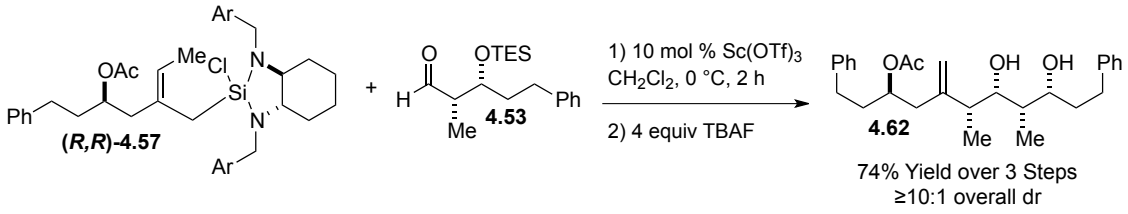

Diene **4.55** (380 mg, 1.55 mmol, 1.0 equiv) was coupled with aldehyde **4.53** (475mg, 1.55 mmol, 1.0 equiv) according to general procedure 2 using diamine **(*R,R*)-4.1**. The crude material was purified by silica gel chromatography (35% EtOAc/Hexanes) to afford compound **4.62** (504 mg, 1.15 mmol, 74% Yield over 3 steps) as a colorless oil. The diastereoselectivity of the reaction was determined to be >10:1 by ^{1}H NMR analysis. $[\alpha]_D$ = +19° (c 1.4, CH_2Cl_2); R_f = 0.3 (30% EtOAc/Hexanes, PMA); ^{1}H NMR (500 MHz, $CDCl_3$) δ 7.35-7.25 (m, 4H), 7.25-7.15 (m, 6H), 5.13 (p, *J* = 6.1 Hz, 1H), 4.90 (d, *J* = 3.9 Hz, 2H), 3.87-3.74 (m, 1H), 3.66 (dd, *J* = 8.7, 2.5 Hz, 1H), 2.82-2.58 (m, 5H), 2.53 (bs, 1H), 2.35 (dt, *J* = 14.9, 7.4 Hz, 2H), 2.20 (dd, *J* = 14.8, 5.3 Hz, 1H), 2.04 (s, 3H), 1.97-1.81 (m, 3H), 1.78-1.61 (m, 2H), 1.11 (d, *J* = 6.8 Hz, 3H), 0.95 (d, *J* = 7.0 Hz, 3H); ^{13}C NMR (125 MHz, $CDCl_3$) δ 170.7, 147.9, 141.8, 141.4, 128.4, 128.4, 128.3, 126.0, 125.9, 113.3, 79.1, 76.1, 72.0, 43.2, 39.9, 38.3, 37.0, 35.9, 32.5, 31.9, 21.1, 16.3, 5.4; IR (cast film) 3404, 2932, 1735, 1496, 1457, 1374, 1242, 1090, 1029, 968 cm^{-1} ; LRMS (FAB+) calc'd for $C_{28}H_{39}O_4$ $[M+H]^+$ 439.61, found 439.40.

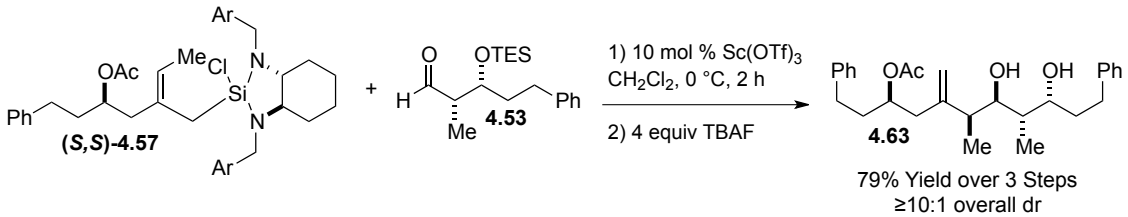

Diene **4.55** (367 mg, 1.50 mmol, 1.0 equiv) was coupled with aldehyde **4.53** (460mg, 1.50 mmol, 1.0 equiv) according to general procedure 2 using diamine **(*S*,*S*)-4.1**. The crude material was purified by silica gel chromatography (gradient 35%, 45% EtOAc/Hexanes) to afford compound **4.63** (520 mg, 1.18 mmol, 79% Yield over 3 steps) as a colorless oil. The diastereoselectivity of the reaction was determined to be >10:1 by ^{1}H NMR analysis. $[\alpha]_D$ = -6° (c 2.0, CH_2Cl_2); R_f = 0.3 (40% EtOAc/Hexanes, PMA); ^{1}H NMR (500 MHz, $CDCl_3$) δ 7.37-7.12 (m, 10H), 5.05-4.95 (m, 2H), 4.93 (s, 1H), 3.88 (d, *J* = 9.8 Hz, 1H), 3.60 (dd, *J* = 8.4, 3.6 Hz, 1H), 3.07-2.88 (m, 2H), 2.80-2.56 (m, 3H), 2.37 (dt, *J* = 12.2, 8.6 Hz, 3H), 2.23 (dd, *J* = 14.2, 6.9 Hz, 1H), 2.05 (s, 3H), 1.99-1.79 (m, 2H), 1.73 (dddd, *J* = 13.5, 9.9, 6.5, 3.0 Hz, 1H), 1.02 (d, *J* = 6.9 Hz, 3H), 0.89 (d, *J* = 7.1 Hz, 3H); ^{13}C NMR (100 MHz, $CDCl_3$) δ 170.9, 147.9, 142.6, 141.3, 128.5, 128.5, 128.4, 128.3, 126.0, 125.8, 114.1, 74.2, 73.7, 72.6, 41.6, 40.6, 39.3, 35.4, 35.3, 33.0, 31.7, 21.2, 12.1, 11.8.; IR (cast film) 3382, 3024, 2932, 1734, 1496, 1459, 1374, 1242, 1030, 970 cm^{-1} ; LRMS (FAB+) calc'd for $C_{28}H_{39}O_4$ $[M+H]^+$ 439.61, found 439.17.

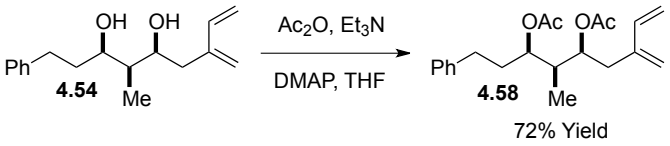

To a solution of diol **4.54** (667 mg, 2.56 mmol, 1.0 equiv) solvated in anhydrous THF (26 mL, 0.1 M) was added Et_3N (1.1 mL, 7.68 mmol, 3.0 equiv) followed by Ac_2O (0.61 mL, 6.40 mmol, 2.5 equiv) and DMAP (156 mg, 1.28 mmol, 0.5 equiv). The mixture was stirred at room temperature and the reaction progress was monitored by TLC analysis. At 2 h, the reaction was concentrated down to a white, salty oil. This crude residue was purified by silica gel chromatography (15% EtOAc/Hexanes) to afford

diacetate **4.58** (630 mg, 1.82 mmol, 72% Yield) as a pale yellow oil. The isolated diene was either used immediately or frozen in a solution of benzene for long-term storage. $[\alpha]_D$ = -3° (c 2.0, CH_2Cl_2); R_f = 0.8 (30% EtOAc/Hexanes, PMA); ^{1}H NMR (500 MHz, $CDCl_3$) δ 7.35-7.24 (m, 2H), 7.24-7.13 (m, 3H), 6.36 (dd, *J* = 17.6, 10.9 Hz, 1H), 5.43 (d, *J* = 17.6 Hz, 1H), 5.20 (td, *J* = 7.1, 3.5 Hz, 1H), 5.16 (d, *J* = 10.9 Hz, 1H), 5.13-5.07 (m, 1H), 5.04 (s, 1H), 4.96 (dt, *J* = 7.9, 5.3 Hz, 1H), 2.69-2.55 (m, 2H), 2.50 (qdd, *J* = 13.8, 7.1, 1.0 Hz, 2H), 2.06 (s, 3H), 2.01 (s, 3H), 2.01-1.94 (m, 1H), 1.94-1.81 (m, 2H), 1.02 (d, *J* = 7.0 Hz, 3H); ^{13}C NMR (125 MHz, $CDCl_3$) δ 170.6, 170.4, 142.3, 141.4, 138.0, 128.4, 128.3, 125.9, 118.7, 114.5, 74.8, 72.2, 38.4, 34.5, 33.2, 31.8, 21.1, 9.5; IR (cast film) 2958, 1736, 1455, 1372, 1236, 1023, 903 cm^{-1} ; LRMS (FAB+) calc'd for $C_{21}H_{29}O_4$ $[M+H]^+$ 345.45, found 345.28.

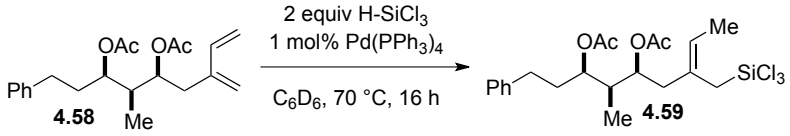

Diene **4.58** (35 mg, 0.10 mmol, 1.0 equiv) was reacted according to the first section of general procedure 2 in a sealed NMR tube. This small scale reaction was performed in C_6D_6 so that intermediate, hydrosilylated compound **4.59** could be observed and confirmed by ^{1}H and ^{13}C NMR. ^{1}H NMR (400 MHz, C_6D_6) δ 7.24-7.11 (m, 2H), 7.11-6.99 (m, 3H), 5.33-5.23 (m, 1H), 5.18 (ddd, *J* = 8.9, 5.6, 4.0 Hz, 1H), 5.12 (dt, *J* = 8.5, 4.1 Hz, 1H), 2.61-2.38 (m, 4H), 2.34 (dt, *J* = 14.9, 0.9 Hz, 1H), 2.21 (dd, *J* = 14.2, 8.9 Hz, 1H), 1.97-1.79 (m, 1H), 1.79-1.67 (m, 2H), 1.70 (s, 3H), 1.65 (s, 3H), 1.38 (d, *J* = 6.9 Hz, 3H), 0.93 (d, *J* = 7.0 Hz, 3H); ^{13}C NMR (100 MHz, C_6D_6) δ 169.7, 169.3, 141.1,

128.4, 128.4, 128.2, 127.9, 127.8, 127.7, 127.5, 127.4, 127.0, 126.0, 125.7, 73.5, 71.6, 41.6, 40.1, 33.7, 32.1, 27.3, 20.2, 20.1, 14.1, 9.6. Some excess trichlorosilane was also observed by ^{1}H NMR (400 MHz, C_6D_6) δ 5.40 (s).

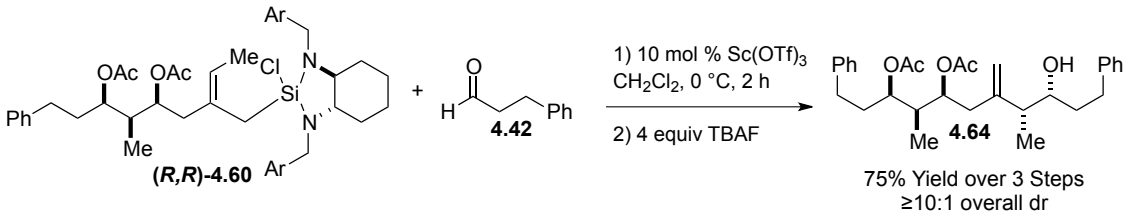

Diene **4.58** (506 mg, 1.47 mmol, 1.0 equiv) was coupled with hydrocinnamaldehyde **4.42** (194 μL, 1.47 mmol, 1.0 equiv) according to general procedure 2 using diamine ***(R,R)*-4.1**. The crude material was purified by silica gel chromatography (20% EtOAc/Hexanes) to afford compound **4.64** (528 mg, 1.10 mmol, 75% Yield over 3 steps) as a colorless oil. The diastereoselectivity of the reaction was determined to be >10:1 by ^{1}H NMR analysis. $[\alpha]_D$ = +29° (c 0.9, CH_2Cl_2); R_f = 0.4 (25% EtOAc/Hexanes, PMA); ^{1}H NMR (500 MHz, $CDCl_3$) δ 7.35-7.27 (m, 4H), 7.27-7.16 (m, 6H), 5.04 (tt, *J* = 8.3, 4.0 Hz, 2H), 4.96 (s, 1H), 4.89 (s, 1H), 3.61 (dq, *J* = 6.9, 3.3 Hz, 1H), 2.87 (ddd, *J* = 15.1, 10.3, 5.3 Hz, 1H), 2.65 (dtd, *J* = 36.3, 9.7, 9.3, 6.4 Hz, 3H), 2.40 (dd, *J* = 14.2, 3.4 Hz, 1H), 2.31-2.16 (m, 2H), 2.07 (s, 3H), 2.00 (s, 3H), 1.98-1.78 (m, 3H), 1.74 (tdd, *J* = 9.8, 6.2, 3.1 Hz, 1H), 1.67 (d, *J* = 2.9 Hz, 1H), 1.01 (d, *J* = 7.0 Hz, 3H), 0.98 (d, *J* = 6.9 Hz, 3H); ^{13}C NMR (100 MHz, $CDCl_3$) δ 170.7, 170.3, 148.1, 142.2, 141.2, 128.5, 128.4, 128.4, 128.3, 126.0, 125.8, 113.6, 74.0, 72.1, 71.5, 43.5, 40.3, 39.3, 36.1, 33.7, 32.9, 32.1, 21.1, 21.0, 12.4, 10.0; IR (cast film) 3444, 3028, 2946, 1735, 1643, 1455, 1373, 1239, 1025, 899 cm^{-1}; LRMS (FAB+) calc'd for $C_{30}H_{41}O_5$ $[M+H]^+$ 481.65, found 481.35.

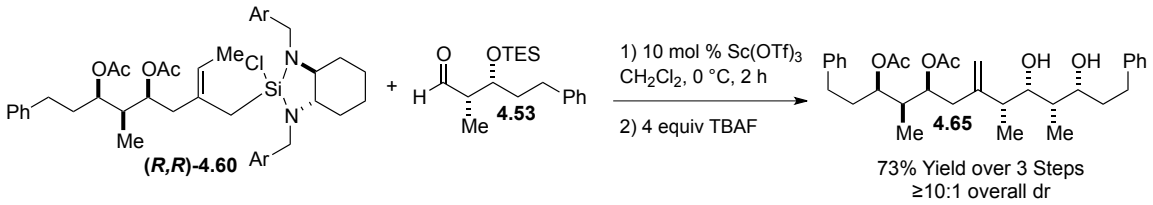

Diene **4.58** (506 mg, 1.47 mmol, 1.0 equiv) was coupled with aldehyde **4.53** (450 mg, 1.47 mmol, 1.0 equiv) according to general procedure 2 using diamine **(*R*,*R*)-4.1**. The crude material was purified by silica gel chromatography (40% EtOAc/Hexanes) to afford compound **4.65** (579 mg, 1.07 mmol, 73% Yield over 3 steps) as a colorless oil. The diastereoselectivity of the reaction was determined to be >10:1 by ^{1}H NMR analysis. $[\alpha]_D$ = +23° (c 1.3, CH_2Cl_2); R_f = 0.4 (40% EtOAc/Hexanes, PMA); ^{1}H NMR (500 MHz, $CDCl_3$) δ 7.35-7.26 (m, 4H), 7.26-7.15 (m, 6H), 5.08-4.97 (m, 2H), 4.92 (d, *J* = 6.1 Hz, 2H), 3.86-3.78 (m, 1H), 3.62 (t, *J* = 5.7 Hz, 1H), 2.95 (d, *J* = 3.9 Hz, 1H), 2.81 (ddd, *J* = 13.7, 10.2, 5.6 Hz, 1H), 2.71-2.54 (m, 3H), 2.41 (ddd, *J* = 18.6, 13.9, 5.3 Hz, 2H), 2.33 (bs, 1H), 2.16 (dd, *J* = 14.2, 9.3 Hz, 1H), 2.08 (s, 3H), 2.02 (s, 3H), 2.04-1.95 (m, 1H), 1.90 (dddd, *J* = 14.9, 11.6, 8.3, 4.8 Hz, 3H), 1.72 (dtd, *J* = 12.6, 5.8, 2.9 Hz, 1H), 1.63 (tdd, *J* = 7.9, 6.0, 5.3, 3.0 Hz, 1H), 1.04 (d, *J* = 6.9 Hz, 3H), 1.00 (d, *J* = 7.1 Hz, 3H), 0.99 (d, *J* = 7.2 Hz, 3H); ^{13}C NMR (125 MHz, $CDCl_3$) δ 171.4, 170.4, 148.4, 142.1, 141.1, 128.5, 128.4, 128.3, 126.1, 125.8, 113.8, 76.9, 74.1, 74.1, 72.3, 41.8, 40.6, 39.1, 38.2, 37.2, 34.0, 32.7, 32.2, 21.1, 21.0, 14.6, 9.9, 6.7; IR (cast film) 3447, 2936, 1735, 1455, 1373, 1237, 1024, 968 cm^{-1} ; LRMS (FAB+) calc'd for $C_{33}H_{47}O_6$ $[M+H]^+$ 539.72, found 539.50.

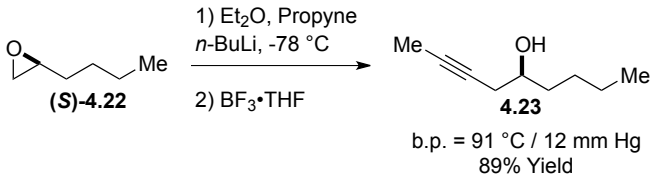

A flame-dried, 500 mL roundbottom flask was equipped with an overhead, mechanical stirrer and charged with Et_2O (250 mL, 0.15 M). The roundbottom flask was cooled to -78 °C, and condensed propyne (ca. 5 mL, 90.0 mmol, 2.4 equiv) was cannulated in from an adjacent volumetric flask also at -78 °C. A 2.5 M solution of *n*-BuLi in hexanes (22.5 mL, 56.3 mmol, 1.5 equiv) was syringed into the cold solution causing the reaction mixture to become white and thick (Note: mechanical stirring of this thick solution was critical to obtain a high yield). After 10 min of stirring the thick solution, (*S*)-1,2-epoxyhexane **(*S*)-4.22** (4.52 mL 37.5 mmol, 1.0 equiv) was added via syringe.[1] After an additional 10 min of stirring, distilled BF_3•OEt_2 (5.1 mL, 41.3 mmol, 1.1 equiv) was added dropwise over 10 min (Note: slow addition of BF_3•OEt_2 was critical for maintaining low reaction temperatures and high regioselectivity of the epoxide opening). The solution was stirred for an additional 30 min before being quenched with sat. $NaHCO_3$ (75 mL) at -78 °C. The resulting mixture was thawed to room temperature over 1 h. The aqueous phase was separated and then back extracted with Et_2O (2 x 100 mL). The combined organic layers were dried over $MgSO_4$, filtered, and carefully concentrated (10-20 °C on the rotary evaporator) to a yellow, salty oil. Distillation (b.p. 91 °C at 12 mm Hg) afforded homopropargylic alcohol **4.23** (4.62g, 33.0 mmol, 88% yield) as a fragrant, colorless oil. $[\alpha]_D$ = +4° (c 4.1, CH_2Cl_2); R_f = 0.7 (25% EtOAc/Hexanes, *p*-Anis - stains orange/pink); ^{1}H NMR (400 MHz, $CDCl_3$) δ 3.71 (tdd, *J* = 6.9, 5.9, 4.5 Hz, 1H), 2.41 (ddq, *J* = 16.5, 5.0, 2.5 Hz, 1H), 2.27 (ddq, *J* = 16.5, 7.3, 2.5

Hz, 1H), 1.90 (bs, 1H), 1.84 (t, J = 2.5 Hz, 3H), 1.59-1.50 (m, 2H), 1.49-1.26 (m, 4H), 0.94 (t, J = 7.0 Hz, 3H); ^{13}C NMR (100 MHz, $CDCl_3$) δ 78.3, 75.4, 70.2, 35.9, 27.8, 27.7, 22.7, 14.0, 3.5; IR (cast film) 3374, 2958, 2929, 2861, 1449, 1124, 1081, 1031, 907 cm^{-1}; LRMS (FAB+) calc'd for $C_9H_{17}O$ $[M+H]^+$ 141.23, found 141.15.

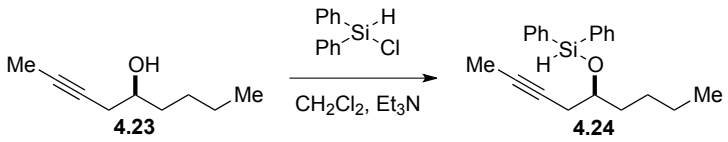

To a solution of alcohol **4.23** (701 mg, 5.0 mmol, 1.0 equiv) solvated in anhydrous CH_2Cl_2 (50 mL, 0.1 M) was added Et_3N (0.91 mL, 6.5 mmol, 1.3 equiv). The resulting mixture was cooled to 0 °C and chlorodiphenylsilane (1.07 mL, 5.5 mmol, 1.1 equiv) was added. The cold bath was removed and the solution was allowed to thaw to room temperature. After 30 min, the solution was concentrated down to a salty oil, retaken in hexanes and filtered over a flame-dried filter frit to remove the white Et_3N•HCl salts. The resulting filtrate was concentrated down to an orange/brown oil. Crude silyl-ether **4.24** was taken on to the next reaction without further purification. ^{1}H NMR (300 MHz, $CDCl_3$) δ 7.75-7.62 (m, 4H), 7.51-7.33 (m, 6H), 5.52 (s, 1H), 4.02-3.88 (m, 1H), 2.39 (dtt, J = 8.4, 5.3, 2.9 Hz, 2H), 1.75 (t, J = 2.6 Hz, 3H), 1.71-1.49 (m, 2H), 1.48-1.18 (m, 4H), 0.87 (t, J = 6.9 Hz, 2H); ^{13}C NMR (100 MHz, $CDCl_3$) δ 134.7, 134.3, 130.2, 127.9, 77.5, 76.2, 73.7, 36.1, 27.5, 27.4, 22.6, 14.0, 3.5.

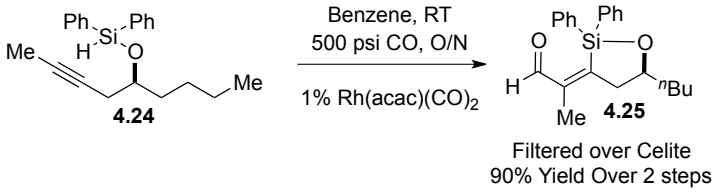

Crude silyl-ether **4.28** (ca. 1.6g, 5.0 mmol, 1.0 equiv) was solvated in anhydrous CH_2Cl_2 (10 mL, 0.5 M) and transferred to a glass bomb-liner. The bomb-liner was inserted into a Parr bomb device, which was sealed and purged three times with CO gas (Note: the bomb was charged to 500 psi and vented down to 100 psi for each purge). The bomb was charged with a final 500 psi H_2 and stirred for 5 min to saturate the solvent with CO. Following this initial saturation, the bomb was vented and temporarily opened to add $Rh(acac)(CO)_2$ (13 mg, 0.05 mmol, 0.01 equiv) to the solution. The bomb was subsequently resealed and purged three times with CO gas before being charged with a final 500 PSI H_2. After 16 h of vigorous stirring, the bomb was vented and opened. The resulting brown solution was concentrated and purified by silica gel chromatography (5% EtOAc/Hexanes) to afford silacycle-aldehyde **4.25** (1.35g, 3.85 mmol, 77% Yield over 2 steps) as a bright yellow oil. (Note: the desired product exhibited mild degradation on silica gel. Though the product was isolated above in high purity, it was also possible to filter the crude residue from this reaction over a short pad of pH 7 buffered SiO_2 gel[4] to afford the desired product in higher yields (ca. 85-90% over 2 steps) with acceptable purity for use in general procedure 2). $[\alpha]_D$ = -8° (c 3.5, CH_2Cl_2); R_f = 0.4 (5% EtOAc/Hexanes, PMA); ^{1}H NMR (400 MHz, $CDCl_3$) δ 9.59 (s, 1H), 7.67 (ddt, *J* = 8.3, 6.6, 1.5 Hz, 4H), 7.52 ? 7.37 (m, 6H), 4.39-4.28 (m, 1H), 3.12 (ddd, *J* = 18.2, 5.5, 1.3 Hz,

[4] pH 7 buffered SiO_2 gel was prepared my adding 10% pH 7 buffer (by mass) to a roundbotttom flask half filled with SiO_2 gel. The resulting mixture was rotated on a rotary evaporated for >12 h (at atmospheric pressure) and then stored for future use.

1H), 2.57 (ddq, *J* = 18.2, 8.2, 1.9 Hz, 1H), 2.00 (t, *J* = 1.5 Hz, 3H), 1.83 (dddd, *J* = 17.3, 10.1, 7.0, 5.1 Hz, 1H), 1.70 (ddt, *J* = 13.5, 10.9, 5.5 Hz, 1H), 1.60-1.32 (m, 3H), 0.94 (t, *J* = 7.2 Hz, 3H); ^{13}C NMR (100 MHz, $CDCl_3$) δ 192.7, 163.7, 144.7, 135.2, 135.1, 135.1, 133.2, 132.8, 130.7, 130.6, 128.2, 128.2, 128.1, 76.1, 41.7, 38.3, 27.8, 22.7, 14.1, 13.3; IR (cast film) 2929, 2858, 1682, 1430, 1263, 1117, 1016, 920 cm^{-1} ; LRMS (FAB+) calc'd for $C_{22}H_{27}O_2Si$ $[M+H]^+$ 351.54, found 351.27.

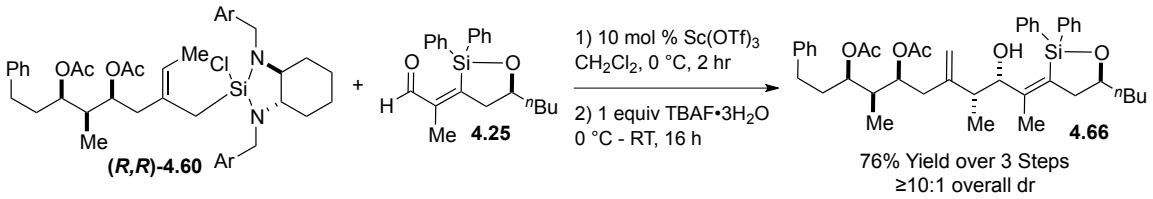

Diene **4.58** (506 mg, 1.47 mmol, 1.0 equiv) was coupled with silacycle-aldehyde **4.25** (516 mg, 1.47 mmol, 1.0 equiv) according to general procedure 2 using diamine **(*R*,*R*)-4.1**. The crude material was purified by silica gel chromatography (15% EtOAc/Hexanes, pH 7 buffered SiO_2 gel[4]) to afford compound **4.66** (783 mg, 1.12 mmol, 76% Yield over 3 steps) as a yellow oil. The diastereoselectivity of the reaction was determined to be >10:1 by ^{1}H NMR analysis. $[\alpha]_D$ = +19° (c 2.5, CH_2Cl_2); R_f = 0.4 (20% EtOAc/Hexanes, PMA); ^{1}H NMR (400 MHz, $CDCl_3$) δ 7.71 (dt, *J* = 6.7, 1.6 Hz, 2H), 7.59 (dt, *J* = 6.6, 1.5 Hz, 2H), 7.51-7.26 (m, 8H), 7.24-7.20 (m, 1H), 7.17 (dd, *J* = 8.0, 1.4 Hz, 2H), 5.18 (dt, *J* = 9.3, 4.5 Hz, 1H), 5.05 (dt, *J* = 7.6, 5.0 Hz, 1H), 5.01-4.92 (m, 3H), 3.54 (qt, *J* = 6.8, 3.4 Hz, 1H), 2.68-2.41 (m, 6H), 2.31 (dd, *J* = 14.2, 9.4 Hz, 1H), 2.05 (s, 3H), 2.05 (d, *J* = 21.6 Hz, 1H), 2.00 (s, 3H), 1.98 ? 1.82 (m, 2H), 1.87 (s, 3H), 1.44-1.08 (m, 6H), 1.01 (d, *J* = 6.9 Hz, 3H), 0.84 (t, *J* = 6.9 Hz, 3H), 0.75 (d, *J* = 6.9 Hz, 3H); ^{13}C NMR (125 MHz, $CDCl_3$) δ 170.7, 170.5, 155.8, 147.2, 141.3, 135.9, 135.1, 134.4, 130.1,

130.1, 130.0, 128.4, 128.3, 127.9, 127.8, 126.0, 114.2, 86.2, 74.3, 72.3, 71.2, 40.5, 40.1, 38.5, 37.2, 36.7, 33.7, 32.1, 27.8, 22.6, 21.1, 21.1, 14.0, 13.9, 11.4, 10.1; IR (cast film) 3464, 2930, 2859, 1735, 1430, 1372, 1238, 1116, 1021, 991 cm^{-1}; LRMS (FAB+) calc'd for $C_{43}H_{56}O_6Si$ $[M+H]^+$ 698.00, found 697.62.

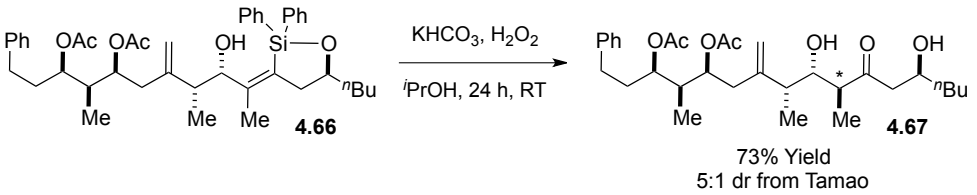

Silacycle **4.66** (783 mg, 1.12 mmol, 1.0 equiv) was solvated in isopropanol (11 mL, 0.1 M). $KHCO_3$ (561 mg, 5.60 mmol, 5.0 equiv) was added to the solution (sparingly soluble) followed by H_2O_2 as a 30% by weight solution in H_2O (1.46 mL, 1.3 ml/mmol, ca. 12 equiv). The reaction mixture was vigorously stirred at room temperature, and the reaction progress was monitored by TLC analysis. After 20 h, the reaction was quenched with brine (10 mL) and extracted with EtOAc (3 x 10 mL). The combined organic phase was dried over $MgSO_4$, filtered, and concentrated to a crude reaction residue. This residue was purified by silica gel chromatography (35% EtOAc/Hexanes) to afford complex polyketide fragment **4.67** (362 mg, 0.68 mmol, 61% Yield) as a colorless oil. The diastereoselectivity of the reaction was determined to be 5:1 by ^1H NMR analysis of the crude reaction residue.[5] $[\alpha]_D = +32°$ (c 1.0, CH_2Cl_2); R_f = 0.4 (40% EtOAc/Hexanes, PMA); ^1H NMR (400 MHz, $CDCl_3$) δ 7.36-7.26 (m, 2H), 7.26-7.15 (m, 3H), 5.10-4.98 (m, 3H), 4.93 (t, *J* = 1.2 Hz, 1H), 4.17-4.07 (m, 1H), 3.72 (dt, *J* = 9.2, 2.7 Hz, 1H), 3.21 (d, *J* = 3.4 Hz, 1H), 2.83-2.69 (m, 2H), 2.70-2.54 (m, 3H),

[5] This ratio was further confirmed upon isolation of the minor methyl diastereomer (72mg, 0.13 mmol 12% Yield) resulting in a combined tamao oxidation yield of 73%.

2.48-2.35 (m, 2H), 2.21 (dd, *J* = 14.1, 9.9 Hz, 1H), 2.09 (s, 3H), 2.05 (d, *J* = 2.8 Hz, 1H), 2.01 (s, 3H), 1.98-1.83 (m, 3H), 1.60-1.26 (m, 6H), 1.07 (d, *J* = 7.0 Hz, 3H), 1.00 (dd, *J* = 6.9, 2.1 Hz, 6H), 0.97-0.90 (m, 3H); ^{13}C NMR (100 MHz, $CDCl_3$) δ 215.8, 170.6, 170.3, 147.7, 141.1, 128.4, 128.3, 126.0, 114.6, 73.9, 73.0, 72.0, 67.5, 50.1, 48.4, 40.5, 39.9, 38.9, 36.1, 33.7, 32.1, 27.7, 22.6, 21.0, 20.9, 14.0, 13.1, 11.1, 10.1; IR (cast film) 3457, 2932, 1736, 1456, 1373, 1238, 1024, 975 cm^{-1} ; LRMS (FAB+) calc'd for $C_{31}H_{49}O_7$ $[M+H]^+$ 533.72, found 533.40.

Stereochemical Proofs. For the coupled polyketide fragments **4.62**, **4.63**, and **4.65**, stereochemical proofs of the newly formed alcohol stereocenter were achieved by Rychnovsky's ^{13}C NMR analysis of acetonides.[2] For complex polyketide fragment **4.67**, the orientation of the methyl stereocenter set during the tamao oxidation was established by nOe analysis from its acetonide derivitive **4.72**. All other stereocenters formed using the methodologies developed in this publication were assigned by analogy to previous work.[3]

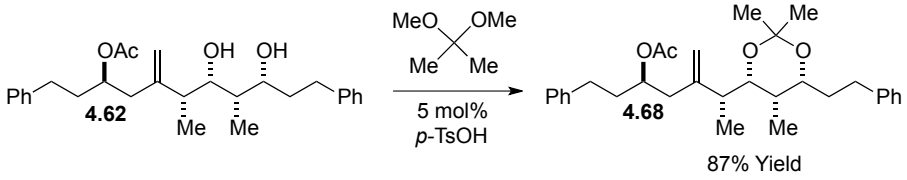

Diol **4.62** (24 mg, 0.055 mmol, 1.0 equiv) was solvated in 2,2-dimethoxypropane (1 mL, 0.05 M). *p*-TsOH•H_2O (ca. 0.5 mg, 0.003 mmol, 0.05 equiv) was added, and the reaction was allowed to stir at room temperature. After 20 min, the reaction was quenched with sat. $NaHCO_3$ and extracted 3x with EtOAc. The combined organic phase was dried over $MgSO_4$, filtered, and concentrated. The resulting residue was purified by silica gel chromatography (7% EtOAc/Hexanes) to afford *syn*-acetonide **4.68** (23 mg, 0.048 mmol, 87% Yield) as a colorless oil. The stereochemistry of the acetonide was verified by ^{13}C NMR analysis (see below). $[\alpha]_D$ = +5° (c 2.3, CH_2Cl_2); R_f = 0.4 (10% EtOAc/Hexanes, PMA); ^1H NMR (400 MHz, $CDCl_3$) δ 7.36-7.26 (m, 4H), 7.21 (ddt, *J* = 7.1, 3.1, 2.0 Hz, 6H), 5.17 (tt, *J* = 7.5, 5.4 Hz, 1H), 4.96-4.85 (m, 2H), 3.78 (ddd, *J* = 8.7, 4.4, 2.1 Hz, 1H), 3.62 (dd, *J* = 10.1, 1.9 Hz, 1H), 2.81-2.55 (m, 4H), 2.42-2.27 (m, 2H), 2.24-2.14 (m, 1H), 2.05 (s, 3H), 2.02-1.84 (m, 3H), 1.59 (dddd, *J* = 13.7, 9.4, 7.2, 4.5 Hz,

1H), 1.46 (s, 3H), 1.43 (s, 3H), 1.39 (dtd, *J* = 6.7, 4.7, 2.3 Hz, 1H), 1.07 (d, *J* = 6.7 Hz, 3H), 0.86 (d, *J* = 6.7 Hz, 3H); ^{13}C NMR (100 MHz, $CDCl_3$) δ 170.7, 146.7, 142.1, 141.7, 128.6, 128.4, 128.3, 126.0, 125.8, 113.4, **99.2**, 77.2, 72.8, 72.2, 42.1, 39.2, 35.8, 34.5, 33.2, 31.8, 31.7, **30.1**, 21.2, **19.8**, 17.9, 5.3; IR (cast film) 2939, 1736, 1455, 1376, 1240, 1199, 1161, 1110, 1027, 1010 cm^{-1} ; LRMS (FAB+) calc'd for $C_{31}H_{43}O_4$ $[M+H]^+$ 479.67, found 479.40.

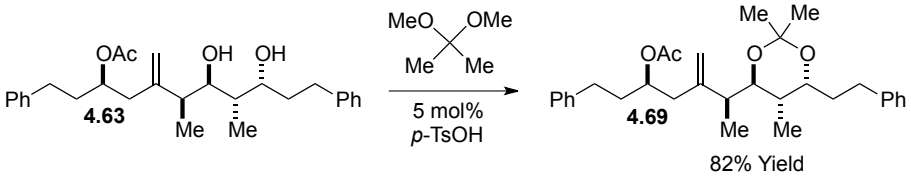

Diol **4.63** (54 mg, 0.123 mmol, 1.0 equiv) was solvated in 2,2-dimethoxypropane (1.2 mL, 0.1 M). *p*-TsOH•H_2O (ca. 1 mg, 0.006 mmol, 0.05 equiv) was added, and the reaction was allowed to stir at room temperature. After 30 min, the reaction was quenched with sat. $NaHCO_3$ and extracted 3x with EtOAc. The combined organic phase was dried over $MgSO_4$, filtered, and concentrated. The resulting residue was purified by silica gel chromatography (7% EtOAc/Hexanes) to afford *anti*-acetonide **4.69** (48 mg, 0.100 mmol, 82% Yield) as a colorless oil. The stereochemistry of the acetonide was verified by ^{13}C NMR analysis (see below). $[\alpha]_D$ = -16° (c 1.4, CH_2Cl_2); R_f = 0.4 (10% EtOAc/Hexanes, PMA); ^{1}H NMR (400 MHz, $CDCl_3$) δ 7.35-7.26 (m, 4H), 7.22 (ddd, *J* = 14.9, 6.9, 1.7 Hz, 6H), 5.11 (qd, *J* = 7.2, 4.8 Hz, 1H), 4.98 (s, 1H), 4.85 (d, *J* = 1.5 Hz, 1H), 3.79 (dt, *J* = 9.2, 4.2 Hz, 1H), 3.30 (dd, *J* = 7.4, 3.7 Hz, 1H), 2.82 (ddd, *J* = 14.7, 10.0, 5.2 Hz, 1H), 2.77-2.51 (m, 3H), 2.38 (dd, *J* = 14.6, 7.4 Hz, 1H), 2.30 (dd, *J* = 14.6, 6.1 Hz, 1H), 2.19 (qd, *J* = 6.7, 3.5 Hz, 1H), 2.04 (s, 3H), 1.91 (dqd, *J* = 10.4, 7.7, 4.0 Hz,

2H), 1.81 (dp, *J* = 14.2, 4.9 Hz, 1H), 1.76-1.68 (m, 1H), 1.63 (dtd, *J* = 13.3, 6.4, 3.2 Hz, 1H), 1.35 (d, *J* = 1.3 Hz, 6H), 1.05 (d, *J* = 6.9 Hz, 3H), 0.86 (d, *J* = 6.8 Hz, 3H); ^{13}C NMR (100 MHz, $CDCl_3$) δ 170.6, 148.1, 142.3, 141.6, 128.4, 128.4, 128.3, 125.9, 125.7, 112.8, **100.3**, 76.9, 72.2, 68.9, 42.6, 40.3, 37.8, 35.8, 32.6, 32.4, 31.8, **25.4**, **23.8**, 21.2, 14.1, 12.3; IR (cast film) 2936, 1736, 1496, 1455, 1378, 1239, 1166, 1140, 1023 cm^{-1}; LRMS (FAB+) calc'd for $C_{31}H_{43}O_4$ $[M+H]^+$ 479.67, found 479.37.

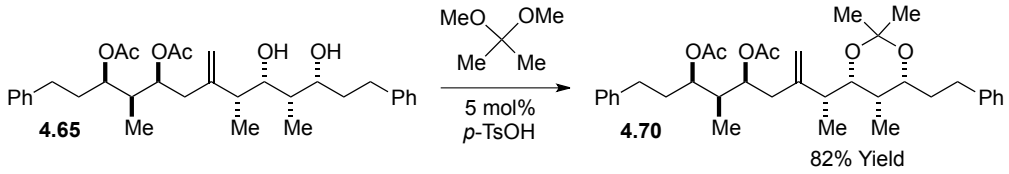

Diol **4.65** (29 mg, 0.054 mmol, 1.0 equiv) was solvated in 2,2-dimethoxypropane (1 mL, 0.05 M). *p*-TsOH•H_2O (ca. 0.5 mg, 0.003 mmol, 0.05 equiv) was added, and the reaction was allowed to stir at room temperature. After 15 min, the reaction was quenched with sat. $NaHCO_3$ and extracted 3x with EtOAc. The combined organic phase was dried over $MgSO_4$, filtered, and concentrated. The resulting residue was purified by silica gel chromatography (10% EtOAc/Hexanes) to afford *syn*-acetonide **4.70** (48 mg, 0.100 mmol, 82% Yield) as a pale yellow oil. The stereochemistry of the acetonide was verified by ^{13}C NMR analysis (see below). $[\alpha]_D$ = +6° (c 2.9, CH_2Cl_2); R_f = 0.3 (10% EtOAc/Hexanes, PMA); ^{1}H NMR (500 MHz, $CDCl_3$) δ 7.35-7.25 (m, 4H), 7.25-7.15 (m, 6H), 5.16 (tt, *J* = 6.7, 2.9 Hz, 1H), 4.99 (q, *J* = 5.9 Hz, 1H), 4.91 (d, *J* = 17.8 Hz, 2H), 3.78 (ddd, *J* = 8.4, 4.3, 2.0 Hz, 1H), 3.60 (dd, *J* = 10.1, 1.8 Hz, 1H), 2.75 (ddd, *J* = 14.2, 9.2, 5.3 Hz, 1H), 2.69-2.54 (m, 3H), 2.30 (dt, *J* = 13.0, 6.6 Hz, 1H), 2.24 (d, *J* = 6.8 Hz, 2H), 2.05 (s, 3H), 2.02 (s, 0H), 2.01 (s, 3H), 1.97-1.85 (m, 3H), 1.59 (dddd, *J* = 13.4, 9.1,

7.3, 4.3 Hz, 1H), 1.45 (d, *J* = 11.1 Hz, 6H), 1.40-1.32 (m, 1H), 1.07 (d, *J* = 6.7 Hz, 3H), 1.00 (d, *J* = 7.0 Hz, 3H), 0.87 (d, *J* = 6.7 Hz, 3H); ^{13}C NMR (125 MHz, $CDCl_3$) δ 170.6, 170.4, 146.7, 142.1, 141.2, 128.6, 128.4, 128.3, 128.3, 126.0, 125.7, 113.6, **99.2**, 77.2, 74.3, 72.8, 72.7, 42.2, 39.3, 36.4, 34.5, 33.6, 33.3, 32.0, 31.7, **30.1**, 21.1, **19.8**, 17.8, 9.9, 5.3; IR (cast film) 2986, 2939, 1736, 1455, 1373, 1233, 1199, 1020, 970 cm^{-1} ; LRMS (FAB+) calc'd for $C_{36}H_{51}O_6$ $[M+H]^+$ 579.79, found 579.33

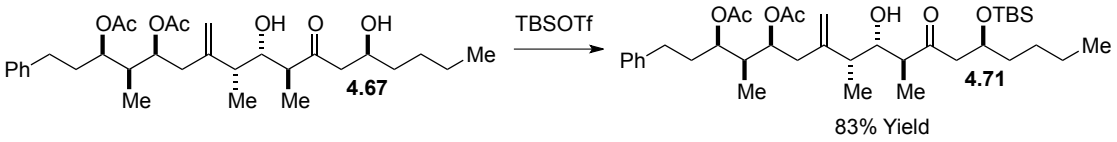

A solution of diol **4.67** (60 mg, 0.113 mmol, 1.0 equiv) solvated in anhydrous CH_2Cl_2 was cooled to -78 °C. 2,6-Lutidine (20 µL, 0.170 mmol, 1.5 equiv) was added followed by TBS-OTf (31 µL, 1.2 equiv). The solution was stirred for 20 min at -78 °C before being quenched with sat. $NaHCO_3$. The cold bath was removed, and the resulting mixture was allowed to thaw to room temperature. The aqueous phase was extracted 3x with CH_2Cl_2, and the combined organic phase was dried over $MgSO_4$, filtered, and concentrated. The resulting residue was purified by silica gel chromatography (15% EtOAc/Hexanes) to afford TBS-ether **4.71** (61 mg, .094 mmol, 83% Yield) as a colorless oil. $[\alpha]_D$ = +23° (c 0.9, CH_2Cl_2); R_f = 0.3 (15% EtOAc/Hexanes, PMA); ^{1}H NMR (400 MHz, $CDCl_3$) δ 7.36-7.25 (m, 2H), 7.25-7.14 (m, 3H), 5.07 (ddd, *J* = 9.2, 5.3, 3.6 Hz, 1H), 5.04-4.94 (m, 2H), 4.91 (s, 1H), 4.24 (dt, *J* = 11.0, 5.5 Hz, 1H), 3.66 (dt, *J* = 8.5, 3.4 Hz, 1H), 2.83-2.51 (m, 4H), 2.35 (dq, *J* = 13.8, 6.1, 4.8 Hz, 2H), 2.21 (dd, *J* = 14.3, 9.7 Hz, 1H), 2.12 (d, *J* = 3.7 Hz, 1H), 2.07 (s, 3H), 2.00 (s, 3H), 1.91 (dq, *J* = 11.1, 7.7, 6.9

Hz, 3H), 1.55-1.39 (m, 2H), 1.31 (qd, J = 6.2, 5.2, 2.4 Hz, 5H), 1.06 (d, J = 7.1 Hz, 3H), 1.00 (dd, J = 6.9, 2.1 Hz, 6H), 0.95-0.80 (m, 12H), 0.10 (s, 3H), 0.05 (s, 3H); ^{13}C NMR (100 MHz, $CDCl_3$) δ 213.5, 170.6, 170.4, 147.8, 141.2, 128.5, 128.3, 126.0, 114.3, 74.0, 73.1, 71.9, 67.8, 51.2, 48.7, 40.4, 40.3, 38.6, 37.3, 33.6, 32.1, 27.2, 25.9, 22.8, 21.1, 21.0, 18.0, 14.1, 13.0, 11.4, 10.2, -4.6; IR (cast film) 3517, 2956, 2931, 2858, 1738, 1459, 1373, 1239, 1025, 976 cm^{-1} ; LRMS (FAB+) calc'd for $C_{37}H_{63}O_7Si$ $[M+H]^+$ 647.98, found 647.51.

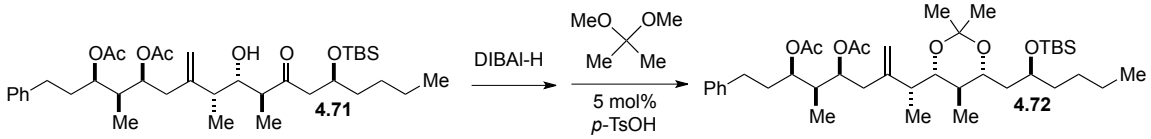

A solution of ketone **4.71** (51 mg, 0.079 mmol, 1.0 equiv) in anhydrous THF (1.6 mL, 0.05 M) was cooled to -78 °C. A 1.0 M solution of DIBAl-H in hexanes (0.24 mL, 0.237 mmol, 3.0 equiv) was slowly added over 1 min. After 30 min, the reaction was quenched with a 1 M solution of tartaric acid at – 78 °C. The resulting mixture was removed from the cold bath and allowed to thaw to room temperature. The aqueous phase was extracted 3x with CH_2Cl_2, and the combined organic phase was dried over $MgSO_4$, filtered, and concentrated. The resulting residue was purified by silica gel chromatography (20% EtOAc/Hexanes) to afford the reduced product. The isolated diol was determined to be an inseparable 2:1 mixture of diastereomers by ^{1}H NMR analysis.

The above mixture of diols (ca. 51mg, 0.079 mmol, 1.0 equiv) was solvated in 2,2-dimethoxypropane (1 mL, 0.08 M). *p*-TsOH•H_2O (ca. 1 mg, 0.004 mmol, 0.05 equiv) was added, and the reaction was allowed to stir at room temperature. After 20 min, the reaction was quenched with sat. $NaHCO_3$ and extracted 3x with EtOAc. The

combined organic phase was dried over $MgSO_4$, filtered, and concentrated. The resulting residue was purified by silica gel chromatography (10% EtOAc/Hexanes) to afford a 2:1 mixture of *syn/anti*-acetonides (45 mg, 0.065 mmol, 83% Yield over 2 steps) as a pale yellow oil. The mixture of diastereomers was repurified by silica gel chromatography (15% Et_2O/Hexanes) to afford a small amount of the major *syn*-acetonide **4.72** for full characterization. The stereochemistry of the major acetonide was verified by ^{13}C NMR analysis (see below). $[\alpha]_D$ = +20° (c 0.9, CH_2Cl_2); R_f = 0.4 (10% EtOAc/Hexanes, PMA); ^1H NMR (400 MHz, $CDCl_3$) δ 7.36-7.25 (d, *J* = 4.6 Hz, 2H), 7.25-7.14 (m, 3H), 5.12 (dt, *J* = 9.0, 4.6 Hz, 1H), 5.00 (q, *J* = 6.0 Hz, 1H), 4.92 (s, 1H), 4.83 (s, 1H), 3.90 (qd, *J* = 8.0, 6.8, 4.0 Hz, 1H), 3.66-3.47 (m, 2H), 2.70-2.52 (m, 2H), 2.46-2.31 (m, 2H), 2.25 (dd, *J* = 14.7, 8.6 Hz, 1H), 2.07 (s, 3H), 2.00 (s, 3H), 1.99-1.85 (m, 3H), 1.72 (ddd, *J* = 13.8, 9.2, 1.5 Hz, 1H), 1.48 (dddd, *J* = 9.1, 7.0, 4.9, 3.0 Hz, 2H), 1.39 (s, 3H), 1.37-1.22 (m, 9H), 1.01 (dd, *J* = 7.1, 2.0 Hz, 6H), 0.92 (s, 12H), 0.79 (d, *J* = 6.5 Hz, 3H), 0.08 (d, *J* = 3.2 Hz, 6H); ^{13}C NMR (100 MHz, $CDCl_3$) δ 170.5, 170.3, 147.9, 141.3, 128.4, 128.3, 125.9, 112.7, **97.4**, 75.4, 74.4, 72.3, 71.2, 68.5, 41.7, 39.7, 39.0, 38.0, 37.8, 35.7, 34.0, 32.0, **30.1**, 26.6, 26.0, 23.0, 21.1, 21.1, **19.9**, 18.1, 14.1, 12.5, 11.8, 10.0, -3.9, -4.4; IR (cast film) 2956, 2931, 2858, 1738, 1461, 1376, 1240, 1202, 1026 cm^{-1} ; LRMS (FAB+) calc'd for $C_{40}H_{68}O_7$ $[M]^+$ 689.05, found 689.48.

nOe Analysis of 4.72:

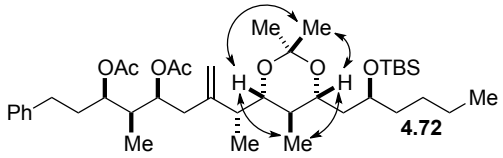

nOe analysis of **4.72** unambiguously confirmed the orientation of the methyl stereocenter set during the tamao oxidation of silacycle **4.66** to ketone **4.67**.

1. Tokunaga, M.; Larrow, J. F.; Kakiuchi, F.; Jacobsen, E. N., *Science* **1997,** *277* (5328), 936-938.

2. Rychnovsky, S. D.; Rogers, B.; Yang, G., *J. Org. Chem.* **1993,** *58* (13), 3511-3515.

3. Kim, H.; Ho, S.; Leighton, J. L., *J. Am. Chem. Soc.* **2011,** *133* (17), 6517-6520.

HPLC Chromatograms for Chapter 4

All racemic dienes were prepared by reacting trichlorosilane **4.38** with the precursor aldehyde in a solution of DMF.

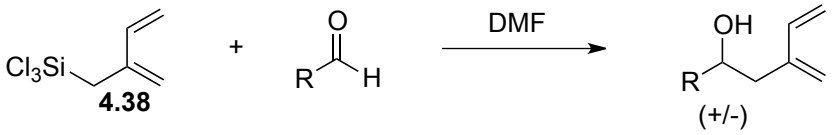

HPLC chromatograms for compound 4.43:

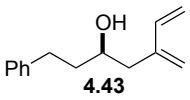

94% ee

Chiralcel OD Column, 5% *i*-PrOH in hexanes, 1 mL/min, 230 nm

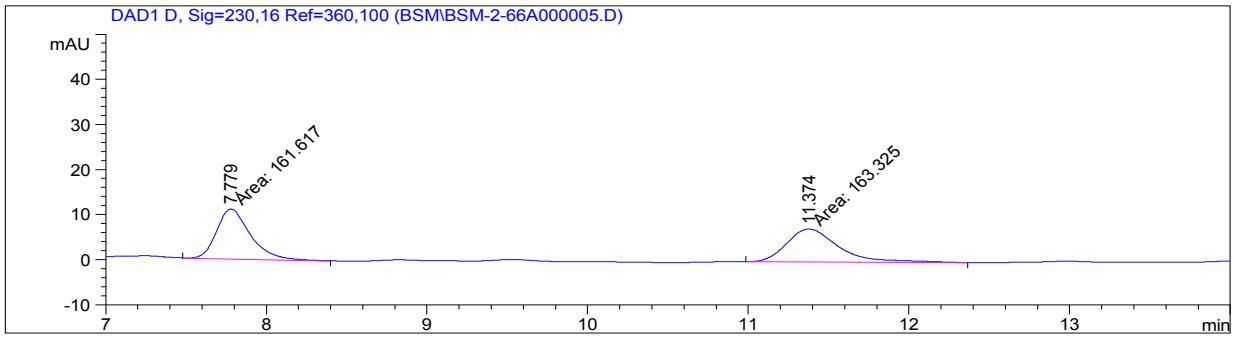

Peak #	RetTime [min]	Sig	Type	Area [mAU*s]	Height [mAU]	Area %
1	7.779	1	MM	161.61710	11.06059	49.7372
2	11.374	1	MM	163.32510	7.30261	50.2628

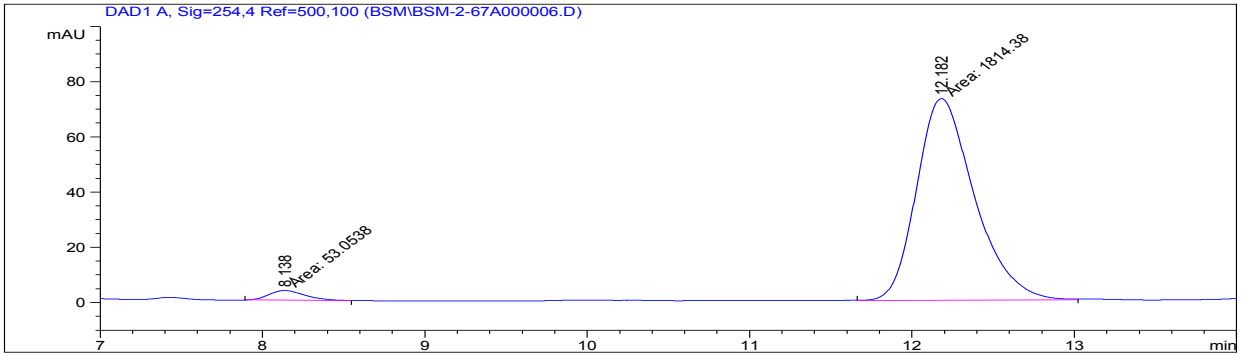

Peak #	RetTime [min]	Sig	Type	Area [mAU*s]	Height [mAU]	Area %
1	8.138	1	MM	53.05380	3.50956	2.8410
2	12.182	1	MM	1814.38416	73.03902	97.1590

HPLC chromatograms for compound 4.45:

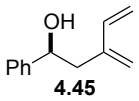

4.45

86% ee

Chiralcel OD Column, 5% *i*-PrOH in hexanes, 1 mL/min, 230 nm

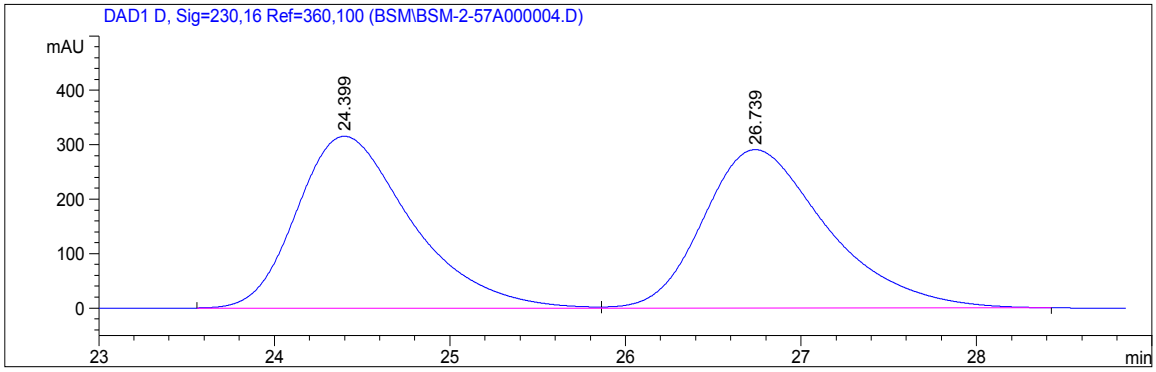

Peak #	RetTime [min]	Sig	Type	Area [mAU*s]	Height [mAU]	Area %
1	24.399	1	BB	1.43269e4	315.72733	49.9893
2	26.739	1	BB	1.43331e4	290.96811	50.0107

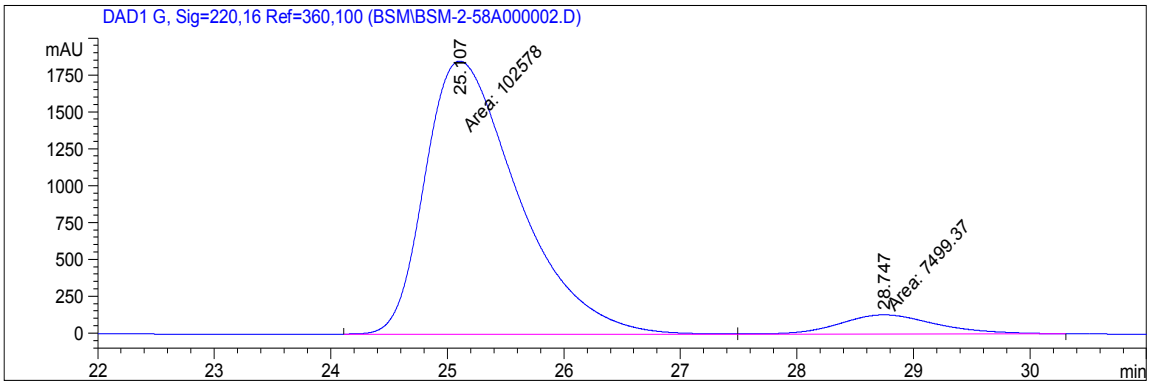

Peak #	RetTime [min]	Sig	Type	Area [mAU*s]	Height [mAU]	Area %
1	25.107	1	MM	1.02578e5	1850.53357	93.1872
2	28.747	1	MM	7499.36816	129.86911	6.8128

HPLC chromatograms for compound 4.47:

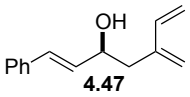

86% ee

Chiralcel OD Column, 5% *i*-PrOH in hexanes, 1 mL/min, 230 nm

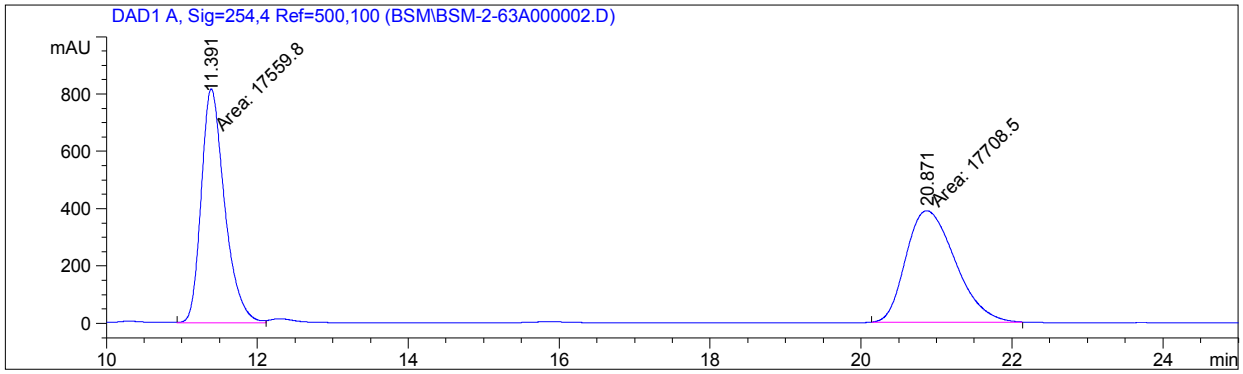

Peak #	RetTime [min]	Sig	Type	Area [mAU*s]	Height [mAU]	Area %
1	11.391	1	MM	1.75598e4	815.82251	49.7891
2	20.871	1	MM	1.77085e4	389.36655	50.2109

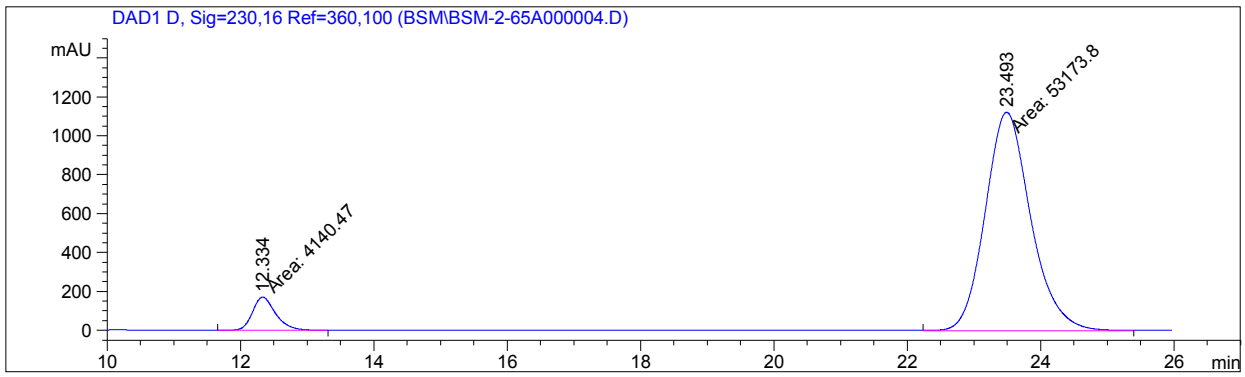

Peak #	RetTime [min]	Sig	Type	Area [mAU*s]	Height [mAU]	Area %
1	12.334	1	MM	4140.47070	170.59232	7.2241
2	23.493	1	MM	5.31738e4	1121.85962	92.7759

HPLC chromatograms for compound 4.49:

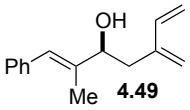

87% ee

Chiralcel OD Column, 5% *i*-PrOH in hexanes, 1 mL/min, 230 nm

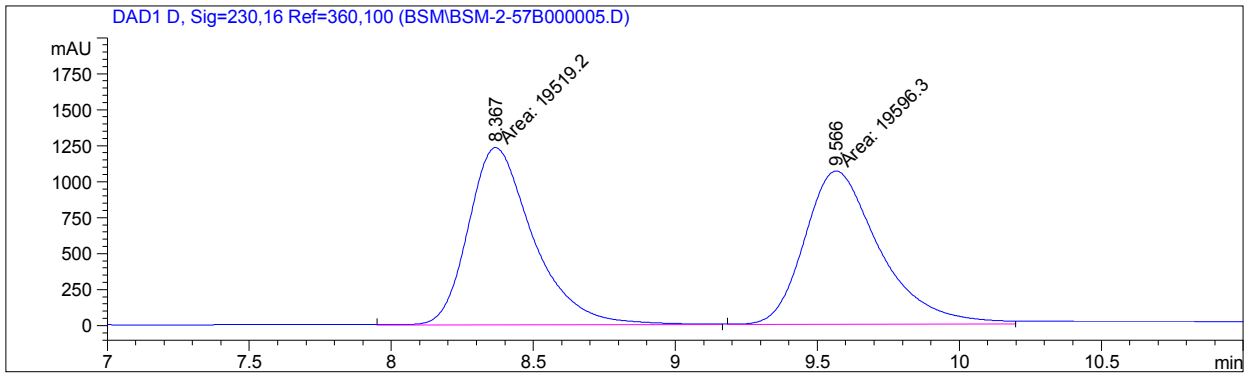

Peak #	RetTime [min]	Sig	Type	Area [mAU*s]	Height [mAU]	Area %
1	8.367	1	MM	1.95192e4	1229.96985	49.9015
2	9.566	1	MM	1.95963e4	1064.27173	50.0985

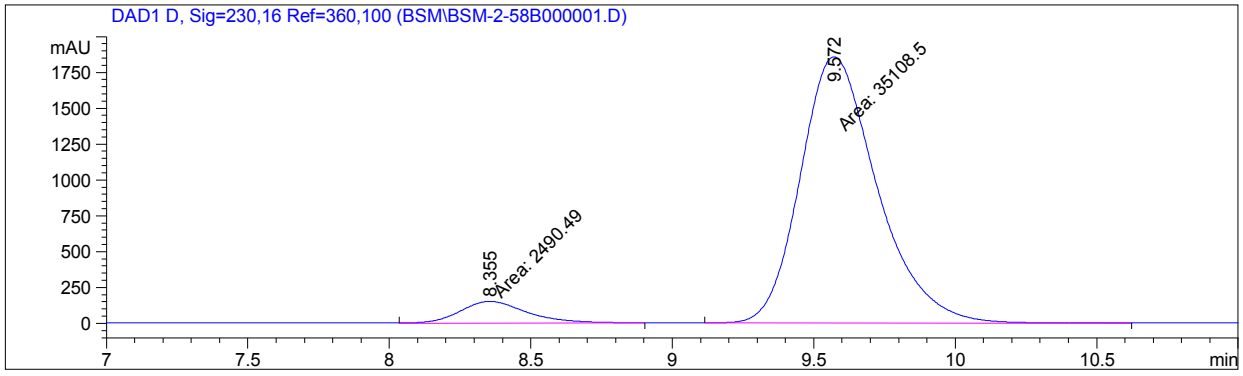

Peak #	RetTime [min]	Sig	Type	Area [mAU*s]	Height [mAU]	Area %
1	8.355	1	MM	2490.49487	151.44154	6.6238
2	9.572	1	MM	3.51085e4	1857.52759	93.3762

HPLC chromatograms for compound 4.51:

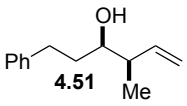

96% ee

Chiralcel AD-H Column, 5% *i*-PrOH in hexanes, 1 mL/min, 254 nm

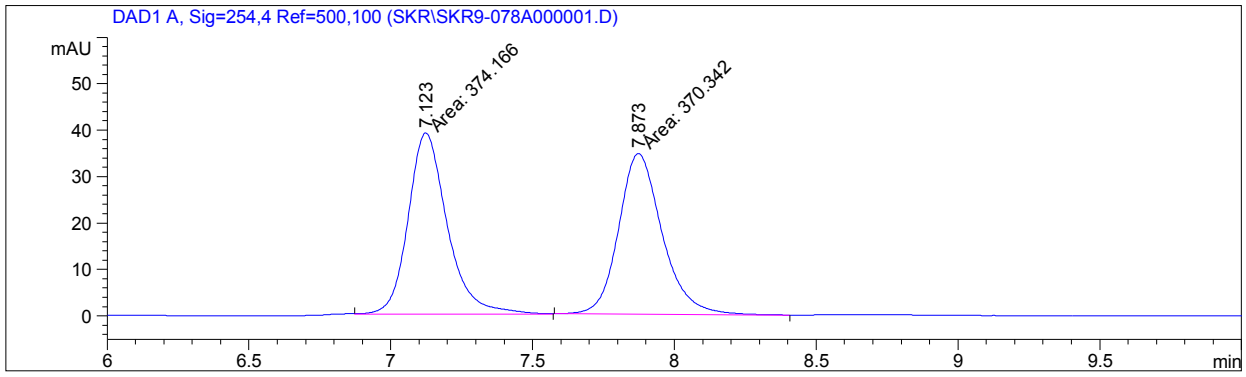

Peak #	RetTime [min]	Sig	Type	Area [mAU*s]	Height [mAU]	Area %
1	7.123	1	MM	374.16617	39.00862	50.2568
2	7.873	1	MM	370.34189	34.64413	49.7432

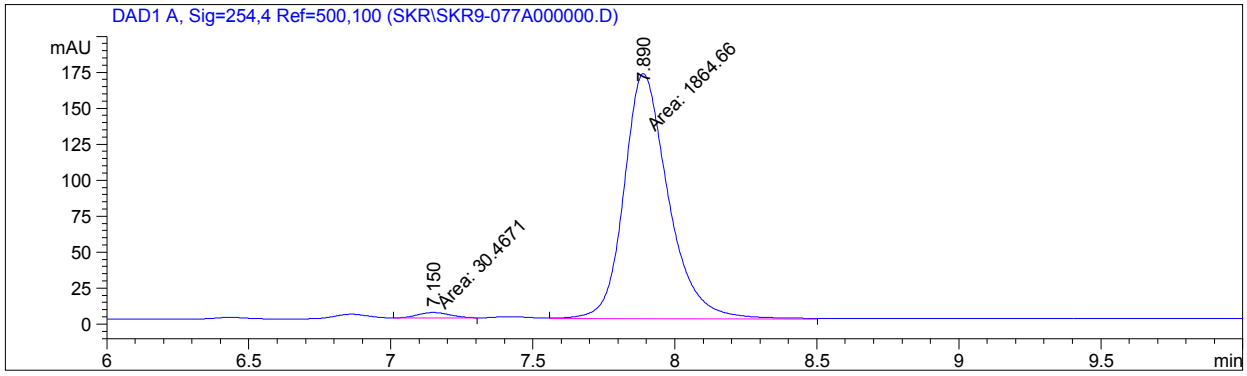

Peak #	RetTime [min]	Sig	Type	Area [mAU*s]	Height [mAU]	Area %
1	7.150	1	MM	30.46707	3.78520	1.6076
2	7.890	1	MM	1864.66418	170.56212	98.3924

Chapter 7: Experimental Information for Chapter 5

General Information. Unless otherwise stated, all chemical compounds were purchased from common commercial sources, and all reactions were carried out under an atmosphere of nitrogen in flame or oven-dried glassware with magnetic stirring unless otherwise indicated. Degassed solvents were purified by passage through an activated alumina column. Thin-layer chromatography (TLC) was carried out on glass backed silica gel TLC plates (250 μm) from Silicycle; visualization by UV light, phosphomolybdic acid (PMA), *p*-Anisaldehyde (*p*-Anis) or potassium permanganate ($KMnO_4$) stain. Gas chromatographic analyses were performed on a Hewlett-Packard 6890 Series Gas Chromatograph equipped with a capillary split-splitless inlet and flame ionization detector with electronic pneumatics control using either a Supelco β-Dex 120 (30 m x 0.25 mm) or Supelco β-Dex 325 (30 m x 0.25 mm) capillary GLC column. HPLC analysis was carried out on an Agilent 1200 Series using either a Chiralpak AD-H (250 × 4.5 mm ID) column or Chiralcel OD (250 × 4.5 mm ID) column. ^{1}H NMR spectra were recorded on a Bruker DPX-300 (300 MHz), Bruker DRX-300 (300 MHz), Bruker AVIII nano bay-400 (400 MHz), Bruker AVIII single bay-400 (400 MHz), Avance III 500 (500 mHz) or a Avance III 500 Ascend magnet (500 MHz) spectrometer and are reported in ppm from $CDCl_3$ internal standard (7.26 ppm). Data are reported as follows: (bs= broad singlet, s = singlet, d = doublet, t = triplet, q = quartet, p = quintet, h = hextet, sep = septet, m = multiplet, dd = doublet of doublets, ddd = doublet of doublet of doublets, dddd = doublet of doublet of doublet of doublets; coupling constant(s) in Hz; integration). Proton decoupled ^{13}C NMR spectra were recorded on a Bruker DRX-300 (300 MHz), Bruker AVIII single bay-400 (400 MHz), Bruker AVIII nano bay-400 (400 MHz), Avance III 500 (500 mHz) or a Avance III 500 Ascend magnet (500 MHz)

spectrometer and are reported in ppm from $CDCl_3$ internal standard (77.0 ppm). Infrared spectra were recorded on a Nicolet Avatar 370DTGS FT-IR. Optical rotations were recorded on a Jasco DIP-1000 digital polarimeter. (APCI)-MS was conducted on a JMS-LCmate LCMS (JEOL).

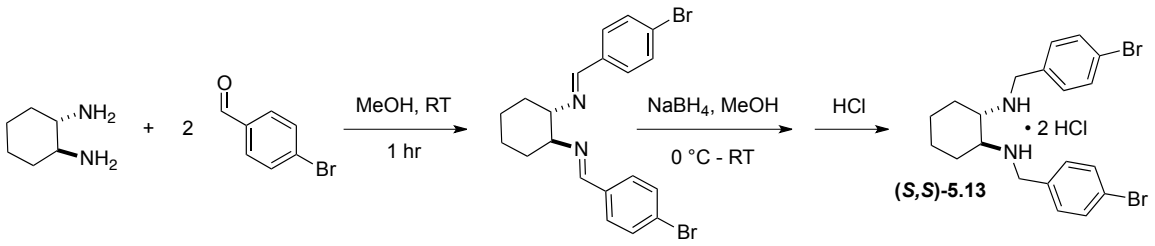

A 5 L, 2-neck roundbottom flask was evacuated and purged with N_2. (*S,S*)-(+)-1,2-Diaminocyclohexane (60g, 525 mmol, 1.0 equiv) was chiseled out in 5g batches and added to the large roundbottom portionwise with minimal air exposure. The diamine was solvated in MeOH (1.3 L, 0.4 M), and the flask was equipped with an overhead, mechanical stirrer and a N_2 line. *p*-Bromobenzaldehyde (195g, 1,050 mmol, 2.0 equiv) was added at room temperature. After 20 min of stirring, newly formed diimine crashed out of the reaction solvent. The heterogeneous mixture was stirred for a total of one hour before being cooled to 0 °C. $NaBH_4$ (43.7g, 1,155 mmol, 2.2 equiv) was added in 5g portions every 5 min until the addition was complete. (Caution: The reaction bubbled vigorously during the $NaBH_4$ addition!). The 0 °C bath was then allowed to expire overnight while the reaction mixture stirred. After 14 h, the reaction mixture was an opaque, solid slurry. Reaction aliquot ^1H NMR analysis confirmed that all diimine had been consumed. The reaction mixture was once again cooled to 0 °C and slowly quenched with deionized H_2O (200 mL). The resulting mixture was transferred portion-wise to a 2-L roundbottom flask and concentrated down to a yellow sludge. This sludge was retaken in Et_2O (800 mL) and H_2O (600 mL), and the roundbottom was reequipped with a mechanical stirrer and cooled to 0 °C. To this mixture, concentrated HCl (300 mL of a 12.1 M solution) was added in

50 mL portions. (Caution: HCl addition caused a strong exotherm and salt formation!). The heterogeneous solution was vigorously stirred for 1 h before being filtered over a large 2-L vacuum filter frit into a 4-L Erlenmeyer flask. A red solution comes through with the desired, white diamine salt remaining in the funnel. The desired solid was washed with 1 M HCl (2 L) solution and then Et_2O (3 L) (Note: Purified Et_2O was used for this wash. A mixture of products was observed when Et_2O stabilized with EtOH was employed). The resulting wet solid was dried by aspirating open to air for 24 h, transferring to a large crystallizing dish and baking in an oven at 85 °C for 16 h to afford clean, dry Diamine•2 HCl **(*S,S*)-5.13** (273g, 520 mmol, 99% yield) as a fluffy white powder. ^{1}H NMR (500 MHz, DMSO-d6) δ 10.20 (bs, 2H), 9.95 (bs, 2H), 8.02-7.50 (m, 8H), 4.25 (dd, *J* = 80.1, 13.2 Hz, 5H), 3.91-3.53 (m, 2H), 2.38-2.23 (m, 2H), 2.21-1.70 (m, 5H), 1.22 (d, *J* = 10.5 Hz, 2H); ^{13}C NMR (100 MHz, DMSO-d6) δ 133.16, 131.90, 131.42, 122.87, 56.56, 47.29, 26.05, 22.65. The remaining characterization data was consistent with previously recorded results.[1]

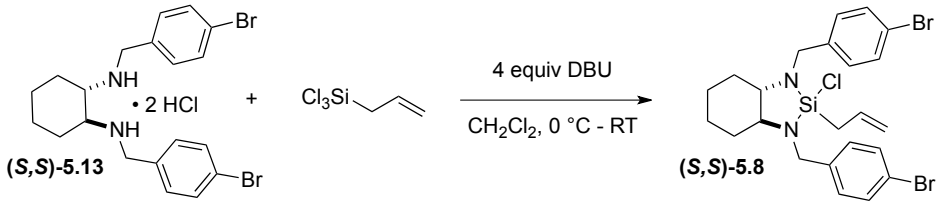

A flame-dried 1 L, 2-neck roundbottom flask was charged with Diamine•2HCl **(*S,S*)-5.13** (52.5g, 100 mmol, 1.0 equiv) and CH_2Cl_2 (330 mL, 0.3 M). The slurry was cooled to 0 °C and allyltrichlorosilane (16 mL, 110 mmol, 1.1 equiv) was added. Distilled DBU (64 mL, 430 mmol, 4.3 equiv) was added to the mixture 0 °C over 10 min. As DBU was added, the white salts

solvated upon deprotonation and the solution took on an amber hue. After an additional 5 min of stirring, the solution was thawed to room temperature. After 1 h, a reaction aliquot NMR showed full conversion to the desired product. The solvent was removed using air-free technique until the resulting oil became opaque and foamy. (Note: air-free technique involved placing the reaction flask in a room temperature water bath, connecting it to an adjacent -78 °C cold-finger and carefully reducing the pressure with a manometer partitioned through the pump manifold. Upon satisfactory removal of solvent, the entire system was back-filled with N_2). Pentane (330 mL) was then added to the oil at room temperature, and the solution was shaken vigorously for 5-15 min until the DBU•HCl salts powdered out into a fine white precipitate. This heterogeneous solution was stirred vigorously for an additional 1 h. The tinted yellow supernatant was collected by filter-cannulation using Teflon tubing into a dry 1 L, 2-neck roundbottom flask. Pentane (100 mL) was added to the remaining DBU•HCl salts and the flask was shaken vigorously. The supernatant was again filter cannulated into the new 1-L, 2-Neck rb. This process was repeated a second time with a pentane (50 mL) wash. The solvent was again removed using air-free technique until the resulting oil became opaque and foamy. The product oil was retaken in boiling pentane (50 mL, 2.0 M) and a seed crystal of previously purified prepared **(*S,S*)-5.8** was added to the flask. The flask was placed in a -20 °C freezer for ≥12 h to fully crystallize the product. While the flask was still cold, the supernatant pentane was rotated away from the solid product and thawed to room temperature. The pentane was removed from the flask via syringe and residual solvent was pumped off under vacuum. The desired solid was broken up in the flask under a flow of N_2 and transferred to a dry, tared flask to afford allyl-silane (***S,S*)-5.8** (46g, 83 mmol, 83% yield) as a white, crystalline solid. ^{1}H NMR (500 MHz, $CDCl_3$) δ 7.48-7.38 (m, 4H), 7.33-7.22 (m, 4H), 5.64 (ddt, J = 15.9, 10.8, 7.8 Hz, 1H), 4.97-4.87

(m, 2H), 4.15 (d, J = 16.2 Hz, 1H), 4.00 (d, J = 15.0 Hz, 1H), 3.85 (d, J = 15.2 Hz, 2H), 2.76 (dddd, J = 33.8, 12.0, 9.2, 3.1 Hz, 2H), 1.88-1.70 (m, 2H), 1.70-1.56 (m, 2H), 1.23-1.05 (m, 2H), 1.05-0.87 (m, 2H); ^{13}C NMR (125 MHz, $CDCl_3$) δ 141.3, 140.4, 131.4, 131.2, 130.1, 129.2, 120.8, 120.5, 116.5, 66.5, 65.6, 48.1, 47.4, 30.9, 30.5, 25.0, 24.9, 24.8. The remaining characterization data was consistent with previously recorded results.[1]

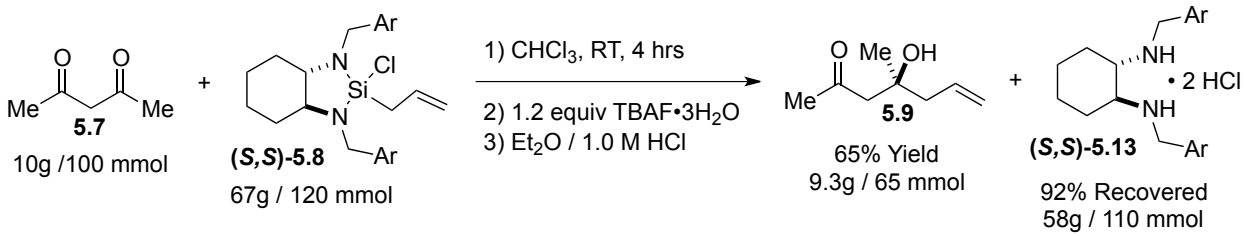

A flame-dried 2 L roundbottom flask was charged with allyl-silane reagent **(*S,S*)-5.8** (66.6g, 120 mmol, 1.2 equiv). The allyl-silane was solvated in anhydrous $CHCl_3$ (1 L, 0.1 M) and the flask was placed in a room temperature water bath. Acetylacetone **5.7** (12 mL, 10g, 100 mmol, 1.0 equiv) was rapidly added via syringe with vigorous reaction stirring. (Note: the external water bath helps to maintain room temperature as the reaction begins with a mild exotherm). The solution becomes bright yellow at first and goes on to turn a dark red with fine white salts floating in the solution as the reaction continues. After stirring for 4 h, the reaction was cooled to 0 °C and TBAF•$3H_2O$ (37.9g, 120 mmol, 1.2 equiv) was added to quench the reaction. The resulting solution was allowed to thaw to room temperature for 1 hr before being concentrated to a thick, red oil. (Note: concentration by rotary evaporation must be done at 0-10 °C to avoid evaporating the desired volatile product). This oil was retaken in Et_2O (500 mL, 0.2 M) and the solution was shaken vigorously to crash out insoluble salts. 1 M HCl (500 mL, 0.2 M, 5.0 equiv) was then added and the roundbottom flask was shaken for an additional ten minutes to

crash out the diamine•HCl salts. This heterogeneous mixture was filtered over a large, coarse filter frit and washed with Et_2O (3 x 300 mL). The filtrate was kept separate from the remaining solids on top of the filter frit. These red/white solids were washed with 1 M HCl (1 L) until the solids were completely white. These white solids were then washed with Et_2O (1 L), aspirated open to air for ≥ 2 h, and baked in the oven at 85 °C for 16 h to afford recovered diamine•2HCl **(*S,S*)-5.13** (58g, 110 mmol, 92% recovered) as a fluffy white powder. The filtrate from above was concentrated at 0-10 °C down to a wet, red oil. This oil was purified directly by silica gel chromatography (gradient 20%, 30%, 50%, 60% Et_2O/Pentane, concentrated at 0-10 °C) to afford keto-alkene **5.9** (9.3g, 65 mmol, 65% yield) as a pale orange oil. The enantiomeric excess of **5.9** was determined to be 89% by chiral GC (see GC trace below). $[\alpha]_D$ = -6° (c 4.7, CH_2Cl_2); R_f = 0.4 (25% EtOAc/Hexanes, PMA); ^{1}H NMR (400 MHz, $CDCl_3$) δ 5.81 (ddt, *J* = 17.5, 10.2, 7.4 Hz, 1H), 5.16-4.97 (m, 2H), 3.83 (s, 1H), 2.64 (d, *J* = 17.3 Hz, 1H), 2.52 (d, *J* = 17.2 Hz, 1H), 2.33-2.19 (m, 2H), 2.15 (s, 3H), 1.20 (s, 3H); ^{13}C NMR (100 MHz, $CDCl_3$) δ 211.2, 134.2, 118.6, 71.6, 51.9, 46.8, 32.1, 27.2; IR (cast film) 3459, 3077, 2977, 2932, 1702, 1641 cm^{-1}; LRMS (FAB+) calc'd for $C_8H_{15}O_2$ $[M+H]^+$ 143.21, found 143.04.

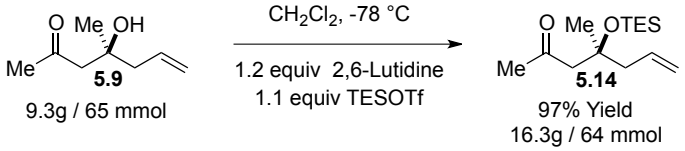

A flame-dried 1 L roundbottom flask was charged with CH_2Cl_2 (650 mL, 0.1 M). Tertiary alcohol **5.9** (9.3g, 65.4 mmol, 1.0 equiv) was added to the flask, followed by 2,6-lutidine (9.2 mL, 78.5 mmol, 1.2 equiv). The roundbottom flask was equipped with a flame-dried 60 mL addition funnel and cooled to -78 °C. TESOTf (16.3 mL, 72.0 mmol, 1.1 equiv) was carefully

added to the addition funnel via syringe and dripped into the cold reaction mixture at a rate of ~1 drop/sec. The addition was complete in ca. 25 min, at which time TLC analysis confirmed full conversion to the desired product. The reaction was quenched at -78 °C with MeOH (3.5 mL, 85.0 mmol, 1.3 equiv) followed by sat. NH_4Cl (250 mL). The resulting mixture was allowed to thaw to room temperature for 1 h. Lutidine salts were observed at the aqueous layer interface, and the organic phase was separated. The organic phase was washed with 1 M AcOH (250 mL), then sat. $NaHCO_3$ (250 mL) before being concentrated to a yellow oil. This oil was retaken in 8% EtOAc/Hex and filtered over a pad of SiO_2 gel (rinsed with four bed-lengths worth of 8% EtOAc/Hexanes – approximately 1.2 L of solvent). The resulting solution was concentrated to afford tertiary silyl-ether **5.14** (16.3 g, 63.6 mmol, 97% yield) as a pale yellow oil. $[\alpha]_D$ = +41° (c 2.0, CH_2Cl_2); R_f = 0.8 (10% EtOAc/Hexanes, PMA); ^{1}H NMR (400 MHz, $CDCl_3$) δ 5.83 (dddd, *J* = 17.0, 10.4, 8.0, 6.6 Hz, 1H), 5.14-4.98 (m, 2H), 2.58 (d, *J* = 13.5 Hz, 1H), 2.46 (d, *J* = 13.5 Hz, 1H), 2.37 (ddt, *J* = 13.6, 6.5, 1.3 Hz, 1H), 2.27 (ddt, *J* = 13.6, 6.5, 1.3 Hz, 1H), 2.17 (s, 3H), 1.31 (s, 3H), 0.95 (t, *J* = 7.9 Hz, 9H), 0.60 (q, *J* = 7.9 Hz, 6H); ^{13}C NMR (100 MHz, $CDCl_3$) δ 208.6, 134.6, 118.2, 75.1, 54.7, 47.7, 32.8, 28.0, 7.3, 7.0; IR (cast film) 2956, 2912, 2877, 1711, 1640, 1457, 1356, 1239, 1139, 1080, 1030, 1005 cm^{-1}; LRMS (FAB+) calc'd for $C_{14}H_{29}O_2Si$ $[M+H]^+$ 357.47, found 357.39.

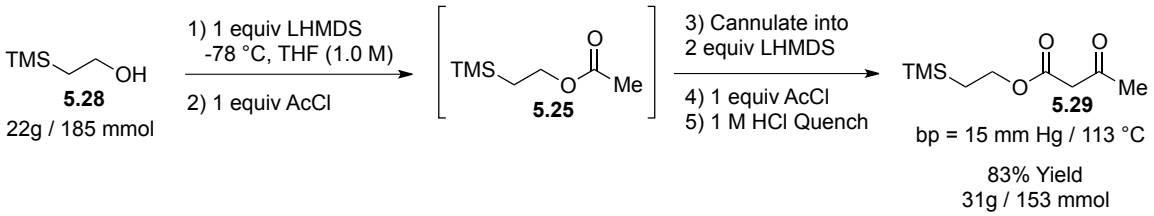

A 100 mL graduated cylinder, a 1 L roundbottom flask equipped with a large stir bar, and a 500 mL roundbottom flask equipped with a large stir bar were flame-dried. A 1.0 M solution of lithium bis(trimethylsilyl)amide (LiHMDS) in THF was cannulated into the dry graduated cylinder for precise measurement and then re-cannulated into the roundbottom flask until the 1 L flask contained 370 mL of LiHMDS (370 mmol, 2.0 equiv) and the 500 mL flask contained 185 mL of LiHMDS (185 mmol, 1.0 equiv). Both flasks were cooled to -78 °C, and trimethylsilylethanol **5.28** (26.5 mL, 21.9g, 185 mmol, 1.0 equiv) was added to the 500 mL flask over 5 min. A mild exotherm was observed and lithiated salts crashed out of the solution. This mixture was stirred for an additional 5 min followed by the addition of acetyl chloride (AcCl) (13.2 mL, 185 mmol, 1.0 equiv) over 2 min. Following AcCl addition, a vigorous exotherm was observed with some white HCl smoke fuming off the reaction. The lithiated salts solvated completely during this process. After 10 min of stirring, the exotherm subsided.

At this point, the reaction mixture containing intermediate ester **5.25** was cannulated into the 1 L flask also at -78 °C. A mild exotherm was observed as well as a thickening of the reaction mixture. The original 500 mL flask was rinsed with dry THF (2 x 20 mL) and cannulated into the 1 L flask. Still at -78 °C, the second equivalent of acetyl chloride (13.2 mL, 185 mmol, 1.0 equiv) was added to the reaction mixture over 1 h via syringe pump. The reaction was stirred for an additional 15 min following the AcCl addition before being quenched by the addition of a 1.0 M HCl solution (300 mL) at -78 °C. The reaction mixture was removed from the -78 °C bath and allowed to thaw to room temperature over 1.5 h before being poured into a 2-L sepratory funnel and diluted with EtOAc (600 mL). The 1 M HCl aqueous layer was separated, and the organic phase was washed with a mixture of 1 M HCl/Brine (200 mL 1 M HCl / 100 mL brine) mixture followed by a final brine wash (100 mL). The organic phase was

dried over $MgSO_4$, filtered and concentrated. Distillation (b.p. 113 °C at 15 mm Hg) afforded *β*-keto ester **5.29** (31g, 153 mmol, 83% yield) as a colorless oil, which exists as a ~10:1 mixture of Keto-Enol tautomers by NMR. R_f = 0.5 (15% EtOAc/Hexanes, *p*-Anis); ^{1}H NMR (500 MHz, $CDCl_3$): Keto Form - δ 4.24 (m, 2H), 3.43 (s, 2H), 2.27 (s, 3H), 1.02 (m, 2H), 0.05 (s, 9H). Enol Form - δ 12.14 (s, 1H), 4.96 (s, 1H), 4.23 (m, 2H), 1.95 (s, 3H), 1.00 (m, 2H), 0.04 (s, 9H); ^{13}C NMR (125 MHz, $CDCl_3$): Keto Form - δ 200.8, 167.4, 63.9, 50.5, 30.3, 17.5, -1.4. Enol Form - δ 90.1, 62.3, 21.4, 17.5, -1.5; IR (NaCl neat) 2956, 2900, 1742, 1720, 1650, 1414, 1361, 1317, 1251 cm^{-1}; LRMS calc'd for $C_9H_{18}NaO_3Si$ $[M+Na]^+$ 225.31, found 226.16.

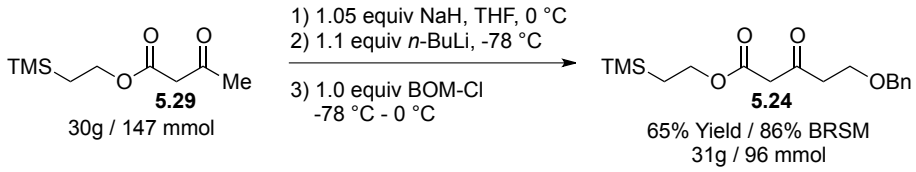

A flame-dried 1 L roundbottom flask equipped with a large stir bar was charged with NaH (60% in suspension in mineral oil, 6.17g, 154 mmol, 1.05 equiv). The NaH was solvated in THF (300 mL, 0.5 M) and the resulting slurry was cooled to 0 °C. *β*-keto ester **5.29** (30g, 147 mmol, 1.0 equiv) was added dropwise over 15 min. During this addition, the solution yellowed and significant H_2 gas evolution was observed. This gas was vented from the reaction vessel using two 16G vent needles. The reaction was stirred for an additional 20 min until the bubbling subsided. The solution was then cooled to -78 °C and *n*-Buli (70 mL of a 2.3 M solution in hexanes, 160 mmol, 1.10 equiv) was added over 20 min. The solution changed color from yellow to dark orange and exothermed throughout the addition. The resulting mixture was stirred for an additional 30 min before BOM-Cl[2] (20.4 mL, 1.0 equiv) was added over 10 min. The solution

was allowed to stir for an additional 10 min before being warmed to 0 °C in an ice bath. As the solution warmed to 0 °C, the solution went from dark orange to yellow. After 30 min, the reaction was quenched at 0 °C by slowly adding 1.0 M HCl (300 mL). After 5 min, the quenched solution was allowed to thaw to room temperature. The mixture was poured into a 2 L sepratory funnel and diluted with EtOAc (600 mL). The aqueous layer was separated, and the organic phase was washed with brine (300 mL). The organic phase was dried over $MgSO_4$, filtered and concentrated. Benzyl alcohol and unreacted starting material **5.29** was removed from the crude mixture by distillation to provide clean compound **5.29** (8g, 39 mmol, 26% recovered, b.p. 113 °C at 15 mm Hg). The remaining distillation residue was purified by silical gel column chromatography (gradient 10%, 15% EtOAc/Hexanes) to afford benzyl ether **5.24** (31g, 96 mmol, 65% Yield, 86% BRMS) as a pale yellow oil, which exists as a ~9:1 mixture of Keto-Enol tautomers by NMR. R_f = 0.4 (15% EtOAc/Hexanes, *p*-Anis); ^{1}H NMR (400 MHz, $CDCl_3$): Keto Form - δ 7.40-7.17 (m, 5H), 4.52 (s, 2H), 4.22 (m, 2H), 3.76 (t, *J* = 6.2 Hz, 2H), 3.48 (s, 2H), 2.84 (t, *J* = 6.2 Hz, 2H) 1.01 (m, 2H), 0.05 (s, 9H). Enol Form - δ 12.18 (s, 1H), 7.40-7.17 (m, 5H), 5.05 (s, 1H), 4.54 (s, 2H), 4.24 (m, 2H), 3.71 (t, *J* = 6.5 Hz, 2H), 2.52 (t, *J* = 6.5 Hz, 2H), 1.03 (m, 2H), 0.06 (s, 9H); ^{13}C NMR (100 MHz, $CDCl_3$): Keto Form - δ 201.6, 167.4, 138.2, 128.6, 127.9, 73.5, 65.2, 63.9, 50.2, 43.3 36.0, 17.5, -1.3; IR (NaCl neat) 3436, 3065, 3032, 2955, 2899, 1742, 1717, 1648, 1496, 1454, 1409, 1367, 1311, 1251 cm^{-1}; LRMS (FAB+) calc'd for $C_{17}H_{25}O_4Si$ $[M-H]^+$ 321.16, found 321.04.

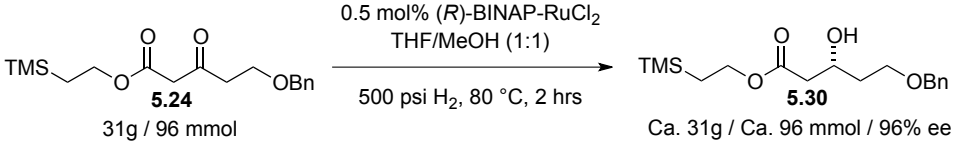

β-keto ester **5.24** (34g, 105 mmol, 1.0 equiv) was transferred to a large glass bomb-liner and solvated in a mixture of THF and MeOH (52 mL of each, 1.0 M total). (R)-BINAP-$RuCl_2$ (420 mg, 0.53 mmol, 0.005 equiv) was added to the solution, which was stirred for about one minute. The bomb-liner was inserted into a large Parr bomb device, which was sealed and purged three times with H_2 gas (charged to 500 psi and vented down to 100 psi for each purge). The bomb was charged with a final 500 psi H_2 and placed in an 80 °C oil bath. After stirring for 2 h at 80 °C, the bomb was carefully removed from the oil bath and allowed to cool to room temperature for an additional hour. Once cool, the bomb was vented, and the reaction mixture was retaken in a solution of 25% EtOAc/Hexanes and filtered over a pad of SiO_2 gel (rinsed with four bed-lengths worth of 25% EtOAc/Hexanes – approximately 1.2 L of solvent). The resulting brown solution was concentrated to a dark brown oil and taken on to the next reaction without further purification. A small portion of this crude material was purified by silica gel chromatography (15% EtOAc/Hexanes) to afford clean alcohol **5.30** for characterization. The enantiomeric excess of **5.30** was determined to be 96% by chiral HPLC (see HPLC trace below). $[\alpha]_D$ = +12° (c 2.0, CH_2Cl_2); R_f = 0.4 (20% EtOAc/Hexanes, PMA); ^{1}H NMR (400 MHz, $CDCl_3$) δ 7.47-7.17 (m, 5H), 4.53 (s, 2H), 4.34-4.13 (m, 3H), 3.84-3.54 (m, 2H), 3.39 (d, J = 3.4 Hz, 1H), 2.49 (d, J = 6.3 Hz, 2H), 1.94-1.73 (m, 2H), 1.10-0.92 (m, 2H), 0.05 (s, 9H); ^{13}C NMR (100 MHz, $CDCl_3$) δ 172.8, 138.3, 128.6, 127.9, 127.8, 73.5, 68.1, 67.1, 63.1, 41.9, 36.3, 17.5, -1.3; IR (cast film) 3506, 2953, 1730, 1454, 1250, 1168, 1100 cm^{-1}; LRMS (FAB+) calc'd for $C_{17}H_{29}O_4Si$ $[M+H]^+$ 325.60, found 325.32.

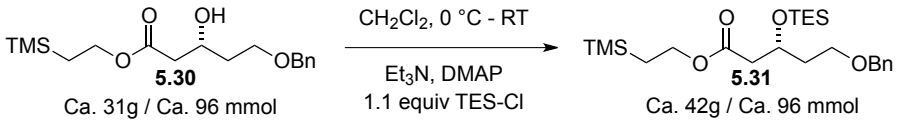

Crude alcohol **5.30** (ca. 34g, 105 mmol, 1.0 equiv) was azeotroped with benzene (350 mL, 0.3 Mz) in a 1 L roundbottom flask to remove adventitious water. The resulting oil was pumped on, purged with N_2, and solvated in CH_2Cl_2 (350 mL, 0.3 M). Et_3N (17.6 mL, 126 mmol, 1.2 equiv) was added to the solution at room temperature. The reaction mixture was cooled to 0 °C and TES-Cl (17.6 mL, 105 mmol, 1.0 equiv) was added over 5 min (the addition of TES-Cl caused a mild exotherm and HCl gas fumed off the reaction). DMAP (642 mg, 5.25 mmol, 0.05 equiv) was added at 0 °C and the reaction mixture was stirred for 5 min before being allowed to thaw to room temperature. The reaction quickly became thick with Et_3N•HCl salts. The reaction progress was monitored by TLC analysis, and showed complete conversion in less than 30 min. At 30 min, the reaction was quenched by adding MeOH (8.5 mL, 210 mmol, 2.0 equiv) to react with any remaining TES-Cl. The resulting mixture was concentrated down to a brown, salty sludge, which was subsequently retaken in a solution 15% EtOAc/Hexanes and filtered over a pad of SiO_2 gel (rinsed with four bed-lengths worth of 15% EtOAc/Hexanes – approximately 1.2 L of solvent). The resulting amber solution was concentrated to a dark amber oil which was taken on to the next reaction without further purification. A small portion of this crude material was purified by silica gel chromatography (15% EtOAc/Hexanes) to afford clean silyl ether **5.31** for characterization. $[\alpha]_D$ = -5° (c 1.7, CH_2Cl_2); R_f = 0.8 (15% EtOAc/Hexanes, PMA); ^{1}H NMR (500 MHz, $CDCl_3$) δ 7.40-7.21 (m, 5H), 4.55-4.45 (m, 2H), 4.33 (dt, *J* = 11.8, 6.2 Hz, 1H), 4.21-4.11 (m, 2H), 3.56 (td, *J* = 6.4, 1.6 Hz, 2H), 2.48 (d, *J* = 6.3 Hz, 2H), 1.91-1.76 (m, 2H), 1.03- 0.97 (m, 2H), 0.95 (t, *J* = 8.0 Hz, 10H), 0.60 (q, *J* = 8.1 Hz, 6H), 0.05 (s, 9H); ^{13}C NMR (100 MHz, $CDCl_3$) δ 171.9, 138.7, 128.5, 127.8, 127.6, 73.1, 67.1, 66.8, 62.7, 43.5, 37.7,

17.5, 7.0, 5.2, -1.3; IR (cast film) 2953, 2876, 1733, 1453, 1414, 1384, 1249, 1164, 1098 cm^{-1}; LRMS (FAB+) calc'd for $C_{23}H_{43}O_4Si_2$ $[M+H]^+$ 439.76, found 439.43.

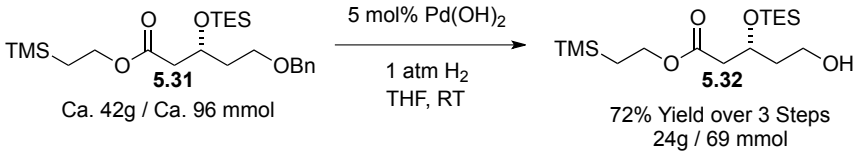

A 1 L roundbottom flask was evacuated and purged with N_2. The flask was charged with Pearlman's catalyst, $Pd(OH)_2$ - 20% by weight (3.69g, 5.25 mmol, 0.05 equiv) and again pump/purged with N_2. THF (100 mL) was added to the $Pd(OH)_2$ to givea black slurry. Crude benzyl ether **5.31** (ca. 46g, 105 mmol, 1.0 equiv) was transferred into the flask with THF (600 mL, 0.15 M total). The roundbottom flask's head space was then purged three times with a 1 L balloon of H_2 gas. A full 1 L H_2 balloon was left on the reaction following the final purge. After 2 h of vigorous stirring, TLC analysis showed mostly the desired primary alcohol with some starting material remaining and some undesired diol formation seen as well. (NOTE: Based on the quality of $Pd(OH)_2$ used in the reaction, reaction times varied from 1.5-6 h. The reaction was carefully monitored by TLC and stopped before overreaction occurred). The reaction mixture was filtered over a pad of celite to remove the activated palladium. The celite was rinsed with EtOAc until the eluent came through as a colorless liquid (ca. 500 mL). The reaction crude was concentrated and purified by silica gel chromatography (gradient 10%, 15%, 20% EtOAc/Hexanes) to afford primary alcohol **5.32** (26.4g, 75.6 mmol, 72% yield over 3 Steps) as a pale yellow oil. $[\alpha]_D$ = -3° (c 2.8, CH_2Cl_2); R_f = 0.25 (15% EtOAc/Hexanes, $KMnO_4$); ^{1}H NMR (500 MHz, $CDCl_3$) δ 4.48-4.30 (m, 1H), 4.23-4.10 (m, 2H), 3.90-3.67 (m, 2H), 2.55 (qd, *J* = 15.1, 6.5 Hz, 2H), 2.26 (t, *J* = 5.4 Hz, 1H), 1.88 (ddt, *J* = 14.4, 7.9, 4.7 Hz, 1H), 1.05-0.95 (m,

2H), 0.98 (d, J = 8.0 Hz, 9H), 0.63 (q, J = 8.1 Hz, 6H), 0.05 (s, 9H); ^{13}C NMR (100 MHz, $CDCl_3$) δ 171.7, 68.5, 62.9, 60.0, 42.8, 39.0, 17.5, 6.9, 6.9, 5.0, -1.3. IR (cast film) 3453, 2954, 2878, 1733, 1459, 1415, 1385, 1310, 1250, 1162, 1090 cm^{-1}; LRMS (FAB+) calc'd for $C_{16}H_{37}O_4Si_2$ $[M+H]^+$ 349.64, found 349.30.

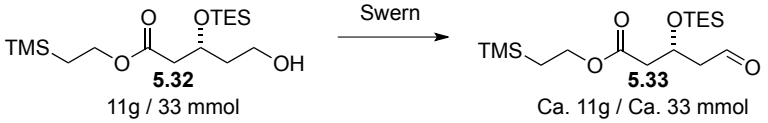

A flame-dried, 1 L 2-neck roundbottom flask was charged with CH_2Cl_2 (350 mL, 0.1 M) and equipped with a flame-dried 60 mL addition funnel at room temperature. Oxalyl chloride (5.5 mL, 64.2 mmol, 2.0 equiv) was added at room temperature and the resulting solution was cooled to -78 °C. DMSO (6.8 ml, 96.4 mmol, 3.0 equiv) was rapidly added (Note: It is important to add the DMSO quickly so the liquid does not freeze in the syringe needle). An exotherm as well as vigorous gas evolution were observed, and the resulting gas was vented with two 16G needles. After stirring the reaction mixture for 20 min, alcohol **5.32** (11.2g, 32.1 mmol, 1.0 equiv) was solvated in CH_2Cl_2 (20 mL) and transferred to the addition funnel. The solution of alcohol **5.32** was dripped into the cold reaction at a rate of ~1 drop/sec. The addition was complete in ca. 30 min, and the addition funnel was rinsed with CH_2Cl_2 (10 mL). The reaction was stirred at – 78 °C for an additional 30 min before Et_3N was added to the reaction via the addition funnel over ca. 15 min. The resulting thick white slurry was stirred vigorously at – 78 °C for an additional 15 min before thawing to room temperature. The solution yellowed and solvated many of the salts as it thawed to room temperature. After 2 h, the reaction mixture was concentrated to a yellow, salty oil, which was subsequently retaken in a solution 15%

EtOAc/Hexanes and filtered over a pad of pH 7 buffered SiO_2 gel[6] (rinsed with four bed-lengths worth of 15% EtOAc/Hexanes – approximately 1.2 L of solvent). The resulting solution was concentrated to a pale yellow oil which was taken on to the next reaction without further purification (Note: the resulting aldehyde was often stored as a solution frozen in benzene overnight, but not for longer than 24 h). A small portion of this crude material was purified by silica gel chromatography (15% EtOAc/Hexanes, pH 7 buffered SiO_2 gel) to afford clean aldehyde **5.33** for characterization. $[\alpha]_D$ = -11° (c 1.4, CH_2Cl_2); R_f = 0.6 (10% EtOAc/Hexanes, *p*-Anis); ^{1}H NMR (500 MHz, $CDCl_3$) δ 9.83 (t, *J* = 2.1 Hz, 1H), 4.67 (qd, *J* = 6.4, 5.1 Hz, 1H), 4.27-4.11 (m, 2H), 2.77-2.59 (m, 2H), 2.64-2.49 (m, 2H), 1.05-0.99 (m, 2H), 0.96 (t, *J* = 7.9 Hz, 9H), 0.63 (q, *J* = 8.1 Hz, 6H); ^{13}C NMR (100 MHz, $CDCl_3$) δ 201.04, 170.90, 64.86, 62.90, 50.97, 42.86, 17.30, 6.76, 4.78, -1.51; IR (cast film) 2955, 2878, 1729, 1459, 1414,1386, 1250, 1165, 1084, 1007 cm^{-1}; LRMS (FAB+) calc'd for $C_{16}H_{35}O_4Si_2$ $[M+H]^+$ 347.61, found 347.36.

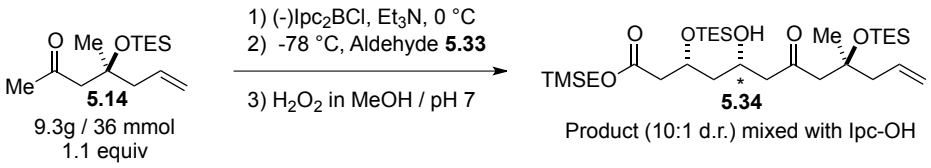

A 50 mL roundbottom flask was flame-dried and used to retrieve (-)-DIP-Chloride[7] (13.6g, 42.5 mmol, 1.3 equiv) from an argon glove-box. This white, crystalline solid was quickly transferred to a flame-dried 500 mL roundbottom flask equipped with a large stir bar, which was subsequently pumped on for 5 min before being back-filled with N_2. The (-)-DIP-

[6] pH 7 buffered SiO_2 gel was prepared my adding 10% pH 7 buffer (by mass) to a roundbotttom flask half filled with SiO_2 gel. The resulting mixture was rotated on a rotary evaporated for >12 h (at atmospheric pressure) and then stored for future use.
[7] Sigma-Aldrich Trademark

Chloride was solvated in Et_2O (140 mL, 0.23 M) and the flask was cooled to 0 °C. Et_3N (6.85 mL, 49.1 mmol, 1.5 equiv) was added to the cold solution with minimal Et_3N•HCl salts observed. Ketone **5.14** (9.34g, 36.4 mmol, 1.1 equiv) was azeotroped with benzene, pumped on, and back-filled with N_2 before being transferred over 10 min to the 0 °C reaction mixture with Et_2O (40 mL, 1.2 M). Upon ketone addition, significant Et_3N•HCl salt formation was immediately observed and full boron enolate formation was confirmed by reaction aliquot NMR. After 30 min of stirring, the reaction mixture was cooled to -78 °C. Crude aldehyde **5.33** (ca. 11.3g, 32.7 mmol, 1.0 equiv) was azeotroped with benzene, pumped on, and back-filled with N_2 before being transferred over 10 min to the -78 °C reaction mixture with Et_2O (40 mL, 1.2 M). Upon aldehyde addition, a mild exotherm was observed. The reaction was stirred at -78 °C for 3 h and then placed in a 0 °C bath for an additional 15 min before being quenched with pH 7 buffer (220 mL, 0.15 M). The resulting mixture was allowed to thaw to room temperature. The aqueous layer was separated from the yellow organic layer and then back extracted twice with Et_2O (200 mL, 100 mL). The combined organic phases were combined in a 2 L roundbottom flask and concentrated down to a yellow, oily mixture. This mixture was retaken in MeOH (220 mL, 0.15 M) and pH 7 buffer (220 mL, 0.15 M) and cooled to 0 °C. H_2O_2 as a 30% by weight solution in H_2O (43 mL, 1.3 ml/mmol, ca. 12 equiv) was added to the cold solution, resulting in a mild exotherm. The mixture was stirred for 5 min before being allowed to thaw to room temperature. After stirring for an additional 30 min, the reaction mixture was diluted with CH_2Cl_2 (250 mL) and the organic phase was separated. The aqueous phase was extracted twice more with CH_2Cl_2 (200 mL, 100 mL). The combined organic phases were dried over $MgSO_4$, filtered and concentrated to a thick yellow oil. Though full chromatographic purification was not required at this point, it was possible to recover all unreacted, starting material ketone through a

partial purification of the reaction mixture by silica gel chromatography (gradient 1%, 5%, 10% EtOAc/Hexanes,) to afford the starting material ketone **5.14** (2.5g, 9.9 mmol, 0.3 equiv) and the impure aldol adduct **5.34** which was taken on to the next reaction without further purification. The diastereoselectivity of the reaction was determined by ^{1}H NMR to be 10:1 dr (inseparable), and a small portion of aldol adduct XX was more rigorously purified for characterization. $[\alpha]_D$ = +20° (c 1.7, CH_2Cl_2); R_f = 0.3 (10% EtOAc/Hexanes, *p*-Anis – stains purple); ^{1}H NMR (500 MHz, $CDCl_3$) δ 5.91-5.75 (m, 1H), 5.13-5.00 (m, 2H), 4.39 (p, *J* = 6.2 Hz, 1H), 4.21-4.09 (m, 3H), 3.32 (d, *J* = 2.6 Hz, 1H), 2.70-2.42 (m, 6H), 2.38 (dd, *J* = 13.6, 6.5 Hz, 1H), 2.28 (dd, *J* = 13.6, 8.0 Hz, 1H), 1.71 (ddt, *J* = 12.4, 9.0, 4.5 Hz, 1H), 1.61 (ddd, *J* = 13.9, 6.6, 3.1 Hz, 1H), 1.32 (s, 3H), 0.96 (td, *J* = 7.9, 1.3 Hz, 20H), 0.61 (p, *J* = 8.0 Hz, 12H), 0.05 (s, 9H); ^{13}C NMR (125 MHz, $CDCl_3$) δ 210.9, 171.8, 134.5, 118.4, 75.2, 67.8, 65.5, 62.8, 54.4, 52.3, 47.8, 43.9, 42.9, 28.1, 17.5, 7.3, 7.0, 5.1, -1.3; IR (cast film) 3532, 2964, 2913, 2878, 1734, 1415, 1379, 1250, 1163, 1083, 1006 cm^{-1}; LRMS (FAB+) calc'd for $C_{30}H_{62}O_6Si_3$ $[M]^+$ 603.07, found 603.61.

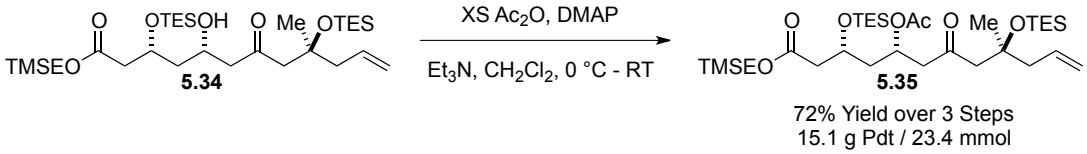

Semi-crude alcohol **5.34** (ca. 19.7g, 32.7 mmol, 1.0 equiv) was azeotroped with toluene, pumped on, and back-filled with N_2 in a 1-L roundbottom flask. THF (220 mL, 0.15 M) and Et_3N (13.7 mL, 98.1 mmol, 3.0 equiv) were added at room temperature, and the resulting solution was cooled to 0 °C. Ac_2O (6.2 mL, 65.4 mmol, 2.0 equiv) and DMAP (1.0g, 8.2 mmol, 0.25 equiv) were added to the cold mixture (Note: excess Ac_2O was employed to acetylate any residual Ipc-OH from the Paterson aldol reaction). After 5 min, the DMAP was fully solvated and the reaction mixture was allowed to thaw to room temperature. The reaction was monitored

by TLC and quenched after 45 min with MeOH (4mL, 98.1 mmol, 3.0 equiv). The resulting mixture was concentrated to a cloudy, amber oil, retaken in a solution 15% EtOAc/Hexanes and filtered over a pad of SiO_2 gel (rinsed with four bed-lengths worth of 15% EtOAc/Hexanes – approximately 1.2 L of solvent). This solution was concentrated down to a crude residue and purified by silica gel chromatography (gradient 1%, 6%, 7%, 60% EtOAc/Hexanes) to afford acetate **5.35** (15.1g, 23.4 mmol, 72% yield over 3 Steps) as a pale yellow oil. $[\alpha]_D$ = -2° (c 2.0, CH_2Cl_2); R_f = 0.5 (10% EtOAc/Hexanes, *p*-Anis – stains purple); ^{1}H NMR (400 MHz, $CDCl_3$) δ 5.83 (dddd, *J* = 16.9, 10.4, 8.0, 6.5 Hz, 1H), 5.26 (tt, *J* = 7.0, 5.4 Hz, 1H), 5.14-4.98 (m, 2H), 4.27-4.06 (m, 3H), 2.85 (dd, *J* = 17.1, 7.0 Hz, 1H), 2.73 (dd, *J* = 17.1, 5.6 Hz, 1H), 2.65-2.41 (m, 4H), 2.37 (ddt, *J* = 13.5, 6.5, 1.3 Hz, 1H), 2.28 (dd, *J* = 13.6, 8.0 Hz, 1H), 2.01 (s, 3H), 1.92-1.75 (m, 2H), 1.31 (s, 3H), 1.07-0.84 (m, 20H), 0.61 (qd, *J* = 7.9, 2.8 Hz, 12H), 0.05 (s, 9H); ^{13}C NMR (100 MHz, $CDCl_3$) δ 206.6, 171.7, 170.3, 134.6, 118.3, 75.2, 67.5, 66.5, 62.7, 54.2, 49.7, 47.5, 42.2, 42.2, 28.1, 21.2, 17.5, 7.3, 7.0, 7.0, 5.0, -1.3; IR (cast film) 2955, 2878. 1739, 1373, 1239, 1166, 1082, 1042, 1009 cm^{-1}; LRMS (FAB+) calc'd for $C_{32}H_{64}O_7Si_3$ $[M]^+$ 645.10, found 645.65.

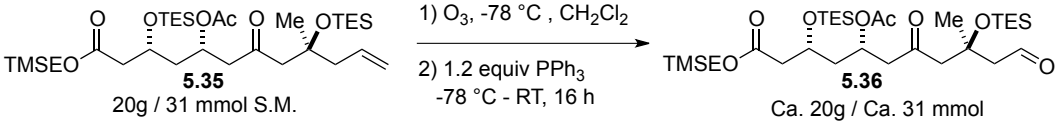

Alkene **5.35** (19.9g, 30.8 mmol, 1.0 equiv) was solvated in CH_2Cl_2 (310 mL, 0.1 M) in a 1 L roundbottom flask. Oxygen was bubbled through the reaction solvent as the flask was cooled to -78 °C. After 5 min, the ozonizer was initiated and O_3 was bubbled throught the -78 °C reaction solvent. After 40 min, the reaction mixture had taken on a dark blue color and TLC

analysis confirmed full conversion of the starting material (R_f = 0.8, 15% EtOAc/Hexanes, *p*-Anis - stains light blue) to the intermediate ozonides (R_f = 0.6, 15% EtOAc/Hexanes, *p*-Anis - stains maroon). After an additional 10 min of O_3 bubbling, the ozonizer was turned off and O_2 was bubbled through the reaction solvent to purge out the excess O_3. After 20 min of purging with O_2, the blue color dissipated. After purging for an additional 20 min, PPh_3 (9.71g, 37.0 mmol, 1.2 equiv) was added at -78 °C. The reaction mixture was removed from the cold bath and allowed to thaw to room temperature under an atmosphere of N_2. As the solution warmed, it took on a pale yellow color. At 15 h, TLC analysis confirmed full consumption of the ozonide, and the reaction mixture was concentrated to a thick yellow oil. This oil was retaken in hexanes (310 mL, 0.1 M), which immediately triturated out most of the crude phosphines. This heterogeneous mixture was stirred vigorously for 10 min before being filtered into a 1 L roundbottom flask. The phosphines were rinsed with additional hexanes (2 x 100 mL) and the resulting filtrate was concentrated down to a yellow oil. The trituration process above was repeated a second time to provide the crude product as a pale yellow oil which was taken on to the next reaction without further purification (crude NMR analysis showed ca. 10 mol% phosphines remained mixed with the desired product). A small portion of this crude material was purified by silica gel chromatography (10% EtOAc/Hexanes, pH 7 buffered SiO_2 gel[8]) to afford relatively clean aldehyde **5.36** for characterization. $[\alpha]_D$ = -13° (c 2.3, CH_2Cl_2); R_f = 0.5 (15% EtOAc/Hexanes, *p*-Anis); ^{1}H NMR (500 MHz, $CDCl_3$) δ 9.81 (t, *J* = 2.5 Hz, 1H), 5.28 (pd, *J* = 7.2, 6.1, 1.8 Hz, 1H), 4.25-4.08 (m, 3H), 2.85-2.59 (m, 6H), 2.56 (dd, *J* = 15.2, 5.1 Hz, 1H), 2.45 (dd, *J* = 15.2, 7.3 Hz, 1H), 2.01 (s, 3H), 1.82 (qdd, *J* = 14.2, 9.9, 4.9 Hz, 2H), 1.43 (s, 3H),

[8] pH 7 buffered SiO_2 gel was prepared my adding 10% pH 7 buffer (by mass) to a roundbotttom flask half filled with SiO_2 gel. The resulting mixture was rotated on a rotary evaporated for >12 h (at atmospheric pressure) and then stored for future use.

1.03-0.88 (m, 20H), 0.68-0.53 (m, 12H), 0.04 (s, 9H); ^{13}C NMR (125 MHz, $CDCl_3$) δ 205.6, 202.0, 171.7, 170.3, 73.6, 67.3, 66.5, 62.8, 54.7, 54.6, 49.6, 42.4, 42.0, 29.2, 21.2, 17.5, 7.2, 7.0, 6.9, 5.1, -1.3; IR (cast film) 2955, 2878, 1732, 1274, 1239, 1166, 1100, 1010 cm^{-1}; LRMS (FAB+) calc'd for $C_{31}H_{62}O_8Si_3$ $[M]^+$ 647.08, found 647.61.

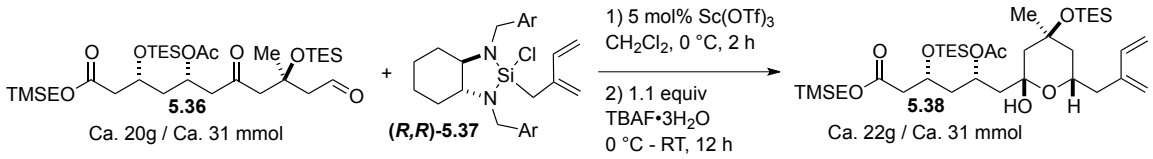

Crude aldehyde **5.36** (ca. 20g, 30.8 mmol, 1.0 equiv) was azeotroped with toluene (2 x 250 mL) in a 1 L roundbottom flask. The flask was evacuated and back-filled with N_2 before being charged with CH_2Cl_2 (310 mL, 0.1 M). The solution was cooled to 0 °C and isoprenylation reagent ***(R,R)*-5.37** (57 mL of a ~0.6 M stock solution in CH_2Cl_2, 34.0 mmol, 1.1 equiv) was added followed by $Sc(OTf)_3$ (759 mg, 1.54 mmol, 0.05 equiv). The solution was vigorously stirred at 0 °C and took on a bright yellow color over time. After 2 h, reaction aliquot NMR analysis indicated that all of the starting material had been consumed, and the reaction was quenched at 0 °C with TBAF•$3H_2O$ (10.7g, 34.0 mmol, 1.1 equiv). The cold bath was allowed to expire overnight as the solution was stirred for an additional 12 h to allow for full silane cleavage and lactol formation. The reaction mixture was concentrated down to a thick amber oil. This crude oil was retaken in a minimal amount of CH_2Cl_2 and filtered over a pad of SiO_2 gel (rinsed with four bed-lengths worth of 10% EtOAc/Hexanes – approximately 1.2 L of solvent) to remove the TBAF and diamine byproducts. The resulting solution was concentrated to a yellow oil which was retaken in 10% EtOAc/Hexanes and subjected to a second filtration over a pad of SiO_2 gel (as above) to remove residual diamine byproduct that bled through the first filtration

(Note: A second filtration was only required due to the large scale of this reaction. When the reaction procedure was performed on ca. 10g of **5.36**, only one filtration was required). The resulting crude yellow oil was taken on to the next reaction without further purification. A small portion of this crude material was purified by silica gel chromatography (8% EtOAc/Hexanes) to afford relatively clean lactol **5.38** for characterization. 1D nOe analysis confirmed that the isolated lactol exists in the expected doubly anomeric form. $[\alpha]_D$ = -13° (c 1.8, CH_2Cl_2); R_f = 0.4 (10% EtOAc/Hexanes, PMA); ^{1}H NMR (400 MHz, $CDCl_3$) δ 6.37 (dd, *J* = 17.5, 10.9 Hz, 1H), 5.97 (s, 1H), 5.28 (d, *J* = 17.6 Hz, 1H), 5.27-5.14 (m, 1H), 5.09 (dt, *J* = 10.4, 4.4 Hz, 3H), 4.24 (dtd, *J* = 13.4, 5.5, 2.7 Hz, 1H), 4.21-4.08 (m, 3H) 2.60 (ddd, *J* = 15.0, 4.4, 2.1 Hz, 2H), 2.41 (dd, *J* = 15.0, 8.2 Hz, 1H), 2.20 (dd, *J* = 13.9, 8.1 Hz, 1H), 2.02 (s, 3H), 2.06-1.89 (m, 2H), 1.89-1.78 (m, 2H), 1.76 (dd, *J* = 13.5, 2.3 Hz, 1H), 1.68 (dt, *J* = 13.5, 2.2 Hz, 1H), 1.56 (d, *J* = 14.5 Hz, 1H), 1.29 (s, 3H), 1.14 (dd, *J* = 13.5, 11.4 Hz, 1H), 1.04-0.86 (m, 20H), 0.60 (qd, *J* = 8.4, 8.0, 2.3 Hz, 12H), 0.04 (s, 9H); ^{13}C NMR (100 MHz, $CDCl_3$) δ 171.9, 170.5, 142.7, 139.0, 118.3, 114.0, 97.0, 74.0, 67.9, 66.8, 64.0, 62.6, 46.6, 45.5, 43.5, 43.5, 42.6, 38.0, 30.7, 21.6, 17.5, 7.1, 7.0, 6.7, 5.1, -1.3; IR (cast film) 3455, 2955, 2878, 1736, 1374, 1244, 1168, 1084, 1044, 1011 cm^{-1}; LRMS (FAB+) calc'd for $C_{36}H_{70}NaO_8Si_3$ $[M+Na]^+$ 738.18, found 737.59.

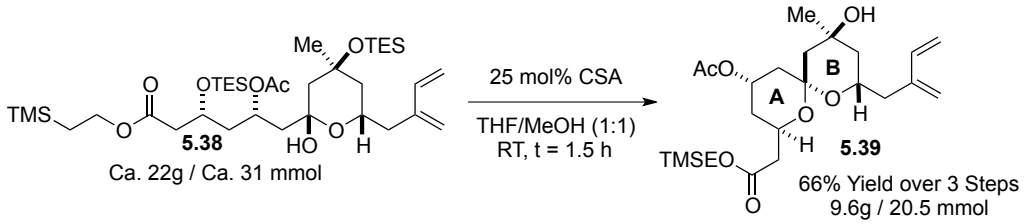

Crude lactol **5.38** (ca. 22g, 30.8 mmol, 1.0 equiv) was solvated with a 1:1 mixture of THF and MeOH (155 mL of each, 0.1 M total) in a 1 L roundbottom flask. CSA (1.79g, 7.71 mmol,

0.25 equiv) was added to the reaction and the mixture was stirred at room temperature. The yellow solution tinged brown over time, and the reaction progress was monitored by TLC. At 1.5 h, the reaction was quenched with Et_3N (3.2 mL, 23.1 mmol, 0.75 equiv) and concentrated. The resulting crude oil was purified by silica gel chromatography (gradient 1%, 15%, 25% EtOAc/Hexanes) to afford clean spiroketal **5.39** (9.6g, 20.5 mmol, 66% Yield over 3 steps) as a single diastereomer. The desired relative stereochemistry of **5.39** was rigorously confirmed by 2D COSY and NOESY analyses. $[\alpha]_D$ = -55° (c 4.1, CH_2Cl_2); R_f = 0.2 (15% EtOAc/Hexanes, PMA); ^{1}H NMR (400 MHz, $CDCl_3$) δ 6.41 (dd, *J* = 17.6, 10.9 Hz, 1H), 5.30 (d, *J* = 17.6 Hz, 1H), 5.18 (dt, *J* = 23.9, 1.6 Hz, 2H), 5.09 (d, *J* = 10.8 Hz, 1H), 5.04 (dt, *J* = 5.7, 2.8 Hz, 1H), 4.43 (dddd, *J* = 11.1, 8.7, 4.4, 2.1 Hz, 1H), 4.30 (s, 1H), 4.31-4.23 (m, 1H), 4.21-4.10 (m, 2H), 2.55 (ddd, *J* = 14.4, 6.5, 1.0 Hz, 1H), 2.51-2.38 (m, 2H), 2.34 (ddd, *J* = 14.3, 6.4, 1.0 Hz, 1H), 2.05 (s, 3H), 2.02 (d, *J* = 15.0 Hz, 1H), 1.81 (dd, *J* = 14.2, 2.4 Hz, 1H), 1.77-1.67 (m, 2H), 1.62 (dd, *J* = 15.1, 3.9 Hz, 1H), 1.60-1.52 (m, 1H), 1.45 (d, *J* = 13.9 Hz, 1H), 1.24 (dd, *J* = 13.5, 11.7 Hz, 1H), 1.16 (s, 3H), 1.00 (ddd, *J* = 9.2, 8.1, 0.9 Hz, 2H), 0.04 (s, 9H); ^{13}C NMR (125 MHz, $CDCl_3$) δ 171.1, 171.0, 142.7, 139.2, 118.0, 113.9, 98.4, 68.0, 66.4, 65.0, 63.3, 62.3, 46.1, 43.6, 40.8, 37.9, 37.4, 34.5, 30.2, 21.6, 17.5, -1.3; IR (cast film) 3530, 2953, 1731, 1402, 1366, 1249, 1209, 1174, 1058 cm^{-1}; LRMS (FAB+) calc'd for $C_{24}H_{41}O_7Si$ $[M+H]^+$ 469.67, found 469.30.

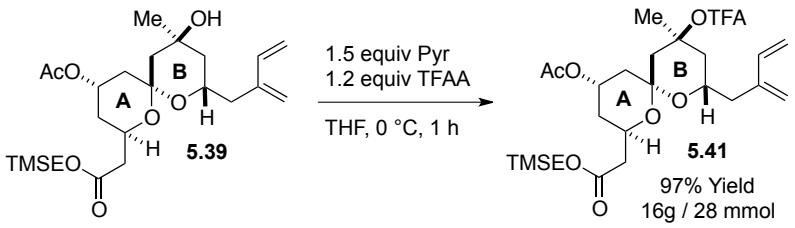

Tertiary alcohol **5.39** (13.7g, 29.2 mmol, 1.0 equiv) was azeotroped with benzene (250 mL) in a 1 L roundbottom. The flask was then evacuated and back-filled with N_2 before being charged with THF (300 mL, 0.1 M). Distilled pyridine (3.5 mL, 44.0 mmol, 1.5 equiv) was added to the solution at room temperature and the resulting mixture was cooled to 0 °C. Trifluoroacetic anhydride (TFAA) (5.0 mL, 35.2 mmol, 1.2 equiv) was added to the cold solution via syringe over 10 min. A minor exotherm was observed upon TFAA addition. The reaction was monitored by TLC and quenched at 0 °C with Et_3N (5.0 mL, 35.2 mmol, 1.2 equiv) after 1 h. Significant smoke was observed as Et_3N•TFA salts formed. After 5 min of vigorous stirring, sat. $NaHCO_3$ (400 mL) was added to the cold solution, causing many salts to crash out of the solution. The resulting mixture was allowed to thaw to room temperature and then diluted with EtOAc (250 mL). The aqueous phase was separated and then back extracted with EtOAc (2 x 200 mL). The combined organic phases were dried over $MgSO_4$, filtered and concentrated. The resulting crude oil was purified by silica gel chromatography (gradient 1%, 15%, 20% EtOAc/Hexanes) to afford clean tertiary trifluoroacetate **5.41** (16.0g, 28.3 mmol, 97% Yield) as a pale yellow oil. (Note: For immediate use, the desired product can simply be filtered over a pad of SiO_2 gel with 20% EtOAc/Hexanes to remove any remaining polar reaction byproducts. Full chromatography was employed to obtain large quantities of highly pure material for long-term storage as a solution frozen in benzene). $[\alpha]_D$ = -68° (c 3.9, CH_2Cl_2); R_f = 0.5 (20% EtOAc/Hexanes, PMA); ^{1}H NMR (500 MHz, $CDCl_3$) δ 6.42 (dd, *J* = 17.6, 10.9 Hz, 1H), 5.30 (d, *J* = 17.6 Hz, 1H), 5.24-5.14 (m, 2H), 5.10 (d, *J* = 10.9 Hz, 1H), 5.04 (t, *J* = 3.2 Hz, 1H), 4.42 (dddd, *J* = 13.4, 7.6, 5.7, 1.9 Hz, 1H), 4.33 (dtd, *J* = 11.4, 6.6, 1.8 Hz, 1H), 4.23-4.08 (m, 2H), 2.85 (dd, *J* = 15.3, 2.2 Hz, 1H), 2.58 (dd, *J* = 14.2, 6.6 Hz, 1H), 2.49 (dd, *J* = 16.2, 5.8 Hz, 1H), 2.36 (dd, *J* = 14.2, 6.8 Hz, 1H), 2.27 (dd, *J* = 16.2, 7.6 Hz, 1H), 2.05 (s, 3H), 2.16 (dt, *J* = 15.0,

2.1 Hz, 1H), 1.97 (dt, *J* = 15.0, 2.1 Hz, 1H), 1.87-1.78 (m, 1H), 1.60 (dd, *J* = 15.0, 4.2 Hz, 1H), 1.57-1.46 (m, 4H), 1.38 (d, *J* = 15.2 Hz, 1H), 1.28 (dd, *J* = 14.1, 11.4 Hz, 1H), 0.98 (dd, *J* = 9.4, 7.7 Hz, 2H), 0.05 (s, 9H); ^{13}C NMR (125 MHz, $CDCl_3$) δ 171.0, 170.9, 156.5 (q, *J* = 41.1 Hz), 142.3, 139.1, 118.4, 114.5 (q, *J* = 286.5 Hz), 113.9, 97.0, 84.3, 66.8, 63.8, 62.7, 61.6, 41.9, 41.0, 40.0, 37.6, 37.5, 33.9, 26.5, 21.6, 17.5, -1.4; IR (cast film) 2953, 1777, 1733, 1377, 1248, 1215, 1151, 1136, 1059 cm^{-1}; LRMS (FAB+) calc'd for $C_{26}H_{40}F_3O_8Si$ $[M+H]^+$ 565.67, found 565.49.

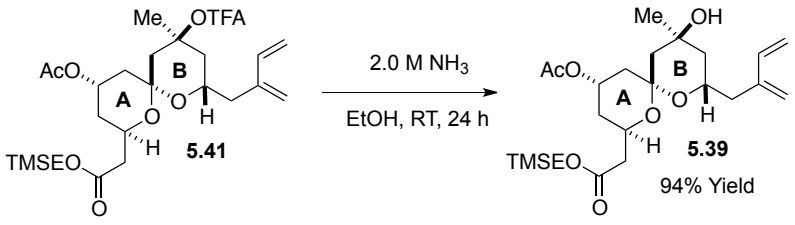

Tertiary trifluoroacetate **5.41** (14mg, 0.025 mmol, 1.0 equiv) was solvated in a 2.0 M solution of NH_3 in EtOH (1 mL). The solution was stirred at room temperature and the deprotection was monitored by TLC. At 24 h, the reaction mixture was concentrated and the resulting oil was purified by silica gel chromatography (15% EtOAc/Hexanes) to afford clean tertiary alcohol **5.39** (11mg, 0.023 mmol, 94% Yield) as a pale yellow oil. The spectral properties of the isolated product were consistent with the characterization data reported above. (Note: This reaction was performed to demonstrate that the removal of the TFA group is both selective and high yielding).

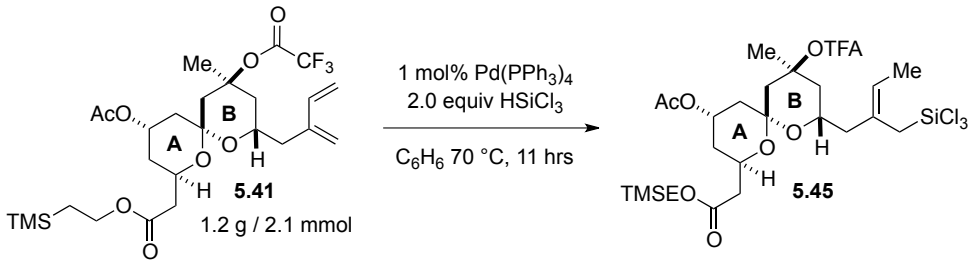

A flame-dried sealed tube was charged with $Pd(PPh_3)_4$ (18mg, 0.015 mmol, 0.01 equiv), evacuated and back-filled with N_2. AB-Fragment Diene **5.41** (847mg, 1.5 mmol, 1.0 equiv) was transferred to the sealed tube in a solution of anhydrous C_6H_6 (15 mL, 0.1 M) under an atmosphere of N_2. Trichlorolsilane (0.30 mL, 3.0 mmol, 2.0 equiv) was added to the solution and the sealed tube was screwed closed. The reaction vessel was placed in a 70 °C bath and the light yellow solution was stirred for 11 h. The resulting light brown solution was allowed to cool to room temperature before being cannulated into a flame-dried, 100 mL roundbottom flask. The sealed tube was rinsed with anhydrous C_6H_6 (2 x 3 mL), and the wash solution was cannulated into the 2-neck roundbottom flask. The reaction mixture was concentrated down to a crude amber oil using air-free technique. (Note: air-free technique involved placing the roundbottom flask in a 40 °C water bath, connecting it to an adjacent -78 °C cold-finger and carefully reducing the pressure with a manometer partitioned through the pump manifold. Upon complete removal of solvent, the entire system was back-filled with N_2). The crude trichlorosilane was taken on to the diamine complexation without purification.

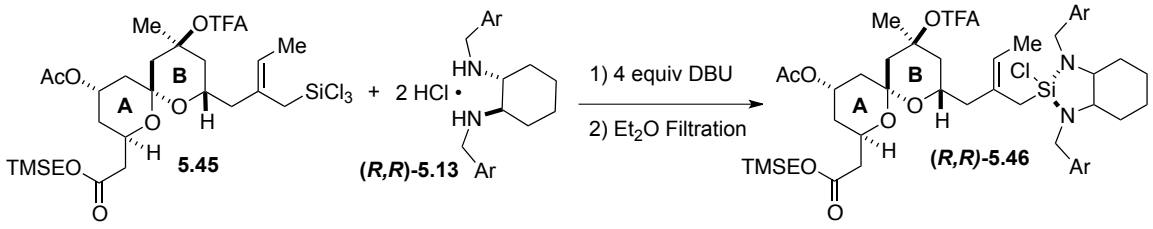

Crude hydrosilylated product **5.45** was retaken in anhydrous CH_2Cl_2 (15 mL, 0.1 M) and diamine•2HCl salt **(*R,R*)-5.13** (788mg, 1.5 mmol, 1.0 equiv) was added at room temperature. The resulting white slurry was cooled to 0 °C and distilled DBU (0.90 mL, 6.0 mmol, 4.0 equiv) was added to the reaction mixture over 10 min. As DBU was added, the white salts solvated upon deprotonation and the solution took on an amber hue. After an additional 5 min of stirring, the solution was thawed to room temperature. After 2 h, the solvent was removed using air-free technique until the resulting yellow oil became opaque and foamy. (Note: air-free technique involved placing the roundbottom flask in a room temperature water bath, connecting it to an adjacent -78 °C cold-finger and carefully reducing the pressure with a manometer partitioned through the pump manifold. Upon complete removal of solvent, the entire system was back-filled with N_2). The resulting oil was retaken in anhydrous Et_2O (15 mL, 0.1 M) and shaken vigorously for 10 min until the DBU•HCl salts precipitated out as a white solid. This heterogeneous solution was stirred vigorously for an additional 6.5 h to until the DBU•HCl salts became a very fine white precipitate. The tinted yellow supernatant was filter-cannulated through a flame-dried, air-free filter frit into a flame-dried, 100 mL roundbottom flask. Et_2O (2x 5 mL) was added to rinse the leftover DBU•HCl salts and the flask was shaken vigorously. The supernatant was again filter-cannulated into the new 100 mL roundbottom flask. The solvent was again removed using air-free technique (room temperature bath) until the resulting yellow oil became opaque and foamy. The resulting angelic-silane **(*R,R*)-5.46** was retaken in anhydrous CH_2Cl_2 (15 mL, 0.1 M) and divided into two equivolume batches for further reaction.

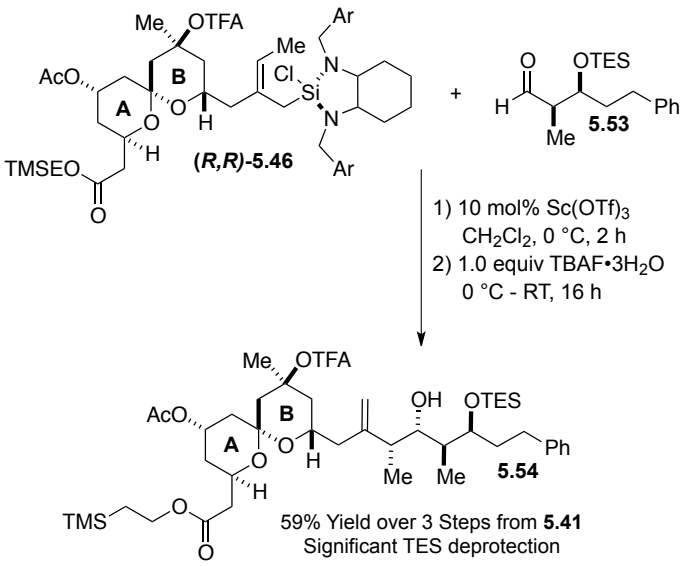

Angelic-silane **(*R,R*)-5.46** (ca. 810 mg, 0.75 mmol, 1.0 equiv) in CH_2Cl_2 (7.5 mL, 0.1 M) from above was cooled to 0 °C. Aldehyde coupling partner **5.53** (230 mg, 0.75 mmol, 1.0 equiv) was added to the cooled mixture followed by $Sc(OTf)_3$ (37mg, 0.075 mmol, 0.10 equiv). The reaction mixture was stirred vigorously at 0 °C for 2 h and then quenched with TBAF•$3H_2O$ (237 mg, 0.75 mmol, 1.0 equiv). The surrounding 0 °C bath was allowed to slowly expire over 16 h. This quenched reaction mixture was then concentrated down to a thick oil and purified by silica gel chromatography (gradient, 15%, 20% EtOAc/Hexanes) to afford coupled fragment **5.54** (383mg, 0.44 mmol, 59% yield over 3 Steps from **5.41**) as a pale yellow oil. $[\alpha]_D$ = -44° (c 2.6, CH_2Cl_2); R_f = 0.4 (20% EtOAc/Hexanes, PMA); ^{1}H NMR (500 MHz, $CDCl_3$) δ 7.32-7.24 (m, 2H), 7.22-7.15 (m, 3H), 5.15 (s, 1H), 5.05-5.00 (m, 2H), 4.38-4.25 (m, 2H), 4.19-4.07 (m, 2H), 4.04 (ddd, *J* = 7.6, 4.8, 2.2 Hz, 1H), 3.66 (dd, *J* = 9.7, 2.2 Hz, 1H), 3.33 (bs, 1H), 2.85 (dd, *J* = 15.2, 2.2 Hz, 1H), 2.78 (ddd, *J* = 13.4, 11.3, 5.3 Hz, 1H), 2.56-2.42 (m, 2H), 2.43-2.34 (m, 2H), 2.29-2.18 (m, 2H), 2.02 (s, 3H), 2.02-1.91 (m, 2H), 1.90-1.75 (m, 3H), 1.60 (dd, *J* = 15.0, 4.3 Hz, 1H), 1.52 (s, 3H), 1.50-1.41 (m, 1H), 1.38 (d, *J* = 15.2 Hz, 1H), 1.32-1.24 (m, 2H), 1.06 (d, *J* = 6.9 Hz, 3H), 1.02-0.92 (m, 11H), 0.82 (d, *J* = 7.0 Hz, 3H), 0.64 (q, *J* = 7.9 Hz, 6H), 0.04 (s,

9H); ^{13}C NMR (100 MHz, $CDCl_3$) δ 171.1, 170.6, 156.4 (q, J = 41.6 Hz) 148.0, 142.4, 128.5, 128.5, 126.0, 114.5 (q, J = 286.9 Hz), 113.4, 96.8, 84.3, 75.7, 72.4, 66.5, 63.6, 62.6, 61.5, 42.5, 41.3, 41.1, 40.1, 40.0, 37.7, 35.4, 33.8, 33.4, 26.5, 21.6, 17.4, 11.5, 10.6, 7.1, 5.3, -1.4; IR (cast film) 3513, 2957, 2882, 1776, 1735, 1378, 1248, 1215, 1164, 1100, 1060, 1000, 977 cm^{-1}; LRMS (FAB+) calc'd for $C_{44}H_{71}F_3O_{10}Si_2$ $[M]^+$ 873.19, found 873.50.

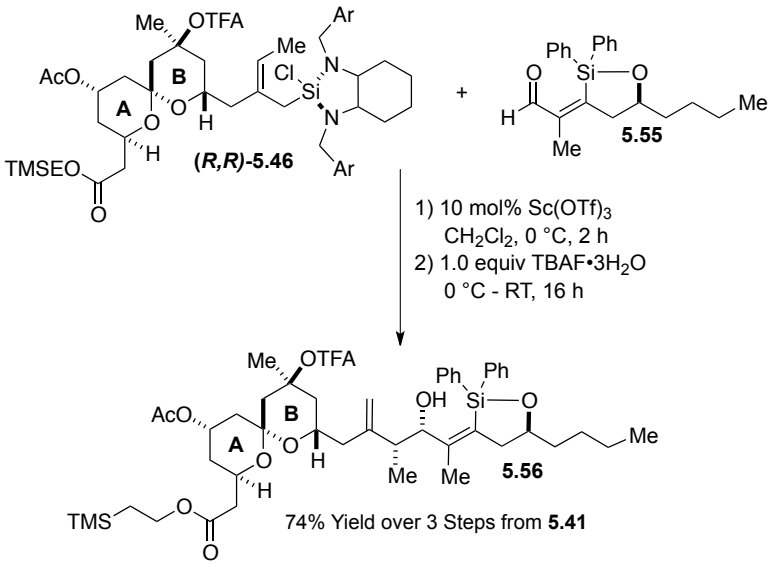

Angelic-silane **(*R,R*)-5.46** (ca. 810 mg, 0.75 mmol, 1.0 equiv) in CH_2Cl_2 (7.5 mL, 0.1 M) from above was cooled to 0 °C. Silacycle-aldehyde coupling partner **5.55** (263 mg, 0.75 mmol, 1.0 equiv) was added to the cooled mixture followed by $Sc(OTf)_3$ (37mg, 0.075 mmol, 0.10 equiv). The reaction mixture was stirred vigorously at 0 °C for 2 h and then quenched with TBAF•3H_2O (237 mg, 0.75 mmol, 1.0 equiv). The surrounding 0 °C bath was allowed to slowly expire over 10 h. This quenched reaction mixture was then concentrated down to a thick oil and purified by silica gel chromatography (gradient, 15%, 20% EtOAc/Hexanes using pH 7 buffered SiO_2 Gel) to afford silacycle **5.56** (508mg, 0.55 mmol, 74% yield over 3 Steps from **5.41**) as a

viscous, pale yellow oil. $[\alpha]_D$ = -33° (c 3.8, CH_2Cl_2); R_f = 0.3 (20% EtOAc/Hexanes, PMA); ^{1}H NMR (500 MHz, $CDCl_3$) δ 7.75-7.65 (m, 2H), 7.65-7.52 (m, 2H), 7.53-7.31 (m, 5H), 5.11 (dd, *J* = 7.2, 1.5 Hz, 2H), 5.05 (t, *J* = 3.2 Hz, 1H), 4.99 (s, 1H), 4.41 (dt, *J* = 13.0, 6.5 Hz, 2H), 4.23-4.07 (m, 2H), 3.54 (bs, 1H), 2.89 (dd, *J* = 15.2, 2.2 Hz, 1H), 2.77-2.67 (m, 1H), 2.63-2.38 (m, 5H), 2.30 (dd, *J* = 16.4, 7.3 Hz, 1H), 2.13 (dt, *J* = 14.5, 2.2 Hz, 1H), 2.02-1.97 (m, 1H), 2.01 (s, 3H), 1.88 (s, 3H), 1.86-1.77 (m, 1H), 1.62 (dd, *J* = 15.0, 4.1 Hz, 1H), 1.58-1.50 (m, 1H), 1.56 (s, 3H), 1.42 (d, *J* = 15.2 Hz, 1H), 1.39-1.08 (m, 9H), 0.98 (t, *J* = 8.5 Hz, 2H), 0.88-0.78 (m, 6H), 0.06 (s, 9H); ^{13}C NMR (100 MHz, $CDCl_3$) δ 170.9, 170.5, 156.3 (q, *J* = 41.1 Hz), 155.9, 147.1, 135.9, 135.1, 135.0, 134.5, 130.1, 130.1, 130.0, 127.8, 127.8, 114.3 (q, *J* = 287.4 Hz), 112.9, 96.7, 86.4, 84.3, 71.2, 66.5, 63.4, 62.5, 61.3, 42.0, 41.7, 40.9, 40.2, 39.9, 37.5, 37.2, 36.8, 33.7, 27.8, 26.4, 22.5, 21.4, 17.3, 14.0, 13.8, 11.4, -1.5; IR (cast film) 3517, 3075, 2961, 2930, 2862, 1777, 1734, 1372, 1249, 1214, 1163, 1059, 1016, 997 cm^{-1}; LRMS (FAB+) calc'd for $C_{48}H_{67}F_3O_{10}Si_2$ $[M]^+$ 917.21, found 917.51.

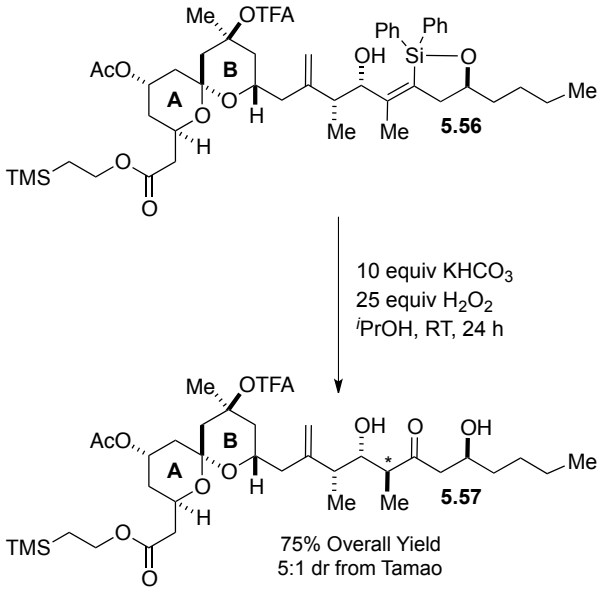

Silacycle **5.56** (440 mg, 0.48 mmol, 1.0 equiv) was solvated in isopropanol (5 mL, 0.1 M). $KHCO_3$ (240 mg, 2.40 mmol, 5.0 equiv) was added to the solution (sparingly soluble) followed by H_2O_2 as a 30% by weight solution in H_2O (0.63 mL, 1.3 ml/mmol, ca. 12 equiv). The reaction mixture was vigorously stirred at room temperature, and the reaction progress was monitored by TLC analysis. After 24 h, the reaction was quenched with brine (10 mL) and extracted with EtOAc (3 x 10 mL). The combined organic phase was dried over $MgSO_4$, filtered, and concentrated to a crude reaction residue. The resulting crude residue was purified by silica gel chromatography (40% EtOAc/Hexanes) to afford keto-diol **5.57** (271mg, 0.36 mmol, 75% yield) as a pale yellow oil. The diastereoselectivity of the isolated product was determined to be 5:1 by ^{1}H NMR analysis. R_f = 0.4 (40% EtOAc/Hexanes, PMA); ^{1}H NMR (500 MHz, $CDCl_3$) δ 5.23 (s, 1H), 5.06-4.99 (m, 2H), 4.44-4.27 (m, 2H), 4.19-4.04 (m, 4H), 3.77 (dt, *J* = 9.3, 2.2 Hz, 1H), 3.22 (bs, 1H), 2.85 (dd, *J* = 15.3, 2.4 Hz, 1H), 2.82-2.76 (m, 1H), 2.73 (dd, *J* = 16.9, 2.5 Hz, 1H), 2.64-2.51 (m, 2H), 2.45 (dd, *J* = 16.7, 7.0 Hz, 1H), 2.35-2.19 (m, 4H), 2.04 (s, 3H), 1.95-1.87 (m, 1H), 1.81-1.72 (m, 1H), 1.65-1.56 (m, 3H), 1.54 (s, 3H), 1.52-1.45 (m, 1H), 1.43-1.24 (m, 7H), 1.15 (dd, *J* = 9.9, 7.0 Hz, 1H), 1.06 (d, *J* = 4.0 Hz, 3H), 1.05 (d, *J* = 4.1 Hz, 3H), 0.95 (dd, *J* = 9.2, 7.9 Hz, 2H), 0.90 (t, *J* = 6.9 Hz, 3H), 0.03 (s, 9H); ^{13}C NMR (125 MHz, $CDCl_3$) δ 216.2, 171.0, 170.8, 156.3 (q, *J* = 41.0 Hz) 147.4, 114.5, 114.3 (q, *J* = 286.7 Hz), 96.9, 84.2, 73.2, 67.6, 66.5, 63.5, 62.7, 61.4, 50.8, 48.4, 42.6, 41.3, 41.2, 40.2, 40.0, 37.7, 36.3, 33.8, 27.9, 26.5, 22.8, 21.6, 17.4, 14.2, 13.1, 11.0, -1.4; IR (cast film) 3497, 2947, 2933, 1778, 1735, 1378, 1249, 1216, 1165, 1136, 1060, 1000 cm^{-1}; LRMS (FAB+) calc'd for $C_{36}H_{59}F_3O_{11}Si$ $[M]^+$ 753.93, found 753.45.

1. Kubota, K.; Leighton, J. L., *Angew. Chem. Int. Edit.* **2003,** *42* (8), 946-948.

2. Connor, D. S.; Klein, G. W.; Taylor, G. N.; Boeckman, R. K.; Medwid, J. B., *Org Synth* **1988,** *50-9*, 101-103.

HPLC chromatograms for compound 5.30:

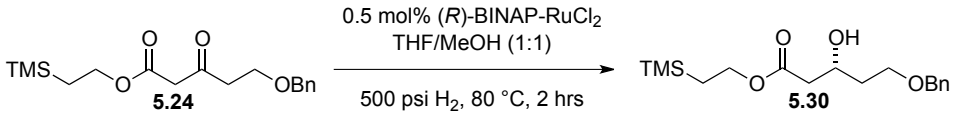

96% ee

Chiralcel AD-H Column, 2% *i*-PrOH in hexanes, 1 mL/min, 254 nm

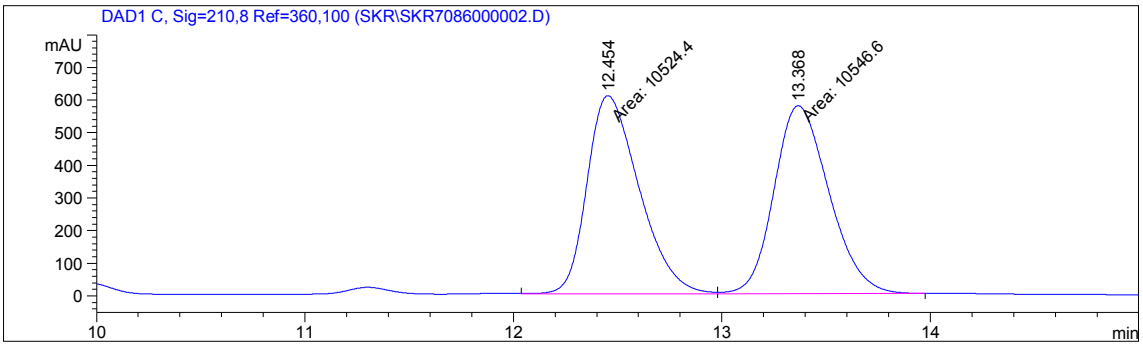

Peak #	RetTime [min]	Sig	Type	Area [mAU*s]	Height [mAU]	Area %
1	12.454	1	MM	1.05244e4	606.62604	49.9473
2	13.368	1	MM	1.05466e4	575.89166	50.0527

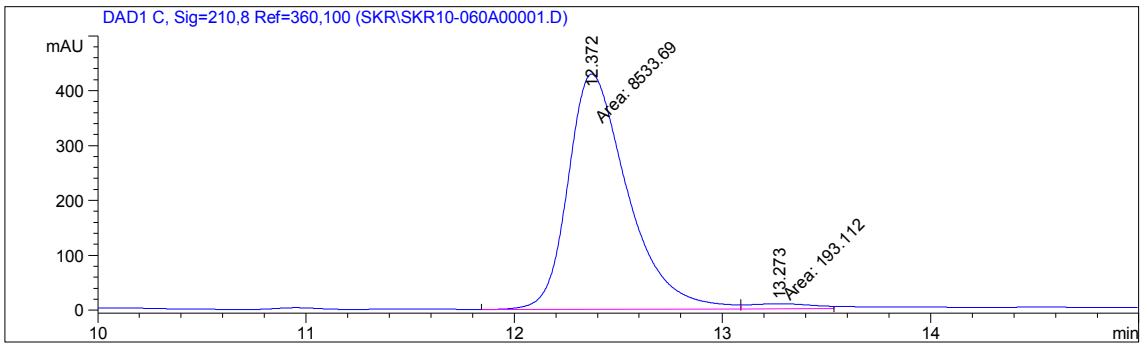

Peak #	RetTime [min]	Sig	Type	Area [mAU*s]	Height [mAU]	Area %
1	12.372	1	MM	8533.68750	428.80310	97.7871
2	13.273	1	MM	193.11183	9.09061	2.2129

GC chromatograms for compound 5.9:

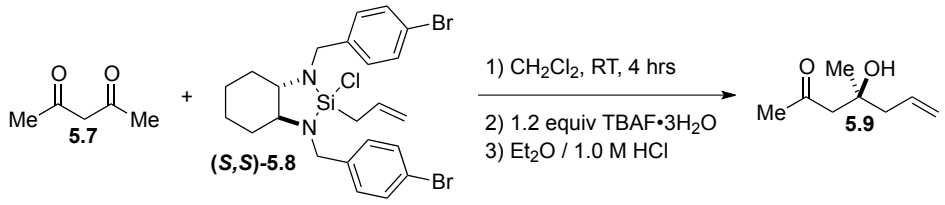

89% ee

Chiral GC Supelco β-Dex 125 and 325, 90 °C Isothermal

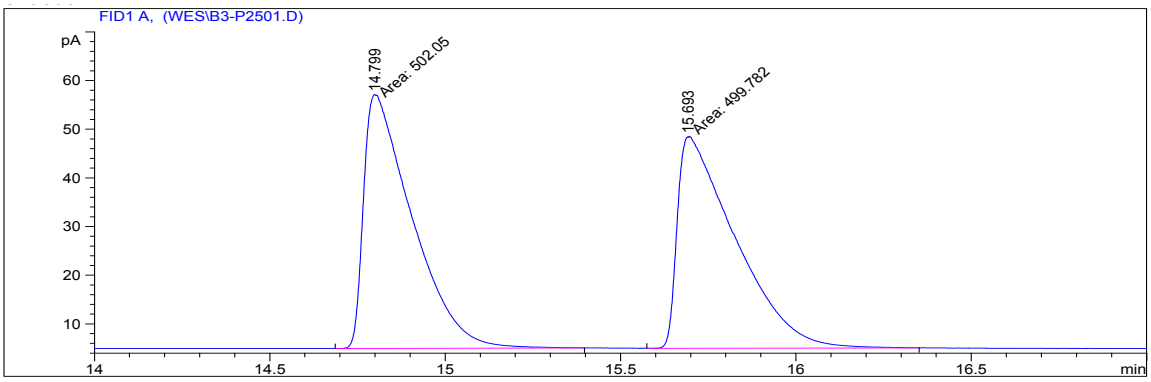

Peak #	RetTime [min]	Type	Width [min]	Area [pA*s]	Height [pA]	Area %
1	14.799	MM	0.1604	502.05014	52.17256	50.11322
2	15.693	MM	0.1913	499.78159	43.53556	49.88678

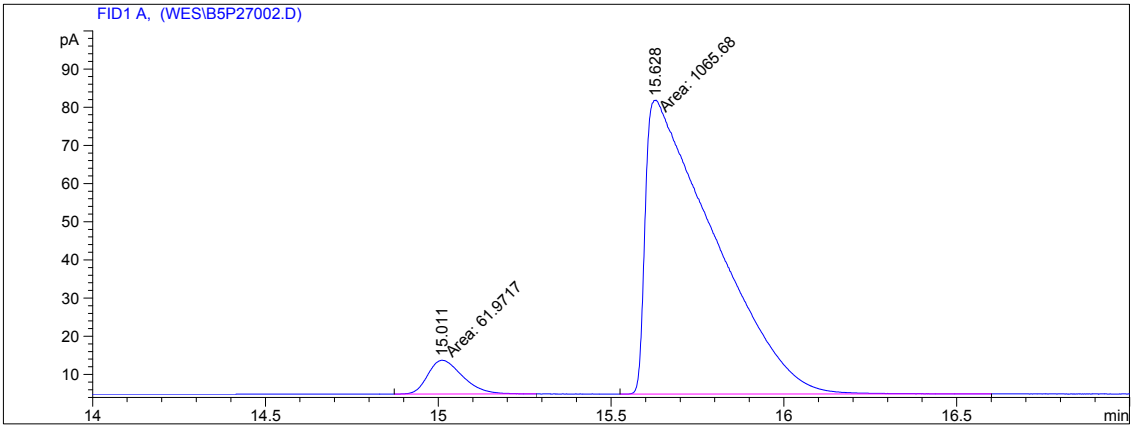

Peak #	RetTime [min]	Type	Width [min]	Area [pA*s]	Height [pA]	Area %
1	15.011	MM	0.1164	61.97166	8.87497	5.49564
2	15.628	MM	0.2308	1065.67969	76.95920	94.50436

Chapter 8: NMR Spectral Data

skr9-123a
Propyne Opening of Epoxyhexane
Distilled Pdt, 1H CDCl3

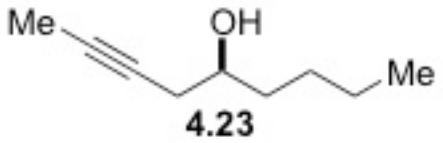

4.23

skr9-123c
Propyne Opening of Epoxyhexane
Distilled Pdt, 13 C CDCl3

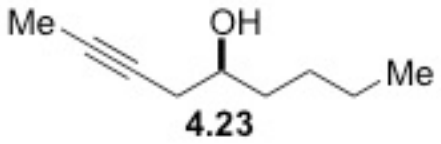

4.23

78.3
75.4
70.2
35.9
27.8
27.7
22.6
14.0
3.5

192

220 210 200 190 180 170 160 150 140 130 120 110 100 90 80 70 60 50 40 30 20 10 0
f1 (ppm)

skr9-124a
Ph2SiClH Rxn w/Homopropargylic Alcohol
Filtered Pdt, CDCl3

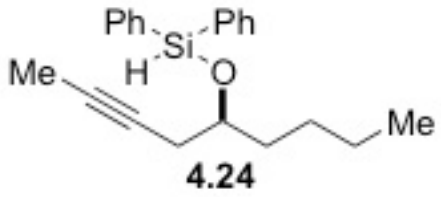

4.24

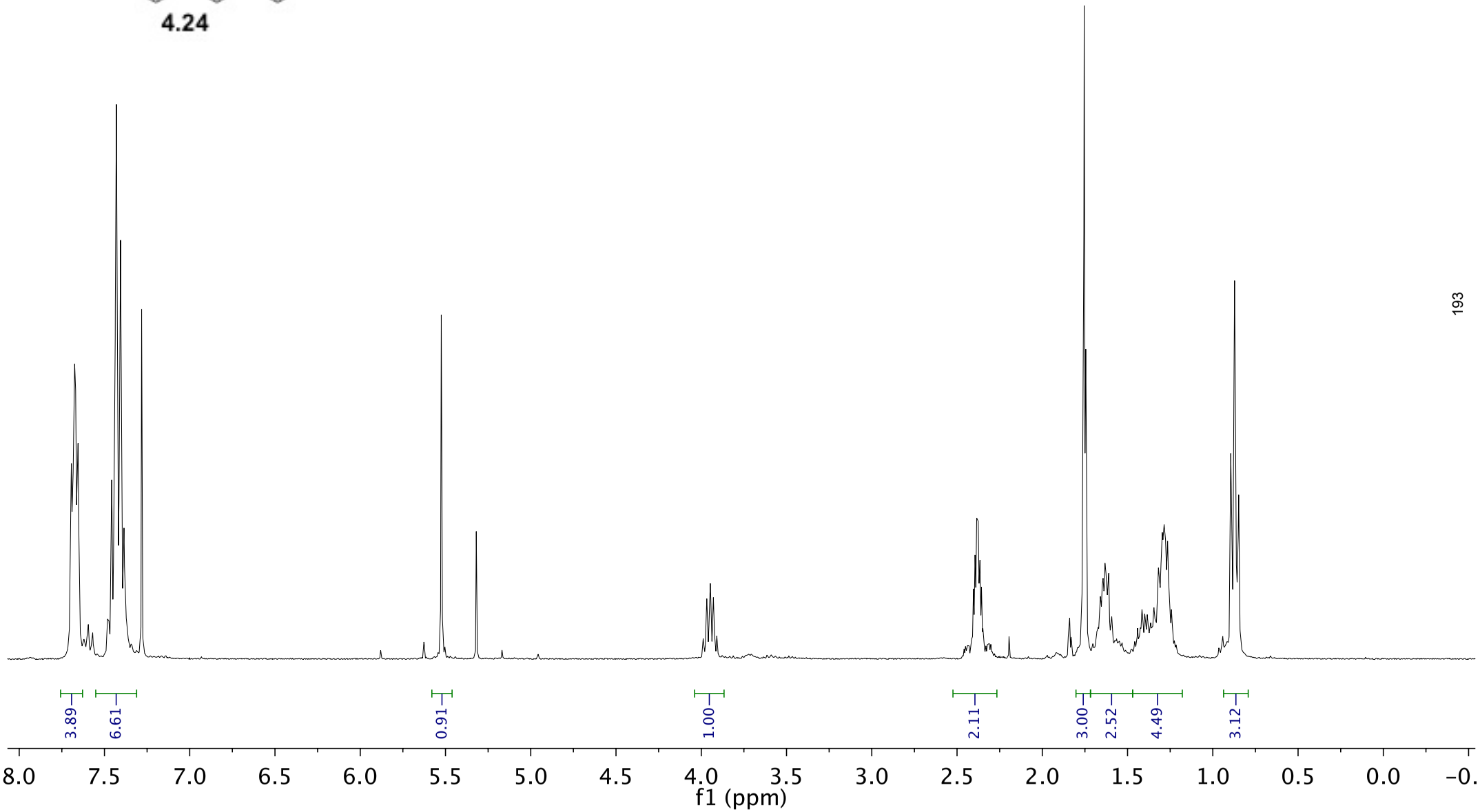

skr10-121c
Ph2SiClH Rxn w/Homopropargylic Alcohol
Rxn Crude Post Filtration, 13C CDCl3

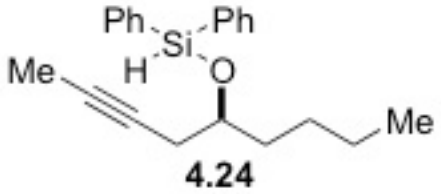

4.24

134.7
134.3
130.2
127.9
77.5
76.2
73.7
36.1
27.5
27.4
22.6
14.0
3.5

194

210 200 190 180 170 160 150 140 130 120 110 100 90 80 70 60 50 40 30 20 10 0 -10
f1 (ppm)

skr10-122a
Silylformylation Rxn (Model Alcohol)
Best Pdt Frxns Flashed w/pH 7 Buffered SiO2 Gel
Azeotroped, 1H CDCl3

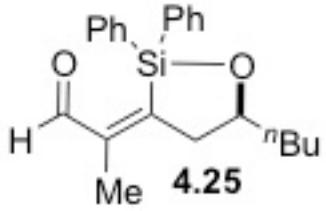

4.25

skr10-122a
Silylformylation Rxn (Model Alcohol)
Best Pdt Frxns Flashed w/ph 7 Buffered SiO2 Gel
Azeotroped, 13C CDCl3

192.7
163.7
144.7
135.2
135.1
133.2
132.8
130.7
130.6
128.2
128.1
76.1
41.7
38.3
27.8
22.7
14.0
13.3

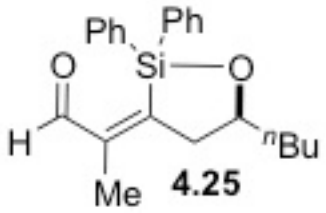

4.25

196

210 200 190 180 170 160 150 140 130 120 110 100 90 80 70 60 50 40 30 20 10 0 -10
f1 (ppm)

skr10-032a
(R,R) Isoprenylation Silane Reagent
Stored in a Solution of CDCl3

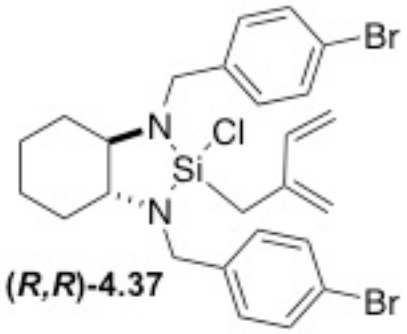

(*R,R*)-4.37

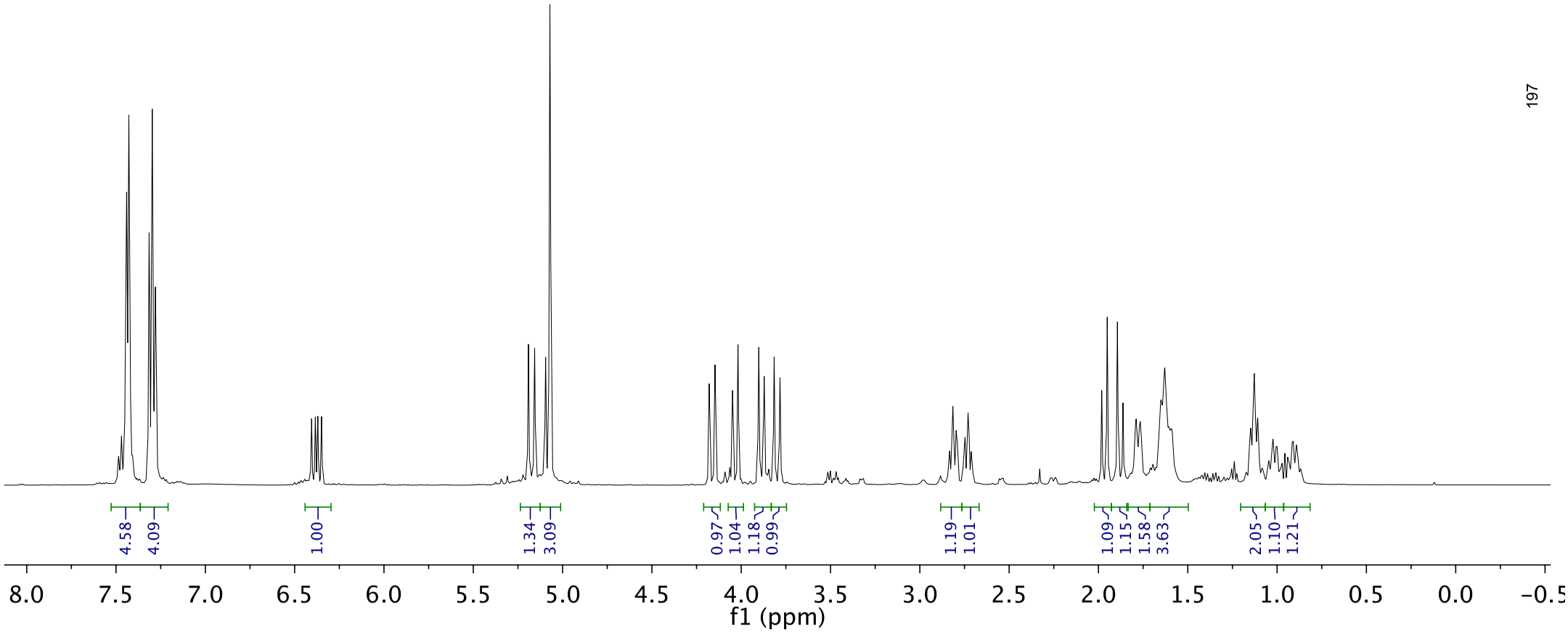

skr10-032c
(R,R) Isoprenylation Silane Reagent
Stored in a Solution of CDCl3 (13C)

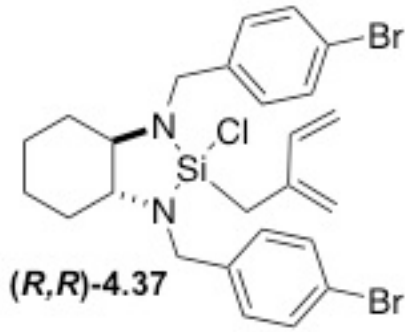

(*R,R*)-4.37

skr9-088a
Distilled Cl3Si-Diene
2nd Frxn, 1H CDCl3

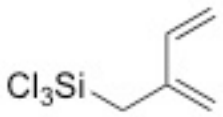

4.38

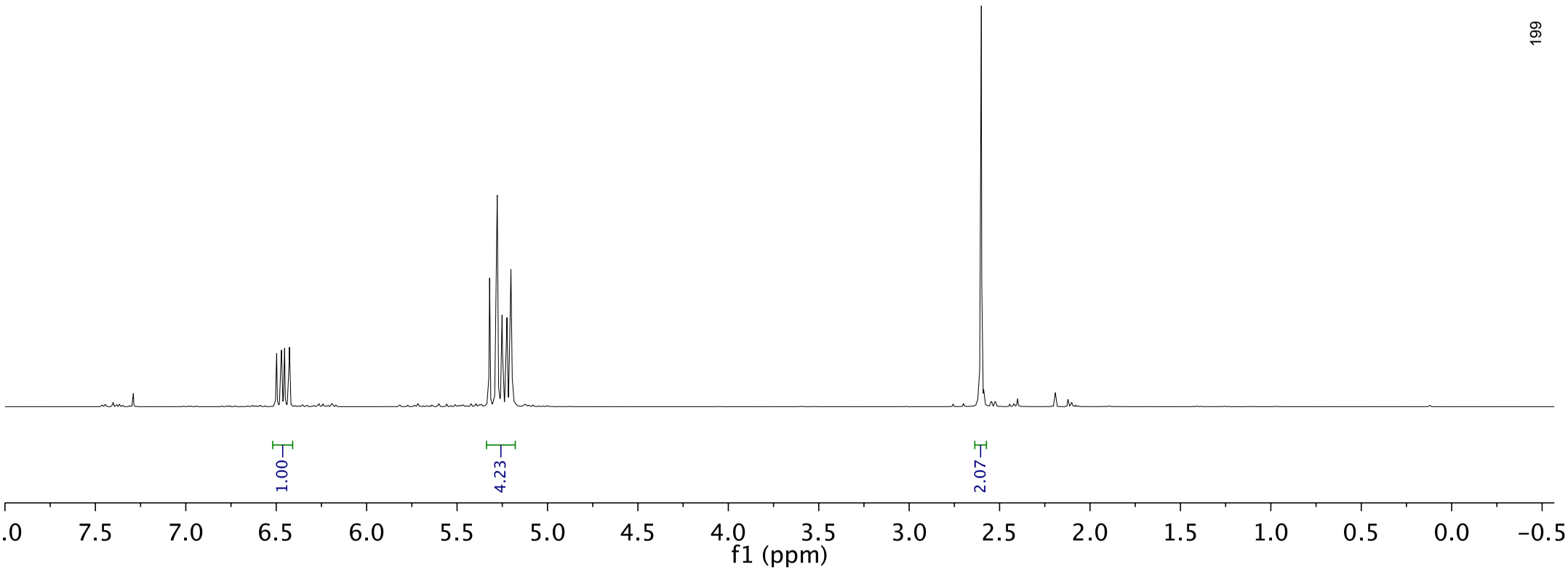

skr9-088b
Distilled Cl3Si-Diene
2nd Frxn, 13C CDCl3

137.9
137.2
119.5
115.3
28.0

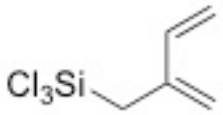

4.38

200

220 210 200 190 180 170 160 150 140 130 120 110 100 90 80 70 60 50 40 30 20 10 0
f1 (ppm)

skr10-031b
H-SiCl3 / Et3N / CuCl Rxn w/AllylBromide
Distilled Pdt (White and Cloudy), CDCl3

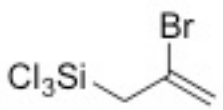

4.41

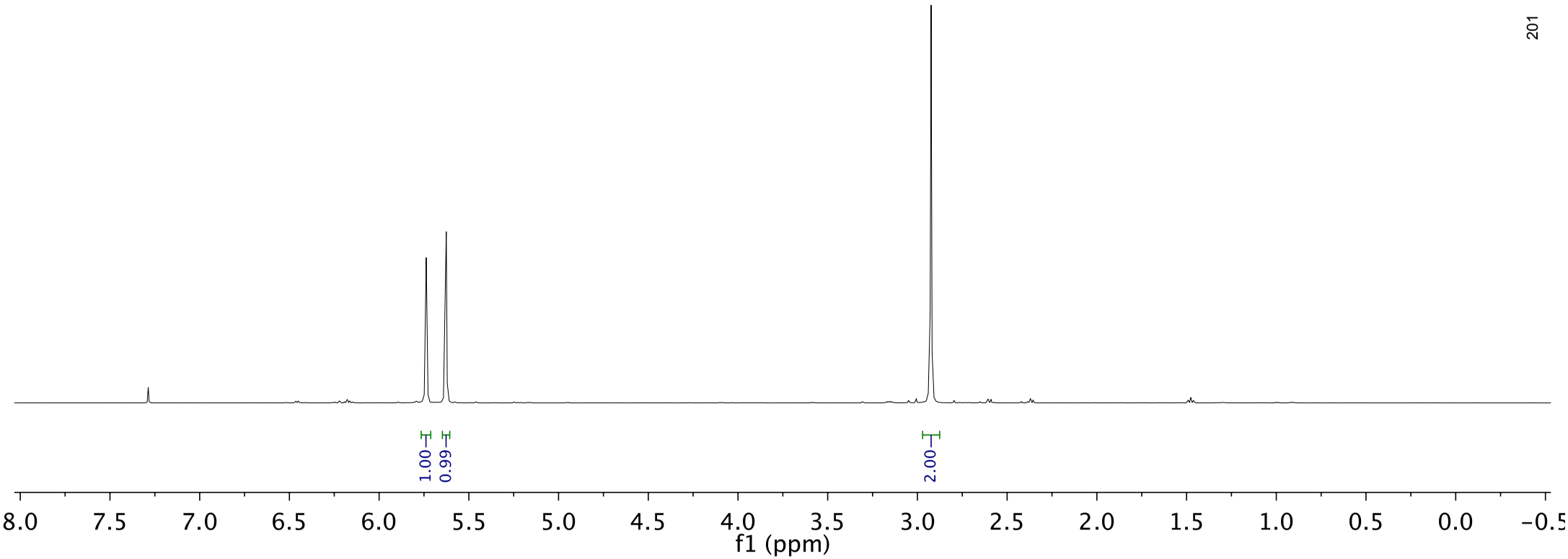

skr10-031c
H-SiCl3 / Et3N / CuCl Rxn w/AllylBromide
Distilled Pdt (White and Cloudy w/HCl), 13C CDCl3

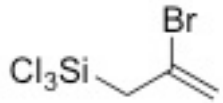

4.41

skr9-057e
Isoprenylation of Hydrocinnamaldehyde
All Pdt Frxns, Concentrate w/CDCl3

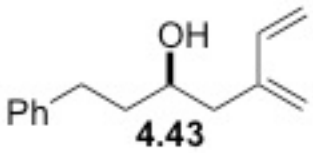

4.43

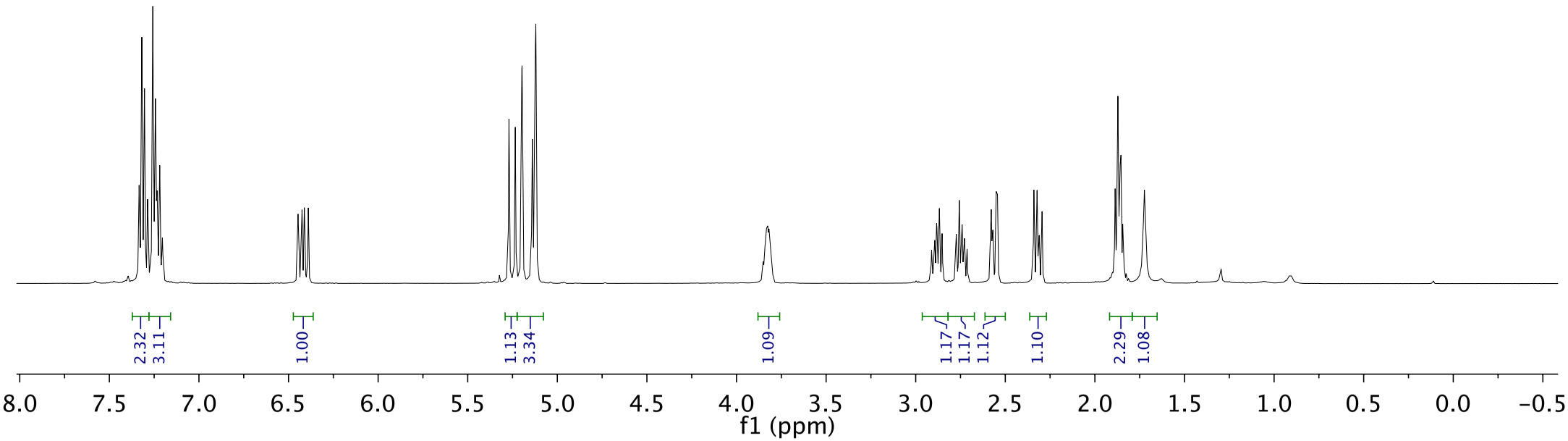

skr9-057f
Isoprenylation of Hydrocinnamaldehyde
All Pdt Frxns, Concentrate w/CDCl3
13C NMR

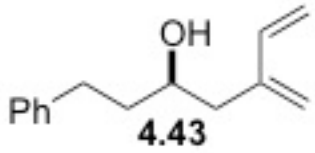

4.43

143.0
142.1
138.4
128.4
128.4
125.8
118.5
114.3
69.1
40.1
38.8
32.1

204

210 200 190 180 170 160 150 140 130 120 110 100 90 80 70 60 50 40 30 20 10 0 -10
f1 (ppm)

bsm2-68h
Reaction C
2nd Column
Pure, CDCl3

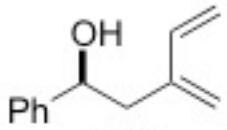

4.45

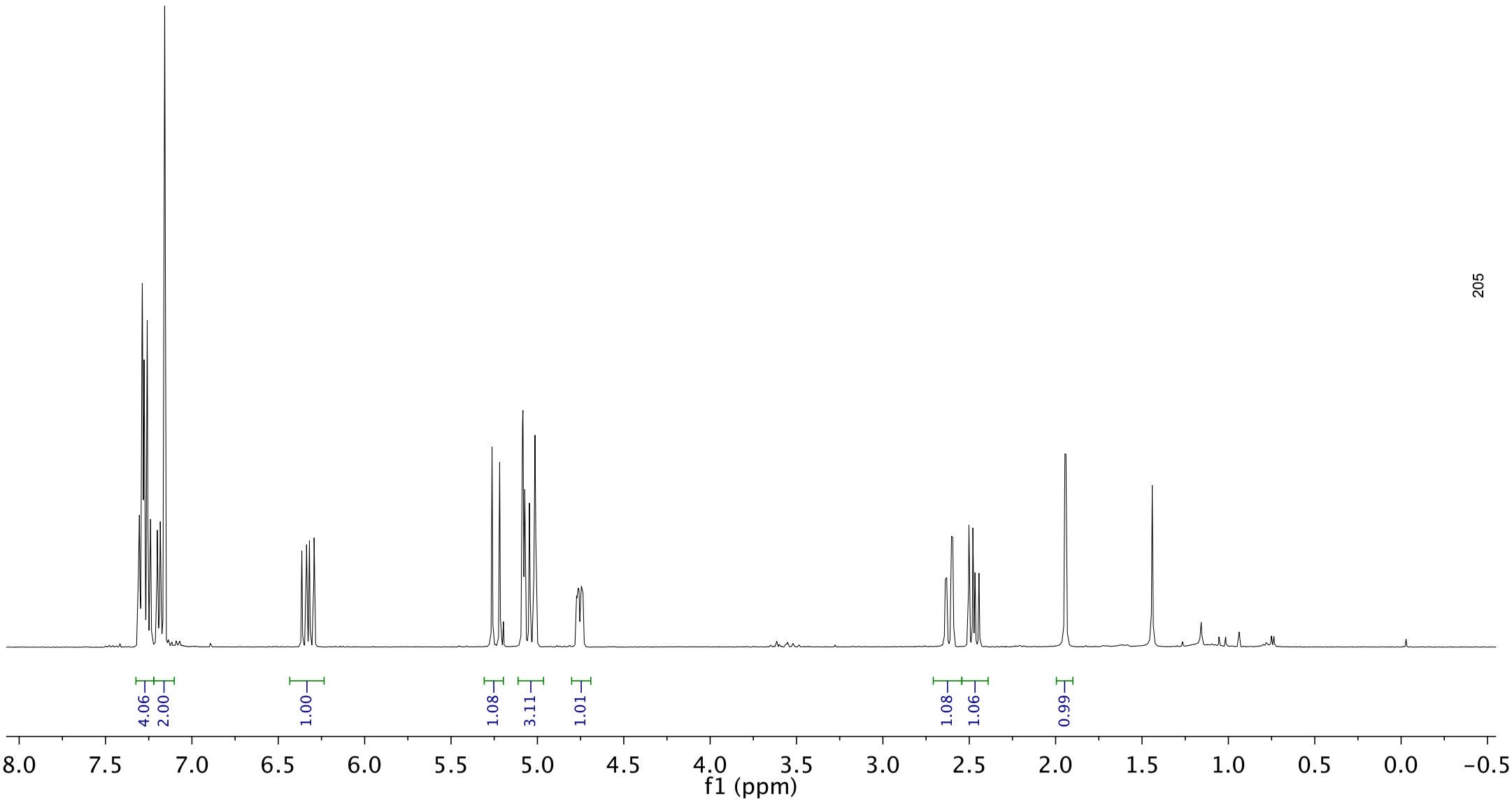

bsm2-68C-C
Reaction C
Carbon
Pure, CDCl3

144.1
142.7
138.3
128.4
127.6
125.8
118.9
114.3
72.2
42.2

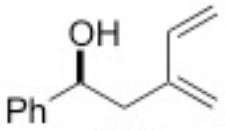

4.45

206

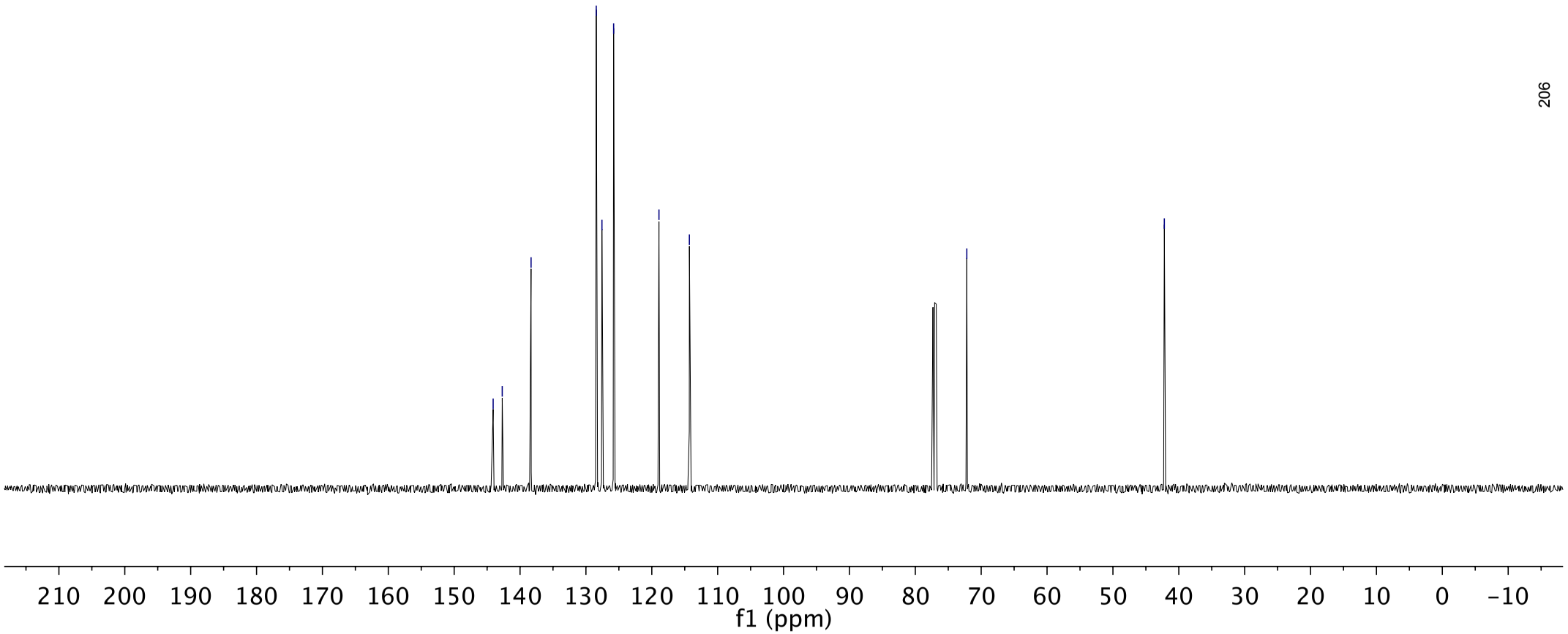

bsm2-68i
Reaction B
2nd Column
Pure, CDCl3

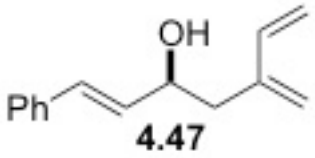

4.47

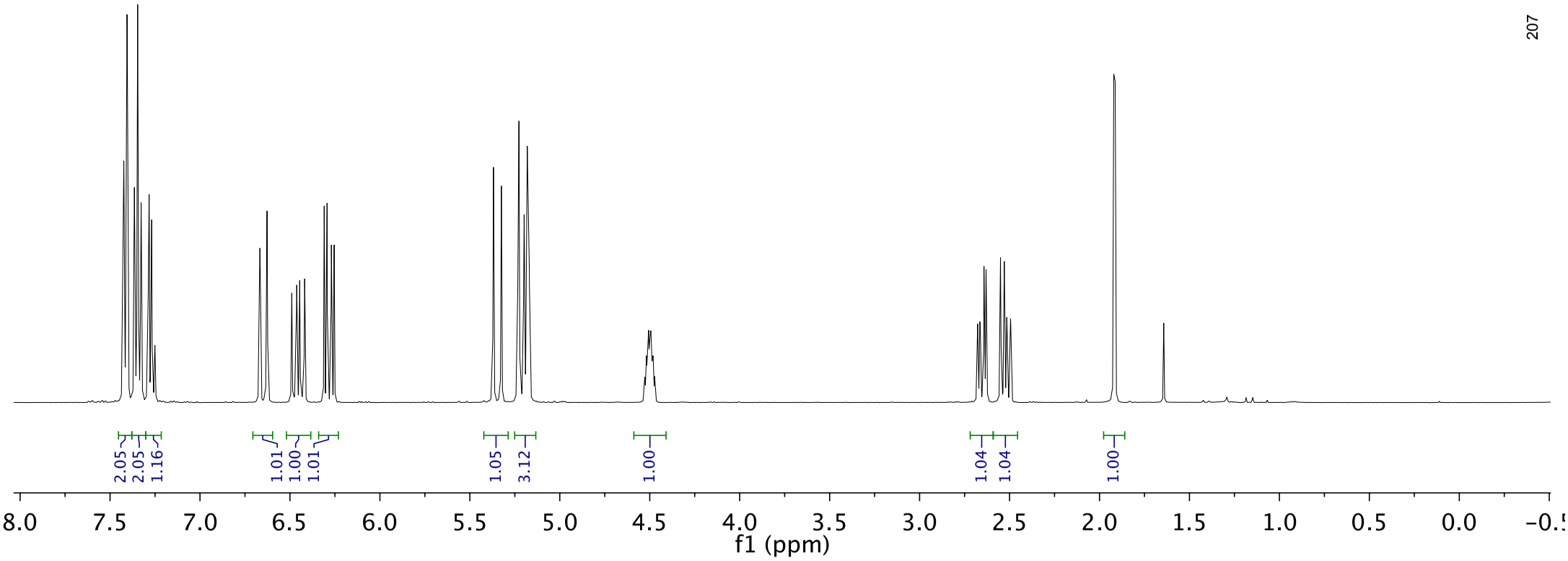

bsm2-68C-B
Reaction B
Carbon
Pure, CDCl3

142.4
138.5
136.8
131.7
130.2
128.6
127.7
126.5
119.0
114.4
70.8
40.1

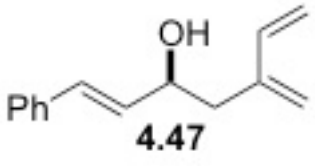

4.47

208

210 200 190 180 170 160 150 140 130 120 110 100 90 80 70 60 50 40 30 20 10 0 -10
f1 (ppm)

bsm2-68g
Reaction D
2nd Column
Pure, CDCl3

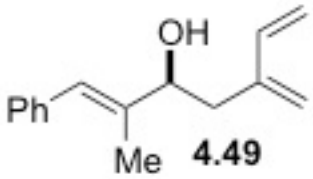

4.49

209

5.56 0.99 1.00 1.07 3.19 0.99 1.05 1.11 3.10 1.03

8.0 7.5 7.0 6.5 6.0 5.5 5.0 4.5 4.0 3.5 3.0 2.5 2.0 1.5 1.0 0.5 0.0 -0.5

f1 (ppm)

bsm2-68C-D
Reaction D
Carbon
Pure, CDCl3

142.9
139.6
138.4
137.6
129.0
128.1
126.5
125.8
118.6
114.3
75.5
38.6
13.6

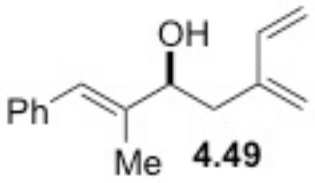

4.49

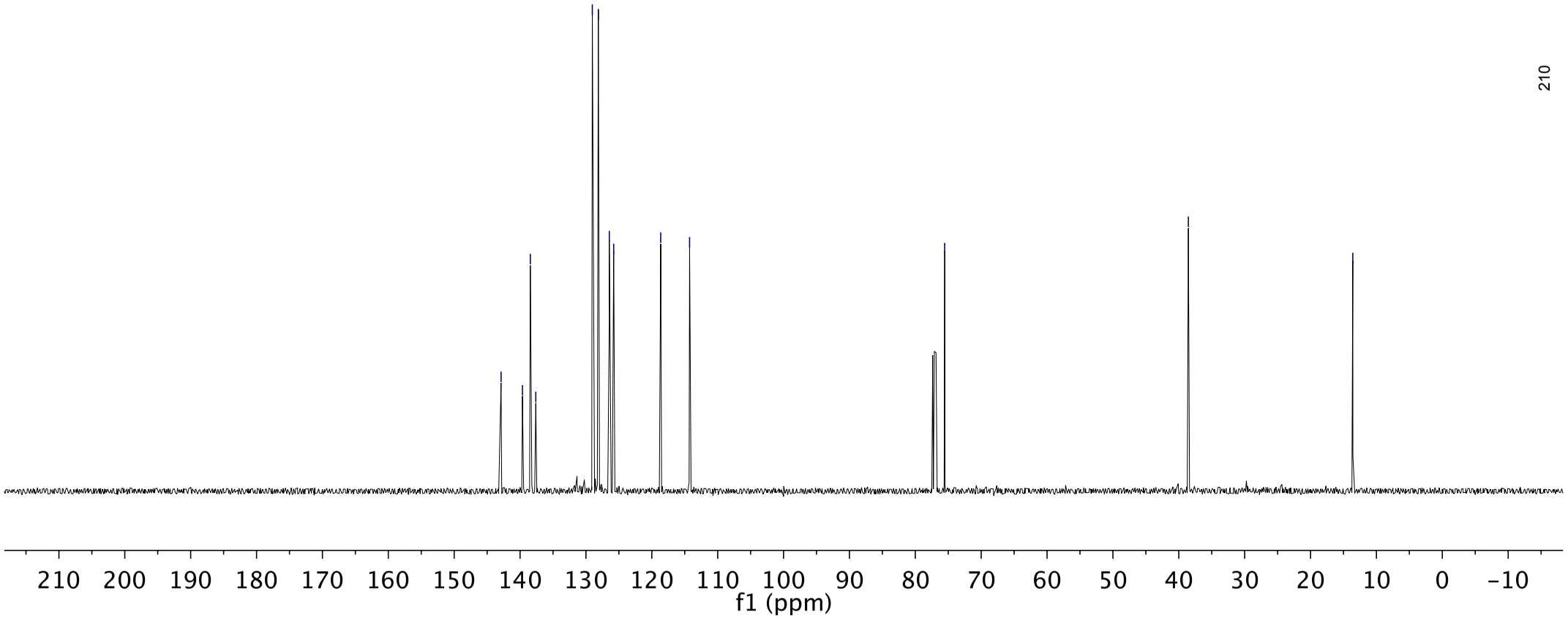

skr9-077d
Cis-Crotylated Hydrocinnamaldehyde
1H NMR, CDCl3

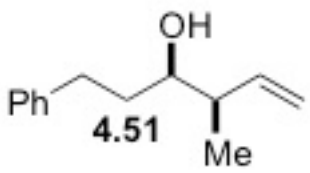

skr9-077e
Cis-Crotylated Hydrocinnamaldehyde
13C NMR, CDCl3

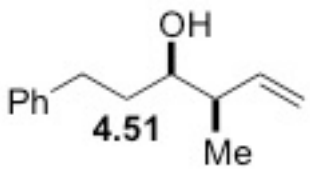

142.3
140.8
128.5
128.4
125.8
115.5
74.1
43.8
35.9
32.5
14.4

212

220 210 200 190 180 170 160 150 140 130 120 110 100 90 80 70 60 50 40 30 20 10 0
f1 (ppm)

skr9-096a
TES Protected Cis-Crotylated Hydrocinnamaldehyde
Reflashed Pdt Frxns, 1H CDCl3

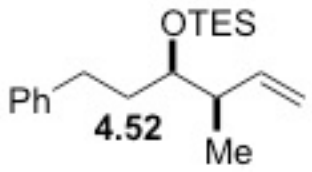

skr9-096b
TES Protected Cis-Crotylated Hydrocinnamaldehyde
Reflashed Pdt Frxns, 13C CDCl3

142.8
141.1
128.4
125.7
114.2
75.9
43.3
36.1
31.8
15.5
7.1
5.3

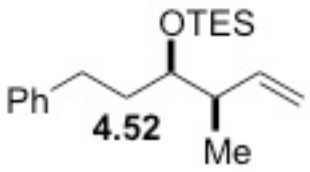

214

220 210 200 190 180 170 160 150 140 130 120 110 100 90 80 70 60 50 40 30 20 10 0
f1 (ppm)

skr9-101a
Ozonolysis w/PPh3
Best Pdt Frxns, 1H CDCl3

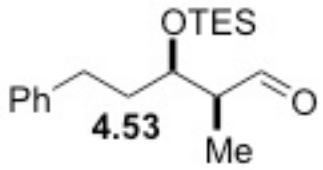

215

1.00 2.93 3.14 1.06 1.14 1.01 1.15 2.22 3.31 9.57 6.47

f1 (ppm)

skr9-101b
Ozonolysis w/PPh3
Best Pdt Frx#5, 13C CDCl3

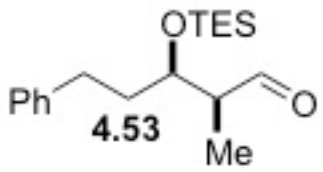

4.53

skr9-102f
Isoprenylated Diol Pdt
Best Pdt Frxns, 1H CDCl3

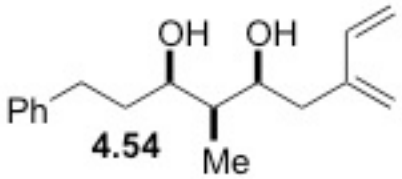

skr9-102g
Isoprenylated Diol Pdt
Best Pdt Frxns, 13C CDCl3

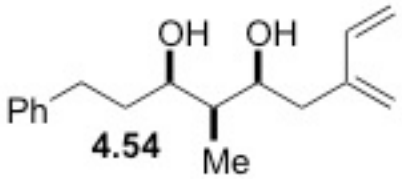

142.9
142.1
138.3
128.5
128.4
125.8
118.4
114.4
76.1
74.7
40.8
37.7
37.0
32.5
4.7

218

f1 (ppm)

skr9-058a
Hydrocinnamaldehyde Derived Diene-Acetate
All Pdt Frxns, Concentrate w/CDCl3

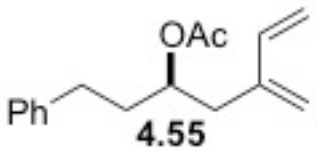

4.55

skr9-058b
Hydrocinnamaldehyde Derived Diene-Acetate
All Pdt Frxns, Concentrate w/CDCl3
13Carbon

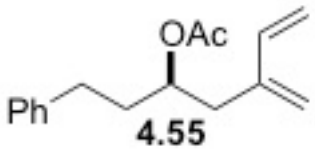

170.7
142.2
141.6
138.3
128.4
128.3
125.9
118.5
114.2
72.4
36.8
35.6
31.8
21.2

220

210 200 190 180 170 160 150 140 130 120 110 100 90 80 70 60 50 40 30 20 10 0 -10
f1 (ppm)

skr9-112a
Acetylated-Hydrocinnamaldehyde Diene
Hydrosilylated for t = 17 hrs at 70 deg C
Rxn NMR, 1H C6D6

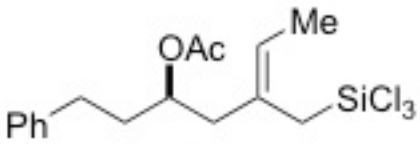

4.56

skr9-112b
Acetylated-Hydrocinnamaldehyde Diene
Hydrosilylated for t = 17 hrs at 70 deg C
Rxn NMR, 13C C6D6

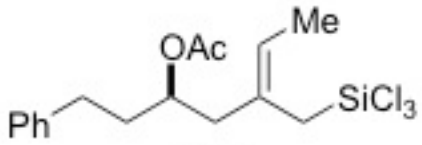

4.56

169.3
141.3
128.4
128.3
127.9 C6D6
127.7 C6D6
127.4 C6D6
126.9
126.0
125.4
71.0
43.5
35.8
31.9
27.4
20.3
14.0

222

220 210 200 190 180 170 160 150 140 130 120 110 100 90 80 70 60 50 40 30 20 10 0
f1 (ppm)

skr9-105a
Bis-Acetylated Diene
Best Pdt Frxns, 1H CDCl3

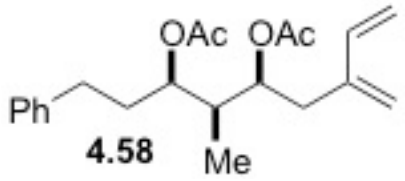

4.58

skr9-105b
Bis-Acetylated Diene
Best Pdt Frxns, 13C CDCl3

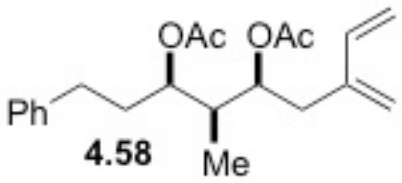

4.58

170.6
170.4
142.3
141.4
138.0
128.4
128.3
125.9
118.7
114.5
74.8
72.2
38.4
34.5
33.2
31.8
21.1
9.5

224

210 200 190 180 170 160 150 140 130 120 110 100 90 80 70 60 50 40 30 20 10 0 -10
f1 (ppm)

skr9-106a
Hydrosilylation of Bis-Acetylated Diene
Rxn at 70 deg C for t = 15 hrs in C6D6 1H

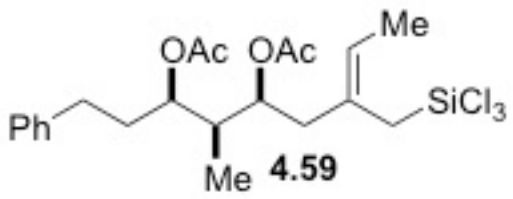

4.59

$HSiCl_3$

4.95 4.50 0.18 1.09 1.12 1.00 5.80 1.21 1.78 6.00 3.04 3.08 3.45

8.0 7.5 7.0 6.5 6.0 5.5 5.0 4.5 4.0 3.5 3.0 2.5 2.0 1.5 1.0 0.5 0.0 -0.5

f1 (ppm)

225

skr9-106b
Hydrosilylation of Bis-Acetylated Diene
Rxn at 70 deg C for t = 15 hrs in C6D6 13C

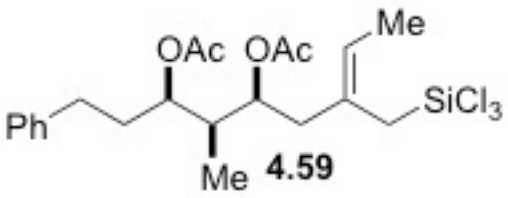

4.59

169.7
169.2
141.1
128.4 C6D6
128.3
128.2 C6D6
127.9 C6D6
127.7 C6D6
127.7 C6D6
127.5 C6D6
127.4 C6D6
127.0
126.0
125.7
73.5
71.6
41.6
40.1
33.7
32.1
27.3
20.2
20.1
14.1
9.6

226

220 210 200 190 180 170 160 150 140 130 120 110 100 90 80 70 60 50 40 30 20 10 0
f1 (ppm)

skr9-061f
(R,R)-Angelic-Silane Rxn w/Hydrocinnamaldehyde
Best Pdt Frxns (Azeotroped), 1H CDCl3

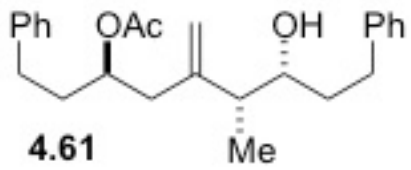

4.61

skr9-061c
(R,R) Angelic-Silane coupled w/Hydrocinnamaldehyde
Best Pdt Frxns (Azeotroped), 13C CDCl3

170.6
148.2
142.1
141.4
128.4
128.4
128.3
126.0
125.8
113.4
71.6
71.1
43.8
41.1
36.1
32.8
31.9
21.1
12.4

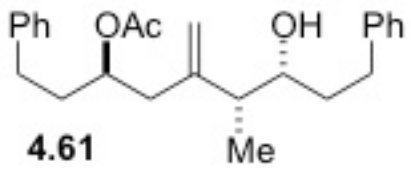

4.61

228

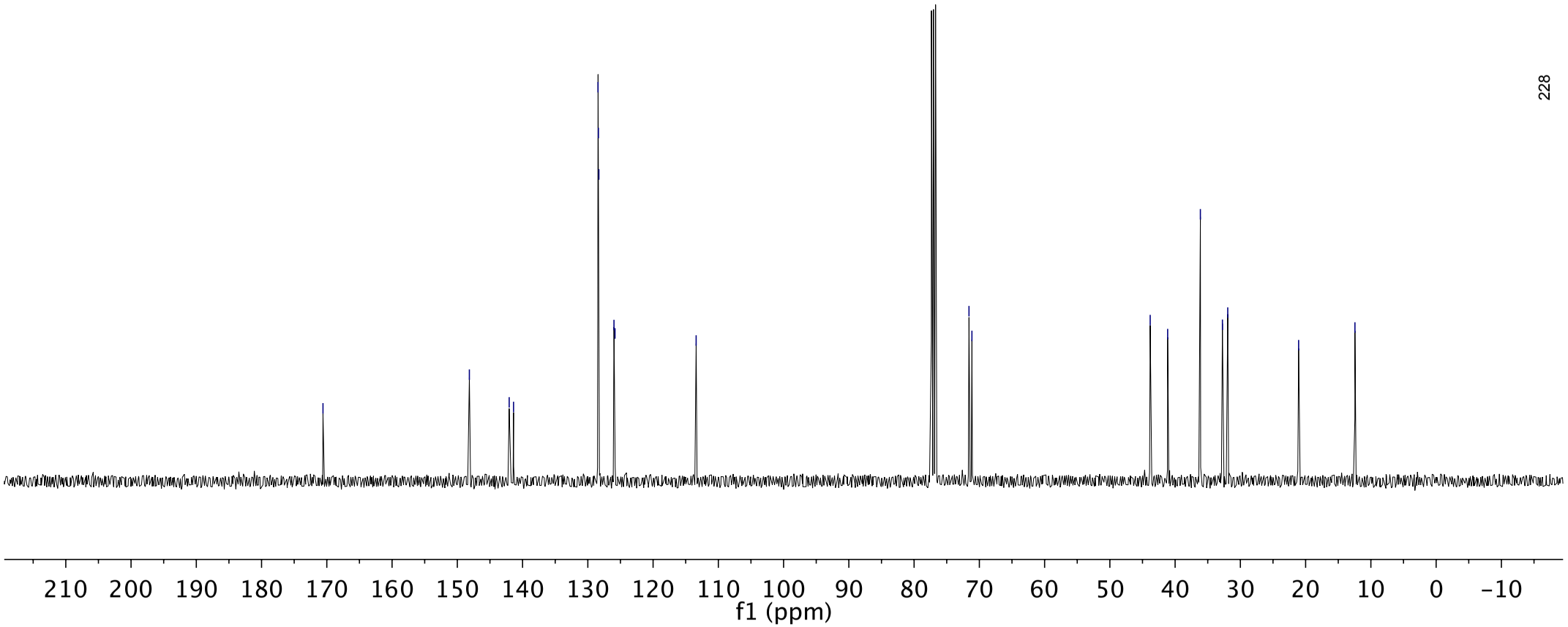

skr9-129e
1x-OAc Diol Angelication Pdt
Best Pdt Frxns, (Azeotroped) CDCl3

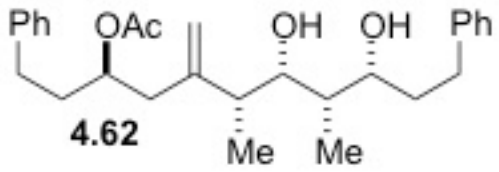

4.62

skr9-129c
1x-OAc Diol Angelication Product
Flashed Best Frxns, 13C CDCl3

170.7
147.9
141.8
141.4
128.4
128.4
128.3
126.0
125.9
113.3
79.1
76.1
72.0
43.2
39.9
38.3
37.0
35.9
32.5
31.9
21.1
16.3
5.4

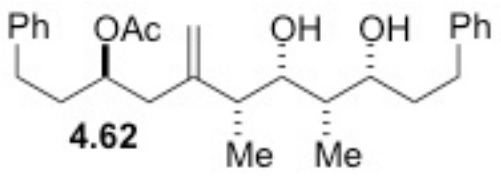

4.62

230

210 200 190 180 170 160 150 140 130 120 110 100 90 80 70 60 50 40 30 20 10 0 -10
f1 (ppm)

skr9-147a
Syn-Anti-Syn Angelication Pdt
Best Pdt Frxns, (Azeotroped) CDCl3

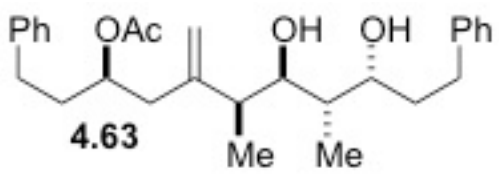

4.63

skr9-047c
Syn-Anti-Syn Angelication Pdt
Best Pdt Frxns, (Azeotroped) 13C CDCl3

170.9
147.9
142.6
141.3
128.5
128.5
128.4
128.3
126.0
125.7
114.1
74.2
73.7
72.6
41.6
40.6
39.3
35.4
35.3
33.0
31.8
21.2
12.1
11.8

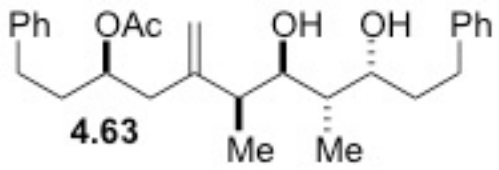

4.63

232

220 210 200 190 180 170 160 150 140 130 120 110 100 90 80 70 60 50 40 30 20 10 0
f1 (ppm)

skr9-135k
2x-OAc, 1x-OH Angelicaiton Pdt
Reflashed Best Pdt Frxns, CDCl3

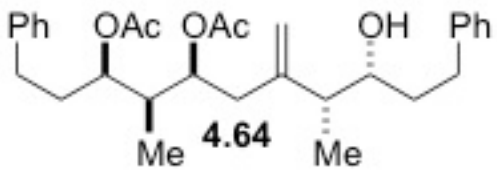

4.64

skr9-135j
2x-OAc, 1x-OH Angelication Pdt
Reflashed for Best Frxns, 13C CDCl3

170.7
170.3
148.1
142.2
141.2
128.5
128.4
128.4
128.3
126.0
125.8
113.6
74.0
72.0
71.5
43.5
40.3
39.3
36.1
33.9
32.9
32.1
21.1
21.0
12.4
10.0

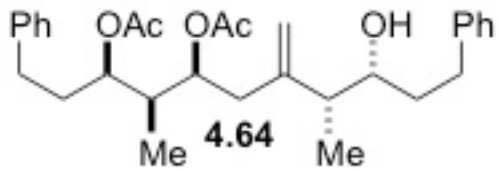

4.64

234

f1 (ppm)

skr9-136d
Angelication Pdt 2x-OAc Diol
Best Pdt Frxns, (Azeotroped) CDCl3

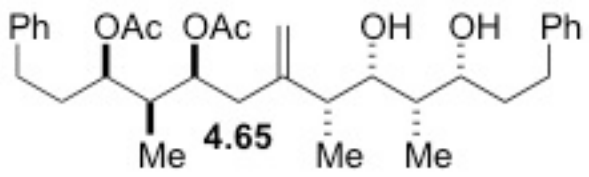

skr9-136c
Angelication Pdt 2x-OAc Diol
Best Pdt Frxns, (Azeotroped) 13C CDCl3

171.4
170.4
148.4
142.1
141.1
128.5
128.4
128.3
126.1
125.8
113.8
76.9
74.1
74.1
72.3
41.8
40.6
39.1
38.2
37.2
34.0
32.7
32.2
21.1
21.0
14.6
9.9
6.7

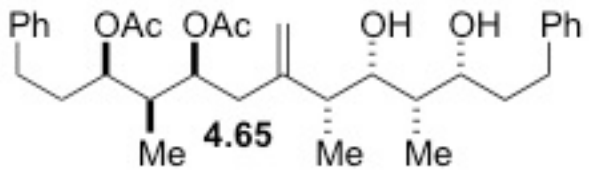

236

220 210 200 190 180 170 160 150 140 130 120 110 100 90 80 70 60 50 40 30 20 10 0 -10 -20 -30 -40
f1 (ppm)

skr9-137b
2x-OAc Silacycle (Angelication Rxn)
Reflashed Pdt Frxns (Azeotroped), 1H CDCl3

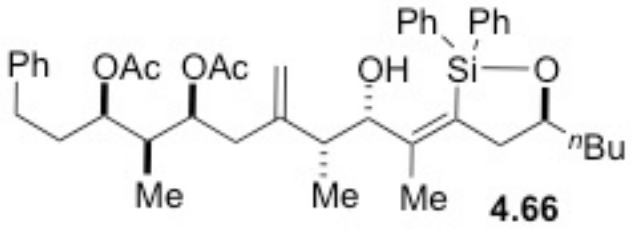

4.66

skr9-137c
2x-OAc Silacycle Angelication Pdt
Best Pdt Fr.ns 1(Azeotroped), 13C CDCl3

177.7
177.4
155.8
147.2
141.3
135.9
135.1
134.4
130.1
130.1
130.0
128.4
128.3
127.9
127.8
126.0
114.1
86.2
74.3
72.3
71.2
40.5
40.1
38.5
37.2
36.7
33.7
32.1
27.8
22.5
21.1
21.1
14.0
13.9
11.4
10.0

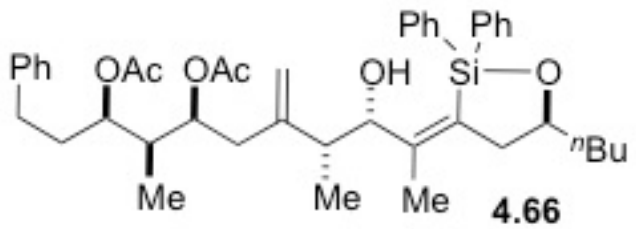

4.66

238

180 170 160 150 140 130 120 110 100 90 80 70 60 50 40 30 20 10 0
f1 (ppm)

skr9-158b
Tamao Oxidation of 2x-OAc Silacycle
Best Pdt Frxns (Main Diastereomer), CDCl3

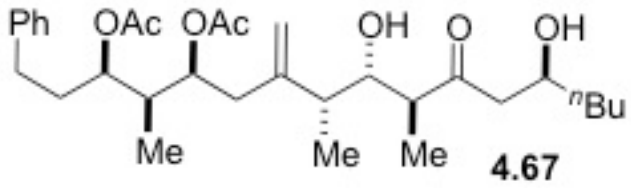

4.67

skr10-017c
Tamao of 2x-OAc Silacycle
Best Pdt Frxns, 13C CDCl3

215.6
170.6
170.3
147.7
141.1
128.4
128.3
126.0
114.6
73.9
73.0
71.9
67.5
50.1
48.4
40.5
39.9
38.9
36.1
33.7
32.1
27.7
22.6
21.0
20.9
14.0
13.1
11.0
10.1

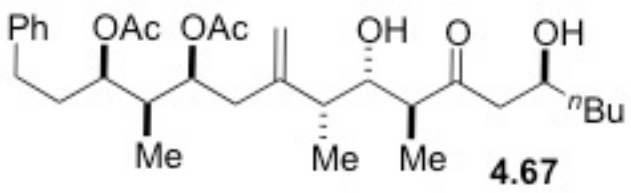

4.67

240

210 200 190 180 170 160 150 140 130 120 110 100 90 80 70 60 50 40 30 20 10 0 -10
f1 (ppm)

skr10-026a
1x-OAc Acetonide Rxn
All Pdt Frxns, (Azeotroped) CDCl3

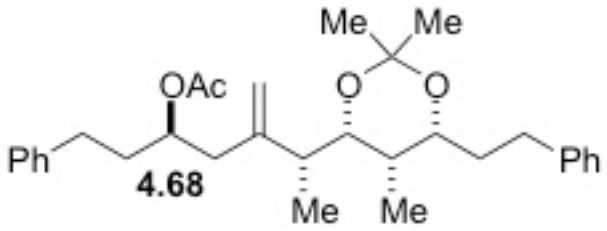

4.68

skr10-026c
1x-OAc Acetonide Rxn
All Pdt Frxns, (Azeotroped) 13C CDCl3

170.6
146.7
142.1
141.5
128.5
128.4
128.3
126.0
125.7
113.4
99.1
77.2
72.8
72.2
42.1
39.2
35.8
34.5
33.2
31.8
31.7
30.1
21.2
19.8
17.9
5.3

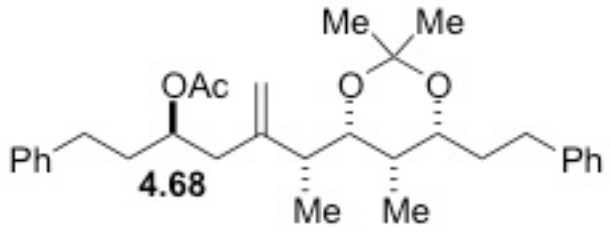

242

220 210 200 190 180 170 160 150 140 130 120 110 100 90 80 70 60 50 40 30 20 10 0
f1 (ppm)

skr10-021b
Syn-Anti-Syn Acetonide Pdt (Reflashed)
Best Pdt Frxns, (Azeotroped) 13C CDCl3

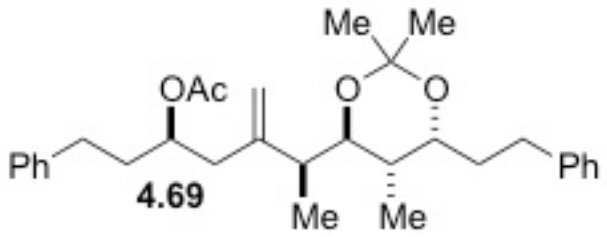

4.69

243

6.03 5.83 1.00 0.94 1.01 1.13 0.99 0.99 3.13 2.11 1.11 3.01 2.27 0.97 1.04 1.15 6.02 3.11 3.19

8.0 7.5 7.0 6.5 6.0 5.5 5.0 4.5 4.0 3.5 3.0 2.5 2.0 1.5 1.0 0.5 0.0 -0.5

f1 (ppm)

skr10-021c
Syn-Anti-Syn Acetonide Product
Flashed Best Frxns, 13C CDCl3

170.6
148.1
142.3
141.6
128.4
128.4
128.3
125.9
125.7
112.8
100.3
76.9
72.2
68.9
42.6
40.3
37.8
35.8
32.6
32.4
31.8
25.4
23.8
21.2
14.1
12.3

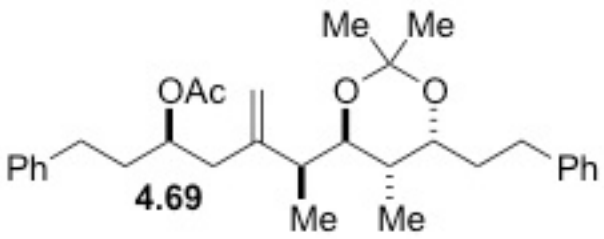

244

210 200 190 180 170 160 150 140 130 120 110 100 90 80 70 60 50 40 30 20 10 0 -10
f1 (ppm)

skr10-027a
2x-OAc Acetonide Fromation
Best Pdt Frxns (yellow), (Azeotroped) CDCl3

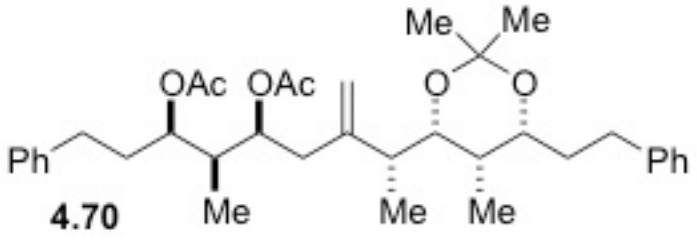

4.70

skr10-027c
2x-OAc Acetonide Fromation
Best Pdt Frxns (yellow), (Azeotroped) 13C CDCl3

170.6
170.4
146.7
142.1
141.2
128.5
128.4
128.3
128.3
126.0
125.7
113.6
99.1
77.2
74.3
72.8
72.7
42.2
39.3
36.4
34.5
33.6
33.3
32.0
31.7
30.1
21.1
19.8
17.8
9.9
5.3

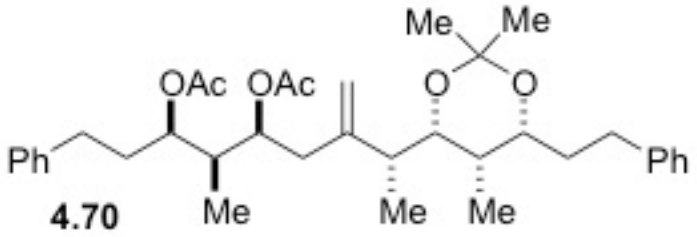

4.70

246

220 210 200 190 180 170 160 150 140 130 120 110 100 90 80 70 60 50 40 30 20 10 0
f1 (ppm)

skr10-018d
TBSOTf protection at -78 deg C
Mono-TBS Protected Pdt (Azeotroped), CDCl3

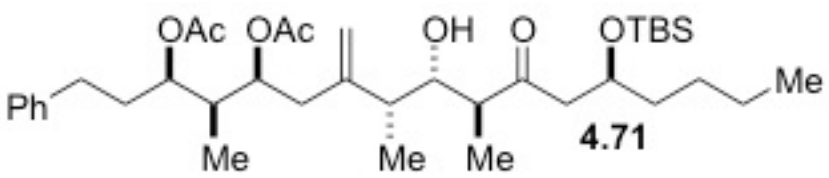

247

2.23 2.97 0.98 2.04 0.97 1.00 0.97 5.13 1.97 1.16 0.96 3.02 3.13 3.11 2.35 4.78 3.38 5.93 12.71 2.99 3.02

8.0 7.5 7.0 6.5 6.0 5.5 5.0 4.5 4.0 3.5 3.0 2.5 2.0 1.5 1.0 0.5 0.0 -0.5

f1 (ppm)

skr10-018c
TBSOTf protection at -78 deg C
Mono-TBS Protected Pdt (Azeotroped), 13 CDCl3

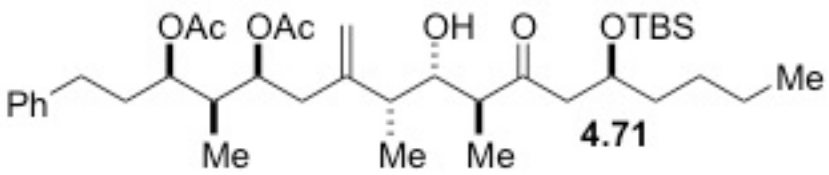

skr10-020b
Acetonide Formation w/p-TsOH
Isolated Syn Diastereomer, CDCl3

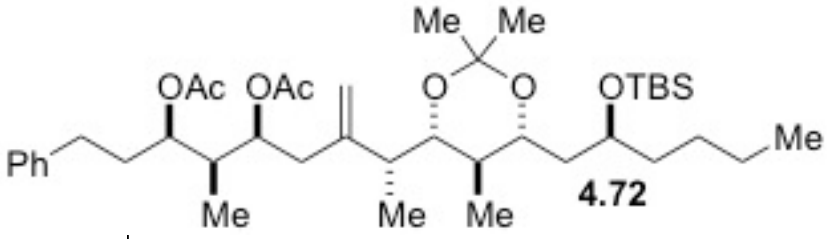

skr10-020d
Acetonide Formation from Tamao Compound
Flashed 1,3-Syn Acetonide, 13C CDCl3

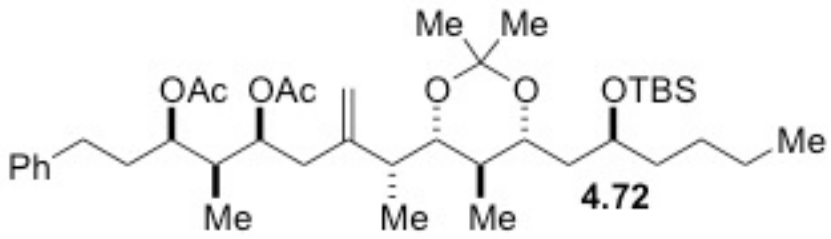

skr10-090d
Synthesized (S,S)-Allyl Diamine Reagent
Concentrated Sample, 1H CDCl3

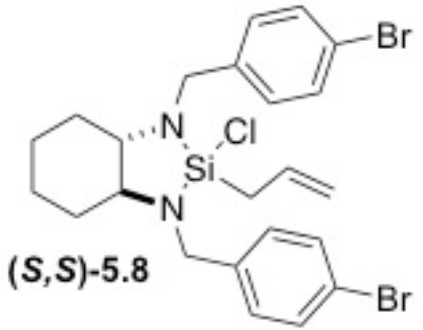

(*S*,*S*)-5.8

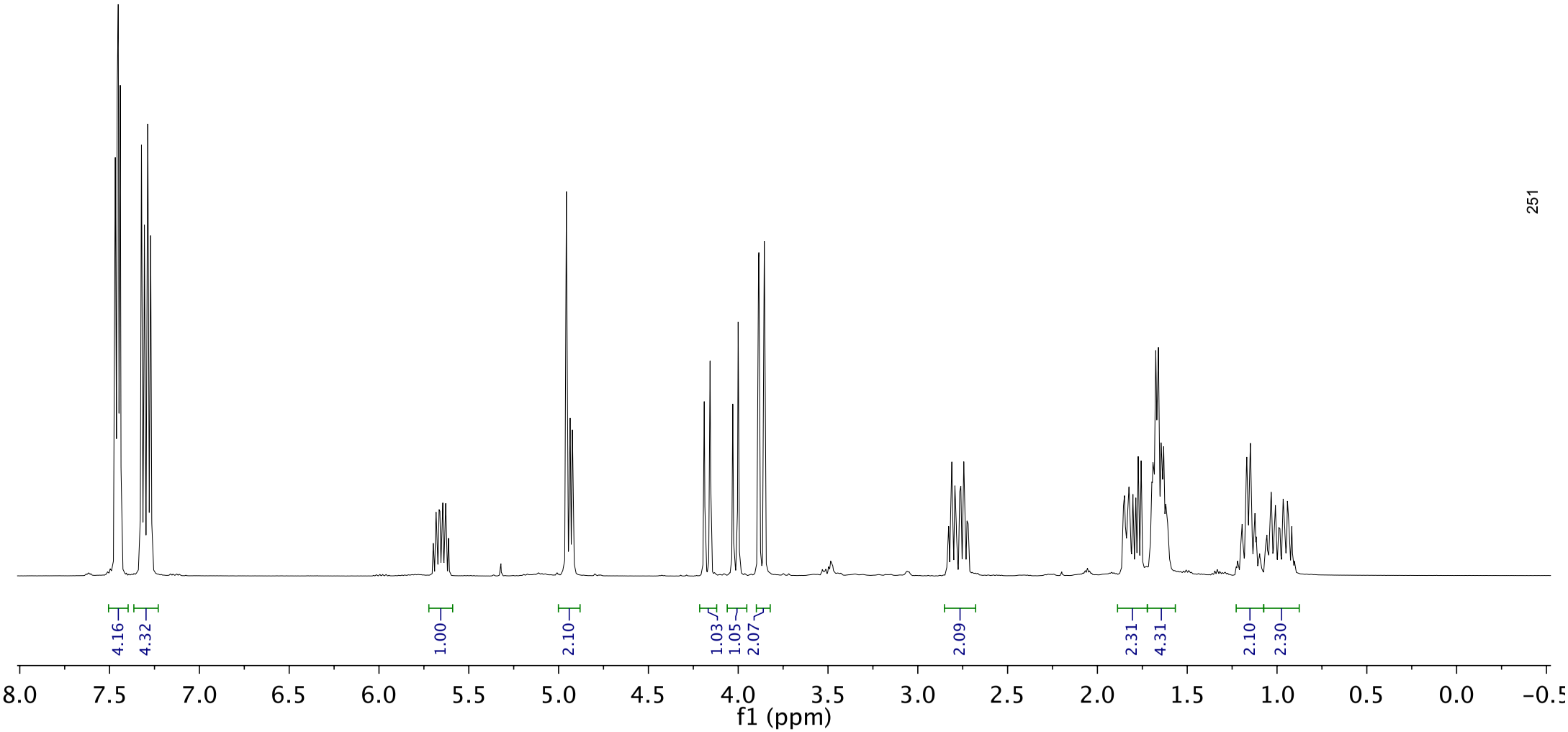

skr10-090e
Synthesized (S,S)-Allyl Diamine Reagent
Concentrated Sample, 13 C CDCl3

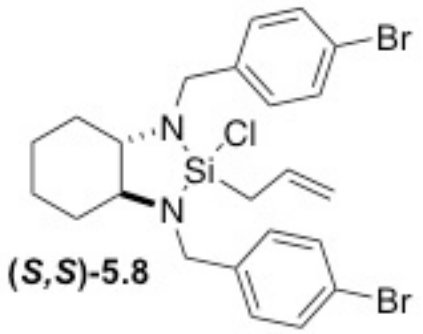

(*S*,*S*)-5.8

141.1
140.2
131.2
129.9
129.0
120.8
120.3
116.3
66.3
65.4
47.9
47.2
30.7
30.3
24.8
24.7
24.6

252

220 210 200 190 180 170 160 150 140 130 120 110 100 90 80 70 60 50 40 30 20 10 0 -10 -20 -30 -40
f1 (ppm)

skr10-091a
(S,S)-Diamine Allylation of Acetylacetone (1g Scale)
All Pdt Frxns, (Azeotroped) CDCl3

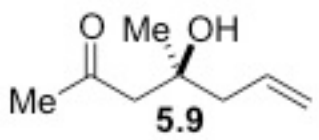

5.9

skr10-091c
(S,S)-Diamine Allylation of Acetylacetone (1g Scale)
All Pdt Frxns, (Azeotroped) 13C CDCl3

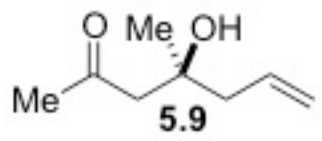

5.9

skr10-092c
(S,S)-Diamine*2HCl Reagent
White Crystalline Solid (Concentrated)
1H Solvated in d-DMSO

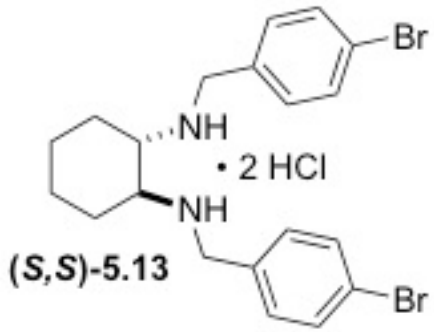

(*S*,*S*)-5.13

skr10-092c
(S,S)-Diamine*2HCl Reagent
White Crystalline Solid (Concentrated)
13C Solvated in d-DMSO

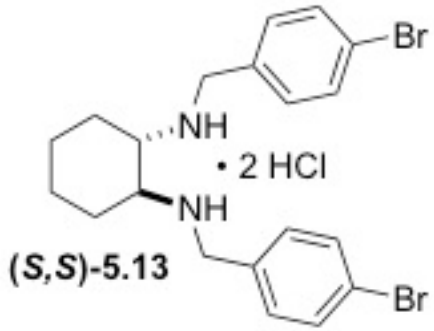

(*S*,*S*)-5.13

133.2
131.9
131.4
122.9
56.6
47.3
26.0
22.7

256

220 210 200 190 180 170 160 150 140 130 120 110 100 90 80 70 60 50 40 30 20 10 0
f1 (ppm)

skr9-016b
3'-OTES Keto-Alkene
Flashed Sample, (Azeotroped) CDCl3

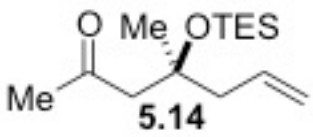

5.14

skr9-016c
3'-OTES Keto-Alkene
Flashed Sample, (Azeotroped) 13C CDCl3

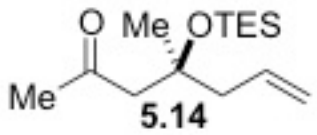

5.14

skr10-069b
BOM-Alkylation (~20g)
Isolated Best Frxn, (Azeotroped) CDCl3

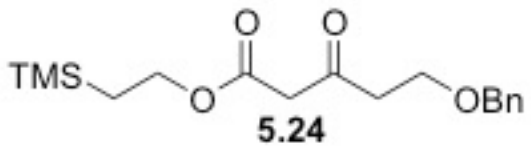

5.24

skr10-069c
BOM-Alkylation (~20g)
Isolated Best Frxn, (Azeotroped) 13C CDCl3

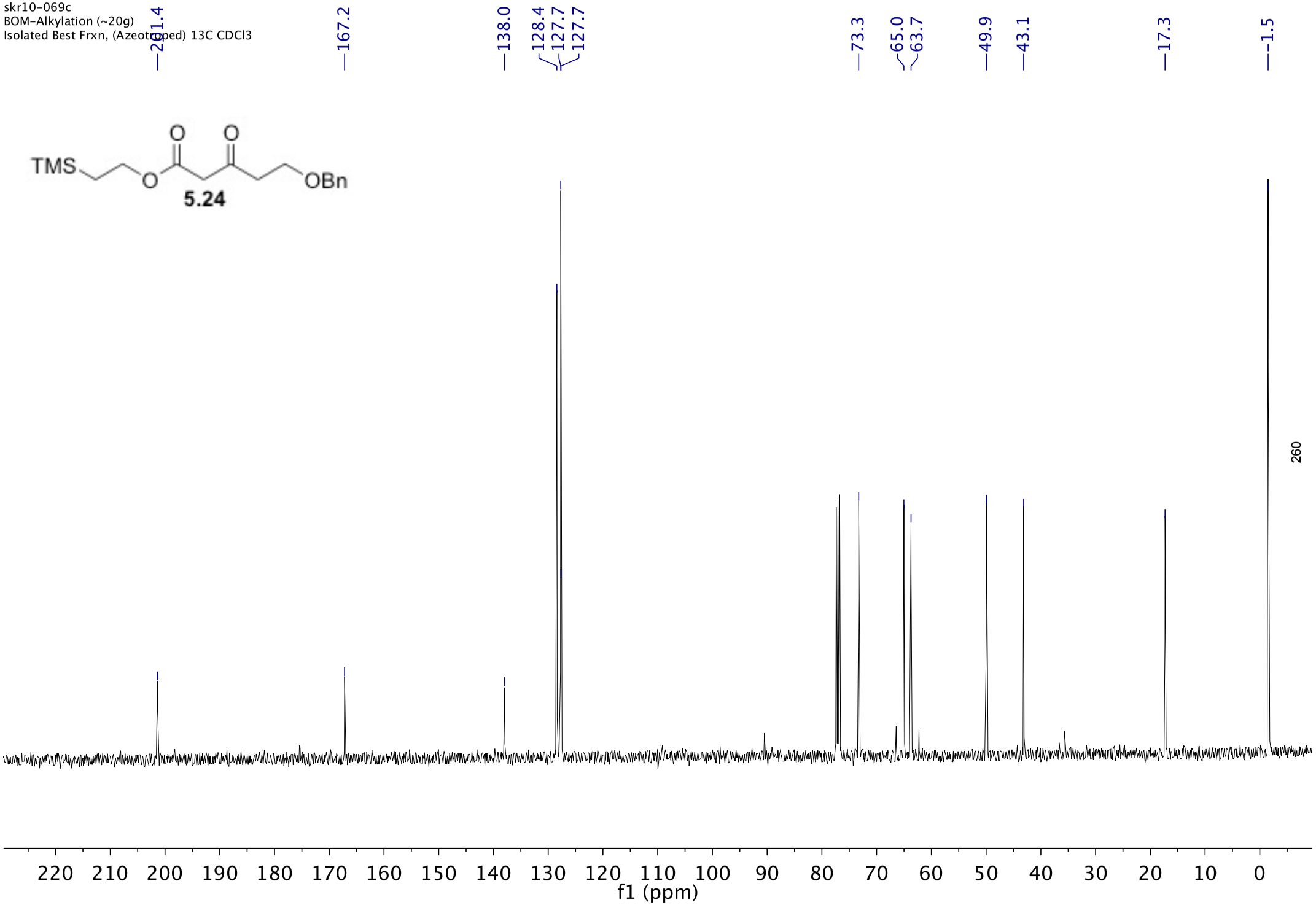

skr10-058d
Two-Pot, Bis-Acetylation of TMS-EtOH
Distillation Frxn 3 (Main), CDCl3

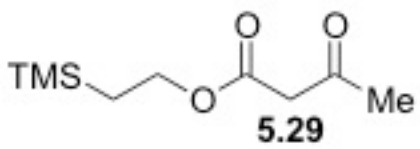

5.29

skr10-058e
Two-Pot, Bis-Acetylation of TMS-EtOH
Distillation Frxn 2 (Main), 13C CDCl3

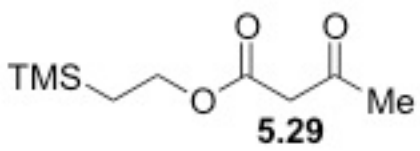

5.29

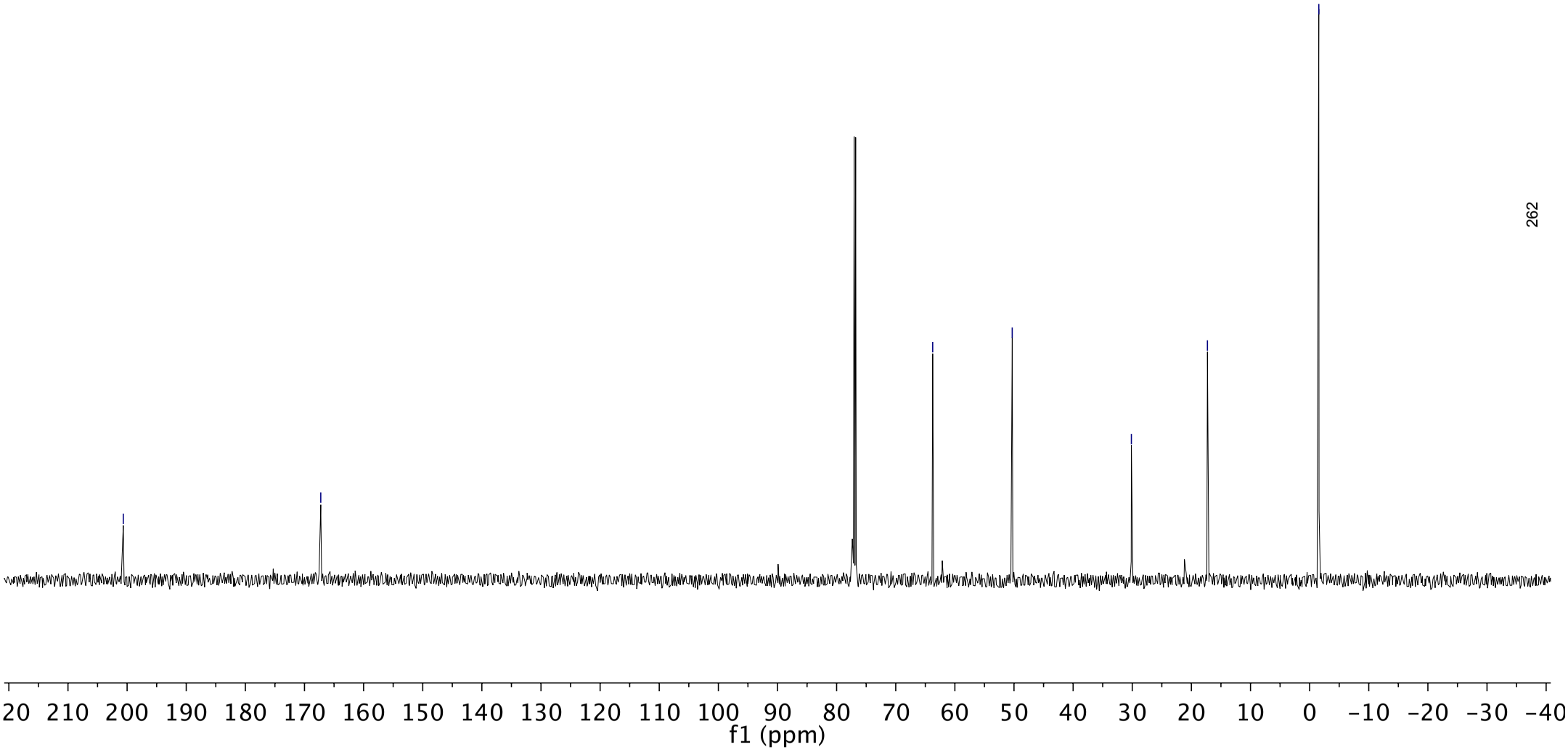

skr10-079a
(R)-Noyori Hydrogenation (Small Rxn)
Best Pdt Frxns, (Azeotroped) CDCl3

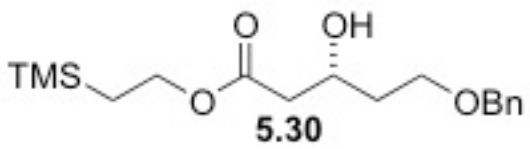

5.30

skr10-079c
(R)-Noyori Hydrogenation (Small Rxn)
Best Pdt Frxns, (Azeotroped) 13C CDCl3

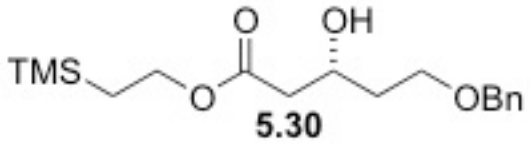

5.30

skr10-061e
TES-Cl Protection of Noyori Crude
Pdt Sample Flashed, (Azeotroped) CDCl3

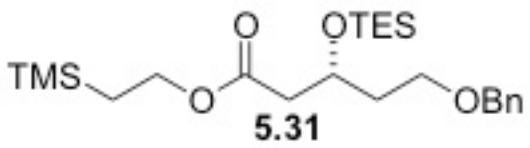

5.31

skr10-061c
TES-Cl Protection on Noyori Crude
Sample Flashed Pdt Frxns, 13C (Azeotroped) CDCl3

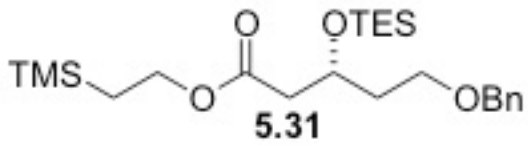

5.31

skr10-089b
Pd(OH)2 Hydrogenation (~60 mmol Rxn)
Reflashed Pdt Frxns, (Azeotroped) CDCl3

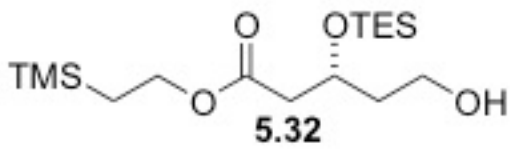

5.32

skr10-089c
Pd(OH)2 Hydrogenation (~60 mmol Rxn)
Reflashed Pdt Frxns, (Azeotroped) 13C CDCl3

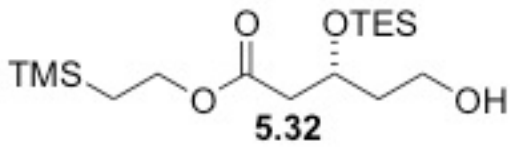

5.32

skr10-093a
Swern Oxidation (Small Scale - 0.1 mmol)
Flashed Best Pdt Frxns, (Azeotroped) CDCl3

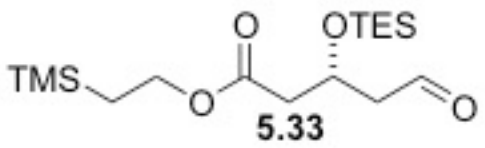

5.33

skr10-093c
Swern Oxidation (Small Scale - 0.1 mmol)
Flashed Best Pdt Frxns, (Azeotroped) 13C CDCl3

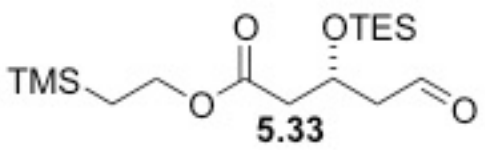

5.33

201.0
170.9
64.9
62.9
51.0
42.9
17.3
6.8
4.8
-1.5

270

220 210 200 190 180 170 160 150 140 130 120 110 100 90 80 70 60 50 40 30 20 10 0
f1 (ppm)

skr10-130g
Large Scale Paterson Aldol
Reflashed Front, Best Pdt Frxns (Azeotroped), 1H CDCl3

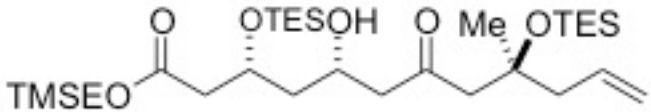

5.34

skr10-130f
Large Scale Paterson Aldol
Best Pdt Fxns (Azeotroped), 13C CDCl3

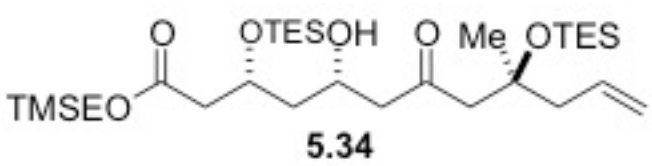

5.34

skr9-024d
Acetylated Paterson Aldol Pdt
Best Pdt Frxns Flashed, (Azeotroped) 1H CDCl3

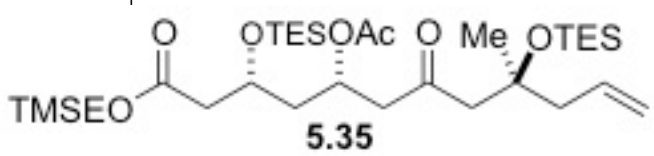

5.35

skr9-024c
Acetylated Paterson Aldol Pdt
Best Pdt Fr's, (Azeotroped) 13C CDCl3

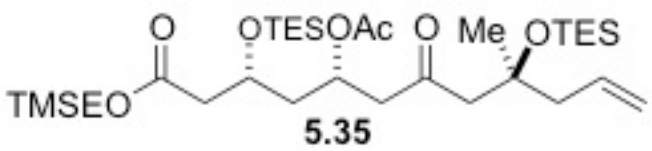

5.35

skr10-142b
Large Scale Ozonolysis Rxn
Flashed pH 7 SiO2 Gel (Azeotroped), 1H CDCl3

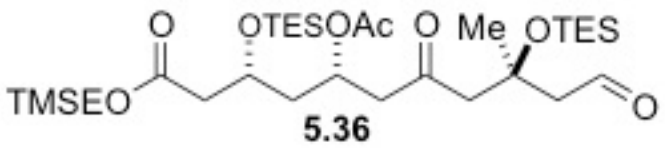

5.36

skr10-142c
Large Scale Ozonolysis Rxn
Flashed pH 7 SiO2 Gel (Azeotroped), 13C, CDCl3

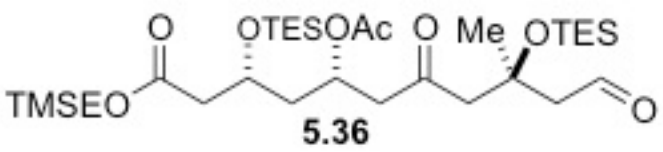

5.36

skr10-143e
(R,R)-Isoprenylated Aldehyde
Best Lactol Pdt (Azeotroped), 1H CDCl3

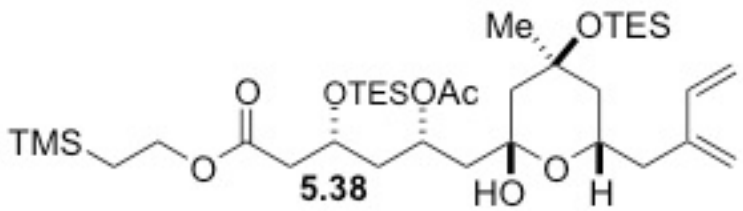

277

1.00 0.92 1.02 1.06 3.14 4.13 1.89 1.03 1.02 3.30 1.83 3.12 1.06 1.70 3.16 1.12 20.90 12.54 9.41

8.0 7.5 7.0 6.5 6.0 5.5 5.0 4.5 4.0 3.5 3.0 2.5 2.0 1.5 1.0 0.5 0.0 -0.5
f1 (ppm)

skr10-143c
(R,R) Isoprenylated Aldehyde
Lactol Pdt (Azeotroped), 13C CDCl3

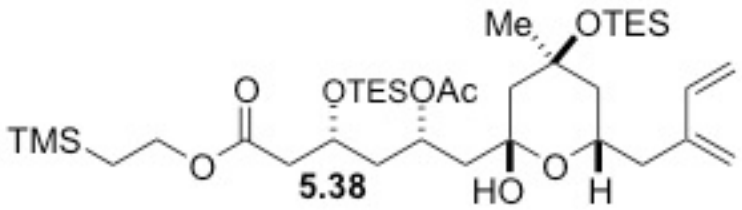

skr10-144w
Spiroketalization (0.25 eq CSA)
Best Pdt Frxn (Azeotroped), 1H CDCl3

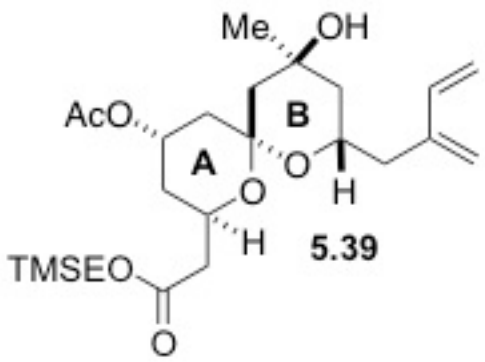

5.39

skr10-144f
Spiroketalization (0.25 eq CSA)
Rxn t = 1.5 hrs, Quenched w/Et3N
Reflashed Best Pdt Frxn (Azeotroped), 13C CDCl3

170.9
170.8
142.5
139.0
117.8
113.7
98.2
67.8
66.2
64.8
63.1
62.1
45.9
43.4
40.5
37.7
37.2
34.3
30.0
21.4
17.3
1.5

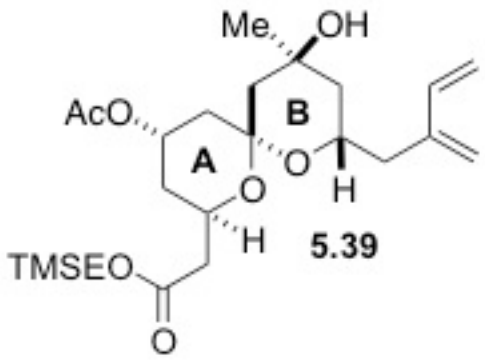

5.39

281

220 210 200 190 180 170 160 150 140 130 120 110 100 90 80 70 60 50 40 30 20 10 0 -10 -20 -30 -40
f1 (ppm)

skr9-030a
3'-OTFA Spiroketal-Diene
Stored for 1 Year in C6H6, 1H CDCl3

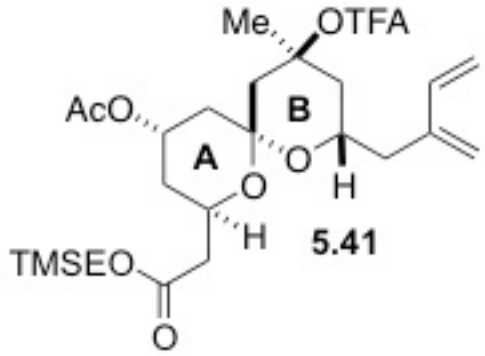

5.41

skr9-030c
3'-OTFA Spiroketal-Diene
Stored for 1 Year in C6H6, 13C CDCl3

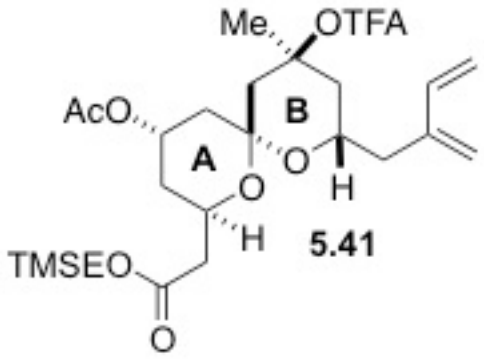

5.41

skr10-156a
AB-Fragment Coupling w/TES-Aldehyde
Best Pdt Frxn (Azeotroped), CDCl3

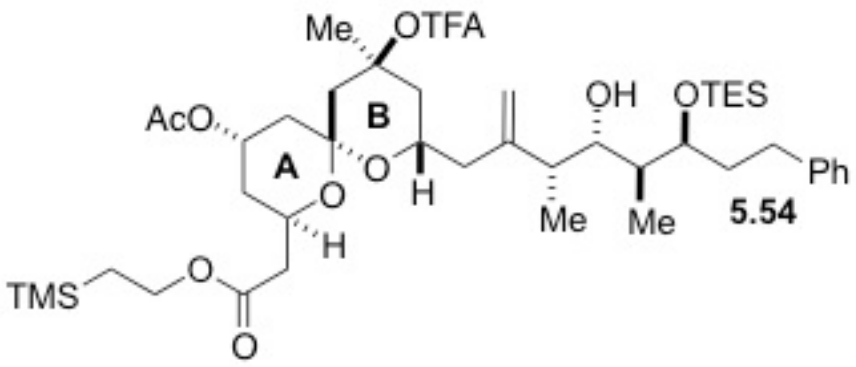

285

2.70 2.91 0.86 1.85 1.85 2.00 0.91 0.89 0.78 0.96 0.90 1.98 1.89 1.90 3.30 1.71 4.02 1.48 3.33 1.15 1.17 1.69 2.75 11.39 2.92 5.88 9.00

8.0 7.5 7.0 6.5 6.0 5.5 5.0 4.5 4.0 3.5 3.0 2.5 2.0 1.5 1.0 0.5 0.0 -0.5

f1 (ppm)

skr9-156c
AB-Fragment Coupling w/TES-Aldehyde
Best Pdt Frxn (Azeotroped), 13C CDCl3

171.1
170.6
156.6
156.2
148.0
142.4
128.5
128.5
126.0
115.9
113.4
113.0
96.8
84.3
75.7
72.4
66.5
63.6
62.6
61.5
42.5
41.3
41.1
40.1
40.0
37.7
35.4
33.8
33.4
26.5
21.6
17.4
11.5
10.6
7.1
5.3
-1.4

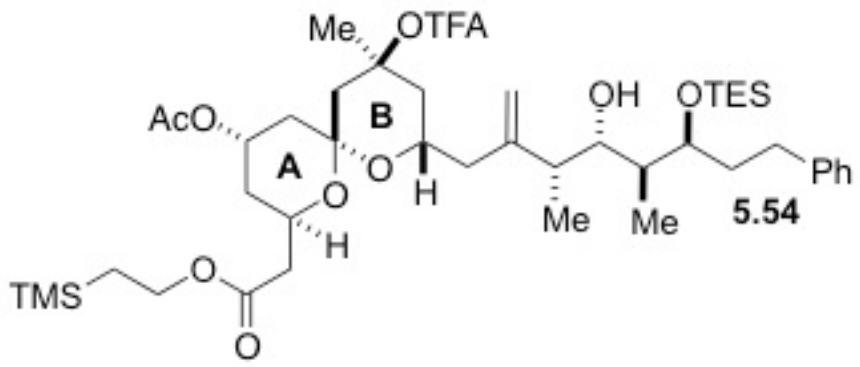

286

210 200 190 180 170 160 150 140 130 120 110 100 90 80 70 60 50 40 30 20 10 0 -10
f1 (ppm)

skr10-157d
AB-Fragment Coupling w/Silacycle-Aldehyde
Best Pdt Frxn (Azeotroped), CDCl3 (Manually Shimmed)

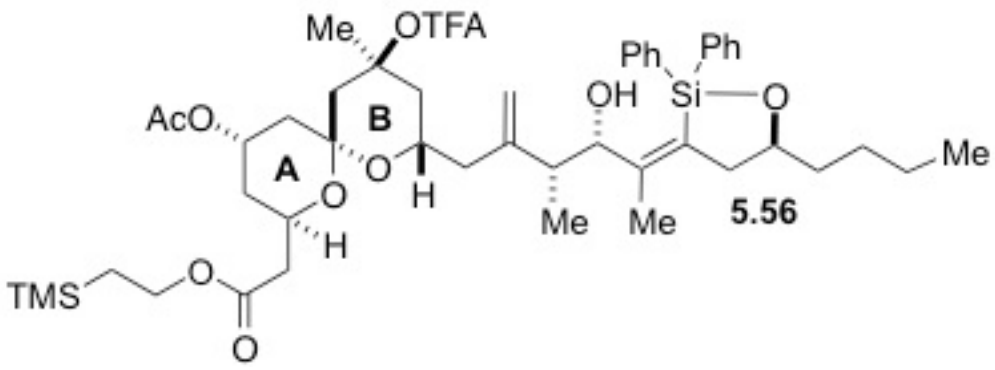

skr9-157c
AB-Fragment Coupling w/Silacycle-Aldehyde
Best Pdt Frx 7 (Azeotroped w/ 10CL6DCl3

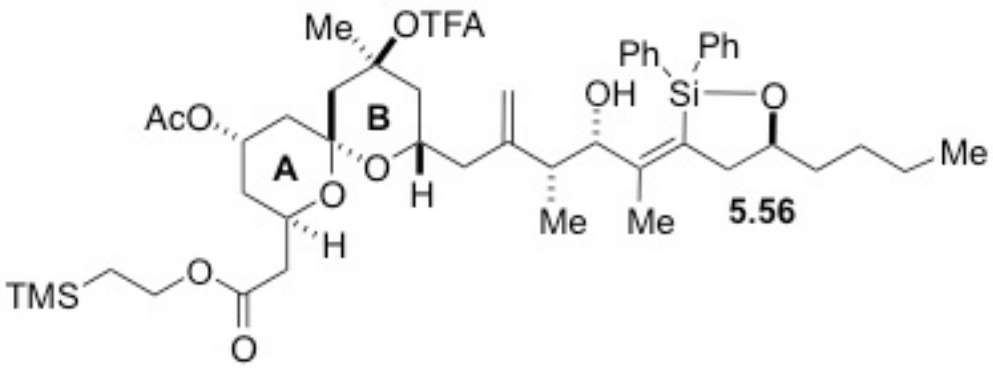

skr10-158h/1
Tamao of AB-Silacycle Coupled Fragment
All Pdt Frxns, CDCl3

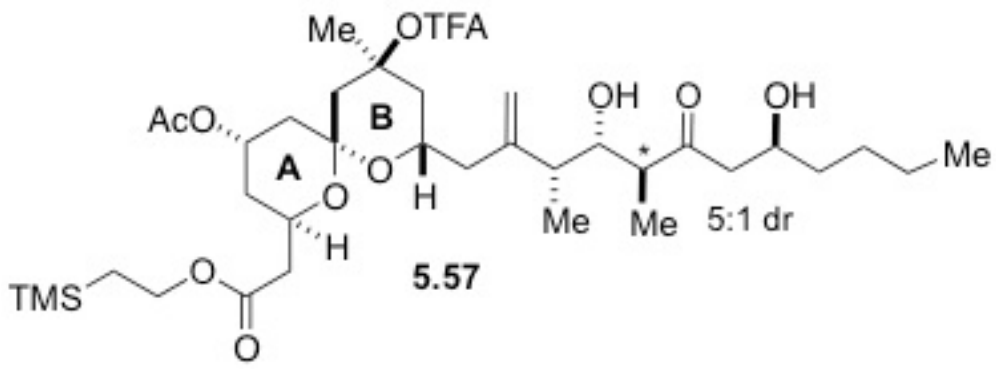

289

1.00 0.30 2.38 0.22 2.83 4.58 0.19 1.05 0.09 0.93 0.10 0.28 4.22 2.96 1.66 5.08 5.39 1.35 1.48 3.22 4.34 3.06 4.59 6.95 1.30 3.26 3.17 3.22 4.83 12.84

8.0 7.5 7.0 6.5 6.0 5.5 5.0 4.5 4.0 3.5 3.0 2.5 2.0 1.5 1.0 0.5 0.0 -0.5

f1 (ppm)

skr10-158i/1
Tamao of AB-Silacycle Coupled Fragment
All Pdt Frxns, 13C CDCl3

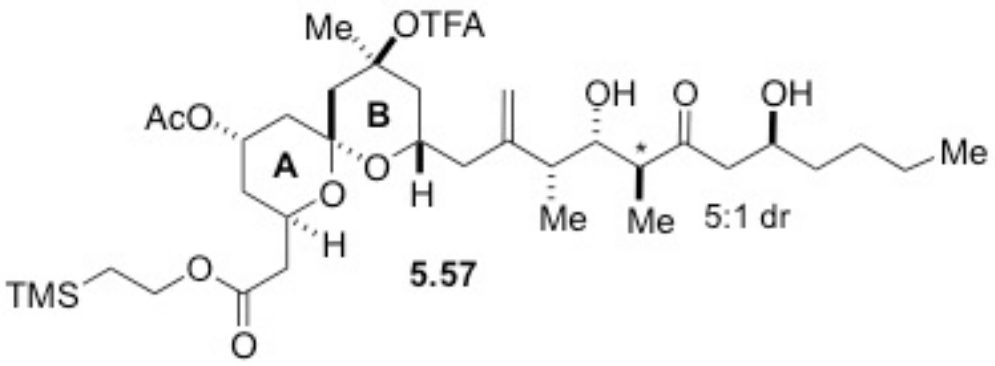

-26.6
171.0
170.8
156.6
156.3
147.4
115.6
114.5
113.3
96.8
84.2
73.2
67.6
66.5
63.5
62.7
61.4
50.8
48.4
41.3
41.2
40.2
37.7
36.3
33.8
27.9
26.5
22.8
21.6
17.4
14.2
13.1
11.0
-1.4

290

220 210 200 190 180 170 160 150 140 130 120 110 100 90 80 70 60 50 40 30 20 10 0
f1 (ppm)